Artificial Molecular Rotors

Gregg S. Kottas,[†] Laura I. Clarke,[‡] Dominik Horinek,[†] and Josef Michl*,[†]

Department of Chemistry and Biochemistry, University of Colorado, Boulder, Colorado 80309-0215, and Department of Physics, North Carolina State University, Raleigh, North Carolina 27695

Received September 8, 2004

Contents

1. Introduction

To many, periodic mechanical conformational motion of molecules is mesmerizing to a degree that is difficult to explain rationally: It is almost as hard to stop watching an image of internal rotation in a molecule as it is to stop watching the flames of a campfire. Perhaps this is one of the reasons why chemists have been fascinated for decades with molecular structures that permit internal mechanical motion at various degrees of complexity, from random flipping to concerted geared motion and to motion intentionally driven in a unidirectional manner. The present review deals with man-made molecular rotors from the point of view of their potential utility for "molecular machinery".

[†] University of Colorado.
[‡] North Carolina State University.

10.1021/cr0300993 CCC: $53.50
Published on Web 04/13/2005

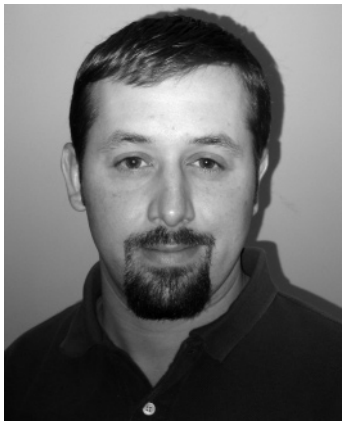

Gregg Kottas was born in 1974 in Buffalo, NY, and received his B.S. in Chemistry from the University of Florida, performing undergraduate research under the direction of Merle A. Battiste. After an internship at the Eastman Chemical Company in Kingsport, TN, he moved on to graduate studies at the University of Colorado at Boulder under the direction of Prof. Josef Michl. Working on the synthesis and surface studies of surface-mounted dipolar rotors, he received his Ph.D. in 2004. Currently, he is a postdoctoral researcher at the University of Münster under the direction of Prof. Luisa De Cola, investigating the synthesis and photophysics of inorganic and organometallic complexes with possible applications for new lighting sources.

Laura Clarke is an Assistant Professor of Physics at North Carolina State University. She received her Master's degree in Physics in 1996 and her Ph.D. in Physics in December 1998 from the University of Oregon under the supervision of Martin N. Wybourne. Her postdoctoral work was conducted in the laboratory of John C. Price at the University of Colorado. Her research focuses on electric, dielectric, and optical measurements of organic materials.

Dominik Horinek was born in 1972 in Freiburg, Germany. He studied Chemistry at the University of Regensburg, Germany, where he got interested in theoretical and computational Chemistry. In 2000, he finished his doctorate in the group of Prof. Bernhard Dick, Regensburg, where he worked on molecular dynamics simulations of matrix isolated molecules. In 2001 he joined Prof. Josef Michl's group at the University of Colorado at Boulder as a Feodor Lynen Fellow of the Alexander von Humboldt Foundation, where his interest is focused on computational studies of surface-mounted molecular rotors.

Photograph and biography for Josef Michl can be found on p 1199.

2. Scope

In the context of nanoscience, it has been customary to use the term *molecular rotor* for molecules that consist of two parts that can easily rotate relative to each other. The rotation is one-dimensional in that it involves changes in a single angle. It is common to view the part with the larger moment of inertia as stationary (the *stator*) and the part with the smaller moment of inertia as the *rotator* (the otherwise more common term *rotor* has been preempted as it refers to the whole molecule), but the distinction is truly unambiguous only if the stationary part is fixed on or within a much more massive object, such as a macroscopic one. In the absence of such mounting, the rotator and the stator both turn around a common axis. In the absence of outside torque, a simple computational procedure relates the possibly quite complicated paths of all the nuclei to the overall rotation of the molecule in the laboratory frame.[1]

In gases, liquids, and certain solids, entire molecules can rotate as a whole around three independent axes, but we will not deal with this phenomenon presently, although molecules rotating in a solid could be referred to as rotors by the dictionary definition[2] of the term ("a part that revolves in a stationary part"). Since internal rotation within molecules is nearly ubiquitous (for instance, all molecules with a methyl group qualify), we further restrict the scope of this review to studies of historical importance, in which groundwork was laid to the current developments, and to studies in which such rotation has been the focus of attention in the context of nanoscience and relevant to the ultimate construction of molecular-size mechanical structures that might perform useful functions. In many borderline instances, we were obliged to make subjective decisions concerning inclusion in the review, and we beg the reader for understanding where we may have erred and also in cases of inadvertent omissions. A particularly difficult distinction has been the separation of pendular motion, which we do not cover, and rotatory motion. We have taken the view that the function of a molecular rotor is continued rotation by 360° or more, and we have not treated exhaustively structures capable of rotating only part way, although some are mentioned in the context of rotational barriers.

We only deal with artificial molecular rotors and pay no heed to naturally occurring protein-based rotors and motors, such as ATP synthase.[3−8] These have been reviewed repeatedly in the recent past.[9−11] Even among artificial rotors, we have arbitrarily decided to deal only with compounds that have been isolated as pure chemical species with a well defined

structure, and not with mixtures. This eliminated from consideration almost all work on polymers. Their internal rotations represent a fascinating subject in its own right, and one only needs to think of crankshaft rotation[12−20] or the work of Gaub and collaborators[21,22] on a bistable nanoscopic machine in which a cis−trans isomerization of azobenzene units shortens a polymer chain and performs nanoscopic work.

We have included both molecular rotors exhibiting thermally induced rotation and those designed so as to be capable of being driven by an external force, such as an electric field or a flow of a fluid. Our emphasis is on experimental results, but we have included computational and theoretical work, and section 3 provides a theoretical background for molecular rotors. It emphasizes the behavior of rotors mounted in a solid or on a surface, reflecting our belief that these situations are most relevant for nanotechnology. Little is said about methods (section 4), which are generally well known and not particularly specific for the study of rotors.

We devote particular attention to molecules that can potentially exhibit unidirectional motion, as opposed to random flipping in either direction. A controlled direction of rotation is often considered as a prerequisite for a motor, even though its dictionary definition,[23] "something, such as a machine or an engine, that produces or imparts motion", does not specify unidirectionality. Many authors use the term molecular motor and molecular rotor interchangeably, but we prefer to reserve the former for molecules designed in such a way that their rotation can actually produce potentially useful work. Useful work is not easily defined on the nanoscale, and we have in mind a process that starts at thermal equilibrium with an external bath and at the end leaves a measurable and desired difference in the system after it is again in thermal equilibrium. Such useful work might be the translocation of a distinct object from one site to another, or the pumping of a fluid, as one would expect of a motor. Although even a real macroscopic motor can most definitely idle at times, converting high-grade energy into heat and achieving nothing else, a rotor that can do nothing but idle will not be referred to as a motor presently. After all, a macroscopic toy spinning top would hardly be considered a motor just because it can rotate, but it is surely acceptable to call it a rotor. We recognize, of course, that this is a matter of personal preference and that at some future time a further synthetic elaboration of such a molecular rotor may convert it into a species capable of actively converting energy supplied to it from the outside into useful work. Still, we prefer to wait with the label *motor* until such elaboration has actually been performed. Although examples of molecular motors based on steady rotatory motion capable of performing useful work are known, to our knowledge none of them are artificial. Useful work-performing artificial molecular structures based on pendular motion, which can also be considered rotatory in nature, are known, but they lie outside the scope of the present review (turning the axis of a liquid crystal, controlling binding events or transport, etc.).

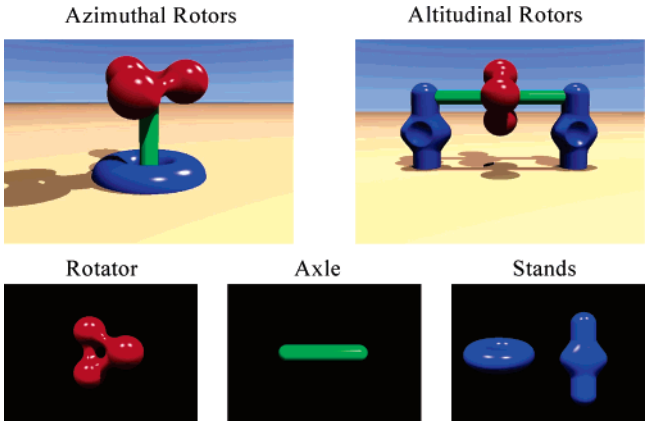

Figure 1. Classification system for surface-bound RS molecular rotors. (See text and Table 1.)

Structurally, one can distinguish rotors in which the stator and the rotator are covalently attached to each other, and those in which they are not (as in catenanes, molecules containing two interlocked rings, and rotaxanes, containing a ring mounted on a rod). We shall only attempt exhaustive coverage of molecular rotors in which the stator and the rotator are covalently linked, which appear not to have been reviewed before. The important and popular subject of rotation in catenanes and rotaxanes has been reviewed elsewhere,[24−26] and we will only briefly mention a few isolated examples. The reader is referred to review articles dealing with catenanes and rotaxanes of the Stoddart type,[27−36] of the Sauvage type,[37−45] of the amide type,[46−50] with catenated cyclodextrins,[51,52] and with dendrimeric rotaxanes.[53] A useful article by Willner and collaborators touches on many issues concerning the use of photoisomerization in possible molecular devices, with an emphasis on rotaxanes and catenanes.[54] Other reviews and monographs have covered catenanes and rotaxanes in general.[55−58]

Molecular rotors of the kind covered in the present review can be classified further according to various criteria. We distinguish rotors that float freely in solution or vapor (section 5), those that are located inside solids (section 6), and those that are surface-mounted (section 7). As discussed above, for solution-phase rotors, the distinction between the rotator and the stator may be ambiguous, as both portions of the molecule rotate with respect to each other. However, for surface-mounted molecules, one can specify whether (i) the molecular rotor provides only the rotator element (an "R rotor"), with the surface acting as a stator, or whether (ii) the stator, rigidly attached to the surface, forms a part of the molecular structure (an "RS rotor"). In addition, the axle of rotation about which the rotator turns can be perpendicular (an azimuthal rotor) or parallel (an altitudinal rotor) to the surface (Figure 1). For rotors in solids, the R and RS distinction can also be made. For a solid formed of molecular rotors, the component molecules will usually contain both a rotary part and some structure which separates adjacent rotators, making them RS rotors. However, plastic crystals are solids made only

Table 1. Definitions for Molecular Rotor Systems

term	definition
molecular rotor	a molecular system in which a molecule or part of a molecule rotates against another part of the molecule or against a macroscopic entity such as a surface or a solid
molecular motor	a molecular rotor capable of producing useful work
Brownian motor or ratchet	a molecular system that undergoes unidirectional motion in response to thermal fluctuations in a nonequilibrium state
rotator	the part of the molecule or system that rotates against the rest (generally taken as that which has the smaller moment of inertia)
stator	the stationary part of the system with respect to which the rotator turns (generally taken as that which has the larger moment of inertia)
axle	the portion of the molecule that carries the rotator and about which the rotator turns; some molecular rotor systems do not contain axles (e.g., a rotor physisorbed onto a surface—an R Rotor (see definition below)
altitudinal rotor	a surface-mounted rotor which turns about an axle parallel to the surface to which it is attached (see Figure 1)
azimuthal rotor	a surface-mounted rotor which turns about an axle perpendicular to the surface to which it is attached (see Figure 1)
R rotor	a surface-mounted or solid-state rotor system without a defined axle, with a surface or bulk solid acting as the stator
RS rotor	a surface-mounted or solid-state rotor system covalently attached to a surface or located within a bulk solid, where the stator is a part of the molecular framework and there is a clearly defined axle about which the rotator turns

of rotators (R rotors). Because a solid has many planes against which rotors could be classified as either altitudinal or azimuthal, such a distinction is not helpful in this case.

Within each category of solution-phase, surface-mounted, or solid rotors, an additional classification can be made by examining the chemical nature of the axle, which is most commonly represented by a single bond, a triple bond, or a metal atom. As will be discussed below, the chemical nature of the bond strongly influences one of the fundamental energy terms in the system, the intrinsic barrier to rotation. We will also discuss systems with no defined axles, such as molecules "incarcerated" in inclusion complexes, physisorbed to a surface, or diffused into solids. Most of these cases involve three-dimensional whole-molecule rotations and are not within our classification system nor within the scope of this review. However, we do briefly mention several such systems which either (i) were important for the discovery of later, related systems or (ii) in and of themselves represent possibilities for molecular-level devices. Table 1 provides definitions for molecular rotor systems that we will use throughout this text.

As alluded to above, we concurrently categorize rotors not only within this structural classification but also by their function, that is, by the nature of their dynamics under a given set of environmental conditions. For instance, for hindered, thermally activated systems, there are rotors with such a small rotational potential energy barrier that reorientation of the rotor is frequent at a sufficient temperature and those where the rotor is strongly hindered and simply sits in the lowest energy configuration, unless the system is perturbed by an external force. Most examples fall between these two extremes. Even a single-rotor system could exhibit both behaviors by altering the temperature, with frequent motion at high temperatures but no reorientation when cold. This example underscores a significant point: the interplay of the various energies in a system determines rotor dynamics (section 3). The structure of the rotor establishes many of these energy terms, such as the barrier to rotation; the remainder are the result of environmental conditions, such as temperature, or a combination of structure and environment, as in the case of a rotor with a permanent electric dipole coupling with an applied electric field or a propeller of a particular shape interacting with a viscous liquid.

Within this categorization based upon dynamics, the first distinction applied reflects the relationship between external forces and the motion of the rotor. We classify systems as driven, when the presence of an external force determines the dynamics of the rotor. In contrast, for systems described here as random, the motion of the rotor is primarily dictated by the thermal energy, although the presence of an external field may affect the static configuration of the system or cause the rotation to be unidirectional. Within the driven category, we distinguish rotors that interact with the driving force via a field, for instance, a dipole rotor interacting with an applied electric field, from those where the interaction is steric, such as in an interlocking system of cogs. Driven motion is further categorized by the efficacy of the driving. Similarly, two types of random rotors are included: (1) those where the thermal energy is the only important energy term and the motion is purely Brownian and (2) rotors where thermal energy is small compared to the intrinsic barrier to rotation and the rotor reorients by thermally activated hopping.

There is a group of authors who use the term "molecular rotors" in a much narrower sense and define them as "fluorescent molecules with a viscosity-sensitive quantum yield that can be used to measure viscosity changes",[59] such as in cell membranes and liposomes.[60−62] These compounds have also been used to study liquid crystals and polymers.[63,64] Such molecules lose their electronic excitation energy by radiation or by intramolecular rotation, in a ratio that depends on the free volume in the environment. Therefore, a simple fluorescence measurement can give information about viscosity changes in a particular medium.

There is a much broader class of molecules that have a partial double bond in the ground state as the axle, which permits a hindered rotation, normally fast at room temperature, and that undergo a twisting conformational change upon electronic excitation. Return to the ground state then can lead to rotation and, hence, *syn*−*anti* isomerization. They are often referred to as TICT (twisted intramolecular charge transfer) molecules. These also fall under our definition of a molecular rotor, but since a comprehensive review on these structures has just been published,[65] we shall only refer to them briefly.

Molecules with a true double bond in the ground state as the axle are usually very highly hindered rotors, but they too can twist upon electronic excitation. Return to the ground state can then lead to a net rotation, and hence, *cis*−*trans* isomerization (e.g., stilbenes,[66,67] rhodopsin,[68] azobenzene[69]). These, too, qualify as molecular rotors under our definition, but instead of reviewing the vast number of all known cases of geometrical isomerization of double bonds, we limit our discussion to several specific examples in which the authors were clearly interested in molecular machines, and we refer the reader elsewhere[54,70] for additional information.

Finally, we need to specify that we do not consider as molecular rotors molecules that are capable of Berry pseudorotation, and we do consider molecules capable of turnstile rotation. Berry pseudorotation generally starts in a trigonal bipyramidal geometry and follows a path along which the axial angle is closing and one of the equatorial angles is opening until the molecule reaches a square pyramidal transition state. The motion then continues until the molecule returns to a trigonal bipyramidal geometry with ligand positions interchanged.[71] In turnstile rotation, a pair of ligands rotates with respect to the other three.[72] Often it is difficult to distinguish whether a mechanism for interconversion of metal-complex isomers involves rotation, pseudorotation, or a dissociation/association process. In this review, we include only those metal systems in which ligand fluxionality is definitely due to rotation of a defined group about a defined axle. The reader is directed to other reviews of fluxionality in transition metal complexes.[73,74]

3. Theoretical Issues

3.1. Overview of Characteristic Energies

We begin with an overview of the general theory and basic behavior of rotor systems. The Langevin equation which describes a one-dimensional rotor system is[75]

$$I\frac{\mathrm{d}^2\theta}{\mathrm{d}t^2} = \frac{-\partial V_{\mathrm{net}}}{\partial\theta} - \eta\frac{\mathrm{d}\theta}{\mathrm{d}t} + \xi(T,t) \qquad (1)$$

Here the thermal bath interacts with a single torsional degree of freedom, θ. The rotator has a moment of inertia I about the rotational axis and moves in a potential V_{net} that encompasses all static or time-dependent interactions between the rotator and the external world. Specifically, the intrinsic torsional potential (reflecting interactions between the rotator and the remainder of the rotor) and the coupling energy between the rotator and any driving field are included in V_{net}. The quantity η is the friction constant (which may be frequency dependent), and ξ is stochastic torque representing thermal fluctuations in the system (T is temperature, and t is time).

A cursory examination of eq 1 indicates that the rotor has one degree of freedom, the ability to turn through a single torsional angle, a situation which is clearly an approximation for molecular structures. However, the other molecular degrees of freedom due to thermal motion of atoms within the rotor are reflected in the frictional and stochastic terms. In other words, the random motion of the atoms within the molecule comprises part of the thermal bath with which the single torsional degree of freedom interacts. As discussed in detail below, this interaction with other degrees of freedom manifests itself in two ways: as random, stochastic torque on the rotator and as a loss mechanism. For instance, torsional and nontorsional modes in a rotor system are inherently coupled, although the extent of this coupling will depend on rotor structure. A driving force designed to turn the rotator may also populate other modes in the rotor (section 3.1.2). From the point of view of eq 1, this results in a need for greater applied torque in order to maintain motion of the rotator, an effect which manifests itself as an increased effective friction constant η.

Although the remainder of section 3 is devoted to an elaboration on the various terms in this equation, some factors are common to the entire discussion and can be addressed here.

3.1.1. Inertial Effects

For a rotor in perfect vacuum at zero temperature, the last two terms on the right-hand side of eq 1 are removed and the elementary result of Newton's second law for angular coordinates is obtained. If we further restrict the system by setting the intrinsic torsional potential and any restorative coupling between the rotator and an applied driving field to zero, the rotor will turn if subjected to external torque. Here, the maximum possible angular acceleration is the ratio of applied torque to the moment of inertia about the rotational axis. After this torque is removed, the energy of the system is purely kinetic and given classically by $\epsilon = L^2/2I$, where L is angular momentum, and $L = -(\partial V_{\mathrm{net}}/\partial\theta)\Delta t$, where, in this case, $-\partial V_{\mathrm{net}}/\partial\theta$ is constant torque applied over a time Δt. A quantum mechanical approach quantizes the angular momentum in packets of $h/2\pi$, where h is Planck's constant, and generates discrete rotational energy levels ϵ

$$\epsilon = \left(\frac{h}{2\pi}\right)^2\frac{J(J+1)}{2I} \qquad (2)$$

where J is the rotational quantum number.[76] Here, the spacing of the levels increases with a decreasing moment of inertia.

For a collection of rotors with nonzero temperature, a comparison of the level spacing to the thermal

energy determines whether the rotor can be treated classically or quantum mechanically. The distribution of rotational energies is given by statistical mechanics.[76] For the systems of interest here, the final two terms in eq 1 are generally not negligible, and inertial effects tend to be small compared to frictional effects.[77,78] Not only is the moment of inertia of the rotators generally minute, but in solution phase, viscous or drag effects can be significant. As discussed in the following subsection, even in solids and on surfaces, analogous interactions cause the motion of the system to be dominated by friction. However, as the size of rotators increases and frictional effects are minimized, inertial effects may become important, and some theoretical literature has addressed this topic.[79−83] Experimental efforts, especially in solids where a protected rotor might rotate in void spaces, unhindered by the overall crystal environment,[84,85] may ultimately probe inertial effects.[86−89]

3.1.2. Friction in Molecular Systems[90]

The final two terms in eq 1 reflect the interaction of the single angular degree of freedom of the rotator with the thermal bath. As mentioned above, the thermal bath includes both internal and external degrees of freedom such as motion of the atoms in the rotator, the atoms in the stator, if present, and the atoms in the surrounding medium (solution, surface, or solid). The explicit stochastic interaction with the bath can be described as torque $\tau(t)$ that varies rapidly in time and is irregular in amplitude. In equilibrium, the average value of $\tau(t)$ is zero. However, if the rotor (due to some external force) is exhibiting directed motion, with an average angular velocity over time $\langle d\theta/dt\rangle \neq 0$, and then this external force is removed, the effect of the thermal bath should be to return $\langle d\theta/dt\rangle$ to zero over some time. This observation would indicate that perhaps $\tau(t)$ can be subdivided into two terms: a rapidly varying part, which has a mean value of zero, and a slowly varying part, which is a function of $d\theta/dt$.

Following this approach, the former term is identified with stochastic torque ξ in eq 1. Its magnitude and sign are purely random, independent of θ or $d\theta/dt$, and it has an average value of zero over the relaxation time of the system. The more slowly varying part of $\tau(t)$ returns the system to equilibrium when conditions change and is associated with the frictional term. Because the specific functional form of the interaction with the thermal bath is unknown, frictional torque is derived by making an expansion of $\tau(t)$ in terms of angular velocity, $d\theta/dt$. The zeroth order term in this expansion, or the value of the function when the angular velocity is zero, is expected to be zero, as discussed above. However, the first-order term in the expansion yields the $-\eta\, d\theta/dt$ term in eq 1, where the minus sign reflects the tendency to reduce the angular velocity. If we assume that the system is only slightly removed from equilibrium, then we can estimate the slowly varying portion of $\tau(t)$ as this first term, obtaining eq 1.

In solid rotor systems, the effect of friction can be thought of as loss of energy from the rotational mode that is being driven by a driving force (discussed in section 3.2.2) to other modes within the rotor, within the stator, or within the larger system, via vibrations.[91,92] Thus, the driving field must continuously provide energy in order to keep the rotor rotating against the thermal motion of the atoms within the structure. This is a very different picture than the inertia-limited rotor discussed in section 3.1.1. In molecular systems, the so-called friction constant, η, is often a function of frequency.[91,92] This result is not surprising, since molecular vibrations have characteristic frequencies and are not expected to all respond similarly to excitations on varying time scales.

For rotating molecules in solution, Stokes' result for friction in a viscous medium can be utilized to establish a functional form for the friction constant η. For a macroscopic spherical rotating object in solution of viscosity β, the friction constant can be written in terms of the measurable quantities of the system

$$\eta = 8\pi\beta a^3 \tag{3}$$

where a is the radius of the sphere.[93] As can be seen from eq 3, as the size of the object or the viscosity of the solution increases, friction grows. While this model, derived in the hydrodynamic limit where the rotating object is larger than the molecules in the solution,[94] is widely used in situations where the molecule as a whole is rotating, even for larger molecules, its utility can be limited.[95−97] Thus, eq 3 serves simply as an illustrative example of the quantitative effects of friction and is not necessarily applicable to the rotors described herein.

3.1.3. The Fluctuation–Dissipation Theorem

With a slightly more detailed analysis, a correlation between the stochastic term, $\xi(T,t)$, and the friction constant can be derived. In particular, the fluctuation−dissipation theorem states[98,99]

$$\eta = \frac{1}{kT}\int_0^\infty \langle \xi(t_0)\, \xi(t_0+t)\rangle\, dt \tag{4}$$

Equation 4 links characteristics of the equilibrium random fluctuations with the friction exhibited when the system is perturbed from equilibrium. The general form of this result was derived by Callen and Welton[100,101] and can be qualitatively understood as follows:[102] Let us set external torque due to V_{net} in eq 1 to zero and examine the system as it is affected by the thermal bath only. If we also neglect the stochastic torque term, the resulting equation for $d\theta/dt$ has a solution $d\theta/dt = (d\theta/dt)_0 \exp(-\eta t/I)$, where $(d\theta/dt)_0$ is the value at $t = 0$. At long times, the angular velocity goes monotonically to zero. However, this result is inconsistent with the equipartition theorem, according to which $\langle (d\theta/dt)^2\rangle = kT/I$ for a one-dimensional system in the absence of external torque.[103] This difficulty is the result of having

neglected the stochastic term. With its inclusion, we find[104]

$$\frac{d\theta}{dt} = \left(\frac{d\theta}{dt}\right)_0 \exp(-\eta t/I) + \int_0^t dt' \exp(-\eta(t-t')/I)\ \xi(t)/I \quad (5)$$

where the second term reflects the integral over time of the angular acceleration due to stochastic torque.

If we use this expression to calculate $\langle(d\theta/dt)^2\rangle$, the square of the first term in eq 5 vanishes at sufficient times due to the decaying exponential. Similarly, the cross-terms have an integral of $\xi(t)$ over a finite time and thus go to zero due to the random nature of $\xi(t)$. However, the square of the final term is second order in $\xi(t)$: it depends on a correlation between ξ at some time t_0 and ξ at time $(t_0 + t)$. If the product $\xi(t_0)$ $\xi(t_0+t)$ is identically zero, equipartition cannot be satisfied. Conversely, for a significant time difference, we expect this correlation to be zero. This is resolved by assuming a correlation function $\langle\xi(t_0)\ \xi(t_0+t)\rangle = 2B\delta(t)$,[104] where the δ function ensures that the correlation is zero for any significant time and B is related to the magnitude of the fluctuating torque. Using this expression, we obtain $\langle(d\theta/dt)^2\rangle = B/\eta I$ at long times. Equating this with the equipartition result yields eq 4.

The friction constant that has been evaluated for molecular rotors according to a definition that was inspired by a simple phenomenological model was found to be a function of frequency,[91,92] indicating that linear response theory is not sufficient. More sophisticated phenomenological models that treat the frequency dependence of η explicitly would probably admit the approximation of linearly responding environment.

The fluctuation−dissipation theorem can be described as the equivalence between the energy removed by friction (dissipated) from the system (the rotor in our case) and the fluctuations of the bath. These fluctuations represent the mechanism by which the rotor is returned to equilibrium when a driving force is removed and by which a steady state is established in the presence of an accelerating force (see, for instance, the discussion in section 3.2.1.2).

3.1.4. Other Energies in the System

The potential energy V_{net} is the sum of all other internal and external energies in the system. Energies of particular importance in this review are the torsional potential, the interaction energy between a dipole and an externally applied field, and dipole−dipole interaction energies.

The internal torsional potential is defined for rotor−stator systems as the potential energy versus angle for turning the rotator about its axis in the absence of external fields. It reflects both interactions between the rotator and the stator and the nature of the axle. Internal torsional potentials are often modeled as sinusoidal functions with n potential minima and a characteristic barrier height, W.[105]

The number of potential minima reflects the symmetry of the system. For instance, azimuthal rotors with threefold rotators, moving against a threefold stand, will generally have three potential minima at locations where the rotor is staggered with respect to the stator. The barriers, or the peaks in the potential energy curve, occur when the rotator and stator are eclipsed. Planar systems, such as those with significant π bonding or other conjugation along the rotational axis, will often have twofold minima. Systems in which the order of the symmetry axis of the rotator is not matched with that of the stator (one is not an integer multiple of the other) will have a multiplicative number of minima. For instance, a fivefold rotator moving against a threefold stator yields fifteen wells. As the number of potential wells increases, the barrier height is usually suppressed, since no purely staggered orientation is possible and the rotator cannot orient itself in a way that significantly reduces interactions with the stator. The energy difference between a "well" and a "barrier" is reduced, effectively decreasing the barrier height, W.

As mentioned in section 3.1, the barrier height amplitude is also a function of the nature of the axle.[106] For instance, a single-bond axis is normally associated with a barrier to rotation in the range of a few kilocalories per mole. Part of this effect is the short length of the σ bond, which leads to significant interactions between rotor and stator. Rotation about triple bonds, in particular acetylene linkages, yields intrinsic barriers that are calculated to be only a few hundred calories per mole.[107,108] Systems where metal atoms act as an axis can exhibit a wide range of barrier heights.

Internal potentials are by definition characteristic of the molecule alone and are generally measured or calculated in the gas phase. Interactions between the rotors and a solution or surface are perturbations to this intrinsic potential. However, in the solid case, the distinction between rotor, stator, and environment can be blurred and an internal potential may refer to the energy surface the rotor experiences in the ordered solid. Given this, and for simplicity, we will generally use the term rotational potential (and the variable W) to be the extrinsic value, reflecting the true potential surface that the molecule experiences due to both intrinsic and environmental influences. Usually, the dominant portion of this rotational potential is the intrinsic torsional potential of the molecule.

A second important energy included in V_{net} is the interaction between a driving field and the rotator. In the discussion below, we will focus on a particularly clear example, the interaction of a permanent electric dipole with an applied electric field. However, the driving interaction energy, U, can be the result of any driving field, such as a stream of atoms or viscous fluid flow. Other driving mechanisms, such as manipulated chemical reactions or electronic excitation with light, rely on modifications to the other characteristic energies in the system, particularly the internal torsional potential, to achieve directed motion. A more detailed discussion of driving fields is provided in section 3.2.2.

Finally, the interaction energy between rotators must also be included in V_{net}. As discussed in section 3.3, rotator−rotator effects can be steric or field-

mediated. As an example of a field-mediated interaction, a pair of dipolar rotators has an interaction energy, U_i, of

$$U_i = \frac{1}{4\pi}\left[\frac{\boldsymbol{\mu}_1\cdot\boldsymbol{\mu}_2}{\mathbf{r}^3} - \frac{3(\boldsymbol{\mu}_1\cdot\mathbf{r})(\boldsymbol{\mu}_2\cdot\mathbf{r})}{\mathbf{r}^5}\right] \quad (6)$$

where $\boldsymbol{\mu}_{1(2)}$ is the dipole moment vector for the first (second) dipole and $\mathbf{r}$ is the position vector between the dipoles.[109,110] The $\mathbf{r}^{-3}$ dependence in eq 6 emphasizes nearest neighbor interactions, but generally, longer range interactions are also important. In principle, the interaction energy of an individual rotator could depend on the relative orientation of every other rotator in the collection. Parametrizing this sort of physical situation into a system with one degree of freedom, as would be described by eq 1, is challenging, and approaches beyond our simple description must be utilized (section 3.3). For a collection of coglike rotators, short range sterics will dominate the motion of the rotator, and this type of interaction can sometimes be described by a torsional potential where the relative angle between neighboring rotators is the important degree of freedom. While we generally consider steric effects to be short range, a body of work on cyanide and other ions in crystals has shown coupling between ion orientation and local strain fields, indicating that the ions may interact via the strain field.[111] This type of interaction would be considered field-mediated in our picture (section 3.3).

3.2. Rotor Behavior in Non-interacting Systems

For mutually non-interacting rotors, rotor behavior is determined by interplay between four important quantities: kT, the thermal energy; W, the magnitude of the rotational potential; U, the interaction energy between the applied driving field and the rotor; $\eta d\theta/dt$, torque due to friction.

Within the present context, we divide rotor behavior into two fundamental categories distinguished by the cause of the dominant motion. In the first, driven motion, the driving field is the cause of the rotation and random thermal effects and friction oppose this rotation. In the second case, random motion, reorientations are due to random thermal effects and only the net orientation is influenced by the other energy terms. By net orientation we mean either the time average (the orientation of one rotator sampled over many times) or, equivalently, the ensemble average (the net orientation of a collection of rotators, that is, the sum of their individual orientations) at a single time. Otherwise stated, the system is ergodic.

Thus, the organization of section 3.2 is as follows. In section 3.2.1, we discuss driven systems, focusing particularly on the coupling of a dipolar rotator and a rotating electric field. Three regimes of response to a driving field are identified: synchronous motion, asynchronous motion, and random driven motion. In section 3.2.2, this discussion is extended to other driving forces. Random motion is then taken up in section 3.2.3. Here, two cases are delineated: Brownian motion, where the system is essentially unconstrained by potential energy surfaces and exhibits purely random motion, and hindered rotation, where the rotor is strongly constrained by the potential energy surface and navigates on that surface by utilizing thermal energy.

Within the discussion of hindered rotation, we will make a brief mention of systems that gain unidirectional motion from thermal fluctuations in a nonequilibrium state. These so-called Brownian motors or thermal ratchets have been extensively reviewed elsewhere.[112,113]

3.2.1. Driven Motion

In the simplest case of driven motion, the interaction energy between the rotator and the driving field is the dominant energy in the system. Consider the specific example of a dipolar rotor interacting with an electric field that is static in magnitude and direction. In this case $U = -\boldsymbol{\mu}\cdot\boldsymbol{E}$, where E is the amplitude of the electric field and the electric dipole has its lowest energy when aligned along the field direction. We specifically assume that the torsional potential of the rotator (W) is small. This means that the energy versus angle for the rotator is dominated by the interaction with the field, given by $U = -\mu E \cos\theta$, where we have placed the electric field direction at $\theta = 0$. This "driving potential" has only one minimum, and thus, the rotator stays more or less aligned with the field. A nonzero thermal energy causes the rotator to oscillate about this position. If the direction of the electric field is altered, say to $\pi/4$, the rotator will respond over some time determined by frictional torque in the system but will ultimately realign with the field. Thus, there is a strong correlation between the orientation of the rotator and the driving field. Furthermore, as we shall see below, the dynamics of the rotator is determined by interactions with the electric field, which places this example in the regime of driven motion. However, with a static electric field, we observe no rotation of the rotor: what is required is an electric field which itself rotates.

Because of its simplicity, it is this picture[91,92] that we shall elaborate upon below. After this illustrative example, we return to the more general discussion in section 3.2.2. We define the frequency at which the electric field direction rotates, ω. If we wish to understand the efficiency of the driving motion, the important variable is the angle between the dipole moment of the rotator (described by $\theta(t)$) and the angle describing the direction of the electric field, which goes as ωt. Thus, the lag angle, $\alpha(t) = \omega t - \theta(t)$, determines the position of the rotor in the rotating field coordinate system. As in the static field case, generally when the rate of rotation is slow and/or the magnitude of the electric field is large, the rotator follows the field. As discussed below, at high frequencies, frictional effects become important and the driving motion is degraded. Similarly, at low field strengths, the thermal energy kT or the magnitude of the torsional potential W become comparable with the interaction energy U and the one-to-one correlation between the rotator and the orientation of the electric field is lost.

Within this picture, we identify three somewhat arbitrary but useful subsets of rotor behavior, delin-

eated by the efficiency with which the driving field determines the position of the rotor at any given time. Synchronous motion occurs when the driving interaction energy is significantly larger than any other energy term in the system. Here, the rotor position is well correlated with the driving field, as in our simple example above with a static field. The asynchronous regime encompasses driven motion that is compromised by drag torque due to friction, the presence of a non-negligible rotational potential, or thermally activated hopping. Despite these loss mechanisms, energy from the driving field still results in directed motion of the rotor and a correlation exists between the position of the driving field and the rotator orientation. As the relative size of the interaction driving energy decreases further, the rotor enters the random driven regime. Here, the knowledge of the position of the driving field has no predictive power in determining the orientation of the rotator at any given time. However, over many cycles, the result of this erratic response is still a rotor more likely to turn in the direction of the rotating electric field than against it. In other words, energy is still being coupled into the rotor motion from the driving field.

3.2.1.1. Synchronous Motion. In synchronous motion ($U \gg kT$ and W, and $\partial U/\partial\theta \geq \eta \mathrm{d}\theta/\mathrm{d}t$), the interaction energy with the driving field, U, is the dominant energy term in the system. In particular, the thermal energy kT and any intrinsic potential W are small compared to U and the torque due to U is able to overcome the torque of friction.

We first set $kT = W = \eta = 0$. Using $U = -\mu E \cos\theta$ and the definition of α above, eq 1 transforms to

$$I\frac{\mathrm{d}^2\alpha}{\mathrm{d}t^2} = -\frac{\partial U}{\partial \alpha} = -\mu E \sin\alpha \approx -\mu E\alpha \qquad (7)$$

where the last equivalence applies for small α. This is the equation of a harmonic oscillator with a characteristic frequency of $(\mu E/I)^{1/2}$, where I is the moment of inertia of the rotator.

Thus, in analogy with the static case, the driving field creates a potential well in which the rotor resides. For a nonzero thermal energy ($T > 0$), the rotator will execute librational harmonic motion within this well while the well and rotator turn with the field. The nonlibrational unidirectional motion of the rotator is purely synchronous, with the rotor executing one and only one turn for each electric field period. The lag angle, α, oscillates about zero, and thus, for N turns, the average lag per turn, $a = \alpha_{tot}/2\pi N$, is zero.[92]

3.2.1.2. Steady-State Motion. Next, we consider a case in which the driving force is less dominant, $U > kT$ and W, and $\partial U/\partial\theta \approx \eta \mathrm{d}\theta/\mathrm{d}t$. We first address the effect of friction while leaving kT and W negligibly small. In this case, eq 1 can be solved for a steady-state solution where net torque on the rotator is zero. In this case, torque due to friction is compensated by torque due to the driving field:

$$\mu E \sin\alpha = \omega\eta \qquad (8)$$

Here we have assumed that $\mathrm{d}\theta/\mathrm{d}t = \omega$ or that the rotator is rotating at the same frequency as the field. In this case, α is a constant. In fact, eq 8 is a constraint on the conditions under which this can occur. As the frequency of motion and, hence, frictional torque increases, the lag angle grows and the driving field exerts more and more torque on the rotor until, at $\alpha = \pi/2$, the driving torque is maximized. Thus, steady-state motion occurs for $\mathrm{d}\theta/\mathrm{d}t = \omega$ and α_0, the constant lag angle, less than $\pi/2$. For a given field amplitude and frequency, α_0 is given by

$$\sin\alpha_0 = \frac{\omega\eta}{\mu E} \qquad (9)$$

By setting $\sin\alpha_0 = 1$, eq 9 can be solved for the minimum field required to obtain synchronous motion for a given frequency, ω.

For model molecular rotors, Michl and co-workers found from molecular dynamics simulations that the friction constant $\eta = \eta(\omega)$ was an increasing function of frequency.[91,92] This results in a frictional torque term that increases as ω^γ, where $\gamma > 1$. Thus, the driving field amplitude necessary to obtain steady-state motion as given in eq 8 may increase dramatically as the frequency increases.

In the energy picture, the driving field has created a potential with minima at $\alpha_0 \pm 2\pi$ and a decreasing slope with increasing α due to the friction term (Figure 2). Now we return random thermal motion to the system. As discussed in the previous section, one consequence is the thermal libration of the rotator within a potential well. Furthermore, as kT increases, the thermal oscillations within a well lead to random thermal jumps, resulting in the rotor occasionally skipping a turn ahead or falling a turn behind the electric field (jumping from one minimum to the next).[91] Thus, the rotor exhibits three types of motion within this "tilted washboard" potential (Figure 2): the dominant synchronous following of the applied driving field ($\Delta\alpha = 0$), thermal librations within the potential well (small $\Delta\alpha$), and thermally activated hops between potential wells ($\Delta\alpha = 2\pi$).

This mechanism of reorientation by thermally activated hopping in the presence of a rotational potential is equivalent to the rotor response in the hindered rotor case, which is discussed in detail in

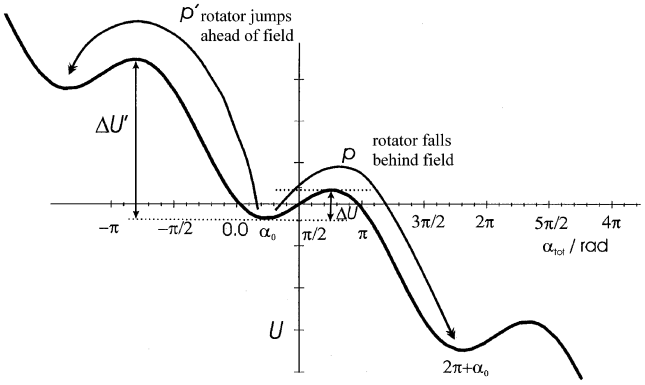

Figure 2. "Tilted washboard" potential of an electric field-driven rotor in a rotating coordinate system. The minima at α_0 are given by eq 8. ΔU ($\Delta U'$) and $\rho(\rho')$ represent the barrier to thermally activated hopping behind (ahead) of the rotating field.

section 3.2.2.2. The difference lies in the origin of the potential. Here, the driving field creates the potential minimum and the thermal effects decrease the efficiency of the driven motion. At $T = 0$, the rotor would rotate perfectly with the field. In the hindered case, there is no dominant unidirectional motion of the rotator, and at $T = 0$, the rotor would be static. The only motion is due to thermal effects, and thermally activated hopping enables the rotor to turn despite the presence of a permanent torsional potential due to its own structure.

Finally, eqs 8 and 9 can be modified for the case where the intrinsic potential, W, is nonzero.[92] It is common to approximate the intrinsic potential by a cosine function, such as

$$V = (W/2)\cos(n\theta) \tag{10}$$

where n is the number of potential wells and a potential maximum has been placed at $\theta = 0$.[105] If the intrinsic torsional potential is included, a third term enters in the steady-state version of eq 1, and eq 8 becomes

$$\mu E \sin\alpha = \frac{\partial V}{\partial \theta} + \omega\eta \tag{11}$$

Because the torsional potential and the induced potential due to the driving field are unlikely to coincide, the requirement for achievement of steady state must hold for all points on the intrinsic potential curve. This indicates that eq 11 must be satisfied for the maximum slope in the torsional potential and leads to the condition

$$\sin\alpha_0 = (\omega\eta + Wn/2)/\mu E \tag{12}$$

Thus, the driving field must overcome both frictional torque and the effect of the intrinsic potential in order to establish synchronous motion. In particular, the driving field must be able to override the intrinsic potential such that new minima correlated to the field orientation are established in place of those dictated by the intrinsic potential, which have an arbitrary orientation with respect to the driving field direction.

3.2.1.3. Distinguishing Synchronous and Asynchronous Motion. Solving eq 9 or 12 for $\sin\alpha_0 = 1$ yields the minimum E field required to produce synchronous motion when random thermal fluctuations are absent. (Asynchronous motion is not defined when $T = 0$: either the rotor moves perfectly with the field at a constant α or it does not rotate at all.)[91,92] For a particular rotor studied, Michl and co-workers[91] found that this field was insufficient to achieve even significant asynchronous rotation at nonzero temperature. The field needed for synchronous rotation is even larger, about twice that needed for asynchronous rotation. Let us return to the tilted washboard potential of Figure 2 and the three mechanisms of motion: synchronous turning, libration about a potential minimum, and thermally activated hopping. Given these modes of motion, the efficiency of the driving can be quantified by the average lag per turn. If, after N turns, the final cumulative lag angle is α_{tot}, then $a = \alpha_{tot}/2\pi N$. Michl and co-workers distinguish synchronous and asynchronous rotation via this "average lag" parameter.[92] In particular, if $0 \le a \le 1/e$, the motion is said to be synchronous. Asynchronous rotation is characterized by values $a < 1$.

To summarize previous statements, in synchronous rotation, the dominant motion is rotation with the applied field. For nonzero friction, the rotator oscillates about a nonzero average lag angle, α_0. Only occasionally do thermally activated hops cause the rotor to skip or jump a turn. Synchronous motion is also possible in the presence of a nonzero torsional potential W, but it requires a larger driving field at a given frequency. The loss mechanism introduced here occurs as the driving well moves through the noncoincident wells of the internal torsional potential. If the rotor is temporarily localized in an internal potential well, the lag angle for that turn increases. Nevertheless, during most turns, the lag angle is close to α_0 and the rotor generally follows the field.

In the asynchronous regime, the rotor does not follow the field perfectly during most rotations, and $\langle d\theta/dt\rangle$ of the rotor can differ significantly from ω. The thermally activated mechanisms which are minimized in the synchronous regime are significant here because kT, $\eta\, d\theta/dt$, and W are no longer negligible. As illustrated in Figure 2, because the barrier to slip behind the field is reduced by the friction term, thermally activated hops that allow the rotor to skip a turn are exponentially more likely than hops that move the rotor ahead of the field (see section 3.2.1.2). As the friction term increases, the washboard potential becomes more tilted, causing barrier heights to decrease and the discrepancy between forward and reverse barriers to increase, allowing for increasingly more rotor slipping. As discussed above, when $W/\mu E$ increases, the rotor may occasionally become trapped in an intrinsic well until a thermally activated event allows it to reenter the minimum created by the driving field. Thus, at low temperatures, the driving force fights the rotational potential. At high temperatures, thermally activated hops decrease the driving efficiency.

As we further increase each of the rotation-opposing terms (kT, $\eta\, d\theta/dt$, and W), we observe rotor behavior that changes from the driven to the random driven regime.

3.2.1.4. Subharmonic Motion in the Asynchronous Regime. A recent computational result has shown interesting subharmonic behavior for a dipolar rotor driven by an oscillating electric field.[114,115] In this case, as the amplitude of the field E is increased, the rotor motion makes a transition from asynchronous to synchronous motion, as expected. However, at high frequencies, rather than a smooth decrease in the average lag per turn a, a distinct plateau at $a = 1/2$ was observed. In a narrow range of field strength and frequency, successful turns with the field alternated with skips where the rotor did not turn, and a qualitative understanding of the origin of this alternation was reached. Such behavior is reminiscent of a phase-locking condition where an innate frequency in the system, f, is "locked" with an applied oscillation, f', where $nf' = mf$ and n and m

are integers. Ultimately, such a conversion of field frequency to rotation frequency suggests the possibility of a single-molecule rotary parametric oscillator.

3.2.1.5. Random Driven Motion. As the friction force is increased further, $U > kT$ and W, and $\partial U/\partial\theta < \eta\ \mathrm{d}\theta/\mathrm{d}t$, torque due to the driving field is insufficient to overcome the frictional response. The lag angle without thermal fluctuations, α_0, is now greater than $\pi/2$, and the response of the rotor differs for each turn of the driving field. Here the knowledge of the position of the driving field has no predictive power in determining the orientation of the rotor. However, over many cycles, the result of this erratic response is still a rotor more likely to turn in the direction of the rotating electric field than against it (a, the average lag per turn, is slightly less than one). Energy is still being coupled into the rotor motion, and the response is driven, although extremely inefficient. For $W = 0$, the average angular velocity, $\langle \mathrm{d}\theta/\mathrm{d}t \rangle$, in this case can be calculated by methods of statistical mechanics:[116]

$$\left\langle \frac{\mathrm{d}\theta}{\mathrm{d}t} \right\rangle = \frac{\omega/2}{1 + (\eta\omega/kT)^2}\left(\frac{\mu E}{kT}\right)^2 \approx \frac{\omega}{2}\left(\frac{\mu E}{\eta\omega}\right)^2 \qquad (13)$$

where the approximate equality holds for $\eta\omega/kT \gg 1$. This expression is second order in $\mu E/\eta\omega$, which is less than one, reflecting the small influence of the driving field on the dynamics of the system. As the driving frequency increases and frictional effects grow, the average angular velocity decreases in direct proportion to the frequency of the field. Thus, the effect of the field decreases at higher frequencies.

3.2.2. Driving Fields

In the above discussion, we have focused on one illustrative scheme for driving torsional molecular motion, based on the interaction of an oscillating electric field with a dipole in the rotator. Here we discuss alternative approaches. Generally, these rotor driving schemes can be divided into three main categories: (i) coupling between a rotator's induced or permanent dipole moment and an oscillating electric field, (ii) chemical reaction or change of the electronic state of the rotor, and (iii) mechanical coupling between the flow of a fluid and the rotator, mediated by molecular collisions. In the discussion below, we give a few examples of each type as illustrations. Many more appear in the subsequent sections.

For driven motion, the energy due to the driving field must overcome any thermal effects, intrinsic barriers in the rotational potential, and dissipation by friction. Below, this is accomplished in two ways. In the first case, as in the discussion above, the energy terms are steady in time (constant driving excitation). A second approach is to create a cycle of excitation events during which the energy terms change. In these cases, individual events in the series may be thermally activated, but for at least one step in the cycle, a driving field is needed. Examples of both approaches appear below.

(i) As described above, a rotating electric field interacting with a permanent dipole associated with the rotator can provide driven motion. This coupling could also be utilized for a rotator with no permanent dipole but with a strongly anisotropic molecular polarizability. The driving field would then both polarize the molecule and interact with the resulting dipole.

Rotating electric fields have been realized by utilizing phase-shifted sinusoidal fields applied to orthogonal electrodes.[117] Another physical realization of a rotating electric field is a rotating linearly polarized laser field.[86,118] In experiments with this "optical centrifuge", light of a nonresonant frequency was used as a controllable source of electric field that interacted with an induced molecular dipole moment (in contrast, in section ii, resonant light is used to excite the rotor molecule to another electronic state).

Modifying the rotational potential by the application of a spatially static, linearly polarized pulse has also been proposed in a theoretical investigation as a mechanism for achieving driven motion in a chiral molecule.[119,120] Here, the unmodified potential is asymmetric and the electric field is used to modulate a particular barrier, allowing the rotor to rotate in the direction of decreasing energy. The authors note that this is only predicted to occur when the laser pulse intensity is greater than a threshold value, indicating that the driving field energy has to overcome the torsional potential for unidirectional motion to occur. If the pulse energy is too low, the rotor moves in both directions, which is consistent with the discussion given above.

(ii) Another approach is to take advantage of the electronic states of the rotor molecules, which generally have different torsional potential energy surfaces. One proposed scheme utilizes this fact in combination with manipulation of librational motion.[121] Here, a femtosecond pulse in the infrared region of the electromagnetic spectrum targets the bond which forms the axle of the rotor, generating librational motion within a minimum of a two-well internal potential for the molecule in its electronic ground state. The torsional angular momentum generated is then calculated to be sufficient to enable the rotator to overcome the different torsional potential in the excited state when a second pulse in the ultraviolet excites the molecule. The induced rotation is predicted to be unidirectional until frictional and thermal effects (not discussed explicitly) slow the motion of the rotator or the system returns to its ground state.

This work builds upon earlier schemes, experimentally realized by Feringa and co-workers, which are discussed at length in section 5.7.1. In one example, the rotator is initially rotated 180° by a light-induced *trans*−*cis* isomerization.[122] The direction of rotation (clockwise or counterclockwise) is determined by steric effects at two stereogenic centers in the molecule. The system can then lower its energy (while remaining *cis*) by inverting these stereogenic centers (which reverses the helicity of the molecule). This relaxation is thermally activated and irreversible, and thus, the relaxation to the lowest energy product is accelerated by raising the temperature. Once the helicity inversion is complete, light is again utilized

to drive the *cis*−*trans* conversion and the steric effects, now reversed, force rotation in the same sense as the *trans*−*cis* step. After another thermally activated helicity inversion, the original configuration is recovered. Thus, by utilizing the stereogenic centers in the molecule and uniquely determining the helicity of the molecule at all times via thermal relaxation, unidirectional motion is achieved.

(iii) A third, and less well explored, category is to use of a stream of gaseous atoms or molecules or a flowing liquid to impart angular momentum to a molecular rotor. Such an approach is restricted to surface-mounted and solid-phase rotors, as the translational motion of the rotor should be minimized compared to the translational motion of the driving atoms. Schematically, the idea is straightforward, and one can immediately conjure ideas of a water wheel or a windmill. We begin with a directed stream of atoms of average velocity v interacting with a rotator that consists of several equally spaced blades. If the rotor cannot move along the direction of the fluid flow and the atoms are significantly smaller than the blades of the rotator, each atom that strikes a blade imparts momentum to the much more massive rotator. The driving torque then is the sum of the momenta per atom, mv, times the distance from the axis, d, summed over all the atoms arriving at the blade in a time interval, Δt, divided by Δt. The geometry of the rotator must be considered in order to induce rotational torque rather than a net linear force on the molecule in the direction of the particle flow. One way to accomplish this is to use a chiral rotator and to flow the fluid in the direction of the axle.[116,123] Such propeller-like structures have been designed and synthesized (see section 5.1) but have not yet been mounted on a substrate, such as a highly transparent grid or a porous membrane through which the fluid can pass. However, molecular dynamics on such azimuthal rotors suggest[123] that rotation will be induced (see section 7.2).

Alternatively, if the flow velocity parallel to the surface varies with the distance from the surface (as expected from the no-slip condition at a solid surface), an achiral altitudinal rotor could be utilized. In this case, the rotational axis might be perpendicular to the flow direction (in analogy to a water wheel), such that the blades furthest from the surface receive more momentum from the collisions than those closer to the surface. An anemometer or s-shaped geometry for azimuthal rotors mounted on an impenetrable surface is also possible. Here the blades tend to be equidistant from the surface but the blade−fluid interaction between opposite blades differs, allowing net torque on the rotator.

As a concluding note, we remark on the necessary and sufficient conditions for unidirectional motion, given the context of the examples above. When a rotor system is in thermal equilibrium, the second law of thermodynamics denies the possibility of unidirectional motion.[113] As discussed above, energy has to be coupled into the system in order to create such motion. Once the energy source is removed, thermal losses will degrade the motion. When the energy source is persistent, a steady state is established where the energy coupled into the system equals the sum of the kinetic energy gained by the rotor and the energy lost to dissipation. A necessary condition for unidirectional motion is that the system be out of equilibrium.

If the driving excitation is strong enough, no other restrictions need to be placed on the nature of the rotor; in particular, it need not be chiral. Interestingly, the driving force creates an asymmetric potential (the tilted washboard in section 3.2.1.2; Figure 2). Such tilted asymmetric potentials are also seen in molecular ratchet systems and in chiral molecules.[119] However, for a system in equilibrium, an asymmetrical potential is not sufficient to produce directed motion. As we shall see below, a rotor in a two-well asymmetric potential will simply execute thermally activated hops back and forth over the lowest barrier between the two wells. We have already discussed one mechanism for getting the system out of equilibrium (driving fields) and will return to this issue in section 3.2.3. For the moment, we conclude that the presence of both an asymmetrical potential and an external perturbation that moves the system out of equilibrium appears to be a necessary condition to achieve unidirectional motion. These effects may be linked, as in the case of a driving field that simultaneously creates an asymmetrical potential and drives the system out of equilibrium, or they may be uncoupled.

3.2.3. Random Motion

Now we turn to the case of random rotor motion. In this regime, rotor reorientations are due to random thermal effects and only the average orientation (as defined in the opening paragraphs of section 3.2) is influenced by the other types of energy available to the system.[124] In contrast, in the driven case, a driving field is necessary for the particular driven motion to occur. Here, the motion of the rotor is essentially unchanged by application of the "driving" field. To clarify this point, imagine a large collection of non-interacting rotors arranged on a two-dimensional grid where motion can be stopped and a "snapshot" recorded showing the orientation of each rotator. If the rotors have no significant rotational potential W and no driving field U is applied, then each snapshot will show an average orientation over the system, $\langle\theta_{sys}\rangle$, of zero. For a system of dipolar rotors, $\langle\theta_{sys}\rangle = 0$ is equivalent to no net polarization. If a rotational potential is added, but the position of the potential minima of adjacent rotors is random, the result is unchanged. Now a driving field is applied. For both random and driven systems, a nonzero $\langle\theta_{sys}\rangle$ is observed. The rotors are more likely to point in the direction of the applied field than against it. The size of this induced polarization is dependent on the interplay of the interaction driving energy with the other energy terms in the problem as described in section 3.3.2 for driven systems and in the sections below for random systems. Thus, the static behavior does not distinguish between random and driven motion. It is the dynamics between the snapshots that determines this categorization. As we

shall see below, in the random collection, the method of reorientation and, to the first order, even the rate of reorientation of the rotor remain unaffected by the presence of the driving field.

We identify two important subsets of random rotor behavior. In the first, which we label random thermal motion or Brownian motion, the thermal energy kT is dominant. In the complete absence of any potential energy dependence on the angle of rotation, either due to intrinsic effects (W) or due to a driving field (U), the orientation of the rotor is random at any given time for a nonzero temperature. If the temperature were lowered to $T = 0$, the rotor would be found at any angle 0 to 2π with equal probability. We quantify the rotor's motion by examining the fluctuation about this zero value of $\langle\theta\rangle$. As discussed in sections 3.1.2 and 3.1.3, frictional effects are linked with thermal effects. Despite the lack of unidirectional motion, friction is still important in this system and the mean square fluctuation of the rotors is inversely related to the friction constant.

Hindered motion is the second subset we examine. In this case, the rotational potential dominates. As in the random thermal case, rotor reorientation is again driven by thermal fluctuations, which are manifest as thermally activated hops over the torsional barrier. Thus, the reorientation rate and even the ability of the rotor to turn at all are strongly dependent on the thermal energy, even though it is not the largest energy term in the system.

Finally, we turn to a very brief overview of potentially useful systems that might utilize random (bidirectional) rotor motion.

3.2.3.1. Random Thermal Motion. In the truly random case, $kT > U$, $\eta\, \mathrm{d}\theta/\mathrm{d}t$, and W, and $\langle\theta\rangle = 0$. By manipulating eq 1 for the case where $\partial V_{\mathrm{net}}/\partial\theta = 0$, ensemble averaging and applying equipartition, and then solving the resultant differential equation, an expression for the magnitude of the fluctuation in θ can be obtained,[125]

$$\langle {\theta_{\mathrm{net}}}^2 \rangle = \frac{2kT}{\eta}\left[t - \frac{I}{\eta}(1 - \mathrm{e}^{-\eta t/I})\right] \qquad (14)$$

where t is time. Here the rotor executes classical Brownian motion in one torsional dimension. At long times, $t \gg I/\eta$, eq 14 reduces to a random walk

$$\langle {\theta_{\mathrm{net}}}^2 \rangle = \frac{2kT}{\eta}t \qquad (15)$$

At very short times, the exponential in eq 14 can be expanded in the small quantity, $\eta t/I$, and the first nonzero term yields

$$\langle {\theta_{\mathrm{net}}}^2 \rangle = \frac{kT}{I}t^2 \qquad (16)$$

where the particle moves as though it had an angular velocity of $(kT/I)^{1/2}$.

For a small but nonzero driving field, a slight preference for orientation in the direction of the applied field is predicted. This is similar to the result for the random driven regime. However, in the random driven case, excessive friction prevents the rotor from following a rotating electric field. If the field were removed, the rotor would have very little rotation because the thermal energy could be quite small. Here, the rotor is always in motion due to the thermal energy. In the rotating electric field case, the average angular velocity $\langle \mathrm{d}\theta/\mathrm{d}t \rangle$ can be calculated from statistical mechanics using the result stated in eq 13, but in a different regime.[91,116]

$$\left\langle \frac{\mathrm{d}\theta}{\mathrm{d}t} \right\rangle = \frac{\omega/2}{1 + (\eta\omega/kT)^2}\left(\frac{\mu E}{kT}\right)^2 \approx \frac{\omega}{2}\left(\frac{\mu E}{kT}\right)^2 \qquad (17)$$

Here, ω and E have the usual meaning of the frequency and amplitude of the field, respectively, and the approximate equality holds for $\eta\omega/kT \ll 1$. Notice that this expression is second order in a small quantity, $\mu E/kT$. To zeroth and first order, $\langle \mathrm{d}\theta/\mathrm{d}t \rangle$ is unchanged by the presence of the field. For low frequencies where $\eta\omega/kT \ll 1$, the system is not limited by friction and $\langle \mathrm{d}\theta/\mathrm{d}t \rangle$ increases with increasing ω. However, the time-averaged value of the angular velocity is always much less than the frequency of the field, due to the $(\mu E/kT)^2$ term.

If the potential U provided by the driving field becomes significant, this random motion becomes increasingly more contained within the rotational well created by the field; that is, it becomes restricted to a smaller set of angles surrounding the potential minimum created by the driving field and $\langle \mathrm{d}\theta/\mathrm{d}t \rangle$ increases as shown in eq 17. Eventually, the thermal motion turns into librations within the well, combined with thermally activated hops ahead of or behind the field. This is the case discussed in section 3.2.1.2.

If the energy of the internal potential W becomes significant, the rotor is again localized to one or more potential minima due to the torsional potential. It librates within the wells and can reorient by hopping, as discussed in the next subsection.

3.2.3.2. Hindered Motion. When $W > U$, kT, and $\eta\mathrm{d}\theta/\mathrm{d}t$, the torsional potential is the dominant energy in the system, and the basic motion of the rotor consists of thermal librations within a well of the torsional potential coupled with occasional thermally activated hops between wells. Thermally activated hopping over the potential barrier is the only method of rotator reorientation. In this regime where $W \gg kT$, the probability of a thermal hop per unit time is proportional to $\exp(-W/kT)$.[126] At low temperatures, thermally activated hops are rare and the rotor rarely reorients. As the temperature increases, thermally activated hops are more common, and at a sufficiently high temperature, the rotor is always in motion and the rate of hopping is nonzero even at equilibrium. If the system is pushed out of equilibrium, hopping provides the only mechanism of relaxation which innately links the relaxation or response rate to the hopping rates. In particular, the relaxation rate, which is a single quantity for each rotor, reflects the interplay between hopping rates into and out of the various wells in the system.

We organize the remainder of the section as follows: First, we discuss the librational frequency. Then we turn to calculation of the relaxation rate, first addressing the case of a small driving signal

applied to a two-well system and finally discussing larger signals and multiple wells.

(*i*) *Librational Frequencies.* In the hindered regime, there are two important frequencies in the problem: the libration frequency of the rotor within the energy well and the relaxation rate (the inverse of the characteristic relaxation time) of the rotor. These scales are generally linked. In particular, the rate of thermally activated hopping is given by[126]

$$\text{rate} = \omega_0 \exp(-W/kT) \tag{18}$$

where ω_0 is an attempt frequency, which is approximately equal to the librational frequency.[127,128]

The librational frequency is often estimated by assuming a harmonic approximation for the small θ portion of a sinusoidal potential with n wells, such as that in eq 10

$$\frac{\mathrm{d}V}{\mathrm{d}\theta} \equiv -k\theta = -\frac{nW}{2}\sin n\theta \approx -\frac{n^2W}{2}\theta \tag{19}$$

where ω_0 is then given as

$$\omega_0 = \sqrt{\frac{k}{I}} = \sqrt{\frac{n^2W}{2I}} \tag{20}$$

and k is the torque constant.

In this treatment, the librational frequency is independent of the thermal energy and depends only on the nature of the torsional potential and the moment of inertia of the rotor. Characteristic libration frequencies for relatively small rotors are on the order of 10^{13} radians/s.[129]

(*ii*) *Response Rate of the Rotor.* The other important frequency, the relaxation rate, can be defined as $1/\tau$, where, for an observable quantity A with an initial nonequilibrium value of A_0 and an equilibrium value of A_s, the system relaxes as[130]

$$A(t) = A_s - (A_s - A_0)\exp(-t/\tau) \tag{21}$$

We begin our discussion by considering a collection of N non-interacting rotors, each possessing the same n-well torsional potential, and determine the equilibrium number of rotors residing in each well. A master equation approach provides a set of equations for the rate of change of N_i, the number of rotors per unit volume in well i:

$$\frac{\mathrm{d}N_i}{\mathrm{d}t} = \sum_j^n [N_j\Gamma_{ji} - N_i\Gamma_{ij}]_{j\neq i} \tag{22}$$

where Γ_{ij} is the transition rate from well i to well j.[131] The right-hand side of eq 22 is a sum of the flux into and out of well i via all the possible processes that can populate or depopulate it. As discussed above, the transition between wells is a result of thermally activated hops and the rates are in the form of eq 18. Therefore,

$$\Gamma_{ij} = \omega_0^i \exp\left(\frac{-W_{ij}}{kT}\right) \tag{23}$$

Here, ω_0^i is the libration frequency in well i and W_{ij} is the barrier which the rotor must overcome in order to hop from the i-th to the j-th well. The set of equations represented by eq 22 along with the conservation equation

$$\sum_i^n N_i = N \tag{24}$$

permit a solution for the system. If we wish to determine the average orientation of the rotor, we must solve eqs 22−24 in the steady-state case, where the rate of change of the N_i is zero. As stated in the opening paragraphs of section 3.2, this is the same as calculating the probability to find a single rotor in a given well or, equivalently, the average number of rotors in the collection residing in a particular well at a given instant.

(iii) Systems with Two Wells. For a two-well torsional potential, we find the expression

$$\overline{N_1}\Gamma_{12} = \overline{N_2}\Gamma_{21} \tag{25}$$

where the bar indicates the equilibrium value. If the wells have equal energies, the barrier surmounted in hopping from well one to well two is equal to that from well two to well one. Thus, the rotors are equally distributed in both wells and $\overline{N_1} = \overline{N_2} = N/2$. The relaxation rate of the system is given by solving eq 22 for the time-dependent case using eq 25, which yields

$$\frac{\mathrm{d}}{\mathrm{d}t}(N_1 - N_2) = -2\Gamma_{12}(N_1 - N_2) \tag{26}$$

where we have used $\Gamma_{12} = \Gamma_{21}$. This is a special case of a general relaxation equation, where the time rate change of a quantity, $A(t)$, is proportional to the distance from its equilibrium value, A_s.[132]

$$\tau\frac{\mathrm{d}A(t)}{\mathrm{d}t} = A_s - A(t) \tag{27}$$

Equation 21 is a solution to such a relaxation equation. Equation 26 fits this form with $(N_1 - N_2)_s = 0$, as expected for wells of equal energy, and $\tau = 2\Gamma_{12}$. Thus, in this case, the relaxation rate of the system is twice the hopping rate between wells.

If a small energy difference between the wells is now introduced such that the energy of well one is lowered by s and that of well two is raised by the same amount (Figure 3), the hopping rates transform to[131]

$$\Gamma_{12} = \omega_0^1 \exp\left[\frac{-(W+s)}{kT}\right] \approx \omega_0^1 \exp\left[\frac{-W}{kT}\right]\left(1 - \frac{s}{kT}\right) \tag{28}$$

and

$$\Gamma_{21} = \omega_0^2 \exp\left[\frac{-(W-s)}{kT}\right] \approx \omega_0^2 \exp\left[\frac{-W}{kT}\right]\left(1 + \frac{s}{kT}\right) \tag{29}$$

where W is the original value of the barrier and the

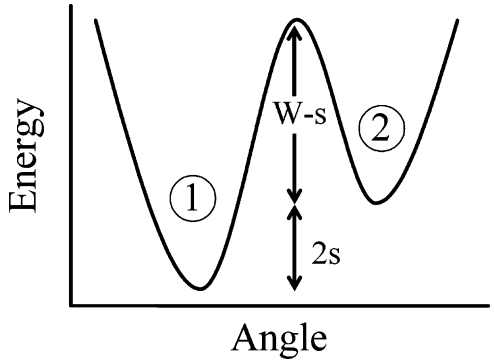

Figure 3. General asymmetrical potential with a lowest barrier height of $W - s$ and an energy difference between the wells of $2s$. Well one is on the left, and well two on the right. In the case of innate asymmetry, s', in addition to an asymmetry caused by the driving field, $2s = 2U + s'$.

last equivalency is for small s/kT. For $\omega_0^1 \cong \omega_0^2 = \omega_0$

$$\overline{N_1} - \overline{N_2} = N\frac{s}{kT} \tag{30}$$

or equivalently, the probability of finding the rotor in well i, P_i, is given as[131]

$$\overline{P_1} \equiv \frac{\overline{N_1}}{N} = \frac{1}{2}\left(1 + \frac{s}{kT}\right); \quad \overline{P_2} = \frac{1}{2}\left(1 - \frac{s}{kT}\right) \tag{31}$$

Equations 30 and 31 confirm that the rotor has a preference to sit in the lowest well, as expected from Maxwell−Boltzmann statistics. For small signals, the population difference is proportional to s.

Again, the relaxation time of the system can be determined by solving eq 22, and the resultant relaxation equation for $N_1 - N_2$ is

$$\frac{\mathrm{d}(N_1 - N_2)}{\mathrm{d}t} = -2\omega_0 \exp\left[\frac{-W}{kT}\right](N_1 - N_2) + 2\omega_0 \exp\left[\frac{-W}{kT}\right]\left[\frac{Ns}{kT}\right] \tag{32}$$

A comparison with eq 27 shows that

$$1/\tau = 2\omega_0 \exp\left[\frac{-W}{kT}\right] \tag{33}$$

Comparing eq 33 with the result obtained when $s = 0$ reveals that, to first order, the relaxation rate is unchanged by the introduction of s. This is consistent with the discussion in the introduction to section 3.2.3. The dynamics of the system is still dominated by the equilibrium thermally activated processes, even under the application of a field.

Physically, a difference in energy between the two wells can result from several causes. In the case where s results from small changes in the environment of each rotor, for instance, disorder due to attachment of a surface-mounted rotor to a rough substrate, s values will differ for each rotor. Averaging over the collection, the effect of the random distribution of values will cancel and no net polarization will be induced. For small s/kT, the relaxation rate of the rotor will also be unaffected.[133] In contrast, imagine each rotor sees an identical asymmetrical torsional potential, and the torsional potential of each rotor is aligned, for instance in a crystalline solid. Here, s will result in a net alignment of the rotors toward the preferred direction. Likewise, when the driving field creates the asymmetry, s can be associated with U, the coupling energy with the driving field. For instance, for dipolar rotors and an applied electric field, the energies of the wells generally aligned with the field are lowered and those of the wells pointing opposite to the field are raised. Thus, the system develops a net polarization pointing in the field direction. For a rotating electric field, this polarization will follow the field direction, provided that changes in the field orientation and magnitude are slow compared to the relaxation time of the system, τ, given by eq 28. However, it is important to remember that while the net polarization follows the field, any given rotor is only slightly more likely to point in the direction of the field than against it. The rotor is still in constant motion, flipping from well to well at the relaxation rate. The case of a dipolar rotor interacting with an electric field is discussed further in the following section.

(*iv*) *Stronger Fields and Saturation.* For clarity, we again take up the interaction of a dipolar rotor with an applied electric field and identify s with the interaction energy, $U = -\mu \cdot E$. Then the quantity $N_1 - N_2$ can be interpreted as proportional to the electric polarization. In light of the analysis in the previous paragraph and in contrast with the discussion of driven motion, it is most helpful here to focus on a static or very slowly changing electric field. For small U/kT, the net rotor alignment increases linearly in U/kT according to eq 30. As the thermal energy increases, the polarization is reduced as random thermal motion decreases the ability of the rotors to align with the field. As U/kT becomes significant, we expect the increase in polarization to slow, as each rotator is already generally pointing in the direction of the field. Such saturation is not taken into account by eq 30, as it was derived only for small U/kT. In the more general case, eq 30 transforms to[134]

$$\overline{N_1} - \overline{N_2} = N \tanh\left(\frac{U}{kT}\right) \tag{34}$$

such that, now, $N_1 - N_2 \rightarrow N$ as $U/kT \rightarrow \infty$. At small U/kT, eq 34 reduces to eq 30.

When U/kT is non-negligible, the time-dependent behavior of $N_1 - N_2$ given by eqs 22 and 23 becomes

$$\frac{2}{\tau[\exp(U/kT) + \exp(-U/kT)]}\frac{\mathrm{d}}{\mathrm{d}t}(N_1 - N_2) = \frac{N[\exp(U/kT) - \exp(-U/kT)]}{\exp(U/kT) + \exp(-U/kT)} - (N_1 - N_2) \tag{35}$$

where the first term on the right-hand side is the equilibrium value of $N_1 - N_2$ from eq 25, τ remains as given in eq 33, and $\omega_0^1 \approx \omega_0^2 = \omega_0$. This equation

fits the relaxation form of eq 27, with a relaxation time of τ' given by

$$1/\tau' = \frac{2}{\tau}[\exp(U/kT) + \exp(-U/kT)]^{-1} = (\Gamma_{12} + \Gamma_{21})^{-1} \approx (\Gamma_{21})^{-1} \quad (36)$$

Physically, the effect of eq 36 is that when the well asymmetry is significant enough to distinguish the rate of hopping into (Γ_{21}) and out of (Γ_{12}) the lowest well, the relaxation rate of the system is dominated by the fastest hopping rate, or the rate of hopping over the lowest barrier. This dominance is a function of the exponential dependence of the hopping rate on the barrier height and indicates that experimental results measuring the relaxation time reflect predominantly the lowest barrier in the system.

This result can also be obtained directly from eqs 22 and 24 by solving for the steady-state populations N_1 and N_2, assuming an arbitrary population distribution at time $t = 0$, which decays toward the equilibrium population with a time constant τ', and then using the time-dependent equations to obtain eq 36.

(v) Innate Asymmetry. As a final topic for the two-well case, we discuss the situation where the well asymmetry, $2s$, results from two causes. In particular, a permanent asymmetry s', for instance due to steric effects, may be associated with the system in addition to the induced well difference due to the driving field U (Figure 3). We return here to the linear response regime where U/kT is small and, for $s' = 0$, eq 30 is valid. For an s' of any size, where each rotor sees an identical asymmetrical torsional potential (for instance, rotors packed in a single crystal)[132]

$$\overline{N_1} - \overline{N_2} \approx N \tanh\left(\frac{s'}{2kT}\right) + N\frac{U}{kT}\cosh^{-2}\left(\frac{s'}{2kT}\right) \quad (37)$$

This is a second-order Taylor series expansion of the exact result in terms of the small quantity U/kT. The first term on the right reflects the innate alignment of the system due to the intrinsic asymmetry, which increases as kT decreases and is independent of the driving field. The second term describes rotor alignment due to the driving field, which is suppressed by the intrinsic asymmetry. As kT decreases, the $\cosh^{-2}$ term decreases the polarization in the direction of the driving field, since the rotors have less thermal energy to overcome the intrinsic well asymmetry and populate the higher well in order to follow the electric field. As kT increases, the effect of the innate asymmetry is reduced and the polarization due to the electric field is limited by random thermal motion of the rotor. For a system with randomly oriented rotors, the first term in eq 36 sums to zero over the rotor collection. Nevertheless, even for a random orientation of rotors, an innate asymmetry still affects the ability of the driving field to align the rotors and the second term remains. At low temperatures, the rotors fall into their lowest wells and do not respond to the field. At higher temperatures, the driving field must overcome random thermal motion.

(vi) Systems with $n > 2$ Wells. For systems with more than two wells, the geometry of the system is reflected in the maximum polarization due to the driving field. For the two-well case, we have assumed a one-dimensional scheme where the two wells are separated by 180° and the driving field points along a line between the two wells: the rotor is either parallel or antiparallel to the field. We now address the more general cases, for rotors with their axis aligned at an angle to the electric field; for randomly oriented rotors; and for rotors with more than two minima in their torsional potential. Again, we use the example of a dipolar rotor interacting with an electric driving field. Here the net alignment of the rotors can be measured as an electric polarization which is given by

$$P_e = \sum_i^n N_i \mu_i \quad (38)$$

for a system with n wells, where μ_i is the projection of the electric dipole $\boldsymbol{\mu}$ onto the electric field direction for well i.[135] Thus, for a two-well system aligned at an arbitrary angle φ to the electric field,

$$\overline{P_e} = (\overline{N_1} - \overline{N_2})\mu \cos\varphi = N \tanh\left(\frac{U\cos\varphi}{kT}\right)\mu\cos\varphi \quad (39)$$

where we have used the result from eq 34. For the case of small U/kT, eq 39 reduces to

$$\overline{P_e} = N\left(\frac{\mu E}{kT}\right)\mu\cos^2\varphi \quad (40)$$

where we have used $U = \mu E$. This result applies to two-well systems where all rotor axes are aligned and reflects the reduction of electric polarization as a result of the misalignment with the electric field.

For a random system where each rotor has a unique angle φ varying from 0 to 2π, the net polarization is

$$\overline{P_e} = \frac{1}{2\pi}\int_0^{2\pi} N\left(\frac{\mu E}{kT}\right)\mu\cos^2\varphi\, d\varphi = N\mu\left(\frac{\mu E}{2kT}\right) \quad (41)$$

Interestingly, the result shown in eq 41 is independent of the number of wells as long as the wells are equally spaced in angle. For instance, for a three-well system,

$$\overline{N_i} = \frac{(\Gamma_{ji}\Gamma_{ki} + \Gamma_{jk}\Gamma_{ki} + \Gamma_{kj}\Gamma_{ji})N}{\sum_{l=1}^{3}(\Gamma_{jl}\Gamma_{kl} + \Gamma_{jk}\Gamma_{kl} + \Gamma_{kj}\Gamma_{jl})} \quad (42)$$

where the subscript indices are independent ($i, l \neq j \neq k$).[136] Combining this result with the projection of the dipole for each well, μ_i, as in eq 38, yields the net polarization. Here the Γ_{ij} values are found from eq 23 using the effective barrier to rotation W_{ij}. The rotational potential in which the rotator moves is now the sum of the initial torsional potential and the contribution from coupling with the electric field. The effective barrier to rotation W_{ij} is obtained by adjust-

ing the initial barrier by the contribution from coupling with the electric field both at the top of the barrier between minima i and j as well as at the well i.[137] Assuming that the initial barriers were identical, that the initial well energies are degenerate, and that the attempt frequencies ω_0^i are similar, the polarization given by eqs 38 and 42 can be expanded as a Taylor series in the small quantity $\mu E/kT$. The first-order term then reduces to the last term in eq 41.

$$\overline{P_e} = \sum_{i=1}^{3} \overline{N_i \mu_i} \cong N\mu\left(\frac{\mu E}{2kT}\right) \tag{43}$$

In the limit of many wells, the barrier to rotation may be sufficiently low as to approximate the rotator as free to rotate in a plane. For an electric field lying in this plane, the average dipole moment, $\langle p_{mol} \rangle = P_e/N$, is given as[138]

$$\langle p_{mol} \rangle = \frac{\int d\phi\, \mu \cos\phi \exp\left(\frac{\mu E \cos\phi}{kT}\right)}{\int d\phi \exp\left(\frac{\mu E \cos\phi}{kT}\right)} \cong \mu\left(\frac{\mu E}{2kT}\right) \tag{44}$$

where the last approximate equality holds for small $\mu E/kT$. Here we have used standard spherical coordinates and placed the electric field along the x axis and the rotator in the $x-y$ plane. For an electric field at an angle γ to the rotator plane, E can be replaced by $E \cos\gamma$.

Finally, if the constraints on the rotor are further relaxed such that rotator can reorient within a set of wells not described a single plane, the maximum polarization will reflect the change in dimensionality of the system. For instance, the extreme example of a free rotor in three dimensions yields[138]

$$\langle p_{mol} \rangle = \frac{\int d\Omega\, \mu \cos\theta \exp\left(\frac{\mu E \cos\theta}{kT}\right)}{\int d\Omega \exp\left(\frac{\mu E \cos\theta}{kT}\right)} \approx \frac{\int_0^{2\pi} d\varphi \int_0^{\pi} d\theta \sin\theta \cos\theta \frac{\mu E}{kT} \cos\theta}{\int_0^{2\pi} d\varphi \int_0^{\pi} d\theta \sin\theta} = \mu\left(\frac{\mu E}{3kT}\right) \tag{45}$$

where the electric field is along the z axis and the traditional notation for spherical coordinates has been used: Ω is the solid angle, θ is the angle between the z axis (E field) and the rotator, and φ is the azimuthal angle in the $x-y$ plane. The approximate equality is for $\mu E/kT \ll 1$. Equation 45 is obtained by expanding the numerator and denominator to first order in the small quantity. The zeroth-order term in the numerator and the first-order term in the denominator integrate to zero.

The parenthetical expressions on the right-hand side in eqs 40, 41, and 43−45 are often referred to as the Curie factor and reflect the decrease in polarization as a result of thermal motion. Comparison of eqs 40, 41, and 45 illustrates the correlation between the Curie factor and the dimensionality of the system. For a truly one-dimensional system, described by eq 40 with $\varphi = 0$, the extreme constraint on the rotor due to the reduced dimensionality is reflected in the polarization. As this dimensional constraint is relaxed, the maximum polarization at a given temperature also decreases. It is important to note, as mentioned above, that this correlation is normally only valid when the well positions are uniformly distributed.

3.2.3.3. Unidirectional Rotation from Random Motion. Thus far, our discussion in section 3.2.3 has focused on bidirectional rotation. When the rotational potential of a rotator is modified by the application of a field, the rotator will be more likely to point in the direction of the field than against it. However, how the rotator acquires this orientation, that is, by rotating clockwise or counterclockwise, is not constrained. This is the most common situation when the motion is thermally driven. However, important exceptions to this normal condition are the so-called thermal ratchets or Brownian motors. Such systems are complex and have been reviewed elsewhere.[112,113] We briefly discuss them here only to make a few important points relevant to our discussion. These systems generally have asymmetrical potentials such as the traditional example of a ratchet and a pawl.[139] However, in thermal equilibrium they do not execute unidirectional motion, as pointed out in our discussion above. The system must be driven out of equilibrium, usually in a cyclic manner, to obtain directed transport. One experimental example of a thermal ratchet in a rotor system is the work of Kelly and co-workers, discussed in section 5.7.2.[140] By utilizing a chemical reaction sequence in combination with thermally activated events, unidirectional motion was obtained without the application of a traditional driving force. The chemical reactions force the system out of equilibrium and create asymmetry in the rotational potential.[140] This is consistent with the general conditions for directed motion in randomly driven systems[113] and the necessary conditions discussed in section 3.2.2 for obtaining unidirectional motion in a driven rotor system. Namely, unidirectional motion is possible only when an asymmetry exists in a spatially periodic potential and the system is driven out of equilibrium.[113] In our scheme, this result applies equally to the driven and random regimes.

3.2.4. Utilizing Rotor Systems in the Random Motion Regime

As a brief conclusion to the discussion of random motion, we mention applications and systems for which bidirectional motion dominated by random thermal effects is useful. The most obvious example is the analogy that we have utilized several times in section 3.2, dipolar rotators interacting with electric fields. A collection of such rotors represents an artificial dielectric built up from individual molecules.[141] Both ordered collections, where the molecules are evenly spaced and identically oriented, and disordered dielectrics are useful. By altering the characteristics of each molecule, the dielectric parameters such as polarization per unit volume and dielectric response time can be tuned. Such work is

already underway for ordered three-dimensional systems[141] but may be particularly interesting for lower dimensional arrays.[81,142] Ordered collections offer the increased possibility of forming ferroelectrics where interactions between rotors are not negligible. Such interacting systems are discussed in section 3.3.

A second area of interest for random motion is applications where the orientation of the rotor is the important observable. Switches or memory elements are examples of this type. Flipping the orientation of a dipole rotator in order to control current flow through a molecule has been proposed,[143] and chiro-optic molecular switches have been developed.[144] For switches or memories, hindered rotors where the rotator orientation is limited to a small number of angles are an obvious choice although strong fields may still have to be applied to reorient or reset such elements. Rotors where rotation can be quenched by a change in the local environment (resulting in a change in the torsional potential) would represent another kind of switch.[145]

3.3. Interacting Rotors

We now turn to situations where the interaction energy between neighboring rotators is important. In this section, we do not discuss the interaction between a rotator and another element of the system, such as a surface for surface-mounted rotors, the stator in an RS rotor, the solvent in a solution-phase system, or the constraining solid for rotors in the solid phase. These effects are included within the non-interacting rotor description above and generally manifest themselves in rotational potentials and as friction.

An interacting rotor system can only be discussed in the context of a collection of rotors. Furthermore, the relative position of the rotors (the spacing between rotors) in such a collection must be well defined. As a consequence of this definition, we restrict ourselves to solid, surface-based, or polymeric systems where adjacent rotators are permanently positioned with respect to each other. Thus, collective effects interest us here: modes or states that are dependent on the orientation of numerous rotors in the collection. However, we point out that work on correlated rotations between different rotators contained in the same molecule,[146] which have been observed in solution-phase systems, may speak to many of the important issues in establishing correlations between rotators on different molecules. This is especially true in the case where the important interaction between rotators is steric, and thus, we touch on such systems briefly below. In the limit that the molecule becomes very large or a polymer is formed, a system with correlated rotations might be considered a collection of several types of rotators, with the various types interacting. Additional examples and a more detailed analysis of correlated rotation within a molecule appear in section 5. Here we restrict ourselves to rotator−rotator interactions between different, but identical, rotators in the collection.

Rotator−rotator effects can be subdivided into two broad categories: field-mediated interactions and steric interactions. Steric interactions involve gearing or physical "contact" between two adjacent rotators. In the field-mediated case, coupling between a property of the rotator, such as an electric dipole moment, and the field produced by the other rotators in the collection is important. We begin by discussing steric interactions and refer the reader to additional examples in the text to follow. Then, we take up field-mediated effects. Few examples of this type yet exist in rotor systems, but dipole−dipole interactions in other materials are well studied and the extension to rotors appears natural and fruitful.

Interaction between rotors can occur both in ordered systems, where the rotators are arranged in a regular array, and in disordered or random collections. When disorder is present, the interaction between rotators differs for different elements in the collection. For steric interactions, this lessens the efficiency of the coupling between rotators while, for field-mediated electrostatic interactions, inhomogeneity is expected to lead to a dipolar glass.[147] Dynamic behavior in the presence of disorder is complex, and we will focus on ordered systems in our discussion.

3.3.1. Steric Interactions

As described above, steric interactions are fundamentally local. In the gear analogy, the teeth of the adjacent rotators are intermeshed such that the motion of each rotor is correlated. Generally, such systems can be described with hindered rotation where there are (at least) two important rotational potentials: one for independent rotation of the two units (gear slipping) and another for correlated rotation. Thus, the steric interactions are manifested in these rotational potentials. Correlated rotational motion of two groups on the same molecule has been observed in "internally crowded" systems where adjacent groups are in particularly intimate contact.[148] Here, independent motion of either rotator is prohibited by a high activation energy. In the gear analogy, this is equivalent to slipping a tooth of one rotator over a tooth of an adjacent rotator. Sterically this is a very unfavorable configuration and thus has a high energy. The thermally activated motion of the system, determined by a rotational potential with the much lower barrier, is both rotators moving in unison.

This local interaction can be extended by stringing together a chain of rotating propeller groups. Such chains of twofold rotators have been studied.[149,150] For one system of this type,[149] two types of motion are predicted. Correlated rotation occurs with a rotational barrier that increases with increasing chain length. Thus, as additional rotators are added, more energy is required to rotate the assembly, which reflects the interacting nature of the system. When a rotator at the beginning or end of the chain is forcibly rotated, localized rotation is also predicted. Here the second rotator in the chain rotates in a correlated way, but the next ring is static with respect to the second rotator and turns with it as one unit. As the chain length increases, the likelihood of localized rotation instead of correlated rotation increases due to the increased barrier to rotation, W. A third mode of motion, torsional oscillations with

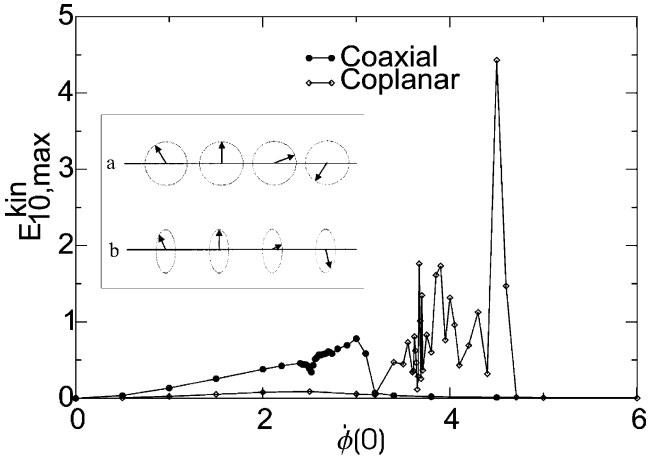

Figure 4. Maximum energy $E^{kin}_{10,max}$ of the 10th dipole in a 25-dipole chain as a function of the angular velocity $\dot{\phi}(0)$ with which the first dipole is excited for coplanar (inset, a) and coaxial (inset, b) rotor chains (see text). Private communication from de Jonge, J. J., and Ratner, M. A. The inset has been reprinted with permission from ref 83. Copyright 1999 American Chemical Society.

an amplitude less than 180°, has also been observed.[150] The energy of this torsional mode and the barrier for correlated rotation are both altered by changing the linkage between the rotators.

3.3.2. Electrostatic Interactions

In the field mediated case, the interactions are extended. Here, the dipole interaction energy, given by eq 6 for a pair of dipoles, is nonzero at all distances. Physical contact of adjacent rotators is not needed, and depending on the size of the dipole moment and the spacing of the dipoles, interactions between non-neighboring dipoles may be important. Here the energy of the system is dependent on the configuration of the dipoles, and a well-defined ground state of the system can be identified. Torsional potentials are generally not useful, and the whole rotor collection is treated as one unit. Because the electrostatic interaction energy is often smaller in magnitude than steric interactions, its effects are generally studied in systems with low torsional barriers and at low temperatures.[151]

Ratner, de Leeuw, and co-workers have modeled one-dimensional arrays of dipolar rotators as classical point dipoles with no torsional potential or friction.[81−83] As might be expected from eq 6, the ground state of this system occurs when all the dipole moments point along a line.[82] A more rigorous result considering long-range dipole−dipole effects gives the minimum energy, V_{min}, as

$$V_{min} = -2(1.202)(N-1)\mu^2/r^3 \qquad (46)$$

for a long chain of N dipoles separated by a distance r.[82] In contrast, for a chain of rotators where the axis of rotation is along the line connecting the rotators, the dipoles cannot point along a line and the ground state occurs when each dipole is antiparallel to its neighbors.[83] We will refer to these two cases as coplanar or coaxial chains, respectively (Figure 4, inset). If the chain is slightly perturbed from this ground state by moving dipole l an angle φ_l from its equilibrium position, it will follow the equation of motion

$$\partial^2\varphi_l/\partial t^2 = -\mu^2/Ir^3\sum_j(2\varphi_l - \varphi_j)/|l-j|^3 \qquad (47)$$

for the coplanar system or

$$\partial^2\varphi_l/\partial t^2 = \mu^2/Ir^3\sum_j \sin(\varphi_l - \varphi_j)/|l-j|^3 \qquad (48)$$

for the coaxial case.[83] Here the sum is over all the other dipoles and $l - j$ is the distance between dipole l and dipole j. These results enable a discussion of how an excitation would travel along the chain. If a periodic solution of the form $\varphi_l = u_k e^{i(kl-\omega_k t)}$ is assumed, the following dispersion relations are obtained:

$$\omega_k{}^2 = 4(1.202)\mu^2/Ir^3 + 2\mu^2/Ir^3\sum_{m>0}\cos(km)/m^3 \qquad (49)$$

$$\omega_k{}^2 + 2\mu^2/Ir^3\sum_{m>0}(-1)^m/m^3[1-\cos(rkm)] = 0 \qquad (50)$$

for the coplanar[82] and coaxial cases,[83] respectively. For the coplanar case, the dispersion curve (ω versus k) has its maximum (which corresponds to the maximum energy) at zero wavenumber ($k = 0$) and drops continuously as k increases to π. At $k = \pi$ (the maximum wavevector) and at $k = 0$, the slope of the dispersion curve is zero, resembling optical phonon dispersion in a Debye-type crystal lattice. The group velocity $|\partial\omega_k/\partial k|$, which defines the speed at which excitations travel along the chain, has its maximum at $k = \sim\pi/2$ and vanishes at $k = 0$ and $k = \pi$. In the coaxial case, the entire system of dipoles can be rotated about its common axis without any change in energy; thus, long wavelength (k small) excitations approach zero frequency in the dispersion curve. The maximum of the dispersion curve is at $k = \pi$, thus resembling an acoustic phonon in a Debye crystal lattice. The group velocity has its maximum at $k = 0$ and is approximately twice the maximum group velocity in the coplanar rotor chain.

These analytical results obtained in the low energy limit have been verified by numerical simulations. The authors used molecular dynamics to study a chain with 100 dipoles.[82,83] In a constant energy ensemble, the central dipole was rotationally excited. Monitoring the kinetic energy of each dipole, the analytically derived dispersion relations were confirmed at temperatures near zero.[82] For $T > 0$, thermal correlations become important. Autocorrelation functions of the dipole orientations and of the Fourier densities were obtained from simulations at different temperatures. The dipole autocorrelation function at low temperatures exhibits regular oscillations which are dampened within less than 20 periods. At higher temperatures, these oscillations disappear due to thermal fluctuations.

Energy transfer for higher excitations was studied on a 25 dipole chain, in which the first dipole was excited.[81] In Figure 4, which shows the maximum

energy of the 10th dipole in the chain as a function of excitation energy of the first dipole, the difference of the coaxial and the coplanar chains is obvious. Low-energy excitations below three reduced energy units ($E \times 4\pi\epsilon_0 r^3/\mu^2$), which are essentially blocked in the coplanar chain, propagate through the coaxial chain as a soliton-like wave. Intermediate excitations with energies of 3−5 units propagate along the coplanar chain but not along the coaxial one. For even higher excitations, there is no significant energy transfer in either case. Hence, the coplanar chain behaves like a crude band filter and the coaxial chain like a high-excitation filter.

Ground-state configurations and stability to thermodynamic fluctuations have been discussed for a series of two-dimensional lattices[142,152−156] where such dipole−dipole-mediated waves as discussed in the one-dimensional case may also be present. In particular, square,[155] rectangular,[155] and hexagonal[156] lattices exhibit anti-ferroelectric ground states.[142] The triangular lattice case has been most studied[142,154,155] and shows a ferroelectric ground state which is stable to fluctuations.[142] Generally, ferroelectric ground states are associated with rhombic lattices (with internal angles of less than 80°) while anti-ferroelectric configurations are consistent with rectangular lattices.[142,155] Possible examples of dipole−dipole or higher order coupling between rotors with very small torsional potentials are discussed in section 7.2.[157,158]

4. Experimental and Theoretical Methods

Most methods used to study rotational processes are generally known to the chemist, and their description is easily accessible in the literature. The most common technique for the study of solution-state rotors is dynamic NMR (or DNMR) spectroscopy.[159−167] More detailed discussions on 2-D NMR techniques are available in recent reviews.[168−170] NMR experiments for observing dynamical processes in solids are also described in other sources.[171−173] Other common techniques such as microwave spectroscopy,[174−177] infrared (IR)[178−180] and Raman[181,182] spectroscopy,[183,184] and circular dichroism (CD) spectroscopy[185,186] are mentioned in the text but will not be discussed here. Instead, we chose to highlight two techniques that may be less well known to chemists, dielectric spectroscopy and molecular dynamics simulations, with references to more thorough treatments.

4.1. Dielectric Spectroscopy

Torsional motion of a rotator is probed by dielectric spectroscopy[187] via coupling of an applied electric field with a permanent electric dipole moment associated with the rotator. Thin films or bulk samples of rotor molecules are treated as a dielectric and are encased in a capacitor which can be either parallel plate or more complex in nature. The molecules add an additional polarization to the empty capacitor, effectively increasing the dielectric permittivity, ϵ, and thus the capacitance. The increase in capacitance is measured as a function of the frequency of an applied oscillating field and as a function of temperature.

Dielectric spectroscopy is often utilized for rotors in the random hindered regime discussed in section 3.2.3.2. Here, the thermally activated relaxation rate is an exponential function of the ratio W/kT. For applied electric fields with a frequency smaller than the relaxation rate of the rotors, the dipoles follow the field and thus contribute to the measured capacitance. As the temperature is decreased, or as the frequency of the applied field increases, the dipolar rotators are no longer able to follow the applied field direction and only the background capacitance of the empty capacitor is observed. Thus, for a constant applied frequency, a step in capacitance is observed at a temperature where the relaxation rate of the dipoles is approximately equal to the applied frequency. The position of this step as a function of applied frequency gives information about the torsional potential in which the rotors move (Figure 3). The amplitude of the change in capacitance provides a measure of the number of reorienting dipoles and the efficiency of rotor alignment with the field.

Because the capacitance due to the rotors is normally a factor of 10^3 or more smaller than the background capacitance due to the empty measurement capacitor, this effect is more easily observed by measuring the capacitor loss. The dissipation factor $\tan\delta$ is measured as a function of applied frequency and sample temperature, and it contains information on the response of the real capacitor, which includes resistive elements, in comparison with that of an ideal purely capacitive capacitor. Experimentally, the loss of the measurement capacitor is usually comparable or smaller in size and has significantly smaller temperature dependence than the loss contributed by the rotors, creating a much more favorable situation for observation of the rotor response.

For a voltage applied across an ideal capacitor, the current observed is exactly 90° out of phase with the applied signal. Introduction of a resistive element, such as a leakage current, alters this phase, and a small fraction of the total current is now in phase with the applied voltage. This deviation from ideal behavior is measured as the angle δ between the true phase and 90°. In a rotor relaxation experiment, the rotors also contribute a resistive (or lossy) component to the capacitor which is reflected in a peak in the measurable quantity $\tan\delta$ as a function of temperature. As mentioned above, for a fixed frequency experiment, the dipolar rotators are unable to respond to the applied field at low temperatures and thus do not contribute to either the capacitance or the dissipation factor. At high temperatures, the rotors respond quickly to changes in the applied field and thus contribute to the capacitance but provide no dissipation. However, at an intermediate temperature, where the relaxation rate of the rotors is similar to the frequency of the applied signal, the reorientation of the molecules contributes partially to the capacitance but, due to the imperfect response, also adds a resistance element to the capacitor. Thus, $\tan\delta$ peaks at a temperature where the relaxation rate of the rotors coincides with the measurement frequency (the same temperature as the step in the capacitance). For a homogeneous system with a

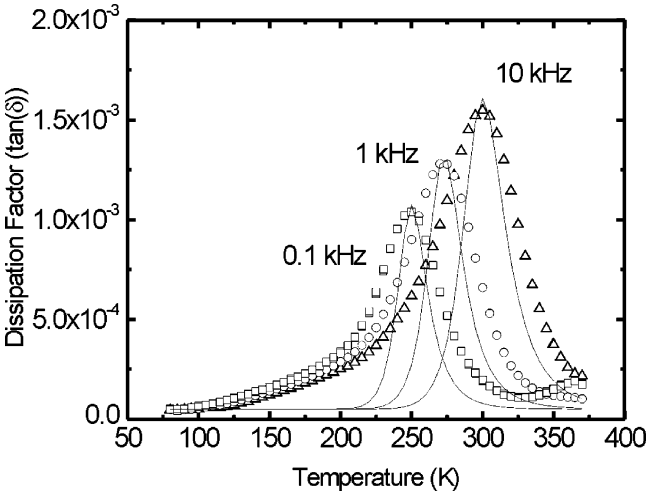

Figure 5. Dissipation factor versus temperature at three frequencies for a microcrystalline array of dipolar fluorobenzene rotors. The solid lines are fits to eq 51 with a lowest barrier ($W - s$ in Figure 3) of 13.7 kcal/mol and s' = 1.9 kcal/mol. The sample contains $\sim 2 \times 10^{15}$ rotors. Reprinted with permission from ref 141.

single relaxation time, the shape and position of the peak can be described by the Debye form:[188]

$$\tan \delta = \frac{C}{C_0} \frac{\omega\tau}{1 + \omega^2\tau^2} \qquad (51)$$

where C is the capacitance due to the rotors, C_0 is the background capacitance, ω is the frequency of the applied field, and τ is the inverse of the relaxation rate discussed in section 3.2.3.2. Plots of tan δ against temperature, obtained at several frequencies, are shown in Figure 5.

A similar experiment can be undertaken in the time rather than the frequency domain.[189] Here, instead of an oscillating excitation, a step change in the potential across the capacitor is imposed and the relaxation (measured via the observable current) is recorded as a function of time. After the fast transient due to the response of the measurement capacitor, an exponential decay in current should be observed for a system with a single relaxation time. This current reflects the alignment of the rotors with the applied field and decays with a time constant equal to the inverse of the relaxation rate. The integrated area under the decay curve is proportional to the number of rotors responding to the applied field. While molecular rotor studies utilizing dielectric spectroscopy are not specifically enumerated here, they are mentioned in the context of specific compounds in the sections to follow.

4.2. Molecular Dynamics

Quantum mechanical (QM) and molecular mechanics (MM) methods are commonly used to construct molecular potential energy surfaces. They can locate minima and calculate energy barriers for various paths. However, a static exploration of the nuclear configurational space provides only an incomplete study of rotor behavior, and molecular dynamics (MD) simulations are required for an understanding of rotor motion. While quantum dynamics methods work at the most accurate level of theory, their excessive computational demand makes them only applicable to very small model systems with a few degrees of freedom. Semiclassical methods are more generally applicable, but large structures require the application of classical molecular dynamics, where all atoms are treated as classical objects moving on a potential energy surface. The equations of motion are then numerically solved introducing a finite time step.[190] A straightforward solution of Newton's equations of motion provides results for a situation in which the number of particles, energy, and volume are constant. In most experiments, temperatures instead of energy and pressure instead of volume are constant. Various methods are available to perform simulations in such ensembles.[190] For typical rotor structures, studies of rotation on a time scale up to nanoseconds are possible. The most severe limitation of MD in rotor studies is that it does not account for zero point vibrations in molecular structures. It has been argued that at very low temperatures this results in pooling of the energy in low-frequency modes.[191]

We do not provide here a list of instances in which MD studies of molecular rotors have been performed but shall mention them in the following sections in the context of the specific molecules that have been investigated.

5. Rotors in Solution

The primary focus of this article is on possible future applications in nanoscience and nanotechnology, where rotors or rotor arrays mounted on surfaces or inside solids are of particular interest. This is reflected in the above discussion of theoretical aspects of rotor motion, and we return to the subject in sections 6 and 7. Up to now, however, by far most molecular rotors have been studied in solution, and this is the subject of section 5. It may appear somewhat disconnected from the other sections, yet it is essential for the appreciation of the topic. After all, the rotor molecules need to be synthesized and their basic characteristics, such as rotational barriers, established before it makes much sense to mount them on surfaces or to examine them inside solids, and such synthesis and characterization are nearly always performed in solution. Besides, to many authors, investigation of molecular rotors freely floating in a solution is fascinating in its own right, and their eventual utility in nanotechnology is of secondary concern.

5.1. Propellers, Gears, and Cogwheels

It can be argued that the first mechanical molecular device was the molecular gear; indeed it is one of the simplest devices that can be designed from molecules. The idea of "correlated", "geared", and "restricted" rotation in a wide variety of molecules is a vast area of research, which can be traced back to the resolution of the first conformationally restricted biphenyl, 6,6′-dinitro-2,2′-diphenic acid, by Christie and Kenner in 1922.[192] The topic has been the subject of many review articles and several books.[148,164−166,193−201]

Presently, we start by defining the nomenclature used for macroscopic gears and use this terminology to describe the molecular counterparts. Then we give a brief historical account of the discovery of molecular propeller systems, which led directly to the notion of gearing in molecules. Finally, we will discuss different systems in turn, in particular, those that led to a deeper understanding of the mechanics of molecular-scale gearing. As mentioned in section 3, we are interested in understanding the factors that affect the intrinsic torsional potential W through steric and electronic effects. Insight into the steric "size" of molecular functional groups, as well as the intrinsic barriers created for the axle about which the rotator turns, is of interest in developing a systematic understanding of the factors that govern rotation. Because the topic has been covered many times before, we choose several examples which we feel illustrate the principles of molecular gearing.

In particular, we do not cover most of the computational work but use one example that we consider particularly striking to illustrate the complex beauty of the subject: Figure 6 illustrates the geared rotation of the eight nitro groups in octanitrocubane, investigated computationally by Hrovat et al.[202]

5.1.1. Nomenclature

The concept of a molecular gear is intended to invoke images of the macroscopic analogues. Indeed, in this review, we use a number of terms that have relations to macroscopic objects, such as turnstiles, motors, wheelbarrows, pinwheels, and gyroscopes, to name a few. To facilitate a discussion of molecular gears, we define some of the nomenclature used in their real-world analogues and extend these definitions to their nanoscale counterparts. There are four main gear classes:[203] *spur gears*, *bevel gears*, *worm gears*, and *spiral* or *helical gears* (Figure 7). *Spur gears* are the simplest and the most commonly used in macroscopic machines and are also the most efficient type of gear, with efficiencies up to 99% in the macroscopic world (Figure 7a). They contain two cylindrically symmetric cogged wheels, with teeth cut parallel to the axis of rotation, and transmit rotary power between parallel shafts. *Bevel gears* transmit rotary power to shafts that are at an angle to one another (most commonly 90°) but lie in the same plane (Figure 7b). The teeth are cut into the frustum of a cone, the apex of which is the point of intersection of the shaft axes. For macroscopic bevel gears of the same size at right angles to one another, the velocity ratio is one-to-one, and these form a special class of gears called *miter gears*. For a velocity ratio other than unity, the smaller of the two gears is referred to as the *pinion* (which applies for the smaller of two gears in any gear system). *Worm gears* transmit rotary power between two shafts that lie in different planes (Figure 7c). A *worm* is a screw cut to mesh with the teeth of a *worm wheel*, which is essentially a spiral spur gear. These gears tend to be very inefficient due to friction and produce much heat during operation. They are typically used in the macroscopic world when one shaft needs to turn at a much slower rate than the other. *Spiral* or *helical*

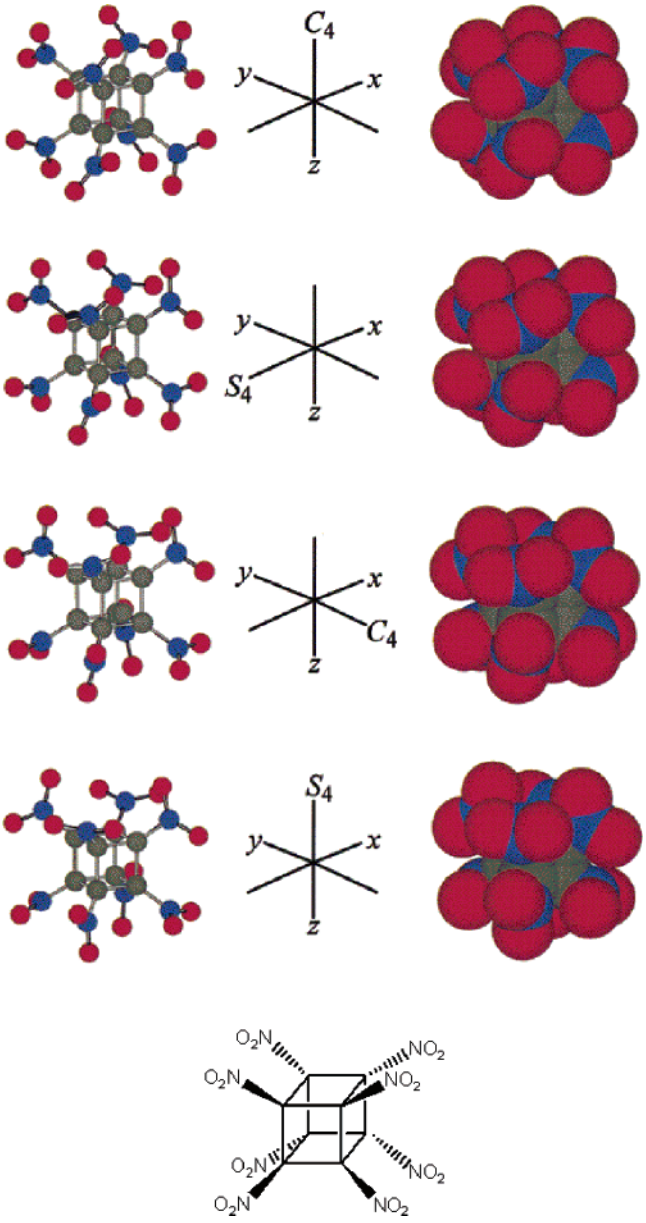

Figure 6. Ball-and-stick, space-filling, and chemical structures of octanitrocubane. Reprinted with permission from ref 202. Copyright 2001 American Chemical Society.

gears are used to transmit rotary power between shafts that are either parallel to each other or at angles to one another, but in different planes. The former is referred to as a *herringbone gear* (Figure 7d). In the macroscopic world, the teeth of a spiral or helical gear are cut at an angle across the face of the gear, which differentiates them from other types of gears. In nanoscopic systems, it can be argued whether spiral and helical gears can be distinguished from other types, such as bevel gears, although the helicity of the individual molecular "teeth" may serve to differentiate them. The efficiency of these macroscopic gears is roughly the following: spur > herringbone > bevel > spiral or helical > worm.

Whitesides and co-workers[204] have defined the nomenclature for *fluidic gears*, those that operate at the fluid/air interface, for millimeter- to centimeter-scale objects. Gearing in the macroscopic systems studied by this group can occur either by classical

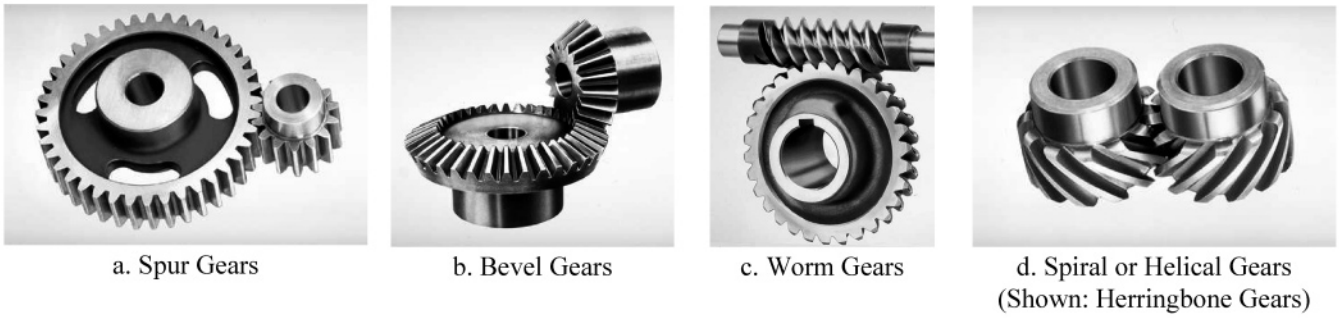

Figure 7. Several types of macroscopic gearing systems. Photographs courtesy of Emerson Power Transmission Corporation (http://www.emerson-ept.com).

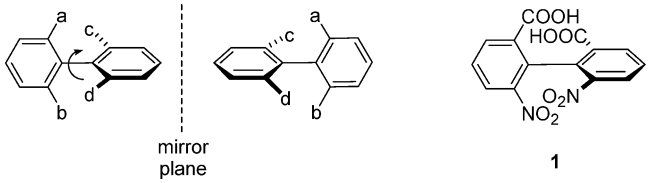

Figure 8. Chirality in biphenyls and the first biphenyl compound separated into enantiomers (**1**).

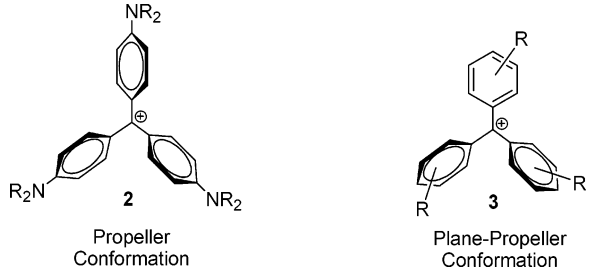

Figure 9. Early proposals for the stereochemistry of molecular propeller systems.

mechanical gearing or by hydrodynamic shear and capillary forces. Fluidic gears generally have differently shaped teeth in comparison to classical analogues and can indeed have no teeth at all. Gearing in such systems is created by menisci formed at the interface, and the shear from the turning gears is transmitted to neighboring gears. Due to the fact that these gears are not in intimate contact, and instead transfer torque through the liquid medium, they have a very low wear potential. However, it is doubtful that the physical phenomena observed in these systems[204] will translate as the size of the objects is decreased, ultimately to the molecular scale. The same, however, can be said about our understanding of mechanical gears in general. This section, and others in the review, will deal with our understanding of how and which macroscopic properties can be transferred to the molecular level.

5.1.2. Historical Account of Molecular Propellers and Gears

In the beginning of the 20th century, chemists began to discover that molecules need not possess a stereogenic center to be chiral. Hindered rotation of groups within a molecule, if slow enough on the time scale of observation, could render a molecule chiral. Therefore, the presence of a stereogenic center in a molecule is a sufficient condition, but not a necessary one, for the molecule to have a non-superimposable mirror image and exhibit chirality. The first experimental examples were in the study of substituted biphenyls (Figure 8), where rotation about a single bond is hindered. It was initially argued whether biphenyls were planar or whether the rings were twisted with respect to one another to overcome steric crowding. The resolution of enantiomers of biphenyls, first observed by Christie and Kenner[192] on 6,6′-dinitro-2,2′-diphenic acid (**1**), proved that the molecules must be twisted to remove planar symmetry. The resolution of a number of other sterically hindered biphenyls,[205−208] anilines,[209−213] and styrenes[214−218] soon followed. The ability of compounds to possess chirality due to restricted rotation was labeled *atropisomerism*[219] (from Greek; *a* meaning not and *tropos* meaning turn or rotate).

Early work on biphenyls and related atropisomeric systems was important in understanding issues related to chirality and energy barriers to rotation as a function of steric interactions. One importance of the discovery is that it led to further research in propeller-like molecules. The first such molecules were the triarylcarbonium ions. Lewis and co-workers[220] investigated the low-temperature absorption and emission spectra of the crystal violet cation (**2**, R = CH_3) and detected different isomers which interconverted with a barrier of ∼2−3 kcal mol^{-1} (Figure 9). They proposed a helical propeller structure, where all the rings are twisted in the same sense. Later, Deno and co-workers[221,222] investigated many variously substituted triarylcarbonium cations and concluded that a "plane-propeller" conformation **3** (one aryl ring planar, the other two twisted) is most likely for substituted trityl cations.

Definitive proof of the helical conformation did not come until the mid 1960s and was made possible by the advent of NMR spectroscopy. Schuster, Kurland, and Colter[223−225] (often abbreviated SKC) measured the ^{19}F NMR of fluorinated *ortho*- and *para*-substituted triphenylcarbonium ions (**4**) in liquid HF (Figure 10). By using temperature-dependent NMR, they were able to observe that the molecule is indeed in a propeller conformation and that it interconverts stereoisomers via "flip" mechanisms, wherein one or more rings rotate perpendicular to the plane containing the central carbon and the three phenyl carbons bound to it (the "reference plane"), while the remaining rings pass through the reference plane (see section 5.1.5 for a more detailed discussion). Propeller-type conformations were soon discovered for the

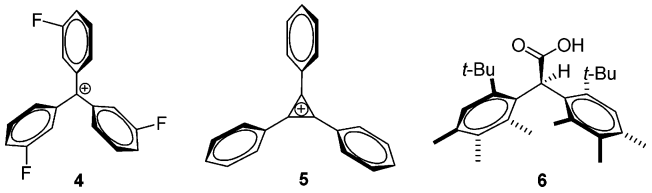

Figure 10. Early propeller systems—phenomenological ancestors of molecular gears.

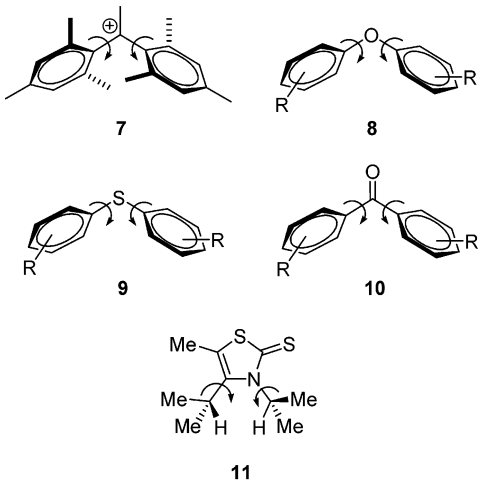

Figure 11. Molecules in early studies on concerted rotations in gearlike systems.

triphenylcyclopropenium ion[226] **5** (by its crystal structure) and in chiral diarylacetic acids (e.g., **6**),[227] which provided the first example of a chiral resolution by chromatography.

However, the importance of the SKC papers was in the use of NMR spectroscopy to view hindered rotation in gearlike systems. Soon after the discovery of propeller systems, investigators began to discover that the rotation of one part of the molecule could effect the rotation of other parts in a correlated fashion. Kwart and Alekman[228] investigated the hindered rotation in dimesitylcarbonium ions (e.g., **7**) and found no temperature dependence on the chemical shifts of the *ortho*-methyl groups (Figure 11). Therefore, even at temperatures as low at −60 °C, they exchange very rapidly. This exchange can be due to nearly unhindered rotation about the arene carbon−central carbon bond or to a concerted rotation of the arene rings wherein the torsional motion of one ring mandates the turning of the second in the opposite direction (disrotation). Steric arguments make the former highly unlikely, and the authors favored the latter explanation, which was supported by calculations. They dubbed this motion the "cogwheel effect", a term that would permeate the literature for many years to come. The phenomenon was also observed in other similar systems in the same year.[229] It should be noted that Adams predicted such a correlated rotation in tetraarylmethanes 18 years earlier, simply by using chemical models: "An examination of the scale models of the tetraphenylmethane molecule reveals a high degree of steric hindrance. It would appear quite difficult for one of the phenyl rings to rotate completely about its bond to the central carbon atom if the positions of the other three rings were fixed. Rotation of the phenyl rings in such a molecule should take place with greatest ease when all four rings rotate simultaneously in a coördinated manner."[230]

With NMR, chemists had a readily accessible and relatively straightforward method to observe concerted rotations in "cogwheel-like" systems, and in the four decades following 1965, the number of papers increased dramatically. Breslow and co-workers[231] revisited the triarylcarbonium ions for geared rotations using DNMR, as did Rakshys et al.[232,233] Other groups investigated similar behavior in diaryl ethers (**8**),[234,235] diaryl sulfides (**9**),[236,237] diphenyl ketones (**10**),[238] and polyarylmethane derivatives (section 5.1.3),[239−241] to name a few. In the 1970s, 1980s, and 1990s and up to the present, many groups have returned to the concept of correlated rotation in a number of systems. Here we will devote the rest of the section to discussing a number of particular areas where the majority of the work has been concentrated. We focus on molecules that most resemble geared systems. Much of the work discussed above and in the following sections, as well as other work, has been discussed elsewhere,[165,166,194,195,242] and a thematic issue on atropisomerism has appeared recently.[243]

5.1.3. Rotation of Alkyls and Related Groups in Molecularly Geared Systems

The simplest alkane to have a rotational barrier is ethane. This is the benchmark for teaching students about rotational isomers and eclipsed and staggered geometries in organic molecules. Since both methyl groups have the same moment of inertia about the C−C axle, one is arbitrarily defined as the stator and the other as the rotator. In the vibrational ground state, and in the absence of outside constraints, both will rotate equally in opposite directions during a hop from one to another staggered minimum. This example illustrates how relative the concepts of rotator and stator in an isolated molecular rotor can be. It also hints at the possible true complexity of the motion that is sometimes simply viewed as a mere turning of one group in a molecule, with the rest of the molecule immobile. Almost inevitably, in the absence of external constraints such as attachment to a macroscopic surface, all atoms in the molecule need to move, and the internal rotation is coupled to a rotation of the molecule as a whole.[1]

The example of ethane also shows that a vast number of molecules could be considered rotors under our classification system. Pitzer and co-workers[244,245] discovered the barrier to rotation in ethane (∼3 kcal mol^{-1}) in their studies on the entropy of gases by statistical mechanics and found that it was not possible to reproduce the entropy without a threefold barrier in the rotation. Early work of Kohlrausch[246] and Mizushima and co-workers[247,248] established the existence of rotational isomers in 1,2-dichloroethane using Raman spectroscopy and dipole moment studies. A review of rotamers in organic compounds determined by vibrational spectroscopy can be found in the book by Mizushima.[247]

In these relatively simple models, it becomes immediately clear that barriers to rotation, which can

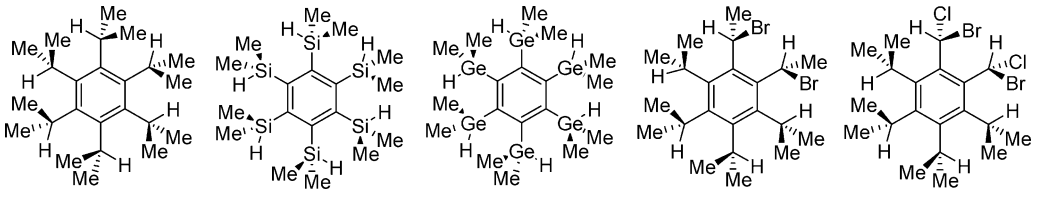

12 13 14 15 16

Figure 12. Benzene rings containing six bulky substituents form tongue-and-groove static geometries. Dynamically, the rotation of one group influences the rotation of the other five in a correlated fashion (cyclic gear systems).

be thought of as a simple gearing model in which a forced turning of one methyl group causes the other methyl group to turn as well, do not need to originate from physical phenomena observable in the macroscopic world. In ethane, the methyl groups do not mechanically mesh as in large-scale gears. The origin of the barrier to rotation and the preference of ethane for an eclipsed conformation are quantum mechanical.[249] This is our first instance where macroscopic mechanical expectations fail at the molecular level. Quantum phenomena often prevent us from "miniaturizing" large mechanical devices to the molecular scale simply.

Since the barriers in these small systems were discovered, a variety of studies followed which measured the activation barriers to rotation in small molecules. The use of NMR spectroscopy to determine rotational barriers was pioneered by Gutowsky and co-workers,[250] who measured the barrier to rotation in *N,N*-dimethylformamide and *N,N*-dimethylacetamide in 1956. An account of the early history of dynamic NMR has been related by Gutowsky.[251] Since then, a number of groups have taken up the study of rotation of alkyl groups and the possibility of gearing. Notably, Roussel, Chanon, Metzger, and associates[197] have coined the term "gear effect" for the meshing of alkyl groups in a number of systems (e.g., **11**, Figure 11). The gear effect is defined by these authors as "nonbonded interactions between anisotropic alkyl groups involving a long-range transmission process of conformational information due to the polyhedral shape of the alkyl groups".[252] These systems behave in a manner analogous to their macroscopic counterparts, but it is difficult to foresee useful work being produced from them. However, the knowledge obtained from these early studies is important in our understanding of the physical consequences of constructing molecular models of macroscopic machines.

A number of groups have investigated rotations in alkylbenzenes,[253−260] benzyl alkali salts,[261−264] benzyl halides,[265−268] substituted aromatic amine derivatives,[269] dialkyl disulfides,[270] methylated pyridinium salts,[252] and variously alkylated phenyl rings.[271,272] A more detailed analysis of rotations of alkyl groups can be found in a number of reviews.[165,166,196,198] However, several investigators[197,273] have cautioned that gearing in alkyl systems is quite complicated and cogwheeling may not be the only mechanism for the rotation of the groups.

Much of the early data available on the rotation of alkyl systems, especially those attached to phenyl rings where the other substituents could be modified, led to the concept of steric "size" in organic molecules. A number of early experiments were summarized by Förster and Vögtle.[274] The use of steric size is important in the design of rotor systems, as it can be used to tune the barrier to rotation in molecules, giving an adjustable synthetic parameter for building rotor systems with useful applications.

Polyalkylbenzenes (Figure 12) have been studied for geared rotation about the $C_{phenyl}-C_{alkyl}$ bond in the presence of the other alkyl groups. Hexaisopropylbenzene (**12**)[254,275−278] was found to have a tongue-and-groove arrangement of isopropyl groups wherein the isopropyl protons sit in the cavity formed by the adjacent isopropyl methyl groups to give an overall C_{6h} symmetric molecule.[279] A lower limit for the topomerization barrier was found to be ($\Delta G^{\ddagger}$) 22 kcal mol^{-1}.[278] Likewise, Mislow and co-workers[280,281] found similar arrangements for hexakis(dimethylsilyl)benzene (**13**) and hexakis(dimethylgermyl)benzene (**14**). In the former, when complexed to $Cr(CO)_3$ (which serves to break the symmetry of the molecule), they found correlated rotation of the alkyl groups with a barrier ($\Delta G^{\ddagger}_{300}$) of 14.2 kcal mol^{-1}. The concept of *conformational cycloenantiomerism* was developed from the study of 1,2-bis(1-bromoethyl)-3,4,5,6-tetraisopropylbenzene (**15**).[282] The gearing of the alkyl groups leads to four stereoisomers (two pairs of enantiomers), where only three would exist in the absence of gearing. If the system exhibited unhindered rotation about all groups, no isomers would exist. In this case, the cyclic structure combined with the steric gearing leads to a situation where *cyclostereoisomers* are observed. Isolation of one enantiomer allowed the authors to determine the cycloenantiomerization barrier (by reversal of the six ring substituents in a concerted fashion) to be greater than 24 kcal mol^{-1} ($\Delta G^{\ddagger}$) by coalescence NMR. Biali and Mislow[283] investigated the geared rotation in a similar compound, 1,2-bis(bromochloromethyl)-3,4,5,6-tetraisopropylbenzene (**16**), and found a barrier ($\Delta G^{\ddagger}_{429}$) of 26.8 kcal mol^{-1} by using saturation transfer NMR ($k = 0.19$ s^{-1}). Similar results were obtained for 1,3,5-tris(diethylamino)-2,4,6-tris(dimethylamino)-benzene, hexakis(diethylamino)benzene, and hexakis(dimethylamino)benzene.[284] Cycloenantiomerization has also been observed in rotaxanes by Vögtle and co-workers.[50]

Hexaethylbenzene (**17**) and derivatives have also been investigated for geared rotations (Figure 13). Mislow and co-workers[285] found that the ethyl groups prefer alternating "up" and "down" conformations with respect to the mean plane of the benzene ring. Similar behavior was observed in hexa-*n*-propylbenzene[286] and hexakis(bromomethyl)benzene.[287] Com-

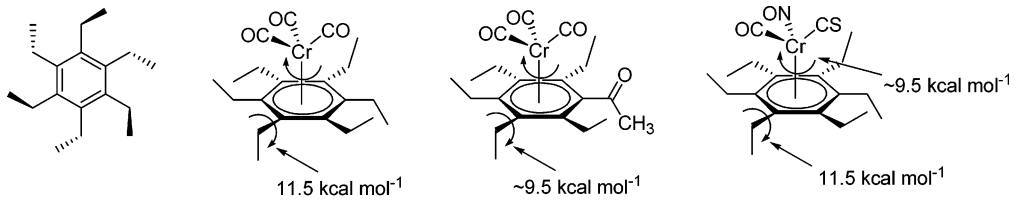

17 18 19 20

Figure 13. Gearing in hexaethylbenzene and organometallic analogues.

plexation of a metal tricarbonyl moiety, such as $Cr(CO)_3$,[285,288] affords a species (**18**) in which the ethyl groups prefer a *proximal* or *distal* relationship with respect to the metal complex and, in the most stable geometry, the carbonyl groups lie directly beneath the distal ethyl groups to minimize steric interactions. The barrier to rotation for exchange of proximal and distal ethyl groups was found to be ($\Delta G^{\ddagger}$) $\sim$ 11.5 kcal mol^{-1}, and the barrier to rotation of the tripodal $Cr(CO)_3$ group was too low to measure (see below and section 5.4.2 for further discussion on rotations of tripodal metal complexes). These complexes represent molecular analogues of bevel gears, with shafts at 90° angles to one another. However, this represents a truly geared system only if the two rotating parts are coupled to each other. Early investigations could not determine this, and synthetic analogues capable of measuring the two barriers were necessary. Also, as explained in section 3, the efficiency decreases when the barriers are mismatched, as the two components cannot orient well.

McGlinchey and co-workers have been interested for some time in the investigation of molecular bevel gears based on hexaethylbenzene−tricarbonylchromium complexes (e.g., **18**)[289,290] and, in particular, in probing whether the rotation of the tripodal base was correlated with the rotation of the ethyl groups. By replacing one ethyl group with an acetyl substituent (**19**), they were able to break the symmetry of the molecule, while keeping the alternating proximal/distal relationship among the substituents, and observe the barrier to rotation ($\Delta G^{\ddagger}$) for the ethyl groups ($\sim$9.5 kcal mol^{-1}) using both solution and solid-state ^{13}C DNMR.[291] However, the barrier to tripodal rotation was still too low to measure. In an elegant experiment, they changed the ligands on the metal to yield the chiral chromium cation $[(C_6Et_6)Cr(CO)(CS)(NO)]^+$ (**20**), which allowed them to separate tripodal rotation from ethyl group rotation.[292] The barrier ($\Delta G^{\ddagger}$) for tripodal rotation was $\sim$9.5 kcal mol^{-1} and the barrier ($\Delta G^{\ddagger}$) for ethyl group rotation was $\sim$11.5 kcal mol^{-1}, which shows that the two processes are not correlated. Siegel and Kilway[293,294] similarly investigated the two processes, but used differentially substituted arenes complexed to $Cr(CO)_3$, and arrived at similar conclusions. In pentaphenylcyclopentadienyliron complex **21**, McGlinchey and co-workers[295,296] also found that tripodal rotation was not geared with phenyl group rotation (Figure 14). Clearly, these systems do not act as true bevel gears. For a more detailed discussion, see reviews by McGlinchey[289,290] and Mislow.[277] Biali and coworkers[297−299] have also investigated the geared

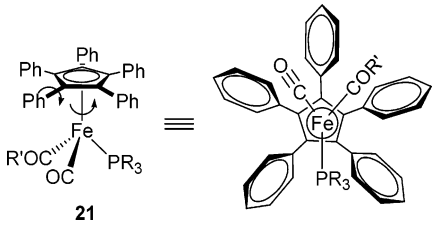

21

Figure 14. Molecular analogue of a bevel gear. However, the rotation of the tripod was not found to be correlated with that of the phenyl groups.

rotation in other polyethylated and related aromatic systems.

More comprehensive treatments of the static and dynamic stereochemistry of alkyl groups can be found in several reviews.[194,197,198,300] Other systems, such as tetraalkylethylenes,[301] tetracycloalkylethylenes,[302] tetracycloalkylmethanes,[303] *ortho*-disubstituted benzenes,[304,305] alkylated propenals,[306] alkylated adamantanes,[307] and 8-(dimethylamino)naphthyl ketones,[308] have also been studied for correlated rotation of the alkyl or related fragment. A number of groups have also investigated cogwheeling of alkyl groups from a computational standpoint.[309−312] Pophristic and Goodman[313] calculated the "gearing" (correlated disrotation) and "antigearing" (rotation in phase) in dimethyl ether. They found that the splitting between the geared rotation and antigeared rotation is due to hyperconjugative effects instead of simple steric factors. This study highlights the inherent difficulty in using macroscopic principles to design molecular machines, as there is no macroscopic analogue of hyperconjugation.

Although many of the geared systems described here and below are not directly applicable to creating "molecular machines", they do provide the basis for understanding the factors involved in correlated rotations, ultimately needed for the design of molecules to be useful as molecular rotors. A requirement for a molecular gear would be the transmission of "information" such as directed motion over a certain distance or over several geared units, as in the cooperative motion of all six alkyl groups on the hexaalkylbenzenes described above. However, the question of how this behavior can be harnessed to make useful molecular devices still needs to be addressed.

5.1.4. Biphenyls

In section 5.1.2, we discussed atropisomerism in biphenyls and the importance that restricted rotation had on the understanding of isomerism with relation

to stereogenic centers; that is, molecules do not necessarily require a stereochemical center to be chiral. Rotational processes are related to the energy difference between the ground-state and transition-state geometries of the molecules in question. For biphenyl-type molecules, for rotation to proceed, the two aryl groups must pass through a geometry in which they are coplanar. Depending on the substituents at the positions located *ortho* to the aryl−aryl bond, the transition state may be low enough in energy such that rotation occurs rapidly at room temperature. If sterically demanding groups are introduced in these positions, isomers will result which do not rotate at room temperature and can be isolated enantiomerically pure (see section 5.1.2).

However, in certain cases, the transition state may be stabilized relative to the ground state to lower the barrier to rotation. Take, for example, the conversion of biphenyl derivative **22** to **23** (Figure 15). Sutherland and Ramsay[314] found (by DNMR, monitoring of the *gem*-dimethyl signals) the barrier to rotation ($\Delta G^{\ddagger}_{375}$) to be 18.8 kcal mol^{-1} for racemization (strictly speaking, "enantiomer interconversion", but we shall retain the convenient abbreviation "racemization"). Rebek and Trend[315] designed the related bipyridyl system **24**, which has a slightly lower barrier ($\Delta G^{\ddagger}_{375}$ = 14.5 kcal mol^{-1}). Bipyridyls are known from X-ray crystal structures to bind to transition metal ions with the aryl rings nearly coplanar. Therefore, metal binding to **24** could actually lower the racemization barrier by stabilizing the transition state. Indeed, this was observed.[315] Complexation with $HgCl_2$ or $ZnCl_2$ reduced the barrier ($\Delta G^{\ddagger}_{213}$) to 10.5 kcal mol^{-1} (Figure 16), and even larger rate enhancements were found in bipyridyls with crown ethers appended, as in **25**−**27** (Figure 17).[316,317] Racemization was observed in **25** with DNMR by monitoring the benzylic protons (shown). Without added metal ions, the lower limit of the barrier for **25a** was found to be ($\Delta G^{\ddagger}$) 24 kcal mol^{-1} (no coalescence up to 165 °C). For **25b** and **25c**, although a singlet was observed for the benzylic protons, the authors did not believe the equivalence was due to racemization and placed the barrier at >24 kcal mol^{-1}. When $PdCl_2$ was added, the activation barriers decreased to 14.6 kcal mol^{-1} ($\Delta G^{\ddagger}_{307}$) for **25a**, 14.0 kcal mol^{-1} ($\Delta G^{\ddagger}_{283}$) for **25b**, and 13.9 kcal mol^{-1} ($\Delta G^{\ddagger}_{283}$) for **25c**, which corresponds to at least a factor of 10^6 at room temperature. In this study, however, the authors contended that the metal binds to the bipyridyl nitrogens and not the crown ether portion of the molecule. This was later disproved[318] by the same authors in the investigation of metal complexation to **26**, which lacks nitrogen binding sites but behaves in an analogous manner to **25a**−**c** when complexed to metal ions.

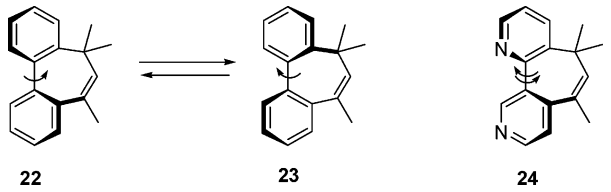

Figure 15. Oscillatory motion in "strapped" biphenyl-type systems.

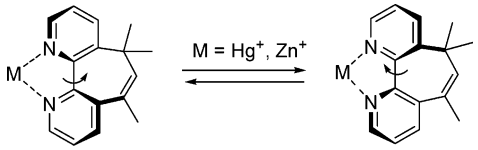

Figure 16. Metal-bound biphenyl-type systems.

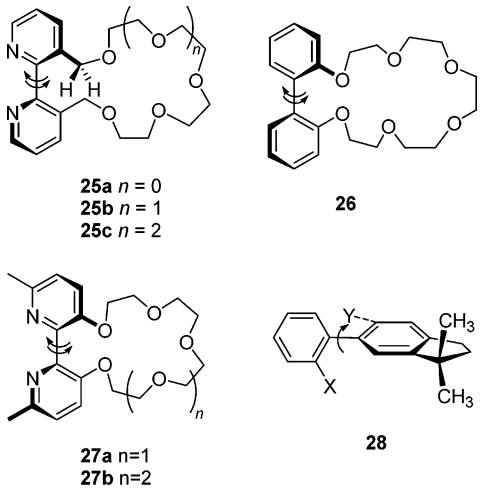

Figure 17. Rotations in some biphenyl-type systems.

Bott, Field, and Sternhell[319] investigated a "rationally designed" biphenyl system to study steric effects in the rotation of biphenyls. Molecule **28** possesses a number of markers which can be used to observe and control rotation. The ability to change the X and Y groups synthetically allowed the authors to test the rotational barrier in terms of steric effects by changing the sizes of the X and Y substituents. In this system, the Y group is only changed slightly to bring the barriers into an acceptable range for DNMR studies, while X is used to test the steric conditions. The prochiral methyl groups on the indane ring are used to observe the rotation in the NMR and are sufficiently removed from the site of the steric interaction in the transition state to not be a factor in the rotational barriers. Changing X and Y should have little or no effect on the ground-state geometry and only affect the transition-state geometry, which is important because a reference level must be defined when a series of compounds are compared. If substitution changed the ground-state and transition-state geometries, no correlation could be attained throughout the series, since there would be no reference point. This compound fits that criterion, as well as others studied in the paper. In all, 33 derivatives were synthesized and measured. From the data, the authors were able to determine the *effective* van der Waals radii of the substituent groups through the series (by changing X, but keeping Y unchanged). Many conclusions about the size of the substituents were as expected: I > Br > Cl > F; SCH_3 > SH; *t*-Bu > *i*-Pr > CH_3; CF_3 > CH_3.

5.1.5. Arene Propellers and Gears

Polyaryl molecular propeller systems draw immediate analogies to macroscopic propellers found on airplanes and boats. The dynamic gearing in systems

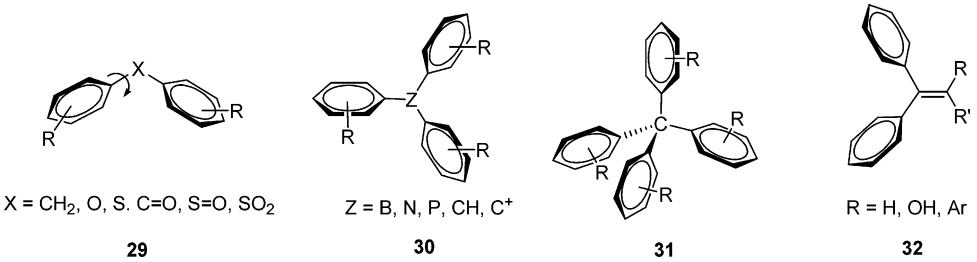

Figure 18. Arene-based propeller systems.

containing multiple arene systems was introduced in section 5.1.1, and a full account of this vast area is beyond the scope of this review. Many reviews have appeared,[148,165,166,194−196,199−201,242,320−322] and the reader is directed to them for a more detailed discussion. Polyarene propellers can generally be classified into two subsets: (a) those arranged around a central atom (Figure 18), as in diarylsulfoxides, diaryl sulfones, diaryl sulfides, diaryl ketones, and diaryl ethers (**29**; X = SO, SO_2, S, CO, respectively),[235−237,323−330] di- and triarylboranes (**30**; Z = B),[331−333] diarylmethanes and derivatives (**29**; X = CH_2),[227−229,238,241,334−340] triarylmethanes (**30**; Z = CH) and trityl cations (**30**; Z = C^+),[220−225,231−233,239,240,331−333,341−347] tetraarylmethanes (**31**),[230] triarylamines (**30**; Z = N),[348,349] triarylphosphines (**30**; Z = P) and derivatives,[350−352] and polyarylated ethanes, ethenes (**32**; R = R′ = H), ethenols (**32**; R = H, R′ = OH), and ethenones,[217,353−359] and propeller chains,[149,150,336] and (b) those described by the rotation about a planar unit such as a benzene ring. This second class includes the triarylcyclopropenium cation (**5**),[226] polyarylated cyclopentadienes, cyclopentadienones (Figure 24),[242,360−362] and benzenes (Figures 22 and 23).[363−367]

In polyaryl propeller systems, the aryl "blades" are twisted in the same sense to yield an overall helicity. If the arene units are differentially substituted, rotation of the groups can lead to isomerization. The rotation of aryl groups in polyarylated molecules is complex, and the interpretation of the data obtained has often been incorrect or at least under debate. From these studies, however, came an important contribution to the understanding of chirality and isomerization in molecules not necessarily containing a stereogenic center. Mislow and co-workers performed the first detailed investigation of correlated rotation in polyphenylated molecules and examined the concept that the torsional motions of two coupled rotors would lead to a situation where the coupled motion of the two units is energetically favored over the independent rotation of the individual units. This was first shown for polyphenylated methanes (**30** and **31**; Figure 18).[200,349] Mislow defined much of the nomenclature and group theoretical arguments that would be used for the decades to come.[148,200,201] Including the use of the SKC nomenclature for "flip" mechanisms, Mislow introduced the concept of *residual stereoisomerism* (also called *phase isomerism* by Iwamura and co-workers[368]), which describes the ability of a system to possess isomers by the sole fact that the rotations of certain units within the molecule are correlated and not independent of the time scale of the observation. In an analogy to macroscopic geared systems, consider two gears that rotate on axes at a distance where the teeth are not intermeshed. In this case, the gears rotate independently of one another and there is no correspondence between the rotation of one and that of the other. On the other hand, if the teeth are meshed, then the rotation of one dictates the rotation of the second. In molecular terminology, as described for arene propellers, if the steric conditions in the system allow for adequate meshing at the temperatures and time scales of the observation, the rotation of one aryl group will likewise dictate the rotations of others in the system. In the macroscopic analogy, one gear rotates clockwise while the other turns counterclockwise. In molecular terms, this is called *correlated disrotation*. If the aryl groups are differentially labeled, isomers will result which cannot interconvert unless there is *gear slippage*, where one or more rings rotate independently of the others in a nonconcerted fashion.

Mislow has labeled the plane containing the central atom and the three aryl atoms bound to it the *reference plane* and defined *stereochemical correspondence* as the relationship that defines the conformations in propeller molecules. A propeller-shaped molecule can invert its helicity by undergoing *n*-ring flips, and the mechanism for inversion changes with the nature of the compound and the steric bulk. For example, highly substituted aryl groups would be unlikely to go through zero-ring flips, because, in the transition state, all the aryl groups must pass through the reference plane simultaneously and become coplanar. For ring flips of $n > 0$, *n* rings rotate in a conrotatory fashion through a plane perpendicular to the reference plane, while the others (for $n = 1$ or 2) pass though the reference plane in a disrotatory fashion. In Figure 19, we show a schematic for ring-flip mechanisms which reverse the helicity of the original molecule. For the three-bladed propeller shown (a ≠ b ≠ c; a, b, c achiral on the time scale of the measurement), if Z = B, eight diastereomeric *dl* pairs result, six from the conformation of each phenyl ring (a, b, c above/below the reference plane) and two from the helicity of the propeller. If Z = CH, a stereogenic center is introduced and 2^5 or 16 diastereomeric *dl* pairs will result (but flip mechanisms only lead to interconversion of diastereomers, not enantiomers). Mislow defines the structure where a ≠ b ≠ c as *maximally labeled*[200] and has tabulated all the possible stereoisomers for different combinations a, b, and c.[199]

Similarly, Biali, Rappoport, and co-workers have extensively studied geared rotations in polyarylated

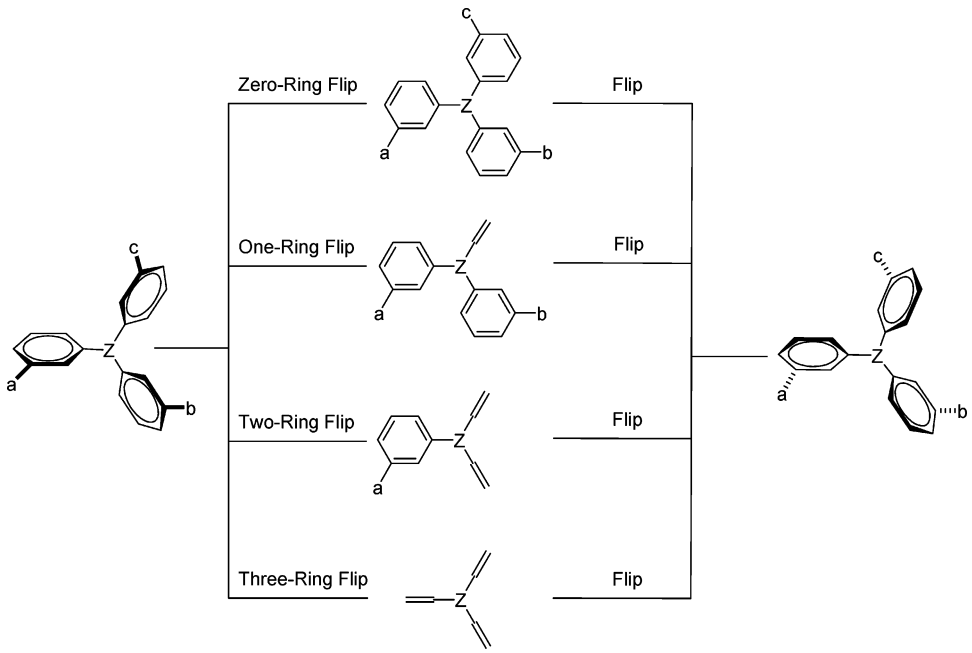

Figure 19. Schematic representation of ring-flip mechanisms for aryl propeller systems. The symbol // represents a phenyl ring oriented perpendicular to the page.

ethenes and ethenones,[356,358,359] and Schlögl et al.[353] found that 1,1′,2,2′-tetraarylethenes (**33**, Figure 20)

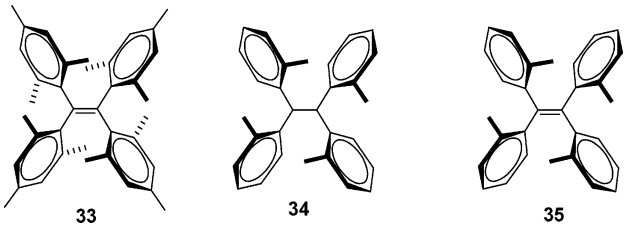

Figure 20. Polyarylated ethene and ethane propeller systems.

could be separated into enantiomers ($\Delta G_{293}^{\ddagger} = 22.2$ kcal mol^{-1}; $t_{1/2} = 38.3$ min at 21 °C). Isomerization was suggested to occur by a two-ring flip mechanism, while, in 1,1,2,2-tetra-*o*-tolylethane (**34**) and tetra-*o*-tolylethene (**35**), Willem et al.[354] found an interconversion of the isomers to proceed via a four-ring flip.

Several groups have investigated "propeller chains",[149,150,336,369] which consist of multiple arene units connected via linking groups (Figure 21), and investigated the transmission of rotational information along the chain. Montaudo et al.[336] first studied a series of substituted dibenzylbenzenes (**36**) by dipole moment and NMR measurements. They found preferred conformations based on the substitution pattern but did not probe the dynamics. Biali and co-workers[149] investigated similar molecules, permethylated dibenzylbenzenes (**37** and **38**), using DNMR and molecular mechanics calculations. In compound **37**, different conformations result from the two possible helicities of the moieties and the arrangement of the phenyl groups on the main chain. However, for a given conformation of the main chain, not all helicities are sterically feasible. Compound **37** also displays an achiral conformation, which is possible for propeller chains with an odd number of rings, while those with an even number of rings must exist in chiral conformations. The lowest energy mechanisms for this molecule to interconvert helicities are a two-ring flip involving the two outer rings ($E_{calc} \sim 7$ kcal mol^{-1}) and a one-ring flip involving the middle ring ($E_{calc} \sim 7.2$ kcal mol^{-1}). One surprising outcome came when driving the rotation of the outer ring in the calculation: while the middle ring was found to rotate in a disrotatory fashion as expected, the third ring did not rotate at all and the behavior was termed "localized disrotatory rotation".[149]

The calculated barrier for the mutual interconversion among all the conformers in **37** was calculated to be 3.9 kcal mol^{-1}. In compound **38**, since all the propeller conformers are chiral (even number of rings), each flip resulted in enantiomerization. Like the case of **37**, the lowest energy flip mechanism proceeds through a geometry in which the rings are alternately coplanar and perpendicular to the reference plane. The barrier to correlated rotation in **38** ($E_{calc} \sim 10$ kcal mol^{-1}) was found to be larger than that in **37**, which is in turn greater than that in the diphenylmethane (**29**; R = pentamethyl, X = CH) analogue also investigated in this paper.[149] In conclu-

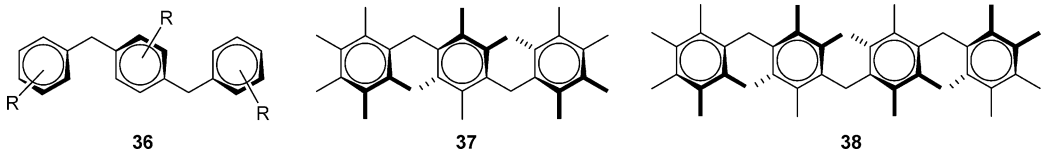

Figure 21. Some examples of propeller chains.

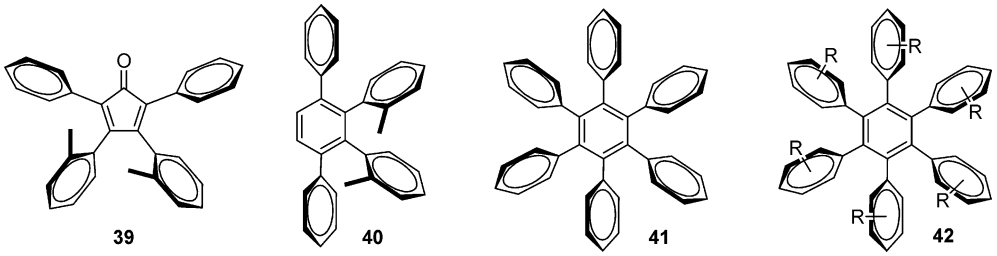

Figure 22. Some examples of aryl propellers on a planar skeleton.

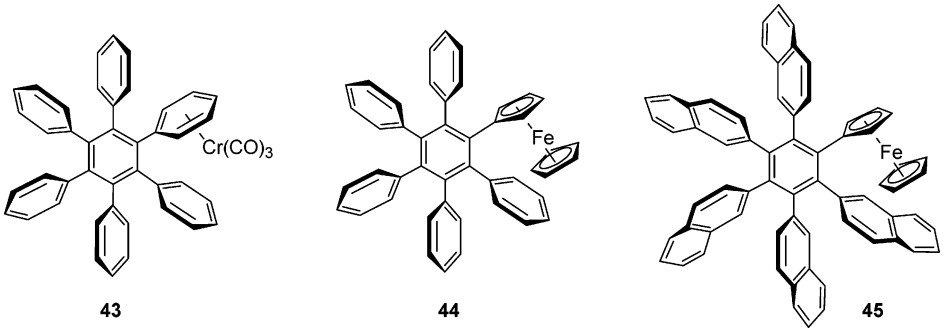

Figure 23. Organometallic polyarylated propeller systems.

sion, the authors found that increasing the chain length decreases the chance of correlated rotation throughout the chain. Instead of minimizing the steric interactions by rotations along the chain, the interactions are in fact localized and the threshold mechanism becomes correlated disrotation involving only two rings at a time.

Most of the barriers to rotation in polyaryl species such as those discussed above are below ($\Delta G^{\ddagger}$) 25 kcal mol^{-1} and thus lead to some isomerization at room temperature. Although barriers as high as ($\Delta G^{\ddagger}$) 30 kcal mol^{-1} ($t_{1/2}$ = 8 months at 20 °C) have been observed in binaphthyl ethers,[325] two-cogged gears have an inherent inefficiency as compared to gears with larger numbers of intermeshed teeth.

Systems in which the geared rotation is about a central, planar unit such as a phenyl ring have also been studied (Figure 22). The first example of a polyarene on a planar skeleton appears to be that of Sundaralingam and Jensen[226] for triphenylcyclopropenium perchlorate (**5**; Figure 10), for which the crystal structure showed a propeller conformation. Hayward-Farmer and Battiste[370] first investigated the tetraarylcyclopentadienone system and polyarylbenzene systems and found that the barriers to rotation were ($\Delta G^{\ddagger}$) 21.8 kcal mol^{-1} in 3,4-bis(*o*-tolyl)-2,5-biphenylcyclopentadienone (**39**) and above ($\Delta G^{\ddagger}$) 25.6 kcal mol^{-1} in 1,2-bis(*o*-tolyl)-3,6-diphenylbenzene (**40**).

Gust and co-workers[363,364] studied rotational isomerism on hexaarylbenzenes in the late 1970s. The static stereochemistry shows that the aryl rings prefer a conformation perpendicular to the central benzene, with librations about the $C_{Ar}-C_{Ph}$ bond in and out of this arrangement. An X-ray structure of hexaphenylbenzene (**41**)[371] had previously shown the phenyl rings to prefer a "propeller" conformation with a ~65° angle with respect to the central benzene, and electron diffraction[372] predicted an essentially perpendicular arrangement of the phenyl rings with librations of ±10° from normal. Gust and co-workers[363,364] used sterically demanding *o*- and *m*-substituted phenyl rings to increase the barriers to rotation. For rings bearing *o*-substituents (**42**; R = Me, OMe), the barriers were as high as ($\Delta G^{\ddagger}$) 38 kcal mol^{-1} for the aryl ring to pass through a transition state in which it is coplanar with the central benzene ring. For *m*-substituted phenyls, the barriers were significantly smaller ($\Delta G^{\ddagger}$ ~17 kcal mol^{-1}). The values have been assigned to one-ring flip mechanisms, followed by rotational relaxation of the other five rings, which inverts the helicity of the molecule. Conversion to the enantiomer would require that all six rings flip, but this is energetically very unfavorable. Pepermans et al.[366,373] also investigated hexaarylbenzenes and found similar results.

McGlinchey and co-workers[374−377] used organometallic labels to differentiate the aryl rings on hexaarylbenzene propeller systems (Figure 23). In hexaphenylbenzene chromium tricarbonyl (**43**),[375] the unhindered rotation of the rings leads to overall C_{2v} symmetry, which is reduced to C_s when the rotation of the phenyl ring bearing the chromium group is slowed on the NMR time scale (−100 °C). The value for the rotational barrier ($\Delta G^{\ddagger}$) of the complexed ring was found to be ~12 kcal mol^{-1}. This is lower than the value obtained by Gust and co-workers, but it was not possible to tell if this was a result of a stabilization effect on the transition state of destabilization of the ground state. Replacing the phenyl-$Cr(CO)_3$ unit by a ferrocene group (**44**), McGlinchey and colleagues[376] found that a propeller conformation was not the lowest energy structure. Instead, as evidenced in the crystal structure, the rings exhibit an incremental progression of twist angle (51° to 120°) with respect to the central benzene ring. The ferrocenyl unit lowers the barrier relative to that of the corresponding chromium tricarbonyl complex **43**, such that propeller interconversions could not be observed on the NMR time scale. To understand the effect of

the ferrocene group on propeller dynamics of phenylated benzenes, larger naphthalene groups were chosen.[377,378] McGlinchey and collaborators[377] synthesized ferrocenylpenta(2-naphthyl)benzene (**45**) and studied it by DNMR and X-ray crystallography. The solid-state structure exhibits disorder at three of the naphthalene rings, and the low-temperature NMR confirms that the molecule is a mixture of rotamers (at least three diastereomers). Clearly, these systems do not represent good candidates for molecular gears, and the authors have suggested[377] even bulkier groups, but it is unclear whether this design scheme will produce nanoscale applications.

Willem et al.[360,361] reinvestigated tetraarylcyclopentadienones (**46**) in the early 1980s and found the interconversion pathways to be one or two sequential one-ring flip mechanisms based on whether the phenyl ring on the carbon α to the ketone or the one on the carbon β to the ketone rotates (Figure 24).

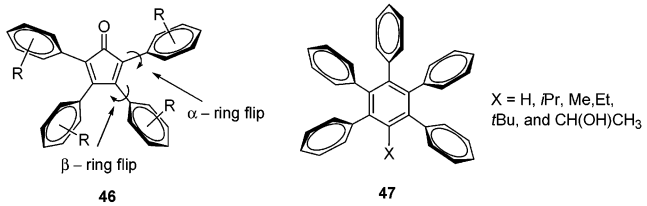

Figure 24. Pentaphenylated planar arene propellers.

They concluded that the threshold mechanism was the uncorrelated rotation of the α-phenyl ring via a one-ring flip. In an similar example, Gust and co-workers[365] observed that phenyl groups in pentaphenylbenzenes (**47**) adjacent to the nonphenylated position rotate much more easily if X is smaller than a phenyl ring. Brydges and McGlinchey[362] used semiempirical calculations and structure−conversion path correlation to study polyphenylated cyclopentadiene and cyclopentadienones (**46**). They concluded that the rotations of the α and β phenyl groups are only partially correlated and describe the threshold mechanism for rotation as a "delayed *n*-ring-flip" mechanism which would not be observable by NMR methods. A flip of the α ring is followed by that of the β ring at some delayed time, indicating that the rotations of the two are not truly geared. This is more evidence for the likelihood that molecular gears based on phenyl−phenyl interdigitation will not find use in the practical world.

A number of groups have also investigated geared rotation in arene systems computationally. Knop and co-workers[379] have investigated tetraphenyl "windmill" systems of boron, carbon, and nitrogen using ab initio (HF) and DFT calculations. They predicted the activation energy for concerted rotation of the phenyl rings to be (E_{calc}) ~5.0 kcal mol^{-1} in BPh_4^-, ~6.4 kcal mol^{-1} in CPh_4, and ~7.9 kcal mol^{-1} in NPh_4^+. A number of reviews[165,194,195,199,201] give a more comprehensive treatment of correlated rotations in arene-based propeller systems.

Gears with planar symmetry ("two-toothed" gears) are terribly inefficient and find almost no use in the macroscopic world. The complex and debated mechanisms for isomerization of geared systems based on arene propeller molecules show this macroscopic observation pertains to the nanoscopic world as well. Again, although the arene-based gear systems are unlikely to find uses in the design of molecular machines, the scientific knowledge gained is likely to help us understand the extent to which the information we have gleaned from the extensive study of simple (or even complex) macroscopic machines will be useful when the same devices are shrunk to the dimensions of molecules. The information obtained from the work mentioned above was instrumental in designing the first truly geared systems, which will be discussed in the next section.

5.1.6. Triptycenes

The laboratories of Iwamura and Mislow[148] reported the first examples of truly geared rotation, in ditriptycyl ethers (Tp_2X; X = O) and ditriptycylmethanes (Tp_2X; X = CH_2). Interestingly, both groups came upon these systems independently and concurrently in the early 1980s.[148] As shown in Figure 25, they consist of two three-toothed gears, and the intermeshing between the phenyl groups on the two triptycenes leads to little or no slippage of the gears, even at high temperatures. In these systems, there is no doubt that rotation of one triptycene unit causes the disrotation of the other in a frame of reference that keeps the central linker atom static. Before discussing the work in this field, a distinction must be made between *static* and *dynamic gearing*.[273] Static gearing is defined as the intermeshing of groups in the ground state due to steric crowding and is commonplace in organic and inorganic chemistry. Dynamic gearing is defined as "the special effect on the rate or mechanism of a process that may be attributed to the intermeshing of a chemical [rotator] with neighboring groups"[201] and is much rarer in the chemical literature (cf. "the gear effect"; section 5.1.3).[197]

Earlier work by Ōki and co-workers[380] had shown that bridgehead-substituted triptycenes (Tps) behave as molecular gears with high barriers to rotation (Figure 26). Ōki and others have investigated triptycenes substituted at the bridgehead with benzyl,[381−383] mesityl,[381,384] and phenoxy[382,385,386] groups.

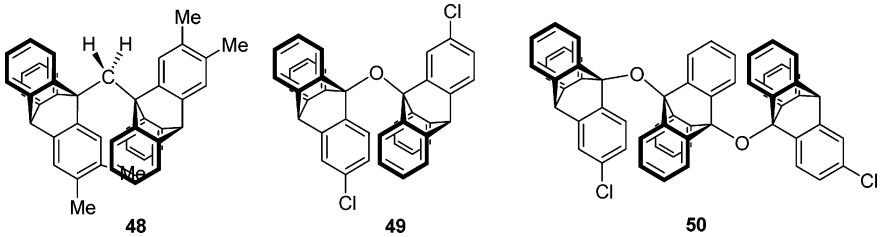

Figure 25. Triptycene-based molecular gears.

Mislow's group and Iwamura's group extended these studies into the ditriptycyl geared systems shown in Figure 25.[148]

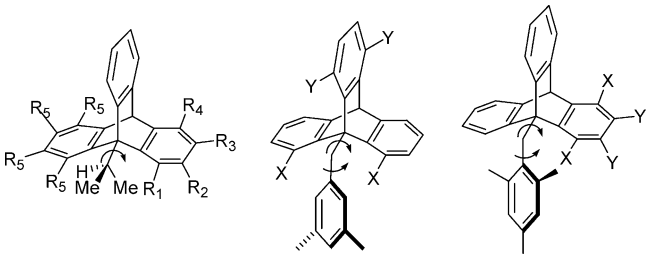

Figure 26. Early triptycene molecular rotors.

Empirical force field calculations[387] predicted a barrier of only 1 kcal mol^{-1} to rotation in Tp_2CH_2 from the C_s ground state through the C_2 transition state, implying that correlated rotation was nearly barrierless. To probe geared rotation by NMR, differentially substituted ditriptycyls needed to be synthesized, and Mislow[387] provided a full permutational analysis for the different types of substitution patterns that would lead to isomers under geared and nongeared rotation. Mislow[388] and Iwamura[389] simultaneously published the realization of this concept in back-to-back papers in 1981 for Tp_2CH_2 and Tp_2O derivatives, respectively. In Tp_2X derivatives with only one substituted triptycene benzene ring, nine isomers are predicted: one achiral *meso* isomer and four diastereomeric *dl* pairs.[387,390] Under the operation of dynamic gearing, some isomers interconvert and only three residual isomers remain: a *meso* isomer (consisting of one achiral conformer and a *dl* pair) and two enantiomeric *D* and *L* residual isomers (each with three chiral conformers). To interconvert isomers, *gear slippage* would have to occur, meaning that one triptycene would temporarily become uncogged from the tooth of the other. Mislow[388] chose to investigate the dimethyl analogue **48**, and Iwamura[389] observed the phenomenon in the chloro analogue **49** (Figure 25). Both found that diastereomers were observable and separable and that the barrier ($\Delta G^{\ddagger}$) to isomerization (gear slippage) was quite high: ~34 kcal mol^{-1} for **48** and >25 kcal mol^{-1} for **49**. After these initial successes, many variations of the original systems were investigated. In all cases, isomer interconversion did not occur at room temperature and the barriers to gear slippage ($\Delta G^{\ddagger}$) exceeded 30 kcal mol^{-1}. The benzene rings on one triptycene fit well into the cleft formed by two of the benzene rings on the other, causing the rotation of one to induce the correlated disrotation of the second and making slippage unfavorable.

Iwamura and co-workers[391] investigated a substituted bis(triptycyloxy)triptycene (Tp′OTpOTp′, **50**) compound to investigate whether dynamic gearing could be observed in doubly geared molecules (analogous to the rotor chains discussed earlier). They found this to be possible with an extremely high activation energy for gear slippage (E_a = 43.2 kcal mol^{-1}), and they proved that stereochemical information from one terminal triptycene unit can be transferred to the other one via the unlabeled central triptycene unit through cooperative geared motions. This system provided the first example of a molecular species that could adequately mimic the behavior of a macroscopic counterpart and the rules that govern rotation, and it demonstrated the inherent advantage of the three-toothed over the two-toothed wheels.

Mislow and co-workers[392,393] also investigated the three-cogged rotors tris(9-triptycyl)cyclopropenium perchlorate (**51**) and tris(9-triptycyl)germanium chloride (**52**), which allowed them to investigate selection rules for molecular gears (Figure 27). If one triptycene rotates, the second must rotate in a disrotatory fashion, while the third would only be allowed to rotate conrotatory with respect to the first. In a cyclic system, this clearly cannot be done, and thus, cogwheeling in this system is forbidden, as one would expect from imagining a macroscopic analogue. As with macroscopic gears, correlated rotation in a cyclic gear system can only occur if the number of cogwheels is even, and this was observed to be the case in the molecular system also. Therefore, rotation in these molecules can *only* occur via gear slippage. This is borne out in the experiment. The high barriers to topomerization ($\Delta G^{\ddagger}$ ~ 20.0 kcal mol^{-1}) in these systems contrast with the low ($\Delta G^{\ddagger}$ ~ 5 kcal mol^{-1}) barriers for correlated disrotation observed in bis(9-triptycyl)methanes, and it is clear that this gearing system does not operate with the same fidelity. The authors conclude: "9-triptycyl systems are therefore the only molecular gears studied to date that match their mechanical counterparts in both static and dynamic properties, i.e., that follow the same classical mechanical laws as gears in the macroworld." Yamamoto and co-workers[394] studied methyltris(9-triptycyl)stannane and benzyltris(9-triptycyl)stannane and arrived at similar conclusions.

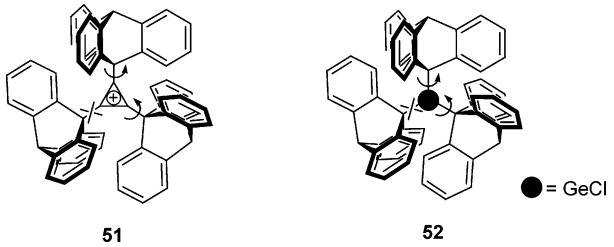

Figure 27. Tris(triptycyl) gears—formally disallowed geared rotation.

For macroscopic systems of this type, geared rotation would not be observed. At the molecular scale, however, thermally activated processes lead to gear slippage. Therefore, although the systems described above represent extraordinary achievements in furthering our understanding of how macroscopic rules relate to systems operating on the molecular scale, the particular exceptions that belong only to the nanoscopic regime must always be kept in mind in both the design of systems and in making claims as to whether those systems will be useful as molecular analogues. The difference is related to the scales at which the different systems operate and the value of kT relative to the barriers present (see section 3). For molecular systems at or around room temperature, kT is usually large enough to randomly excite rotational and vibrational modes that permit motion over barriers. Since molecular machines will most

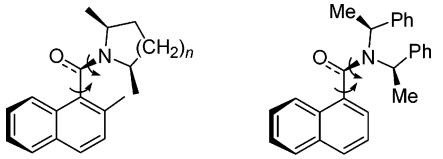

53a (n = 1)
53b (n = 2)

54

Figure 28. Aromatic amide gears.

likely run at room temperature or higher, this is an important point. However, it does not preclude the use of molecules in the fabrication of useful devices, because these random motions could possibly be harnessed and thermally activated rotation of molecules could help in the design of nanodevices. It is in this endeavor where truly important contributions to our understanding of the design and implementation of molecular machines will be realized. We have already briefly discussed Brownian motors in section 3, and we will discuss other examples of harnessed random motion in the later sections.

A more detailed discussion of gearing in these systems is available.[148,201] Triptycenes are synthetically accessible by addition of benzynes to anthracenes. However, the conditions for the in situ formation of benzyne are quite harsh and some functional groups are not tolerated. Protecting groups and subsequent substituent manipulation may be needed. Since these molecular gear systems represent the first true nanoscopic representation of a macroscopic gear, it will be interesting to see if work continues toward the development of geared systems with larger numbers of teeth per gear. Organometallic chemistry offers a wide variety of interesting structures with angles between units at fixed values, and the synthesis of *miter gears* (bevel gears held at 90° angles to one another; section 5.1.1) and other variations seems plausible. In sections 5.1.8 and 5.4 we will discuss some aspects of gearing in organometallic systems.

5.1.7. Aromatic Amides

Rotations about aryl-C=O groups in aromatic amides have been known for some time, and a number of interesting systems have been developed by exploiting the partial double bond character[161] of the structure and by introducing sterically demanding groups on both the aromatic ring and the amide nitrogen. Atropisomerism can be observed in substituted benzamides whose *o*-positions carry groups larger than a proton.[395] The C=O group then lies more or less perpendicular to the plane of the aromatic ring,[396,397] and the barrier to rotation can be high enough ($\Delta G^{\ddagger}$ between 25 and 40 kcal mol^{-1}) that enantiomers can be resolved[398−403] and the barriers to rotation of the amide unit can be measured.[404,405] Clayden and co-workers have used their experience in making chiral aromatic amides,[406−408] for use in stereocontrolled reactions,[409−416] toward the creation of "geared" molecular systems (Figure 28).[417,418] Using a sterically hindered 2-methyl-1-naphthamide system bearing a chiral pyrrolidine (**53a**), they found that aryl-CO bond rotation ($\Delta G_{306}^{\ddagger}$ = 26 kcal mol^{-1}) was correlated with C−N bond rotation ($\Delta G_{306}^{\ddagger}$ = 24 kcal mol^{-1}).[417] However, in this case, the barrier to slippage is quite low and the authors prefer to say that Ar−CO rotations are "gated" by C−N rotations. In a similar system, Johnston et al.[419] replaced the dimethylpyrrolidine by a dimethylpiperidine unit (**53b**) and found that the barrier to gear slippage in this system was extremely high and rotation occurred concertedly with a better than 99% efficiency. They proposed a disrotatory cogwheeling mechanism for the rotation. Clayden and co-workers[418,420] also designed molecule **54**, in which correlated and uncorrelated rotations could easily be distinguished. The NMR shows a mixture of diastereomers, and because correlated rotations only interconvert enantiomers, and not diastereomers, variable-temperature NMR should only cause the coalescence of some of the peaks and not others if the rotations are geared. This is indeed what was found, and the authors concluded that correlated rotation accounted for more than one-third of the rotational processes, with a rate of approximately 10 Hz at room temperature. For less hindered amides, C−N rotation occurs more slowly than Ar−CO rotation and the processes are not correlated. As the steric hindrance increases, the rate of Ar−CO rotation decreases until the two appear to have the same rate, giving rise to geared rotation. Once again, this points out the importance of synthetic tunability in designing, studying, and improving molecular systems.

As in previous examples, although these systems are important in furthering our understanding of geared systems and expanding the "tool box" with which synthetic chemists can work, aromatic amide systems would appear to lack the fidelity to rival their macroscopic counterparts on the nanoscale. Although synthetically accessible, aromatic amides are relatively reactive, and the two-toothed gears discussed here suffer from the same problems as those discussed above for the phenyl systems. Amines also suffer from stereochemical complications due to nitrogen inversion, which must be taken into account when determining whether such systems have useful applications. However, in these cases, it did not provide an insurmountable impediment to their study.

5.1.8. Gearing in Organometallic and Inorganic Systems

A number of groups have investigated rotations in organometallic and inorganic molecules, some of which were discussed in previous sections where relevant. Hellwinkel et al.[421] investigated rotations in propeller molecules in naphthyl-substituted spirophosphoranes (**55**) as a function of the substituent (X) in the 8-position of the naphthalene unit (Figure 29). They found the size sequence X = $N(CH_3)_2$ > OCH_3 > CH_3 ≈ Br ≈ Cl > F > H > electron pair, where the electron pair was carried by an aza nitrogen (**56**). This important information on steric size was alluded to in section 5.1.3. Knowledge of such factors arms the synthetic chemist with an arsenal of possible functional groups to either increase of decrease rotational barriers when designing the synthesis of a molecular target.

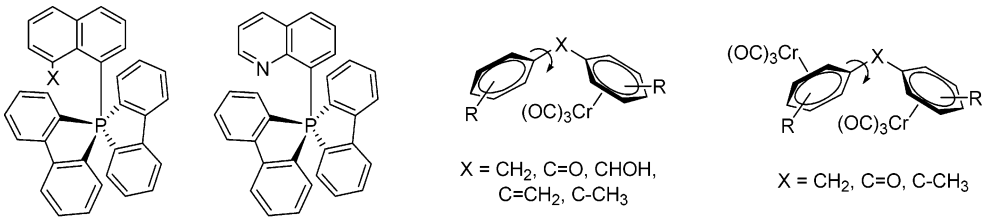

55 56 57 58

Figure 29. Examples of organometallic gears.

Trahanovsky, Kowalski, and Avery[422] first investigated the dynamics of monochromium tricarbonyl complexes of diarylmethanes, diaryl ketones, diarylmethanols, and diarylethenes (**57**), and they suggested that the rotation of the complexed ring was correlated with that of the uncomplexed ring. Barriers for the uncomplexed ring were in the range of ($\Delta G^{\ddagger}$) 14−20 kcal mol^{-1}. Weissensteiner, Scharf, and Schlögl[338] studied mono- (**57**) and bis(tricarbonylchromium) (**58**) complexes of diarylmethanes, diarylethanes, and diaryl ketones. They concluded that adding an additional $(CO)_3Cr$ did not change the barrier dramatically, which implies either that there was a change in the ground-state and the transition-state geometries or that the rotations were not correlated to begin with.

Aylett and Taghipour[423] discussed the possibility of "multiple-cogwheel" rotation in $ISi[M(CO)_5]_3$ and $Si[M(CO)_5]_4$ (M = Mn, Re) clusters (**59**; Figure 30).

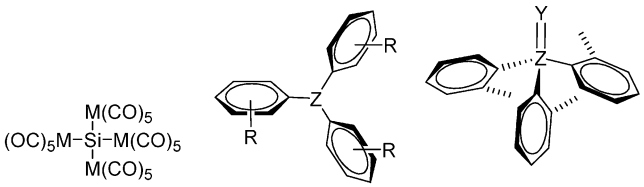

59 60 61

Figure 30. Some other organometallic gears.

Due to the highly congested nature of the complexes, it was deemed likely that the rotation of one $M(CO)_5$ group would include the concerted rotation of the others. However, they could only conclude this via molecular models and infrared data because low solubilities of the compounds precluded NMR studies. Were this an example of geared rotation, it would represent a cyclic gear system of four four-toothed gears (one metal−carbonyl bond is axial and would not contribute to gearing). In section 5.1.6, we discussed the selection rules for cyclic gear systems, with four in an array being allowed. This compound would be an example of such a system, and barriers to gear slippage in this or related compounds would be an interesting investigation, especially in the solid state. In section 6, we will mention some examples of geared rotations in the solid state.

Many organometallic counterparts of the organic compounds discussed above were also studied as geared systems. Binsch and co-workers[350] studied phosphorus and arsenic analogues of triarylmethanes (**60**), and Howell et al.[351] investigated the silicon and germanium analogues as well (Figure 30). The latter group also investigated the effect of a chalcogen attached to the phosphorus atom (**61**) and found that the barrier to rotation roughly scales with the van der Waals radius of the chalcogen (O < S < Se). Here, the rotationally isotropic atomic group contributes to the rotational barrier, likely due to steric repulsions of the chalcogen electron cloud from that of the rotating phenyl rings and well as changing the valence angles about the phosphorus.

McGlinchey and co-workers[424] have combined the chemistry of triptycenes (section 5.1.6) with that of chromium coordination to phenyl rings[425] in their attempt to synthesize a molecular brake. They synthesized 9-indenyltriptycene and complexed it to a chromium tricarbonyl fragment (**62**), hoping that the metal fragment will be movable between the five- and six-membered rings of the indene (Figure 31). Depro-

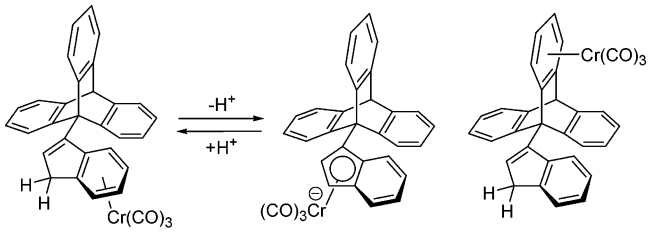

62 63 64

Figure 31. Organometallic gearing systems on a triptycene scaffold.

tonation is known to create a haptotropic shift ($\eta^6 \rightarrow \eta^5$) of the metal fragment to the five-membered ring (**63**),[289] and protonation reverses the process, as shown in Figure 31. However, the chromium tricarbonyl preferred the triptycene phenyl groups over the benzene ring of the indene, and only compound **64** was isolated. The barrier to rotation ($\Delta G^{\ddagger}$) in this molecule was found to be ~13 kcal mol^{-1} by line shape NMR analysis.

Other inorganic and organometallic systems studied for dynamic gearing and hindered rotations include tetrakis(pyridine)ruthenium(II) complexes,[426] iron-diene complexes,[427] osmium clusters,[428,429] bulky silanes,[430−432] and chiral arylamido aluminates.[433]

5.2. Rotation in Nonsandwich Porphyrins

Porphyrins, metalloporphyrins, and their linked arrays are important in the study of light-harvesting antennae and as synthetic models of photosynthetic reaction centers. Porphyrin arrays have also been used in the study of energy transfer for use in solar energy conversion and in molecular electronics. In 2000, a ten-volume compendium called *The Porphyrin Handbook*,[434] covering all aspects of porphyrin chemistry, was published.[435] Because this compen-

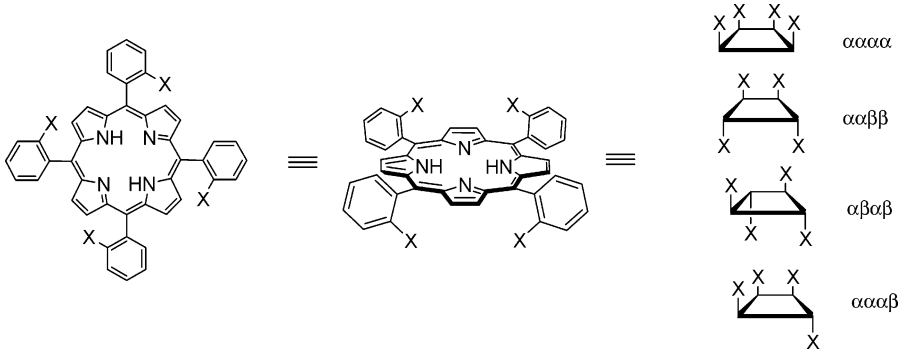

Figure 32. Atropisomeric forms of tetra(*o*-X-phenyl)porphyrins.

dium covers porphyrins in chemistry, physics, biology, medicine, and materials science, we will give only a brief overview of rotational processes in porphyrins. Reviews of electron transfer in molecules mimicking photosynthetic systems, with a large focus on porphyrin systems, have been written by Wasielewski,[436,437] Harriman and Sauvage,[438] and Hayashi and Ogoshi.[439] For a discussion of porphyrins studied for use in molecular devices and machines, the book by Balzani et al.[26] can be consulted. The barriers to rotation in dodecaarylporphyrin dications, 5,15-diarylporphyrins, and 5,15-diaryl-2,3,7,8,12,13,-17,18-octaalkylporphyrins were reviewed by Medforth.[440,441]

5.2.1. Rotation of Phenyl Groups in Phenylporphyrins (PPs)

The rotation of the phenyl groups in substituted and unsubstituted 5,10,15,20-tetraphenylporphyrins (TPPs) has been known since the 1970s, and within the last 30 years, many other rotational processes in porphyrins have been studied. Recently, Medforth[441] has published a review of rotational processes in diamagnetic porphyrins, concentrating on work published since two early reviews appeared.[442,443]

The rotation of phenyl rings in TPP and substituted derivatives is very similar to the atropisomerism observed in biphenyls and related systems discussed in section 5.1.2, and the nomenclature is often the same. For a phenyl group to rotate, it must pass through the plane of the porphyrin, much like two aryl rings in a biphenyl must become coplanar in the transition state (Figure 8). Typically, *ortho*-substituted phenyls and some *meta*-substituted phenyls give rise to atropisomerism observable on the NMR time scale, which has almost solely been used to observe and measure activation barriers for such processes. In a conformationally immobile system, four atropisomers exist for TPPs, differing by the location of the substituent above (α) or below (*β*) the porphyrin plane: αααα, ααα*β*, α*β*α*β*, and αα*ββ* (Figure 32).

Gottwald and Ullman[444] were the first to observe rotation of the phenyl rings in TPPs (Figure 33) in tetra-*o*-hydroxyphenylporphyrin (*o*-OH-TPP; **65**). Due to the relatively large barriers to rotation, they isolated the four isomers on silica gel and studied the isomerization crudely by thin-layer chromatography separation followed by spectroscopic identification. Isomerization at room temperature occurred with a first-order rate constant of $(1.5 \pm 0.5) \times 10^{-5}$ s^{-1}, which corresponds to an activation barrier ($\Delta G^{\ddagger}_{293}$) of 24.0 kcal mol^{-1}. To test whether distortion from planarity of the porphyrin ring ("ruffling"[445]) occurred in the transition state, they made the more rigid copper metalloporphyrin (**66**), but they found that the activation barrier increased only slightly to ($\Delta G^{\ddagger}_{293}$) 25.4 kcal mol^{-1}. Metalated porphyrins are not as flexible as their free-base congeners and are thus not as susceptible to ruffling. This makes the passage of the sterically demanding phenyl group through the plane of the porphyrin more difficult, and the resulting activation energy for the rotation is thus higher. However, the small change indicated that the ruffling may not be very important. Soon after, Walker and Avery[446] discovered atropisomerization in nickel(II) tetra-*o*-tolylporphyrinate [Ni(*o*-tol-TPP), **67**], and they found the barrier to rotation to be at least ($\Delta G^{\ddagger}$) 26 kcal mol^{-1} using DNMR. Because of experimental limitations, they could not determine the exact value.

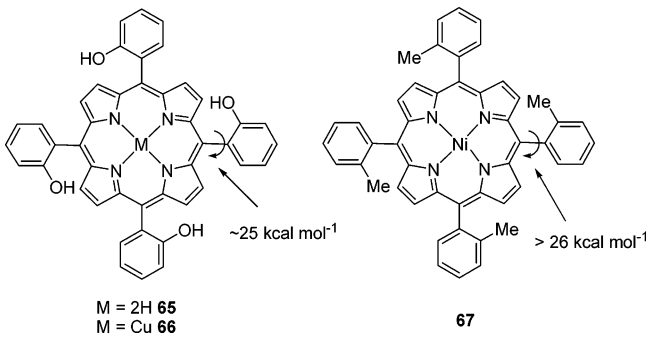

Figure 33. Early tetraphenylporphyrin systems for the study of phenyl ring rotation.

After these initial successes in observing atropisomerism in TPPs, Eaton and Eaton[447−452] published a series of papers discussing rotation in substituted metalated TPP complexes of Ru(II), In(III), Ga(III), and Ti(IV) (**68**−**76**, Figure 34) bearing axial ligands (which render them asymmetrical). Depending on the metal and the ligand, they found activation energies ($\Delta G^{\ddagger}_{298}$) between 13.0 and more than 23 kcal mol^{-1} using DNMR (Table 2). For *o*-Me-TPP complexes of In and Ru (**77**), the barriers were too high to measure by DNMR.[450] Reference 451 provides a comprehensive table of $\Delta G^{\ddagger}_{298}$, $\Delta H^{\ddagger}$, $\Delta S^{\ddagger}$, E_a, and rate constant data for a variety of Ru(III), In(III), and Ti(IV) complexes, and reference 452 has a similar table for Ga(III) complexes.

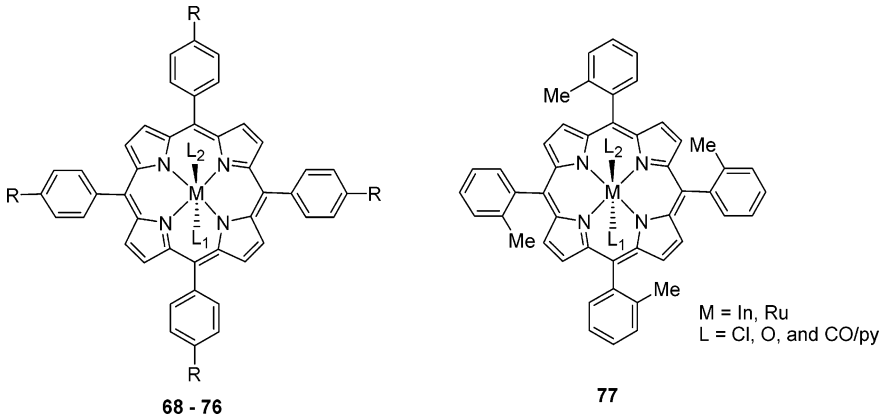

Figure 34. Octahedral porphyrin complexes exhibiting hindered rotation of the phenyl groups. For **68**−**76**, R, M, L_1, and L_2 are defined in Table 2.

Table 2. Characteristic Energies for Phenyl Group Rotations in Metalated Tetraphenylporphyrins Bearing One or Two Axial Ligands on the Metal, as Shown in Figure 34

M	R	L_1	L_2	$\Delta G^{\ddagger}_{298}$ (kcal mol^{-1})	compd	ref
In	*i*Pr	Cl		16.2	**68**	450
Ti	*i*Pr	O		15.6	**69**	450
In	CF_3	Cl		17.0	**70**	450
Ti	CF_3	O		16.3	**71**	450
Ru	CF_3	CO	THF	17.5	**72**	450
In	CH_3	CO		>20	**73**	450
Ru	CH_3	CO	Py	>20	**74**	450
Ru	*i*Pr	CO	EtOH	19.9	**75**	448
Ru	*i*Pr	CO	DMP	18.6	**76**	447

Gust and co-workers[453] investigated the DNMR of H_2TPPs and diprotonated H_4TPPs (Figure 35). They found an activation barrier ($\Delta G^{\ddagger}_{433}$) of 25.9 kcal mol^{-1} for H_2(*o*-OMe-TPP) (**78**) and a slightly lower barrier ($\Delta G^{\ddagger}_{388}$ = 23 kcal mol^{-1}) for the dication **79**. Similarly, for di-*o*-OMe-TPP, they found $\Delta G^{\ddagger}_{433}$ = 25.2 kcal mol^{-1} for the parent **80** and $\Delta G^{\ddagger}_{388}$ = 21.8 kcal mol^{-1} for diacid **81**. The diacids are known to be less conformationally rigid than the free-base porphyrins, which are in themselves less rigid than metalated porphyrins, and this accounts for the lower barrier to phenyl rotation. Hatano et al.[454] studied the dynamics of *o*-CN-TPP (**82**) and found an activation energy (E_a) of about 21 kcal mol^{-1} for the rotation of one phenyl group. Medforth and co-workers[455] investigated atropisomerism in TPPs with *o*-carborane appended to the *meta*-position of the phenyl rings (**83**). For the free-base porphyrin, they found a barrier to rotation of ($\Delta G^{\ddagger}_{323}$) ~17 kcal mol^{-1}, while the zinc

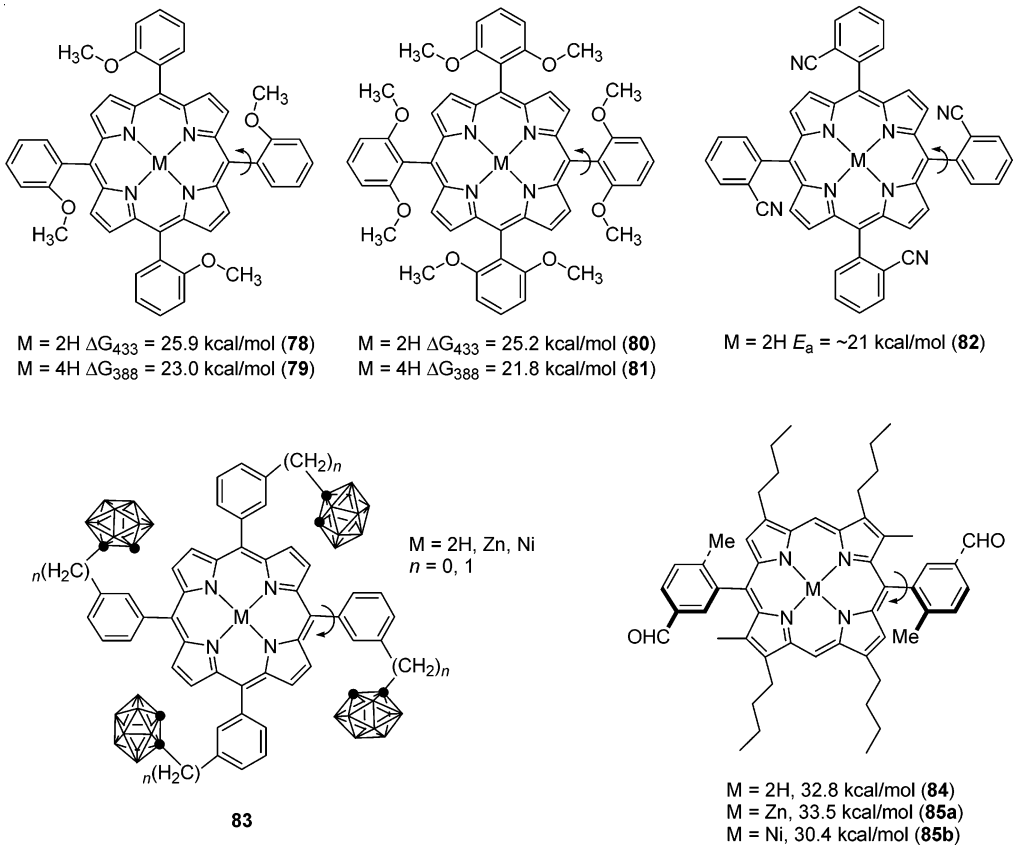

Figure 35. Barriers to rotation in substituted phenylporphyrins.

derivative had a barrier ($\Delta G^{\ddagger}$) of 18−19 kcal mol^{-1} and the nickel metalloporphyin had a barrier ($\Delta G^{\ddagger}_{243}$) of about 13 kcal mol^{-1}. Such barriers are lower than those typical for *ortho*-substituted TPPs but are higher than normal for *meta*-substituted TPPs, indicating the steric "size" of the carborane unit. Officer and co-workers studied atropisomerism in diphenylporphyrins containing *ortho*-methyl and *meta*-carboxaldehyde groups (**84**−**85**) as a function of the central unit (2H, Zn, and Ni). The barriers to rotation were similar to those for TPPs containing *ortho*-substituents ($\Delta G^{\ddagger} \sim 30-33$ kcal mol^{-1}) and agreed well with those for similar diphenylporphyrin systems.[456] These early results provided the groundwork for understanding the factors that influence the rotation about the $C_{porph}-C_{Ph}$ single bond. The ability of the porphyrin ring to distort from a planar structure lowers the activation barrier to rotation. However, the barrier is tunable, depending on the nature of the substituent on the aryl rings and on the state of the porphyrin ring (free-base, diacid, or metalated form). The choice of the metal serves to further fine-tune the relative energy to rotation of the phenyl rings.

In their studies on iron porphyrins as mimics for oxymyoglobins and oxyhemoglobins, Collman and co-workers were interested in the αααα-isomers of TPPs (Figure 32) bearing steric groups in the *ortho*-positions of the phenyl rings to form "picket fence" porphyrins.[457,458] The idea was to create a hydrophobic pocket by placing all the substituents on the same side of the porphyrin ring, which mimics the natural system and allows oxygen to enter where it is protected from other species by the pickets. In this way, they were able to crystallize the first iron porphyrin complex with bound dioxygen. Collman has reviewed his work in the field,[457] and others have investigated "picket fence" porphyrins[459−465] as models for naturally occurring heme systems.

Similar systems dubbed "pocket porphyrins" have also been studied by Collman and co-workers.[466,467] In these compounds, three of the *ortho*-substituents are bound (ααα) to form a cap, and the fourth substituent is in the β position, which forms a "pocket" on the α face for reversible oxygen binding. This work represents an elegant way to take advantage of the intrinsic rotational barriers in porphyrin molecules to make useful systems, in this case, to study biologically important molecular models. Whitten and co-workers[468,469] have studied tetraamido-TPPs similar to those investigated by Collman and collaborators (Figure 36). They performed a detailed study of the activation barriers to rotation (Table 3), both thermally and photochemically, for the free bases, the diprotonated forms, and metal containing complexes of tetra-*o*-propionamido-TPP (**86**−**91**), tetra-*o*-hexadecanamido-TPP (**92**−**97**), and tetra-*o*-pivalamido-TPP (**98**−**103**). Nickel(II) complexes gave the lowest barriers to rotation in all cases. This is not surprising, since Ni−TPP complexes are nonplanar in the solid state, indicating that deformation is possible and leads to a pathway for easier phenyl group rotation. As expected, they found that the zinc(II) complexes gave the highest barriers to rotation:

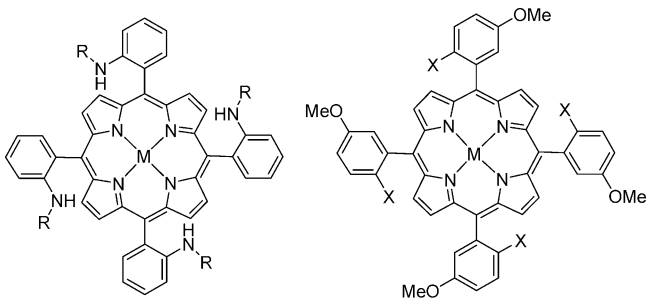

Figure 36. Picket fence porphyrins. See text for explanation of R and X groups.

Table 3. Characteristic Energies for the Rotation of Substituted Phenyl Groups in the Amido "Picket-Fence" Porphyrins Shown in Figure 36

M	R	$\Delta G^{\ddagger}_{383}$ (kcal mol^{-1})	compd	ref(s)
2H	$C(O)CH_2CH_3$	29.1	**86**	469
4H	$C(O)CH_2CH_3$	26.4	**87**	469
Ni(II)	$C(O)CH_2CH_3$	25.8	**88**	469
Cu(II)	$C(O)CH_2CH_3$	29.7	**89**	469
Pd(II)	$C(O)CH_2CH_3$	31.0	**90**	469
Zn(II)	$C(O)CH_2CH_3$	31.4	**91**	469
2H	$C(O)(CH_2)_{15}CH_3$	29.1	**92**	468, 469
4H	$C(O)(CH_2)_{15}CH_3$	26.5	**93**	468, 469
Ni(II)	$C(O)(CH_2)_{15}CH_3$	25.8	**94**	468, 469
Cu(II)	$C(O)(CH_2)_{15}CH_3$	29.6	**95**	468, 469
Pd(II)	$C(O)(CH_2)_{15}CH_3$	31.1	**96**	468, 469
Zn(II)	$C(O)(CH_2)_{15}CH_3$	31.2	**97**	468, 469
2H	$C(O)C(CH_3)_3$	30.6	**98**	468, 469
4H	$C(O)C(CH_3)_3$	28.3	**99**	469
Ni(II)	$C(O)C(CH_3)_3$		**100**	469
Cu(II)	$C(O)C(CH_3)_3$	31.4	**101**	469
Pd(II)	$C(O)C(CH_3)_3$	31.7	**102**	469
Zn(II)	$C(O)C(CH_3)_3$	32.2	**103**	469
2H	$C(O)OCH_3$	27.5[a]	**104**	471
Zn(II)	$C(O)OCH_3$	29.2[a]	**105**	471

[a] $\Delta G^{\ddagger}_{363}$ (kcal mol^{-1}).

Zn−TPP complexes are known to be the least deformable planar metal−TPP complexes in the solid state. Although the free-base and diacid compounds gave slightly higher barriers to rotation than the nickel(II) complexes, they were lower than all the other metals, presumably because they are more easily deformed. The diprotonated forms gave lower values than the free bases.

In general, the pivaloyl group gave higher barriers than the other groups, which indicates that the size of the *tert*-butyl group is more important than the chain length. The authors also found isomerization by photochemical activation of the porphyrins. In a study of triplet-excited porphyrins, Knyukshto et al.[470] found that rotational motion (libration) of the phenyl groups and the resultant deformations of the porphyrin ring led to shortened triplet lifetimes at room temperature. Photochemical isomerization via an electronically excited state offers another parameter by which rotational processes can be exploited.

The ability to change the rotational barriers by interconverting functional groups is a topic we have already touched upon and will continue to encounter throughout the article. Understanding structure−function relationships is of the utmost importance in designing and improving systems for nanoscience

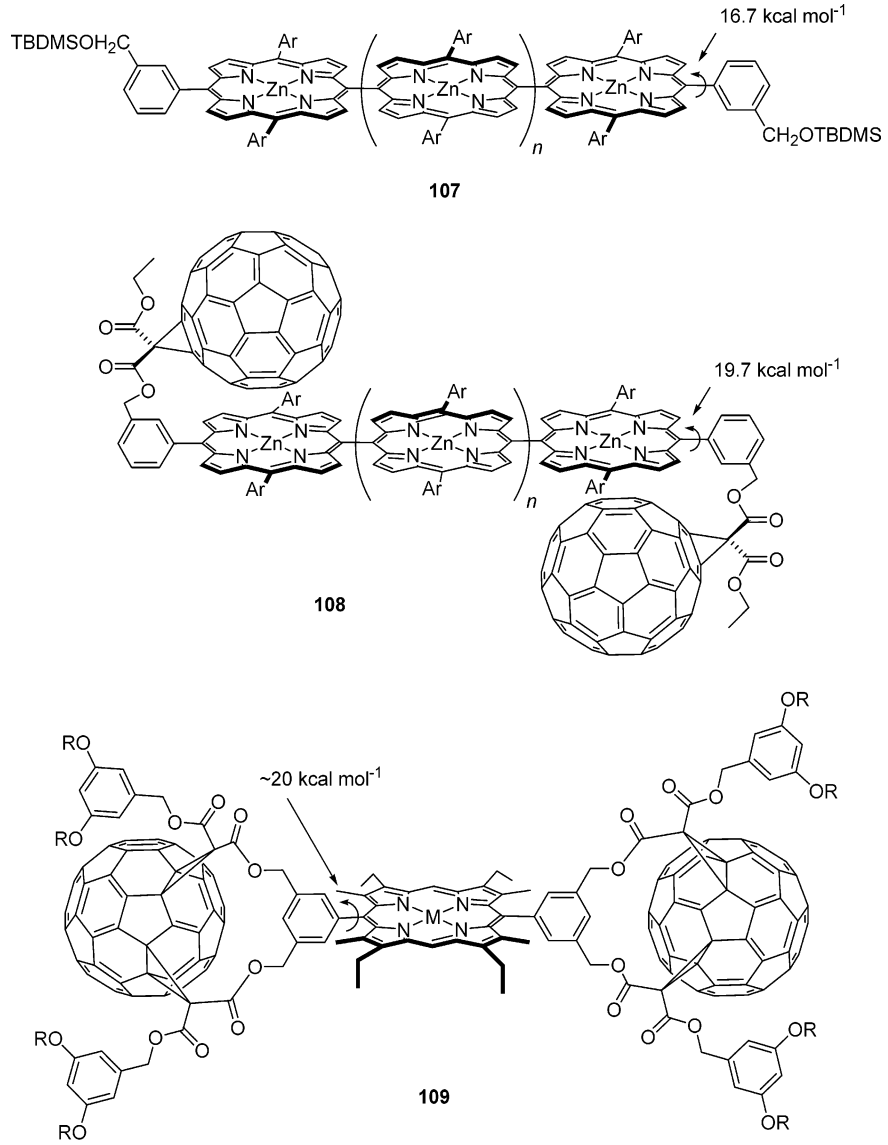

Figure 37. Porphyrin arrays with appended fullerene groups (TBDMS = *tert*-butyldimethylsilyl).

applications, and insight into steric effects on ground and transition states is one such parameter. Hatano et al.[463] performed detailed kinetic studies of rotation in tetra-*o*-amino-TPP and tetra-*o*-pivaloylamino-TPP. In comparing their data with those of other groups, they found the size order pivaloylamino > hexadecylamino ~ NH_2 > CN > MeO ~ OH. Fujimoto et al.[471] have investigated tetra-*o*-methoxycarbonyl-TPP "picket fence" porphyrins (**104**−**105**; Table 3). For the free base, they found an activation energy ($\Delta G^{\ddagger}$) of 27.5 kcal mol^{-1}; for the zinc(II) porphyrin it increased to ($\Delta G^{\ddagger}$) 29.2 kcal mol^{-1}. Sternhell and co-workers[472] studied the tetra-*o*-halide-TPP series (**106**; X = F, Cl, Br, I), similar to work by their laboratory on biphenyls.[319] Predictably, they find that rotation is fastest for fluorine and decreases through the series as the halide size increases. The barriers ($\Delta G^{\ddagger}_{340}$) were 22.9 kcal mol^{-1} for F,[473] 29.5 kcal mol^{-1} for Cl, 30.6 kcal mol^{-1} for Br, and 33.5 kcal mol^{-1} for I. These data for steric size agree well with those discussed previously.

Recently, Diederich and co-workers[474−477] have observed atropisomerization in porphyrin systems with appended C_{60} groups[478] in their investigation of molecular dyads for photosynthetic mimics. In precursor **107** (Figure 37, $n = 0$), the barrier to rotation ($\Delta G^{\ddagger}_{298}$) about the phenyl rings was 16.7 kcal mol^{-1}.[476] Upon appending two fullerene molecules to give compound **108** ($n = 0$), the barrier ($\Delta G^{\ddagger}_{298}$) rose to 19.7 kcal mol^{-1} when monitored by DNMR. Therefore, they deduced that the attractive interaction between the fullerene and the porphyrin increased the free energy to rotation by ~3.0 kcal mol^{-1} (the C_{60} is sufficiently removed as not to be involved in steric interactions in the transition state). In solution, **108** ($n = 0$) preferentially adopts a conformation where the fullerenes sit on opposite sides of the molecule, giving the C_2 symmetric structure shown in Figure 37. The same applies for the higher homomer ($n = 2$). In solution, the compound with three porphyrin units (**108**, $n = 1$) exists as a mixture of syn (C_{60} rings on the same side; C_{2v} symmetry) and anti (C_{60} rings on opposite sides; C_{2h} symmetry) forms in a ~1:1 ratio. Similarly, Diederich and co-workers investigated fused TPP systems with appended C_{60} molecules, but they did not examine the dynamics of isomerization.[477] Nierengarten et al.[479] have shown isomerization in 5,15-diphenylporphyrins bound to

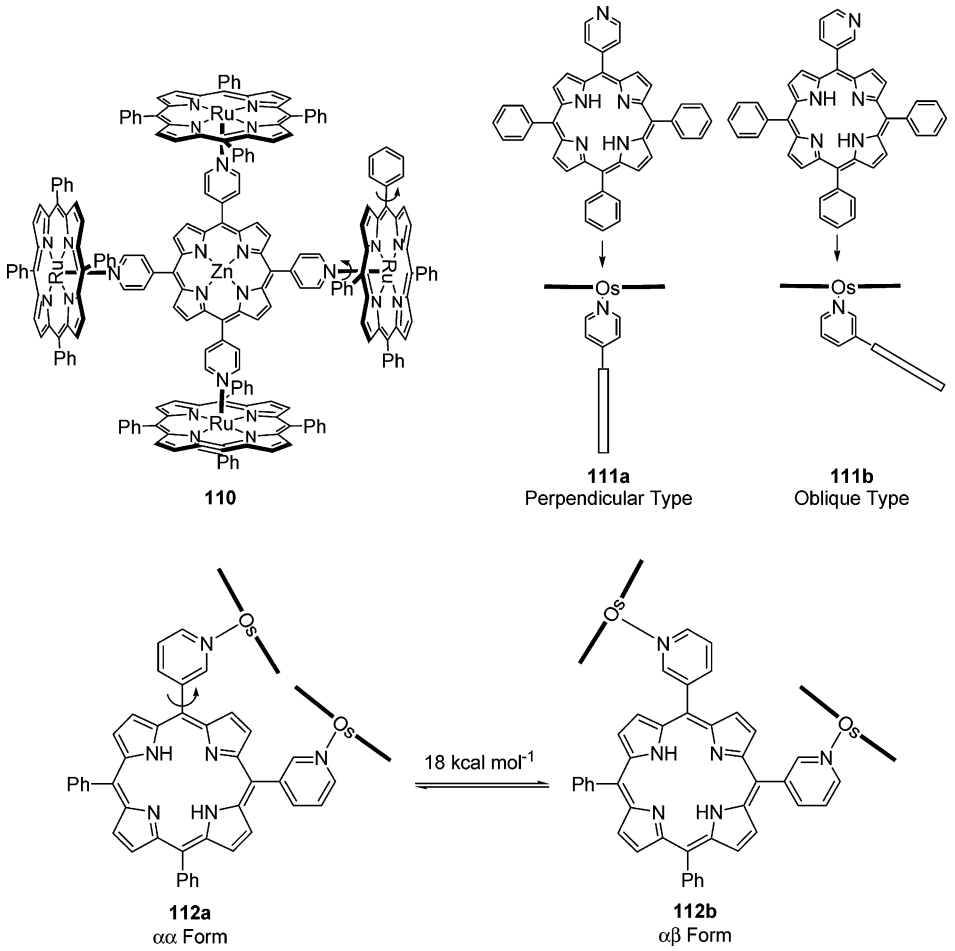

Figure 38. Rotors based on pyridylporphyrins.

fullerenes via benzyloxy tethers at the two *meta*-positions (**109**). They found a barrier ($\Delta G^{\ddagger}_{298}$) of ~20 kcal mol^{-1} for rotation about the phenyl−porphyrin bond.

Calculations have also been used to understand the structure−function relationship in phenylporphyrins and have aided the understanding of transition-state structures in these systems. Okuno et al.[480] have investigated phenyl ring rotations in phenylporphyrins using DFT. Not surprisingly, they found that in the transition state, which brings the phenyl ring into coplanarity with the porphyrin plane, the porphyrin ring distorts to avoid steric interactions with the *ortho*-hydrogens on the phenyl ring. The phenyl ring itself does not undergo significant distortion from planarity, and this was further supported by a calculation on the smaller biphenyl system. The authors concluded that porphyrin deformation contributes significantly to the barrier to rotation (and atropisomerism) observed in phenylporphyrins, and the introduction of *ortho*-substituents on the phenyl ring increases the steric bulk and hence the extent to which the porphyrin ring must deform to accommodate a coplanar transition state.

Avilov et al.[481] have used semiempirical methods (ZINDO) to look both at the steric conditions related to rotation and at the electronic effects of nitro-substituted phenyl groups, with the nitro group in the *ortho*-, *meta*-, or *para*-position. Like Okuno and co-workers, they found that severe deformations of the porphyrin ring accompanied phenyl rotation, especially when the nitro group was in the *ortho*-position. Because the porphyrin rings maintain their structures after the rotation, the distortion in the transition state does not appear to be prohibitive in the design of molecular machinery based on this design principle (molecules do not fatigue in the same manner that macroscopic analogues do). If one considers the usefulness in solid-state applications or situations where the porphyrin units are close-packed on a surface, the distortion of the porphyrin ring may indeed be a problem. However, one could argue that no rotation at all would be observed in such highly congested environments.

5.2.2. Rotations Involving Pyridylporphyrins (PyPs)

The ability to make multiporphyrin units based on the coordination of pyridine(s) on one unit to a metal center on another has led to fascinating architectural arrays.[482−485] Alessio et al.[486] synthesized an "open-box shaped" pentamer (**110**) consisting of a central, free-base, or zinc-complexed tetrapyridylporphyrin (TPyP) and four Ru−TPPs coordinated via a pyridine−Ru bond (Figure 38). They found a relatively simple NMR spectrum, indicating a highly symmetrical molecule in which all the Ru−TPPs rotated freely on the time scale of the observation, even though the individual phenyl groups showed atropisomerism. Similarly, Imamura and co-workers[487−491] have investigated ruthenium(II) and osmium(II) por-

phyrin oligomers based on mono-, di-, tri-, and tetrapyridylporphyrins. Systems with 4-pyridyl groups were called "perpendicular type" (**111a**), and those based on 3-pyridyl groups, "oblique type" (**111b**). Using an oblique type dipyridylporphyrin and complexing it to two Os(II) porphyrins (**112**), the authors found two distinct forms in the NMR spectrum—αα (**112a**) and αβ (**112b**)—which are atropisomers of each other (Figure 38). Coalescence of the two peaks in a variable-temperature NMR experiment occurred around 355 K, but evaluation of the activation parameters was impossible due to decomposition of the compound at this temperature. They estimated the interconversion barrier ($\Delta G^{\ddagger}_{355}$) between **112a** and **112b** to be about 18 kcal mol^{-1}, which is similar to barriers observed in TPPs, although lower than those observed in tetra-*o*-substituted-TPPs. Such an architecture could possibly be used for molecular switching devices, but they would have to be addressable in a simple way. Also, the stability of the compound makes it a questionable choice for molecular electronics applications where process temperatures are often higher than the decomposition temperature for this compound.

Allesio and co-workers[492] have also investigated an oblique-type PyP: a mono-3-pyridyl porphyrin bound to a Ru(II)−TPP. Again, rotation of the Ru−TPP about the Ru−N bond is fast, as evidenced by the equivalence of the phenyl groups in the NMR, while the individual rotations of the phenyl rings are slow at room temperature. Subsequently, Allesio et al.[493] investigated a pentameric complex of tetra-3-pyridyl-PyP [and its Zn(II) analogue] with Ru(II)−TPP and dubbed the resulting structure a "flying saucer". Surprisingly, they found unhindered rotation about the porphyrin−pyridine bond to make all 16 phenyl rings on the Ru−TPP equivalent (although hindered rotation about each phenyl−porphyrin bond was observed).

Miskelly and co-workers[494] were able to separate the metal complexes [Zn(II), Cu(II), and Ni(II)] of tetramethylated *o*-TPyP salts into their atropisomers and found them to be stable for more than a month at room temperature both in the solid state and in solution. This is encouraging for applications in information storage devices. Sanders and co-workers[495,496] and Osuka and co-workers[497] have also studied porphyrin arrays based on PyP scaffolds. The former group[498] observed atropisomerism in dipyridylporphyrins bearing osmium carbonyl clusters (Figure 39). They obtained a mixture of *cis* (**113a**) and *trans* isomers (**113b**) from the reaction of 5,10-dipyridylporphyrin with $Os_3(CO)_{10}(NCMe)_2$, but no attempt to determine the rotational barrier was made. A recent review by Imamura and Fukushima[499] has highlighted advances in self-assembled metalloporphyrin oligomers, and a number of recent reviews have concerned the wide synthetic design space available for multi-porphyrin arrays,[500,501] including PyPs.

In the above sections, we focused on the almost trivial rotational processes in PPs and PyPs and showed how such a simple rotation (analogous to a rotation in a biphenyl molecule) can be exploited to make interesting systems and possibly useful ones. In particular, Collman has used the hindered rotation of phenyl groups to synthesize and study molecules related to naturally occurring systems, and several examples of rotationally switchable molecules have been shown. In the next section, we discuss larger arrays and the rotational processes that occur in them.

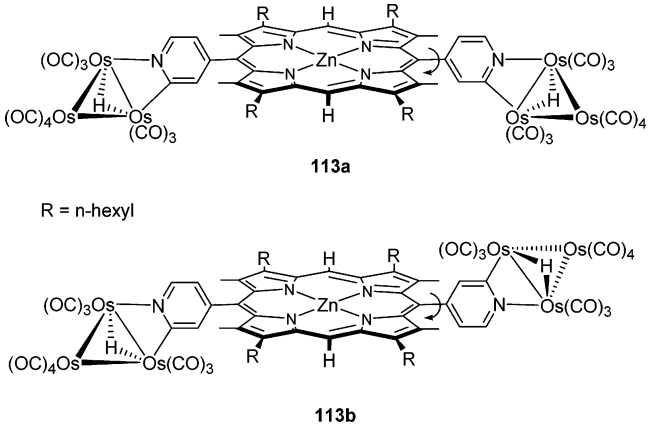

Figure 39. Isolated rotational isomers of dipyridylporphyrins coordinated to osmium clusters.

5.2.3. Rotations Involving Nonsandwich Porphyrin Arrays

Thus far, we have concerned ourselves with rotations involving groups (phenyl and pyridine) directly bound to the meso-positions of the porphyrin. Other investigators have studied systems with direct meso−meso linkages, linking through ethynyl groups, and other types of connections between porphyrins. Rotations in this miscellaneous category of compounds will be covered in this section. The rotation of alkyl, alkenyl, and amino groups attached to porphyrins and the rotation of axial ligands attached to the metal in metalloporphyrins was reviewed by Medforth.[441] The impetus of the work described in this section is derived from the desire to link porphyrin systems together in order to study electron transfer and other processes which occur in multiply linked porphyrins. Although electron transfer is not necessarily a rotational phenomenon, several groups have exploited rotational motion as a means of probing electronic communication.

Arrays of porphyrins linked to one another or to other molecules which can act as donors or acceptors (or both) with respect to the porphyrin is another area of interest, predominantly for making synthetic analogues of naturally occurring photosynthetic molecules.[436,502] Structure−function relationships in these systems are highly important in understanding the factors that govern energy transfer, and the literature in this area is very detailed in this respect. Lindsey and co-workers have been interested in studying systems based on TPP systems linked by ethynes as light-harvesting arrays (**114**−**119**).[503,504] In these compounds (Figure 40), they investigated energy transfer from a zinc porphyrin to a free-base porphyrin and found that the efficiencies are greater than 90% even though the ethyne linker couples the two porphyrins only weakly.[505,506] When *o*-methyl groups were placed on the phenyl group connected

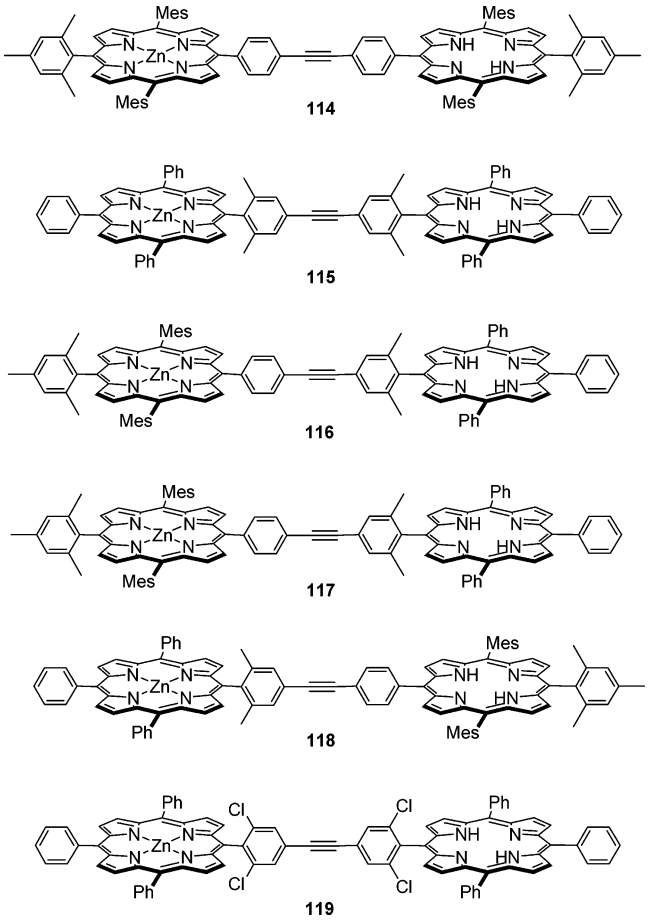

Figure 40. Linear porphyrin arrays.

to the ethyne linker (**115**), thus disrupting the ability of the porphyrin and the phenyl group to adopt a coplanar arrangement via rotation, a 4-fold decrease in the electron-transfer rate was observed.[507] Lifetime measurements also supported the fact that the energy transfer is a through-bond and not a through-space interaction. By placing chloro groups in the *o*- and *o*′-positions of the phenyl groups on the linker (**119**), the authors were able to look at both a steric and an electronic effect of the linker.[508] The results were very similar to those obtained with the tetra-*o*-methyl system, and the effect was determined to be steric, and not electronic, in nature, confirming earlier conclusions that coplanarity of the phenyl groups on the linker is necessary for efficient energy transfer. A more detailed study of the effects of rotation and the flexibility of the ethyne linker was performed[509] and showed that the phenyl groups prefer a coplanar arrangement but that the barrier to rotation (E_{calc}) about the triple bond is only about 0.8 kcal mol^{-1}. Considerable flexibility in the ethyne linker was also discovered, which could have a dramatic impact on energy transfer.[509]

To test whether rotation of the porphyrin units was important in energy transfer, Lindsey and collaborators[510] constructed "molecular box" **120** consisting of four TPPs connected via four ethyne linkers to form a square, which ensured coplanarity of the porphyrin units (Figure 41). The corners of the square were alternating zinc and free-base porphyrins. They found no difference in the energy-transfer rates in

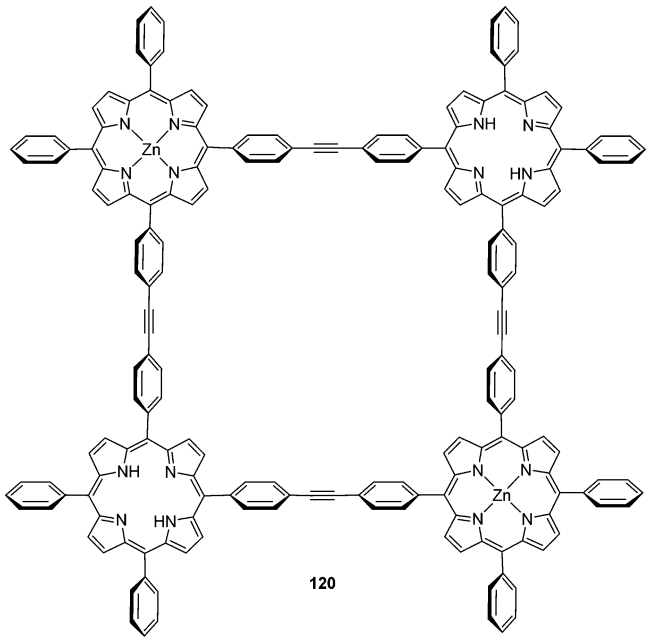

Figure 41. A porphyrin "square".

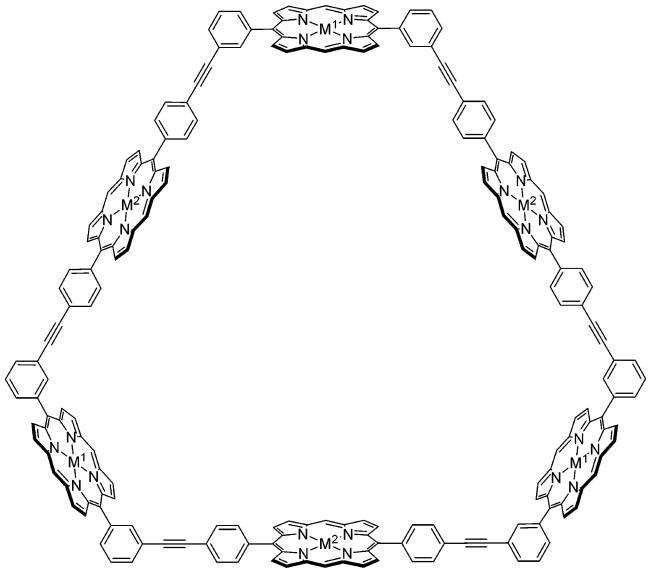

Figure 42. Hexameric porphyrin wheel. M^1 = Zn; M^2 = 2H.

this ensemble versus the linear system (both without groups that would hinder rotation of the linker). By synthesizing a "hexameric wheel of porphyrins"[511] (Figure 42), they concluded that frontier orbitals on the phenyl groups were more important to electronic communication than were torsional motions about the ethyne bonds. Lindsey and co-workers have reviewed their progress in this area[503] and recently[512,513] have shown that hindered rotations of appended aryl groups significantly alter the excited-state properties in related 5,5′-aryl-substituted bis(dipyrrinato)metal complexes.

Albinsson and co-workers[514−522] have investigated diporphyrin arrays connected via bridge molecules (B = benzene, naphthalene, anthracene, and bicyclo[2.2.2]octane) through *meso*-phenylethyne (PhCC) linkers in their research on triplet energy transfer (TET) (Figure 43; M = Zn, M′ = 2H). To interpret the results, they performed time-dependent density

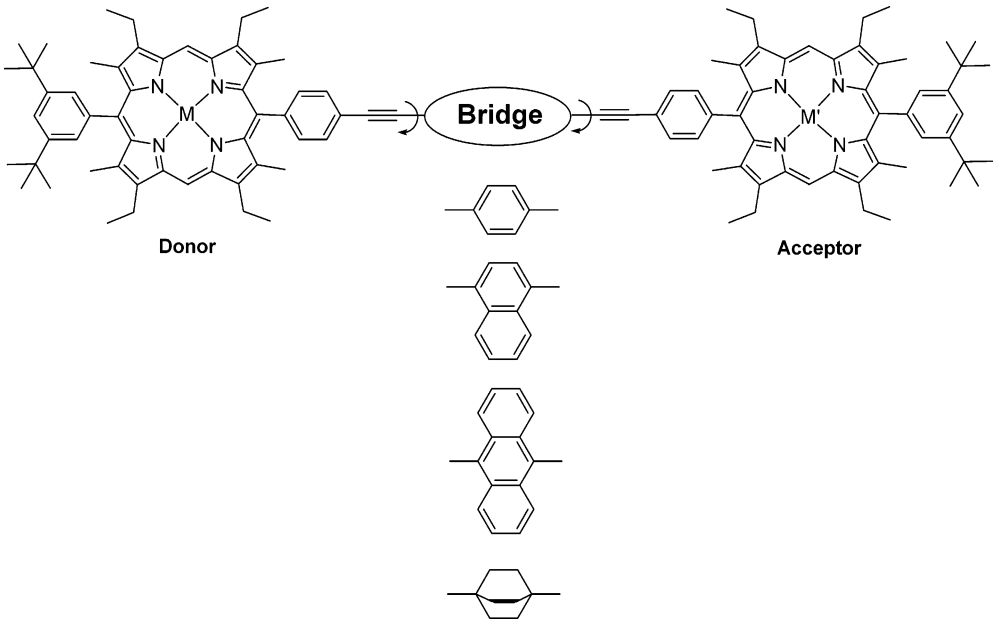

Figure 43. Donor and acceptor porphyrin systems separated by molecular bridge molecules.

functional theoretical (TD-DFT) calculations to determine the extent to which the torsional angle of the bridge molecule affects electron transfer.[519] They found no coupling when the bridge molecule was orthogonal to the porphyrin plane, in which the porphyrins were rotated and the PhCC−B−CCPh was kept coplanar. When the porphyrin−phenyl dihedral angle was set to 60° and the bridge molecule was rotated, the coupling was again found to be largest when the bridge was coplanar and significantly reduced in the twisted rotamer. The bicyclo-[2.2.2]octane bridge has been shown experimentally and computationally[516] to be a poor TET coupler, indicating the process is likely through-bond and not through-space. Albinsson and co-workers[517,521] have also studied hole transfer from gold to zinc porphyrins linked by the bridges described above (Figure 43; M= Zn, M′ = Au^+) and arrived at similar conclusions.

Okuno and Mashiko[523] have also studied the effects of torsional motion on excitation energy transfer (EET) using TD-DFT in a diphenylethyne linked diporphyrin system composed of one zinc porphyrin and one free-base porphyrin. They conclude that rotation affects the zinc porphyrin and not the free-base porphyrin. Such rotation induces an avoided crossing on the excited-state potential energy surface, and the EET is caused by a nonadiabatic interaction around the avoided crossing.

The synthesis of "windmill-like" arrays of porphyrins linked through direct meso−meso bonds has been investigated by Osuka and co-workers.[524−526] They made large arrays by connecting porphyrins through their meso-positions with phenyl groups or phenylacetylenes or by direct meso−meso coupling.[527−529] For a 1,4-phenylene linked trimer, where the two central porphyrins are meso−meso linked (to create a hexamer), they determined the barrier to rotation ($\Delta G^{\ddagger}$) of a peripheral porphyrin to be about 16 kcal mol^{-1}. In a "dodecameric porphyrin wheel"[530] (Figure 44), they found that the outer and inner porphyrinic β protons and the eight aromatic protons

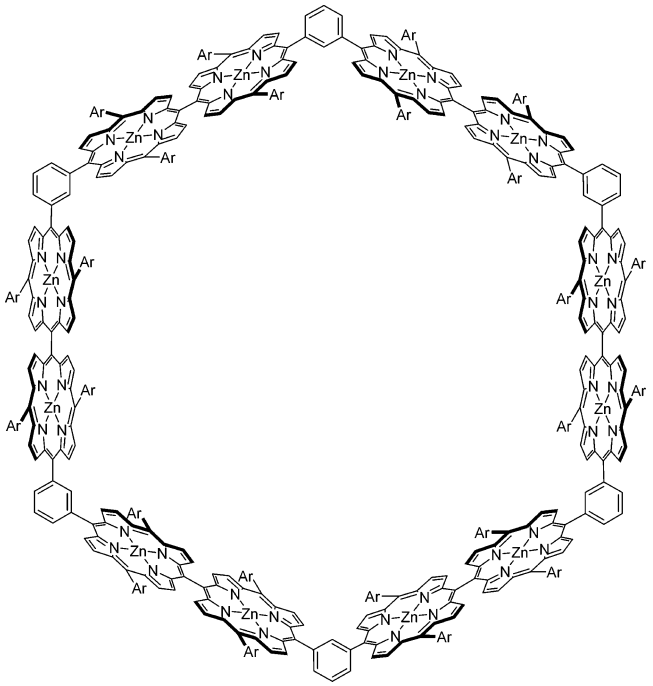

Figure 44. Dodecameric porphyrin array.

on the *meso*-aryl positions are different due to restricted rotation. However, little is known about rotational processes and their effect on energy transfer in theses systems. Recently, Aida and co-workers[501] have reviewed progress in the field of light-harvesting antennae.

Other groups have studied systems in which porphyrins have been coupled by spacers represented by benzene,[531−534] biphenyl,[535] anthracene,[536] phenanthrene,[537] butadiyne,[538−547] ethyne,[548−550] and other structures.[551,552] Although not looking at rotation per se, Helms et al.[553] performed an interesting study pertaining to the effect of rotational processes on electronic coupling. They investigated the rate of electron transfer between two free-base porphyrins as a function of the twist angle of the biphenyl-derived bridging group: phenanthrene (0°), dihydro-

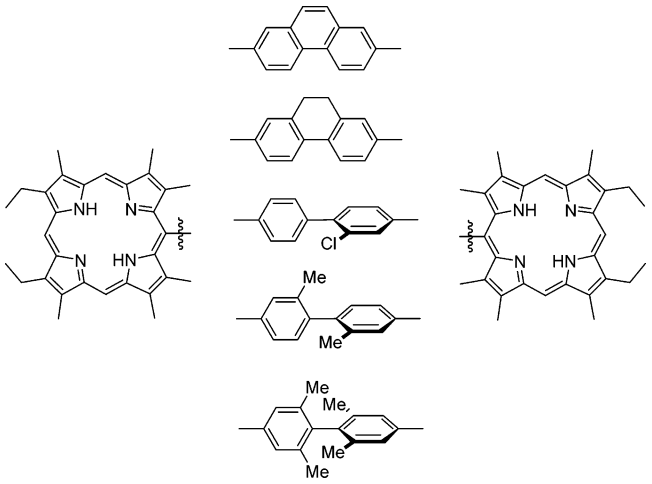

Figure 45. Porphyrin units with spacers possessing restricted dihedral angles.

phenanthrene (20°), *o*-chlorobiphenyl (60°), *o*,*o*′-dimethylbiphenyl (70°), and 2,2′,6,6′-tetramethylbiphenyl (90°) (Figure 45). They found that the rate of electron transfer was highly dependent on the phenyl−phenyl angle and displayed a surprising cos 2θ relationship with a maximum at angles of 0° and 90° and a minimum at 45°. The findings of this study are important in understanding the relationship between the porphyrin-bridge angles in these systems but are in sharp contrast to the findings of Lindsey[554] and Albinsson,[519] who found that little or no electronic coupling (or at least a large decrease in the transfer rate) was found for their systems when the bridging units could not achieve coplanarity or the activation barrier was high. The results of Okuno and Mashiko,[112] stating that the rotation has a dominant effect on the zinc porphyrin, may be relevant in reconciling this discrepancy.

Lin and Therien[549] investigated a series of six bisporphyrins linked by ethyne and butadiyne groups coupled at the meso−meso (**122** and **126**), meso−β (**123** and **125**), or β−β positions (**121** and **124**) on the two rings (Figure 46). Three factors affected the degree of excitonic and electronic coupling in these systems: (i) the length of the bridge (ethyne > butadiyne in a series), (ii) the positions to which the bridge is coupled (meso−meso > meso−β > β−β, in the absence of steric effects), and (iii) steric factors which modulate the rotational space which the porphyrins can sample. The meso−meso ethyne (**122**), meso−meso butadiyne (**126**), and meso−β butadiyne linked (**125**) dimers all had calculated barriers to rotation of less than 1 kcal mol^{-1}. Highly efficient electronic coupling was found in all these cases, decreasing in the order meso−meso ethyne > meso−meso butadiyne > meso−β butadiyne. The meso−β ethyne linked (**123**) dimers cannot rotate, but librations led to some excitonic coupling. Both β−β linked compounds (**121** and **124**) have barriers to rotation, but the butadiyne analogue can achieve planarity by rotation while the ethyne cannot, and enhanced coupling was found in the butadiyne linked molecule. In this case, the ability to achieve coplanarity outweighs the lesser effectiveness of the linker (butadiyne vs ethyne).

Intramolecularly linked porphyrins, systems in which a porphyrin is linked to itself by a tether, have been known since the early 1970s, and some representatives are shown in Figure 47. Also known as "strapped porphyrins"[555] (**127**−**129**), "cyclophane porphyrins",[556] "capped porphyrins"[557−559] (**132**−**133**), "basket-handle porphyrins"[560] (**131**), "crowned porphyrins",[561] "picnic-basket porphyrins"[562] (**131**), "coronet porphyrins"[563] (**130**), and "gyroscope porphyrins"[564] (**134**), most have been studied as synthetic

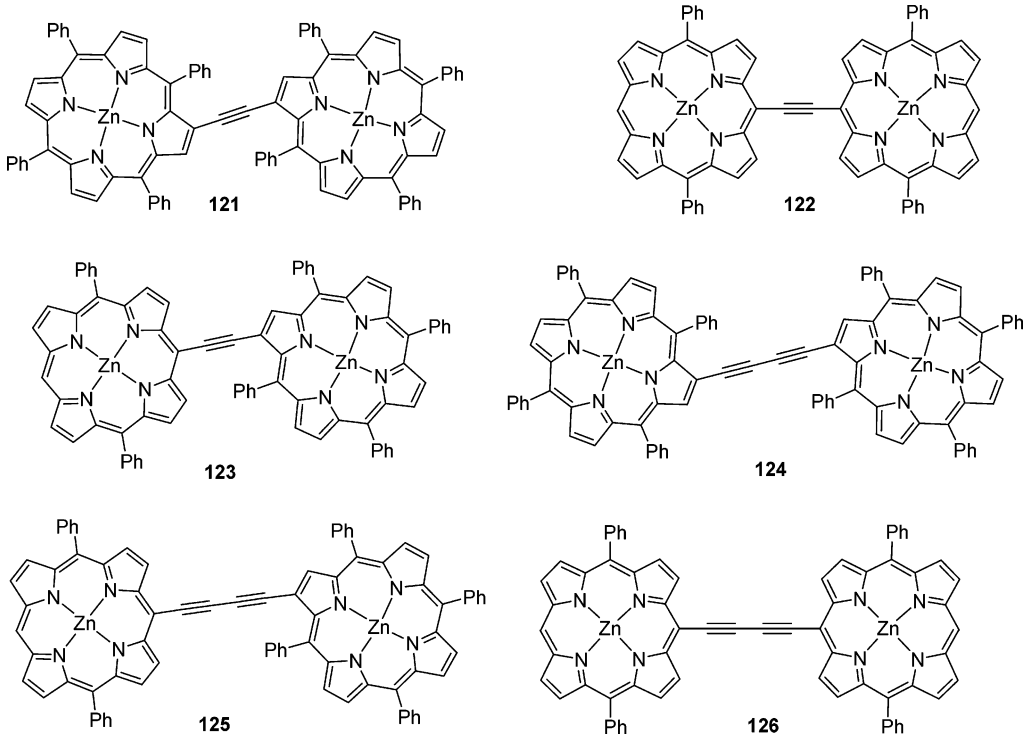

Figure 46. Ethyne-, butadiyne-, and *meso*−*meso* linked porphyrins.

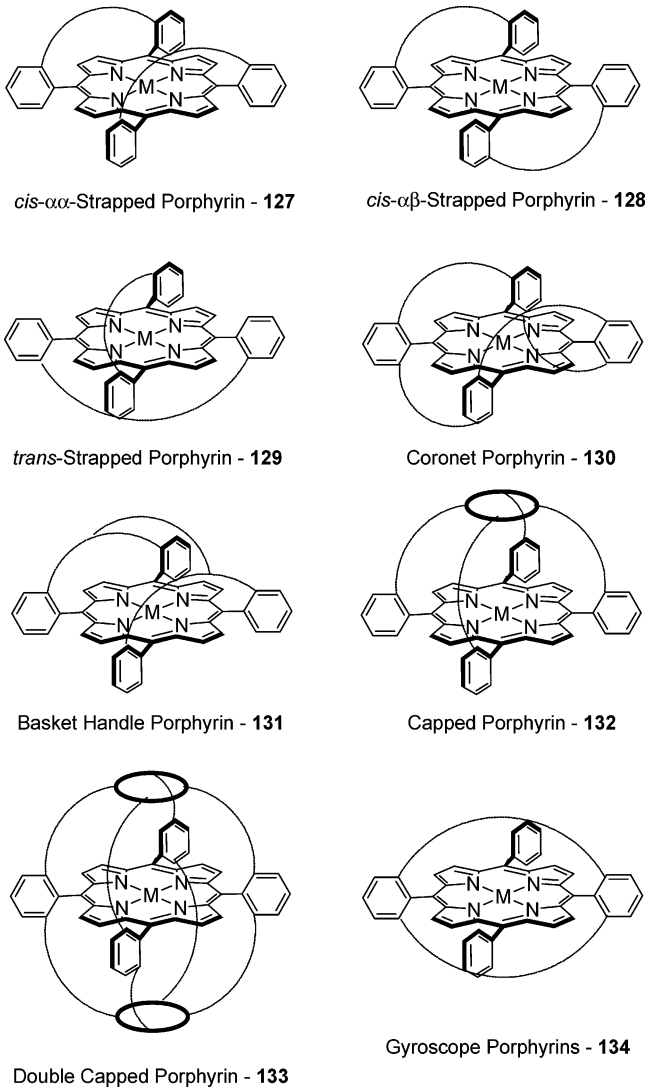

Figure 47. Intramolecularly linked porphyrins.

mimics for myoglobin and hemoglobin. The concept of putting a "protecting" strap over one side of the porphyrin to protect the dioxygen binding site is analogous to Collman's "picket fence" and "pocket" approach for reversibly binding oxygen. Although many papers have appeared,[555–579] few have discussed rotation of the porphyrin through the cavity created by the strap or rotation of individual units in the strap itself. In some cases, rotation would not be observable or even possible. For example, the basket-handle (**131**), capped (**132**), and double-capped (**133**) porphyrins are locked and cannot rotate. Depending on the chain lengths in the tethers, some of the other structures shown in Figure 47 also may not be able to rotate (see below). An early review on "protected hemes" was written by Traylor.[580]

To the best of our knowledge, Sanders and co-workers[581,582] were the first to study rotation in strapped molecules. In looking at quinone-capped porphyrin **135** (Figure 48), they found that rotation of the porphyrin through the cavity created by the strap, which leads to racemization of the two chiral forms, was slow on the NMR time scale. They also found that the quinone unit rotated rapidly through the cavity created by the tethers and the porphyrin. Furthermore, they discovered that the whole en-

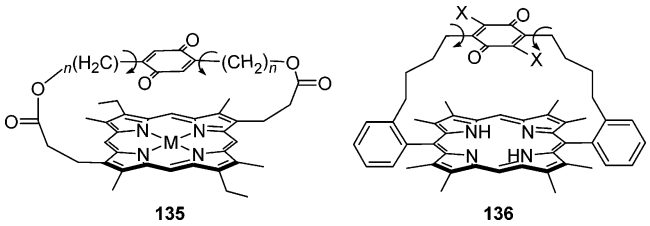

Figure 48. Quinone-capped porphyrins.

semble relaxes by spinning around the fourfold axis of the porphyrin. In unsubstituted porphyrins, this spinning motion would by accompanied by very little solvent disruption (due to its disklike nature) and therefore relaxation would be faster (smaller T_1). In the capped porphyrins, the T_1 values were viscosity dependent because rotation of the porphyrin requires the cap to displace more solvent. Upon addition of magnesium(II) to the porphyrin, the quinone adopts a preferred conformation with one carbonyl pointing toward the metal center, although rotation is still fast for the quinone moiety as a whole at room temperature.

Staab and co-workers performed a more detailed study on the rates of rotation of quinone-capped porphyrins[583–588] in their studies of photoinduced electron transfer in such systems.[589,590] For a series of 1,4-quinone-bridged structures (**136**), they investigated the barrier to rotation upon changing the substituents (X) in positions 2 and 5 as well as by changing the porphyrin structure from octamethyl- (**136**) to tetramethyltetraethyl-5,15-diphenylporphyrin.[583] For X = H, Me, Cl, and Br, they observed no splitting of the β-methyl signals down to 150 K. For X = OMe, they observed such a splitting with an activation barrier ($\Delta G^{\ddagger}_{192}$) of ~9.3 kcal mol^{-1}. They also studied a dimethoxyhydroquinone derivative for comparison. For X = CN, a much higher barrier ($\Delta G^{\ddagger}_{339}$) of about 17 kcal mol^{-1} was found for the hydroquinone unit. Replacing four methyl groups by ethyl groups in the porphyrin raised the barrier to rotation only slightly (~0.4 kcal mol^{-1}). The authors also observed a "swinging bridge" motion of the quinone due to the flexibility in the tethers.

Lindsey and co-workers[591] have performed a detailed study on porphyrins bearing meso linked straps with different lengths and rigidities (Figure 47). In particular, they examined the dynamics of the tethers moving from one porphyrin face to another. In the case of *o,o′* linked porphyrins **127** and **128**, the barriers to rotation were high enough that the isomers were separable by HPLC, whereas *m,m′* linked porphyrins could not be separated with chromatography but could be observed spectroscopically. For these molecules, activation barriers ($\Delta G^{\ddagger}$) of about 16 kcal mol^{-1} were observed for rotation through the strap, which are similar to values presented above for atropisomerism in "unstrapped" molecules.

Gunter and co-workers[592–594] have developed a catenated porphyrin system where a smaller ring is interlocked with the strap on the porphyrin (Figure 49). These catenanes are of the Stoddart type[26–36] and self-assemble in solution. The tetracationic unit can easily rotate about the central hydroquinone unit, but

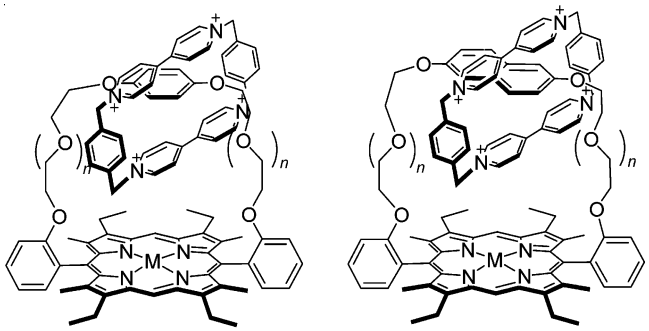

M = Zn, *n* = 1 **137a**
M = Zn, *n* = 2 **137b**
M = 2H, *n* = 1 **138a**
M = 2H, *n* = 2 **138b**

M = Zn, *n* = 2 **139a**
M = 2H, *n* = 2 **139b**

Figure 49. Catenated porphyrin systems.

the porphyrin containing ring cannot rotate through the tetracationic unit (*pirouetting* in the nomenclature of Stoddart[27,595]) due to the steric bulk of the porphyrin unit. In **137b**, the rotation of the tetracationic unit about the hydroquinone unit has an appreciable barrier $\Delta G^{\ddagger}_{262} = 12.9$ kcal mol^{-1}; $k = 104$ s^{-1}).[592] For the shorter chain Zn derivative (**137a**), the barrier increased as expected ($\Delta G^{\ddagger}_{316} = 14.4$ kcal mol^{-1}; $k = 445$ s^{-1}).[592,593] The free-base porphyrins (**138a** and **138b**) showed a similar behavior. In the case of the electron richer 1,5-naphthoquinol unit shown in **139a** and **139b**,[593,594] the barriers to rotation ($\Delta G^{\ddagger}_{332}$) were determined to be 15.7 kcal mol^{-1} for both molecules. To control the rotation of the tetracation unit in the cavity of the porphyrin macrocycle, the authors used protonation of the free-base porphyrins (**138a**, **138b**, and **139b**). The self-assembly of such structures is controlled by a template effect, in which the electrostatic interactions between the porphyrin and the tetracationic unit allow the molecule to be formed in nonstatistical yields. If this interaction were broken in the assembly process, low yields of the catenated structures would result. However, once the catenane is formed, removing the favorable interaction could lead to interesting properties, as the two units can no longer dissociate.

When the porphyrin is in its free-base from, the viologen unit of the tetracationic macrocycle sits above the porphyrin. When the porphyrin is protonated, the viologen unit avoids it due to electrostatic repulsions and the *p*-xylylene unit sits above the porphyrin. For the phenyl-linked porphyrin with the shorter strap (**138a**), upon protonation, the viologen unit moves farther away from the porphyrin ring and the rate of rotation of the tetracationic unit about the hydroquinol stator actually increases (1000 s^{-1}; $\Delta G^{\ddagger}_{238} = 12.9$ kcal mol^{-1}) relative to the case of the unprotonated porphyrin (80 s^{-1}; $\Delta G^{\ddagger}_{238} = 14.2$ kcal mol^{-1}). For the porphyrin with the longer strap (**138b**), the rotational rate of the protonated porphyrin was found to be 1500 s^{-1} ($\Delta G^{\ddagger}_{298} = 12.6$ kcal mol^{-1}), which is comparable to the case of the unprotonated system (1500 s^{-1}; $\Delta G^{\ddagger}_{298} = 12.7$ kcal mol^{-1}). Therefore, protonation has little effect on rotation rate in this case, but the tetracation prefers to have the xylyl group over the porphyrin ring and the flexibility in the tether allows the entire paraquat unit to displace from the center of the porphyrin. For the case with the long strap and the naphthyl unit in the porphyrin macrocycle (**139b**), the rates for the protonated (5 s^{-1}; $\Delta G^{\ddagger}_{298} = 16.2$ kcal mol^{-1}) and the unprotonated (10 s^{-1}; $\Delta G^{\ddagger}_{298} = 15.7$ kcal mol^{-1}) forms were not very different.

These data show that there is an interplay between electrostatic and steric effects. Although the protonated porphyrin might be predicted to yield increased barriers to rotation due to electrostatic repulsions, these repulsions in and of themselves cause the flexible linker to move farther from the porphyrin, and thus, the steric hindrance to rotation is reduced. For the data given above, these contributions to the rotational barrier appear to balance in this system.

Face-to-face porphyrin dimers and trimers (two or three porphyrins linked to each other through tethers with the porphyrin planes parallel) were pioneered by Collman and co-workers.[596−603] However, the early workers were interested in catalysts for the electroreduction of oxygen to water, and rotational processes in such systems were not investigated. Later, face-to-face porphyrins and porphyrin aggregates gained renewed interest in models for naturally occurring electron-transfer systems.[604−612] The first example of rotation of one porphyrin inside the cavity formed by the other porphyrin and the two tethers was provided by Sanders and co-workers,[577] as determined by the simplicity of the NMR spectrum. However, they did not attempt to determine the barrier to rotation. In a subsequent paper,[613] they synthesized two new structures with different tethers (Figure 50). In compound **140** with symmetrical

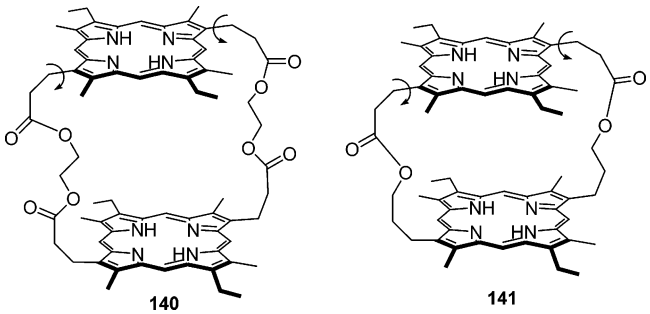

Figure 50. Face-to-face porphyrins.

tethers, rotation is slow on the NMR time scale at room temperature, and it exists as a 2:1 mixture of meso and racemic forms due to the lack of symmetry in the porphyrin. No saturation transfer was observed between the isomers, and the authors placed an upper limit of 1 s^{-1} on the interconversion rate. Protonation to the tetracation led to an isomeric ratio of 3:2 (meso:racemic), presumably because the mutual repulsion of the two charged species widens the inter-porphyrin distance and thus allows for easier rotation, as observed in the catenated system discussed above. Incorporation of zinc(II) favors the meso isomer with a higher than 50:1 selectivity. The authors attributed this to greater porphyrin−porphyrin interaction in this isomer compared with the racemic one. The compound **141** with unsymmetrical (and shorter) tethers also existed as two isomers (syn and anti) and interconversion by rotation is not

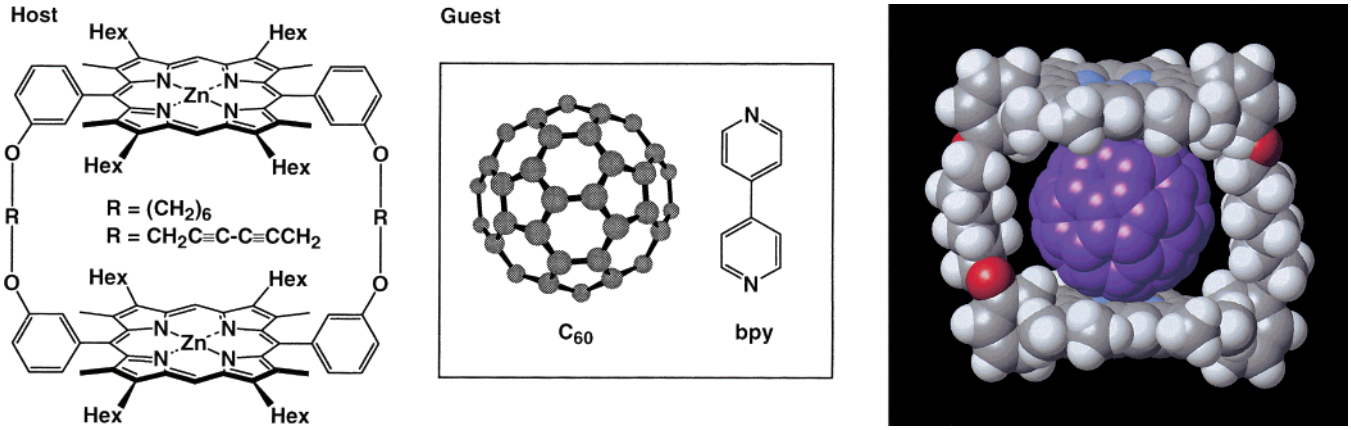

Figure 51. porphyrin complex that encapsulates fullerenes. Reprinted with permission from ref 617. Copyright 1999 American Chemical Society.

possible. Protonation and metalation have no effect on the isomer ratio. Both compounds also experience a fluxionality based on the ability of one porphyrin to "slide" to a different position relative to the other. On the basis of results obtained from this work, Sanders and Hunter[614] developed a simple model for $\pi-\pi$ interactions as a predictive method for designing molecules that favor $\pi-\pi$ interactions and have used it to design host−guest systems.[615,616]

Encapsulation of fullerenes into porphyrin dimer compounds was investigated by Aida and co-workers[617−621] in a cyclophane-type molecule (Figure 51) and by Reed and co-workers[622] in "molecular tweezers". A system developed by Shinkai and his collaborators[623] employed a porphyrin tetrad which could rotate about a *p*-terphenyl axle (Figure 52) to

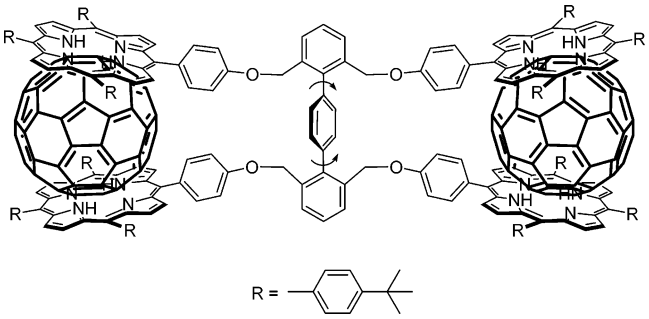

Figure 52. Multiporphyrin system that can bind two C_{60} molecules cooperatively.

selectively bind two C_{60} molecules. Another C_{60} rotor based on porphyrins, in which the porphyrin complexes do not rotate with respect to one another, but about a cental butadiyne axis, was also investigated.[624] This porphyrin tetramer was used to show cooperative binding to bidentate amines. Aida has also developed an oscillator based on a porphyrin−fullerene system (Figure 53) and recently used cyclophane−porphyrin systems to extract fullerenes larger than C_{76} from mixtures created in the combustion-based industrial production of C_{60} and C_{70}.[625]

5.3. Rotations about Triple Bonds

Early computational work by Liberles and Matlosz[626] investigated diarylacetylenes semiempirically (CNDO and INDO). In particular, they were interested in the effect of orbital overlap of the p-orbitals of the aryl rings with those on the ethyne unit and whether this would lead to a planar structure or one in which the phenyl rings were mutually perpendicular, given that the triple bond has two mutually orthogonal π systems. They found that the twisting potential is very flat, and they concluded that the perpendicular geometry was more stable by ~1 kcal mol^{-1}. The nature of the methods used makes the latter result doubtful. Several groups have calculated the bond rotations about groups attached to a carbon−carbon triple bond using ab initio levels of theory and also found them to be very low.[107,108,627] The barriers (E_{calc}) are in the range of 0.4−1.1 kcal mol^{-1} for diphenylacetylene derivatives[107,627] and less than 10 cal mol^{-1} for bis(trimethylsilyl)acetylene.[108] Ito and co-workers[628] measured the torsional motion in tolane (diphenylacetylene) in a supersonic free jet and obtained a value inside this range (202 cm^{-1} ≈ 0.6 kcal mol^{-1}).

However, as we have seen before, if the steric environment around the groups attached to the ethynyl group prevents easy rotation, then the barriers can become quite high. To measure barriers about triple bonds by conventional techniques, such as DNMR, sterically hindered analogues must be synthesized. In particular, the steric interaction of the groups must *bridge* the length of the triple bond (~4.0 Å for X−C≡C−Y[629]). Oki, Toyota, and coworkers found large barriers in substituted bis(triptycyl)ethynes (**142a**−**143h**),[630−633] bis[di(*o*-aryl)phenyl]acetylenes (**144a**−**144c**),[634] and bis(1-phenyl-9-anthryl)ethynes (**145a**−**145d**),[635] and supported the results by molecular mechanics calculations (Figure 54). Table 4 shows the rotational barriers for these sterically hindered diphenylacetylenes. For the ditriptycene molecules, barriers in the range of 9−17 kcal mol^{-1} were found, with the barrier increasing as a result of the steric size of the substituents on the triptycene phenyl groups. As shown in section 5.1, the methoxy group is actually "smaller" than the methyl group, likely due to the ability to avoid steric interactions by rotations about the Ph−O and O−CH_3 bonds, whereas a methyl group is more rigid and cannot avoid steric interactions as easily. The halogen series also shows the predicted trend: upon increasing the van der Waals radii in going from

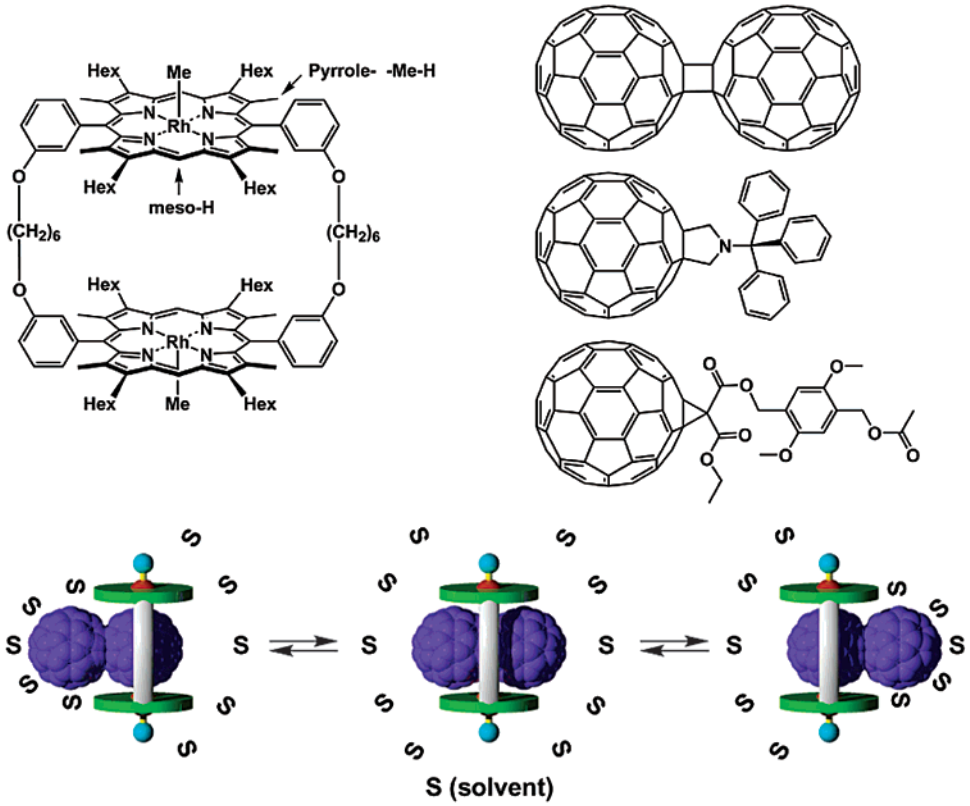

Figure 53. Molecular oscillator based on fullerene encapsulation to a porphyrin face-to-face dimer complex. Reprinted with permission from ref 620. Copyright 2002 American Chemical Society.

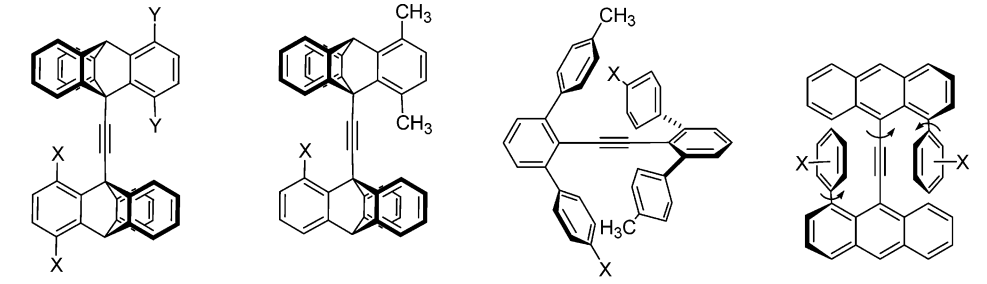

142a X = Y = H
142b X = H, Y = CH_3
142c X = H, Y = OCH_3
142d X = CH_3, Y = CH_3
142e X = CH_3, Y = OCH_3
142f X = OCH_3, Y = OCH_3

143a X = F
143b X = Cl
143c X = Br
143d X = I
143e X = Ph
143f X = Mes
143g X = Ph-CC-
143h X = (1-naph)-CC-

144a X = CH_3
144b X = CH_2Br
144c X = CH_2OCH_3

145a X = 4-CH_3
145b X = 4-*i*-Pr
145c X = 3-*i*-Pr
145d X = 3,4-(*i*-Pr)$_2$

Figure 54. Hindered rotation about triple bonds.

fluorine (**143a**) to iodine (**143d**), the rotational barriers ($\Delta G^{\ddagger}$) increase from 11.6 to 17.3 kcal mol^{-1} (Table 4). This observation has been made repeatedly throughout this text. With larger substituents such as phenyl (**143e**) and mesityl (Mes; **143f**), the barriers were found to be 15.7 and 18.8 kcal mol^{-1}, respectively. For compounds **143g** and **143h**, the authors found severe deformations of both acetylene groups in the crystal structure,[632] which likely accounts for the lower than expected values for the rotational barriers (17.5 kcal mol^{-1} for **143g** and 17.8 kcal mol^{-1} for **143h**). Overall, in this series, the rotational barriers increased in the order H < F < OCH_3 < Cl < CH_3 ≈ Ph < Br < I ≈ arylethynyl < Mes. This hierarchy is similar to that seen in other systems.

In bis[di(*o*-aryl)phenyl]acetylenes (**144a**−**144c**), the barriers were too low to measure and were estimated to be about 7 kcal mol^{-1} ($\Delta G^{\ddagger}$).[634] For bis(1-phenyl-9-anthryl)ethynes (**145a**−**145d**), the authors were able to measure the barriers.[635] Using dynamic NMR (total line shape analysis), they found two dynamic processes: rotation of the two anthracene units about the acetylenic axis and rotation of the phenyl groups about the C_{Ar}−anthracene bond. For the most sterically hindered molecule (**145d**), the barrier to rotation ($\Delta G^{\ddagger}_{273}$) about the acetylene bond was an extraordinary 18.0 kcal mol^{-1} while that about the phenyl ring ($\Delta G^{\ddagger}_{273}$ = 11.9 kcal mol^{-1}) was similar to that found in other structures (section 5.1.4). Phenyl ring rotation was in the vicinity of 10−12 kcal mol^{-1} for all compounds, and the anthracenyl rotation scaled as the steric bulk of the substituent ($\Delta G^{\ddagger}_{273}$ = 11.5 kcal mol^{-1} for **145a**, 11.3 kcal mol^{-1} for **145b**, and ~17.5 kcal mol^{-1} for **145c**). The two processes

Table 4. Activation Barriers for Rotation in the Hindered Diphenylacetylene Compounds Shown in Figure 54

compd	$\Delta G^{\ddagger}_{273}$ (kcal mol^{-1})	ref
142b	10.1	630
142c	8	630
142d	15.4	630
142e	12.7	630
142f	9.4	630
143a	11.6	631
143b	14.7	631
143c	16.7	631
143d	17.3	631
143e	15.7	632
143f	18.8	632
143g	17.5	632
143h	17.8	632
144c	<8	634
145a	11.5	635
145b	11.3	635
145c	~17.5	635
145d	18.0	635

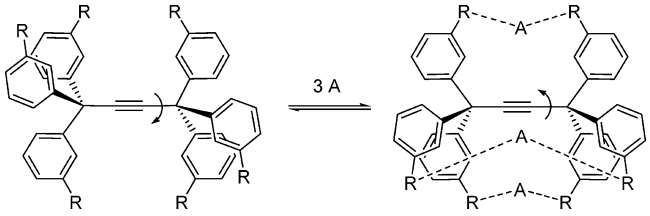

Figure 55. Design scheme for a pinwheel receptor where the rotationally flexible recognition elements can bind three analytes cooperatively, where R is a recognition element and A is an analyte. Reprinted with permission from ref 636. Copyright 2000 American Chemical Society.

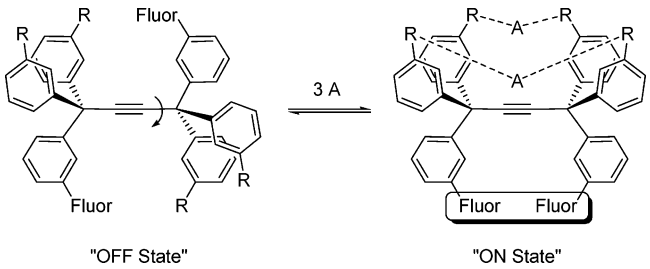

Figure 56. Pinwheel receptor with a fluorescent tag for readout. Reprinted with permission from ref 637. Copyright 2001 American Chemical Society.

appear to be independent of each other, although the authors could not rule out some correlated effects.

Molecular rotors containing triple-bond and butadiyne axles, with possible applications to chemical sensing, were developed by Glass and co-workers[636−638] for the fluorescent sensing of analytes. The first-generation pinwheel receptor bears three coordination sites for the binding of analytes and an acetylene spacer (Figure 55), while the second-generation system has two binding sites with a third site occupied by two fluorophores which form an excimer upon excitation, with a butadiyne spacer (Figure 56). Binding of an analyte will bring the fluorophore pair in close proximity, and excitation will cause excimer formation. This allows for the molecule to be probed for analyte binding. Such a system may have uses in memory devices where the presence of excimer emission could equal a binary "1", while the absence would correspond to a "0".

In these systems, binding of the first molecule has the highest energy because the rotor must rotate into the preferred conformation. After the first binding has occurred, and the entropic price has been paid, subsequent bindings have lower energies. This is termed a *positive allosteric effect* and will be discussed in greater detail in section 5.4.4.

5.4. Rotations of Molecular Carousels (Sandwich Complexes)

We define a molecular carousel as a compound consisting of two or more planar (or nearly planar) "decks" which rotate and remain parallel to each other. An alternative formulation would be the name molecular sandwich complexes. However, we feel that the term sandwich complex includes molecules which may not rotate, whereas a carousel naturally brings about the image of rotation.

5.4.1. Metallocenes and Related Complexes

Metallocenes (**146**) are perhaps the simplest type of molecular carousel (Figure 57). Since the discovery

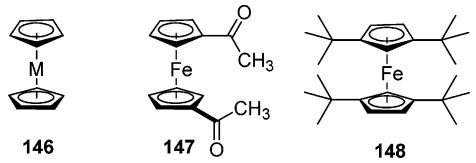

Figure 57. Metallocenes and substituted metallocenes.

of ferrocene (**146**; M = Fe)[639] and its subsequent structural determination,[640,641] many groups have studied the barrier to rotation in the parent and its derivatives. Early computational papers[642,643] and dipole moment measurements of substituted ferrocenes[644] predicted "free"[645] rotation of the cyclopentadienyl rings about the iron axle. Holm and Ibers[646] were the first to experimentally determine a barrier to rotation in ferrocene ($\Delta G^{\ddagger} = 1.8$ kcal mol^{-1}) as well as in ruthenocene (**146**; M = Ru; $\Delta G^{\ddagger} = 2.3$ kcal mol^{-1}) by line shape analysis of the solid-state NMR spectrum. Mulay and Attalla[647] also found a small barrier ($\Delta G^{\ddagger} = 2.3$ kcal mol^{-1} at 68 K) for ferrocene, and the barriers in cobaltocene (**146**; M = Co), nickelocene (**146**; M = Ni), and chromocene (**146**; M = Cr) were all measured to be ($\Delta G^{\ddagger}$) 1.8 ± 0.2 kcal mol^{-1}.[648]

Over the ensuing years, many groups have investigated the rotational processes in metallocenes and their derivatives. In particular, inserting bulky groups on the cyclopentadiene (Cp) rings increases the barrier to rotation and, if the steric hindrance is high enough, makes the barriers to rotation within the region accessible by solution-phase dynamic NMR analysis ($\Delta G^{\ddagger} > \sim 5$ kcal mol^{-1}). Simply putting one acetyl group on each ring (**147**) already increases the barrier[649] to over 11.0 kcal mol^{-1}, and putting two *tert*-butyl groups on each ring (**148**) further hinders the rotation such that it occurs with a barrier[650] of 13.1 kcal mol^{-1}.[651]

A number of groups have also investigated concerted rotations of more than one group in substituted metallocene compounds. For example, Castel-

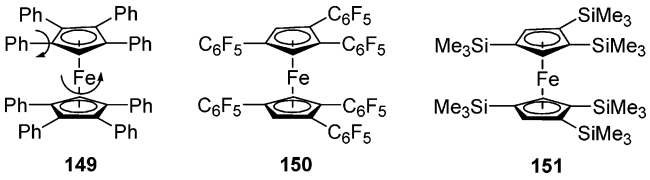

Figure 58. Substituted metallocenes with two rotational processes and the possibility of geared rotation (Ph = phenyl; C_6F_5 = pentafluorophenyl).

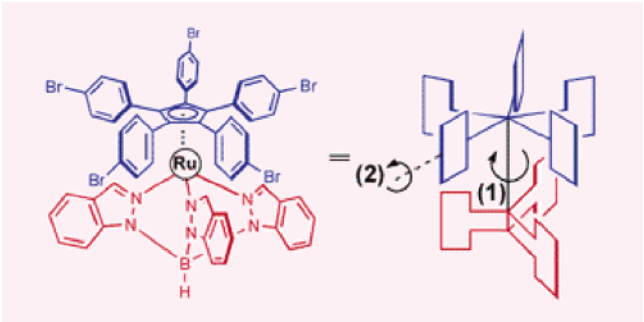

Figure 59. Organometallic "molecular turnstile", showing (1) rotation about the ruthenium axle and (2) rotation of the phenyl rings. In order for the rotation (1) to occur, the phenyl rings must rotate out of their nearly perpendicular arrangement to allow passage of the indazolyl groups. Reprinted with permission from ref 657. Reproduced by permission of The Royal Society of Chemistry.

lani et al.[652] synthesized bis(tetraphenylcyclopentadienyl)iron(II) (**149**) to investigate both the rotation of the cyclopentadienyl rings and the reorientation of the phenyl groups in the process (Figure 58) in attempt to determine if they were correlated. The barrier ($\Delta G^{\ddagger}_{178}$) to phenyl group rotation (cogwheeling) was found to be 9 kcal mol^{-1} at −95 °C while the cyclopentadienes were still rotating rapidly. Deck and co-workers[653] studied [1,2,4-$(C_6F_5)_3C_5H_2]_2$-Fe (**150**) by ^{19}F DNMR and observed two dynamical processes: (1) the rotation of the aryl groups with respect to one another and (2) the rotation of the two cyclopentadiene rings. The activation energy (E_a) for the rotation of the Cp rings in [1,2,4-$(C_6F_5)_3C_5H_2]_2$-Fe (**150**) was found to be 11 kcal mol^{-1}, which is similar to that found for [1,2,4-$(Me_3Si)_3C_5H_2]_2$Fe (**151**) (11.0 kcal mol^{-1})[654] and [1,2,4-$(Me_3C)_3C_5H_2]_2$Fe (15.3 kcal mol^{-1}) (not shown).[655]

Interestingly, polyphenylated metallocene molecules do not have very high barriers to rotation as one might have expected for such a crowded system. It was postulated[656] that the phenyl rings can rotate slightly out of their preferred geometry to allow for passage of the other substituents, which corresponds to a geared ("concerted") rotation.

This was also observed by Launay and co-workers[657] in their work on a "molecular turnstile". They have synthesized a ruthenium sandwich complex with a pentakis(*p*-bromophenyl)cyclopentadiene deck and another deck consisting of a hydrotris(indazolyl)-borate ("scorpionate"[658]) group (Figure 59). In such a crowded molecule, and as evidenced in the X-ray structure, it is quite surprising that they could not observe hindered rotation of the cyclopentadiene ligand [the rotational barrier ($\Delta G^{\ddagger}$) was less than 10 kcal mol^{-1}] or the phenyl groups on the cyclopentadienyl ring. NMR indicated that the indazolyl groups fit into the pockets created by the phenyl groups on the opposite deck, as evidenced by their greater shielding. Therefore, the authors proposed a rotational mechanism wherein the phenyl rings twist out their nearly perpendicular arrangement as the indazolyl rings pass and then settle back into their perpendicular state. The authors noted that such a design is well suited for functionalization for surface attachment, and they hope they will then be able to control the direction of rotation. Surface attachment with concomitant observation of rotation would be an important step in the direction toward molecular electronics (see section 7.2).

Okuda[656] and Long[659] have written reviews with some discussion of rotation in metal complexes with sterically demanding cyclopentadiene ligands. Examples of fluxional behavior in metallocenes and related complexes can also be found in a number of other places.[242,660−662]

Several groups have investigated hindered rotation in tetraarylcyclobutadienecyclopentadienylcobalt complexes (Figure 60). Rausch and co-workers[663] studied such complexes bearing two phenyl rings in positions 1 and 3 and mesityl groups in positions 2 and 4 on the cyclobutadiene (Cb) ring (**152**). They found restricted rotation about the cyclobutadiene−mesityl bond with an activation energy E_a of 10.5 kcal mol^{-1} ($\Delta G_{298}^{\ddagger}$ = 13.7 kcal mol^{-1}) and facile rotation of the cyclopentadiene as low as −60 °C. Takahashi and co-workers[664] have studied tetraarylcyclobutadienecyclopentadienylcobalt complexes bearing bulky chiral (−)-menthyl groups on the cyclopentadienyl ring (**153**). The menthyl group on the Cp ring resides between two phenyl groups on the Cb ring and hinders the rotation of the phenyl rings, which induces a helical chirality to the molecule due to concomitant restriction of the Cp−Co−Cb bond rotation. Stevens and Richards[665] have designed an interesting system in which the four phenyl groups on the cyclobutadiene are cogged with a three-toothed triptycene molecule attached to the cyclopentadiene unit (**154**). Although spectral changes were noted using variable-temperature NMR, the evidence was inconclusive as to whether the two cogs were actually coupled in this system. However, it represents a novel design for the synthesis of molecular gears, even though a three-toothed gear meshed with a four-toothed gear would be inefficient (see section 3 for further elaboration).

Metallacarboranes were recently investigated for electrical, redox, and photochemical switchable rotation by Hawthorne et al.[666] The bonding in metallocarboranes is related to that in metallocenes, but complexes of the former tend to be more stable than those of the latter. This group took advantage of this stability to make a two-state molecular switch that interconverted via rotation about the metal ion axis (Figure 61). In **155a**, the oxidation state of the nickel is +4, and these complexes are known to prefer the *cisoid* geometry with the carbon vertexes on the same side of the molecule,[667,668] while in the +3 oxidation state nickel prefers a *transoid* conformation like that shown in **155b**.[668−670] The authors exploited these preferences to induce a 4π/5 (144°) rotation by

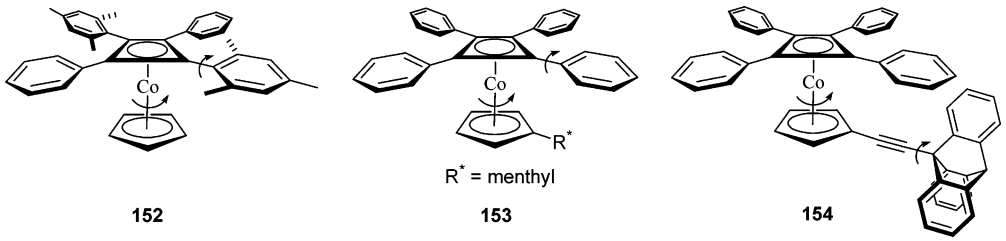

Figure 60. Rotation in tetraarylcyclobutadienecyclopentadienylcobalt complexes.

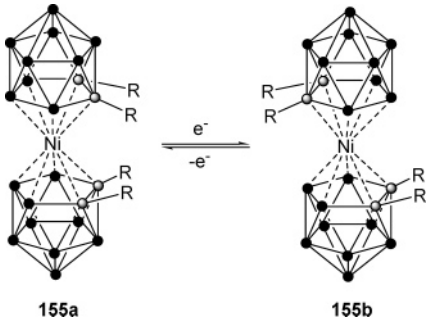

Figure 61. Electron-driven molecular rotor prepared from carboranes, where the light circles are carbon atoms and the dark circles are boron atoms. For the parent molecule in this class, R = H.

changing the oxidation state of the metal both eletrochemically and photochemically. Photon-driven rotation was observed using resonance Raman and luminescence spectroscopy and supported with time-dependent DFT calculations. With this energy input, an electron is promoted to the lowest unoccupied molecular orbital (LUMO) and the molecule relaxes via rotation.

The authors of the study proposed several systems in which unidirectional rotation could be observed, an important step toward making true molecular motors (see section 5.7). One advantage of the carborane systems over similar metallocene systems is the ability to substitute the cage further for multiple functionalization. One possibility alluded to in the paper was surface attachment (see section 7.2). Such molecules on a surface could be photochemically switched and represent "1s" and "0s" in a binary system. If the rotamers could be "read" and "written" with different wavelengths of light, ultracompact storage media (such as a compact disk) would be one example of an application, with one bit equal to one molecule.

5.4.2. Piano-Stool (Half-Sandwich) Transition Metal Complexes and Related Compounds

The so-called piano-stool complexes are half-sandwich complexes bearing one cyclopentadienyl ligand and up to six other ligands. We have already discussed several examples in section 5.1, and here we only briefly mention several others. The parent compound of this class, from which its name is derived, is the $CpM(CO)_3$ complex **156**, which bears resemblance to a three-legged piano stool (Figure 62). In this section, we include compounds that are structurally similar to the parent but are neither metallocenes (section 5.4.1) nor multicyclopentadienyl compounds (section 5.4.3).

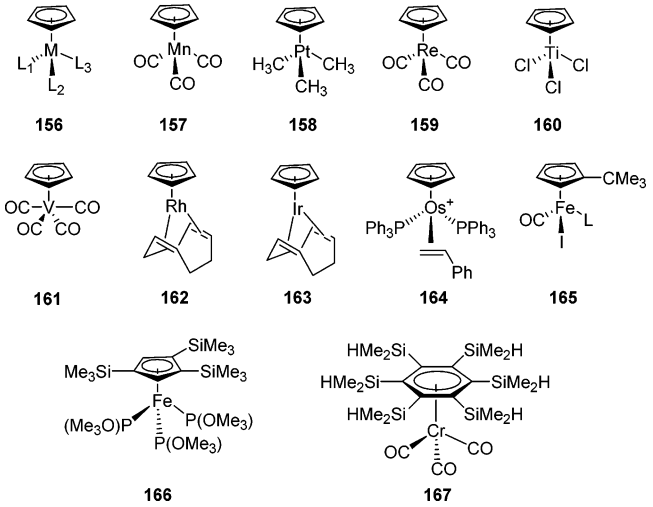

Figure 62. Some half-sandwich metal complexes.

Figure 62 shows a variety of such single-Cp piano-stool complexes that have been investigated, with structures **156** through **160** showing typical examples. The barrier to rotation in solid **157** was studied by both quasi-elastic neutron scattering (QENS)[671] and spin−lattice relaxation NMR measurements.[672] QENS gave a value of 4.0 kcal mol^{-1}, which would appear to be high for this relatively unhindered molecule, and NMR T_1 measurements provided a more likely value of 1.7 kcal mol^{-1} ($\Delta G^{\ddagger}$). A larger than expected value was also obtained for **158** (4.9 kcal mol^{-1})[673] using mechanical spectroscopy.[674] Similarly, Gilson et al.[672] measured the barriers to rotation in **159** and **160** by spin−lattice relaxation NMR and found similar values ($\Delta G^{\ddagger}$) of 1.71 and 1.70 kcal mol^{-1}, respectively. Earlier, they had measured the barrier in **161** and found it to be a seemingly high 2.3 kcal mol^{-1}, which is the upper limit measured for ferrocene.[675] Several half-sandwich complexes with cyclooctadiene (COD) "stools" have been measured by Mann and co-workers[676] using ^{13}C spin−lattice relaxation experiments. For the rhodium complex (**162**), these authors obtained a barrier ($\Delta G^{\ddagger}$) of ~1.9 kcal mol^{-1}, and for the iridium complex (**163**) it was ~1.7 kcal mol^{-1}. Recently, Mynott and co-workers[677] found restricted rotation of an unsubstituted Cp ring in $(\eta^5\text{-Cp})M^+(Ph_3P)_2(\eta^2\text{-}CH_2CHPh)$ complexes for M = Ru and Os (**164**).

Much like metallocenes, compounds bearing only one Cp group normally exhibit fast rotation at room temperature, unless they are substituted with bulky groups on the ring or the metal ligands are bulky enough to hinder rotation. By substituting the Cp ring with a *tert*-butyl group as shown in **165**, hindered rotation was observed when $L = PPh_3$, but no value was obtained for the barrier.[678] Okuda[679] found

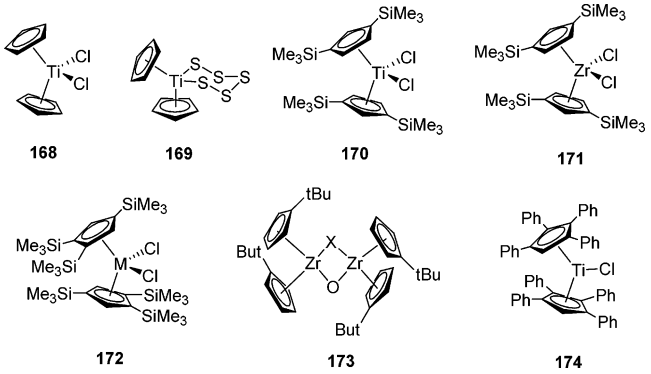

Figure 63. Metal complexes with multiple cyclopentadienyl ligands.

no hindered rotation in **166**, which is surprising given the bulkiness of the Cp substituents and the ligands, whereas **167** is an example of a highly hindered arene piano-stool compound with a barrier to rotation of 13.9 kcal mol^{-1}.

A full discussion of rotation of the ligands and the Cp ring is beyond the scope of this review, and we direct the reader to the reviews of Albright,[661,680] Okuda,[656] Coville et al.,[681] and McGlinchey,[290] which give more in-depth coverage of the rotational processes in these molecules. Albright[661,680] has reviewed the early results on arene-based half-sandwiches with chromium tricarbonyl tripods, including benzene, cyclobutadiene, cyclopentadiene, cycloheptatriene, and other polyene complexes. More recently, McGlinchey[290] has reviewed slow tripodal rotations in sterically hindered arene−chromium complexes (see also section 5.1.3 for a discussion of geared rotation in such complexes).

Activation energies for piano stool complexes are in the range of 2−13 kcal mol^{-1}. Similar trends are followed as in the metallocene series: larger substituents and smaller metals lead to larger barriers to rotation. However, as the above short discussion indicates, it is not trivial to predict the rotational properties based on these criteria alone. More work in this area must be completed before predictive methods in rotational potentials can be used to tune the properties of these compounds for applications in molecular machinery. The ability to substitute different ligands on the metal permits the functionalization of such compounds, for example, for surface attachment.

5.4.3. Complexes Bearing More Than One Cp Ring

A number of other groups have studied organometallic complexes bearing more than one cyclopentadienyl ring. Although these complexes are not true "sandwich" compounds, they will be treated in this section (Figure 63). In 1959, the barrier to rotation of cyclopentadiene groups in Cp_2TiCl_2 (**168**) was measured[646] in the solid state using the T_1 relaxation NMR method and the barrier ($\Delta G^{\ddagger}$) was found to be a scant 0.5 kcal mol^{-1}. Increasing the steric bulk around the titanium atom by replacing the chlorine ligands with cyclopentasulfide (Cp_2TiS_5; **169**) increases the barriers ($\Delta G^{\ddagger}$) to rotation about the Cp rings.[675] Two barriers were found, 1.8 and 2.1 kcal mol^{-1}, for equatorially and axially positioned Cp ligands. The two rings have different steric environments and rotate at different rates. Increasing the steric bulk on the Cp ligand also increases the barrier to rotation. Thus, in $[(Me_3Si)_2Cp]_2TiCl_2$[682] (**170**) and $[(Me_3Si)_2Cp]_2ZrCl_2$[683] (**171**), the barriers ($\Delta G^{\ddagger}$) in solution were found by the coalescence NMR technique to be ~8.9 and ~9.0 kcal mol^{-1}, respectively. When three trimethylsilyl groups were investigated (**172**), the barrier ($\Delta G^{\ddagger}$) increased predictably to 11.2 kcal mol^{-1} for the zirconium complex and 11.0 kcal mol^{-1} for the hafnium complex (Hf has a larger ionic radius). Similarly, bridged cyclopentadienyl complexes of the type **173** which have μ-oxo and -chalcogen bridges were investigated. For X = O, the barrier for rotation ($\Delta G^{\ddagger}_{206}$) was found to be 9.6 kcal mol^{-1} and increased to ($\Delta G^{\ddagger}_{222}$) 11.0 kcal mol^{-1} for the larger selenium ion (X = Se).

When four phenyl groups are placed on the Cp rings as in $(Ph_4Cp)_2TiCl$ (**174**), the Cp rings do not have an observable barrier to rotation, while the phenyl groups rotate with a barrier of ~10 kcal mol^{-1} (Figure 63).[684] Therefore, there is no correlation between the two types of rotation. A more detailed analysis can be found elsewhere.[656,659] A review of cluster complexes bearing facial arene ligands, including dynamic behavior, has been recently written by Wadepohl.[685]

Bis(cyclopentadienyl) complexes of the type discussed above resemble macroscopic bevel gears—gears with shafts at angles to one another but in the same plane (see section 5.1.1).

5.4.4. Bisporphyrinato and Related Complexes

Porphyrins will form 2:1 complexes with larger metal ions wherein the metal lies between two porphyrin rings to form a carousel structure such as that shown in Figure 64. This is in contrast to the

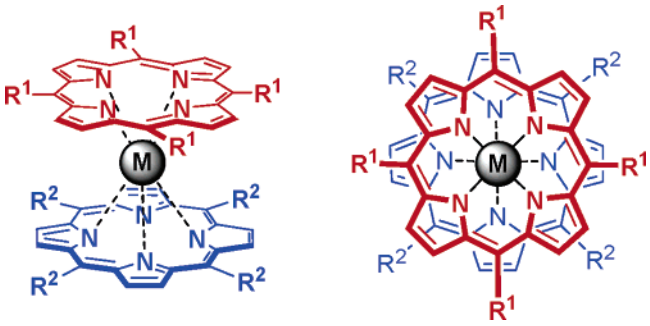

Figure 64. Side (left) and top (right) views of a bis(porphyrinato) metal (M) sandwich complex.

metal binding we saw in section 5.2. Suslick and coworkers[686] and Buchler et al.[687−689] first looked for possible rotations in such bisporphyrinato complexes but were unable to detect any rotation of the two porphyrin complexes with respect to one another about the axle comprised of the metal atom. The former group investigated zirconium(IV) complexes and observed no rotation by NMR analysis up to 150 °C. No isomerization was observed upon refluxing in toluene for 2 h. The phenyl rings, however, did rotate. The latter group studied both cerium(IV) and zirconium(IV) double-decker complexes and also concluded that rotation about the metal ion axis does

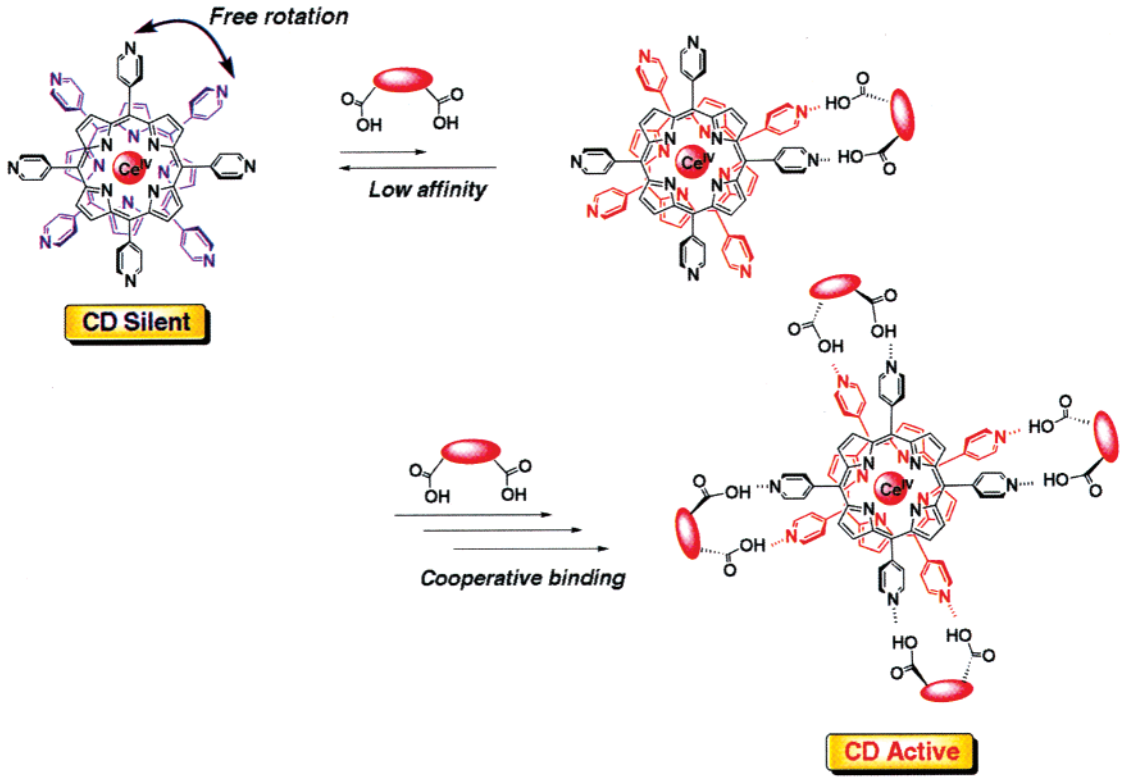

Figure 65. Cooperative binding via a rotational mechanism in cerium(IV) bis(porphyrinato) complexes. Reprinted with permission from ref 705. Copyright 2001 American Chemical Society.

not occur. In the case of the cerium(IV) complexes, they were able to detect (though not separate) two isomers caused by hindered rotation of the complexes.

Aida and co-workers[690] reinvestigated cerium(IV) and zirconium(IV) complexes, resolving the enantiomers using chiral HPLC. They confirmed that the zirconium complexes were stable to thermal racemization (refluxing toluene; 2 h), but they found that the cerium(IV) complexes isolated underwent facile racemization, even at 10 °C. They further determined by a scrambling experiment that dissociation followed by recombination of the porphyrins was not responsible, and they proposed that mutual rotation of the porphyrin rings was responsible for the racemization. The ability to rotate and the rates were found to be dependent on the steric bulk of the ligands and the size of the central metal atom. Addition of acid promoted rotation in the zirconium(IV) complexes.

This led to a "controversy"[691] in the literature as to whether bis(tetraarylporphyrinato) complexes did or did not rotate. It was pointed out that if rotation was a little too slow for observation on the NMR time scale, it could not be observed using coalescence NMR experiments. Indeed, these authors did not observe coalescence up to 150 °C (in DMSO-d_6), but they found it difficult to isolate the enantiomers even at room temperature due to their facile racemization. Tashiro et al.[692] found that the rate of rotation (and thus racemization) of chiral cerium double-decker complexes is greatly accelerated by reduction of the metal center and that oxidation retards the acid-induced rotation of zirconium complexes.

Shinkai and co-workers[693] exploited the ability of the cerium(IV) complexes to rotate to show that molecular recognition in such compounds could lead to a positive allosteric effect. The complex bore four pyridine groups on the phenyls, and the authors investigated the binding of dicarboxylic acids (Figure 65). As discussed in section 5.3, when the first substrate is bound, the entropic price is paid (lost rotation of the porphyrin rings), and binding of subsequent substrates is favored because the molecule is already conformationally locked. Previous work[694,695] had shown that a similar porphyrinatoiron(III) complex did not show cooperative binding due to a tilt in the rings after the first substrate binds, leading to a negative allosteric effect (binding of the first substrate precludes binding of additional ones). The authors have also shown[696,697] recognition for chiral dicarboxylic acids using complexes bearing two 4-pyridyl groups on each of the decks. Interestingly, the chiral induction was kept even after removal of the guests, and this "chiral memory" could be preserved for 3 days at 0 and 1 year at −37 °C (Figure 66). The authors identified such systems as possibly useful for "molecular memory systems". This is an example of a molecular rotor system useful in memory applications, although the racemization may be too fast for immediate utility at ambient temperature. Clearly, more work must be performed to slow the thermal racemization, and the synthetic ability to introduce steric interactions into molecular systems could play a role in achieving this goal.

These authors[698] also demonstrated a similar system which binds oligosaccharides preferentially based on their chirality. Similarly, Shinkai and co-workers have shown cooperative binding of silver ions to the π-faces of the aryl groups on the porphyrin decks,[699] saccharide (Figure 67) and oligosaccharide binding to modified double deckers in aqueous environ-

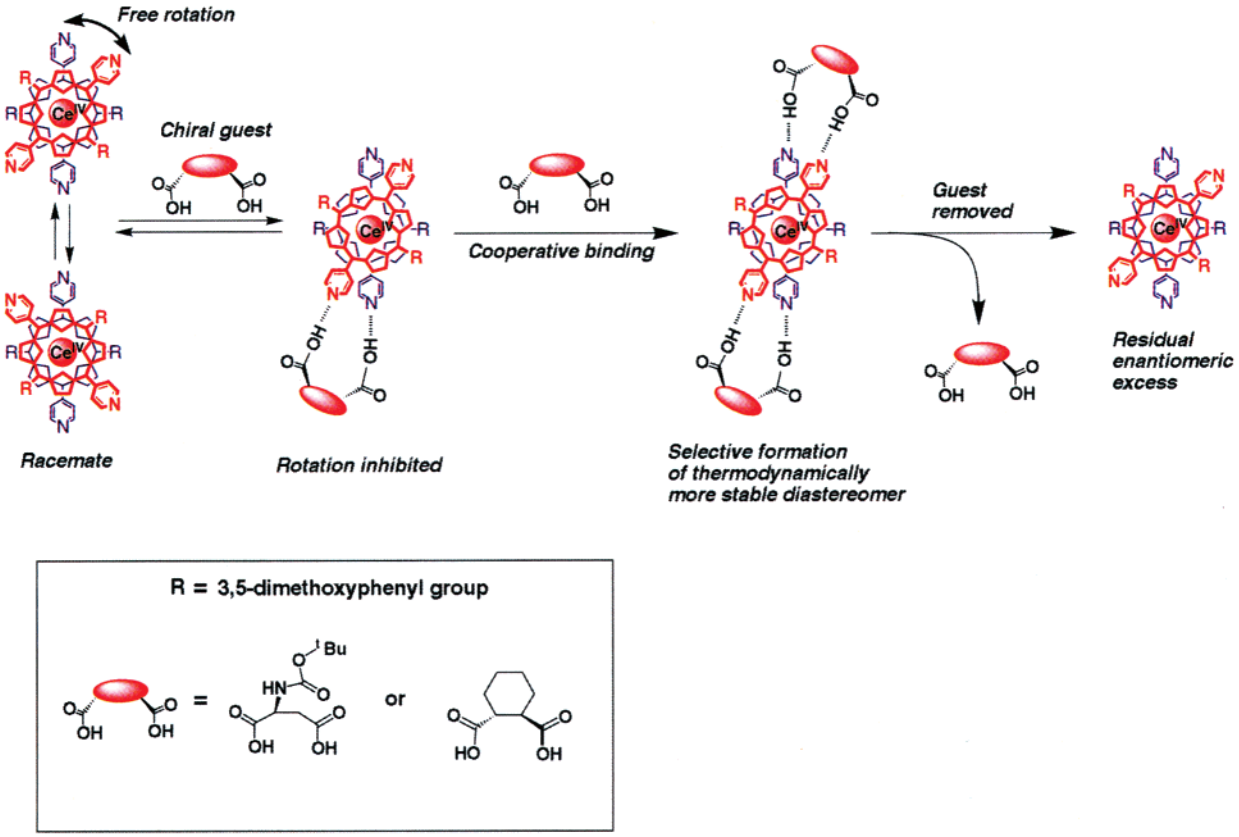

Figure 66. Cooperative binding in a cerium(IV) bis(porphyrin) complex. Reprinted with permission from ref 705. Copyright 2001 American Chemical Society.

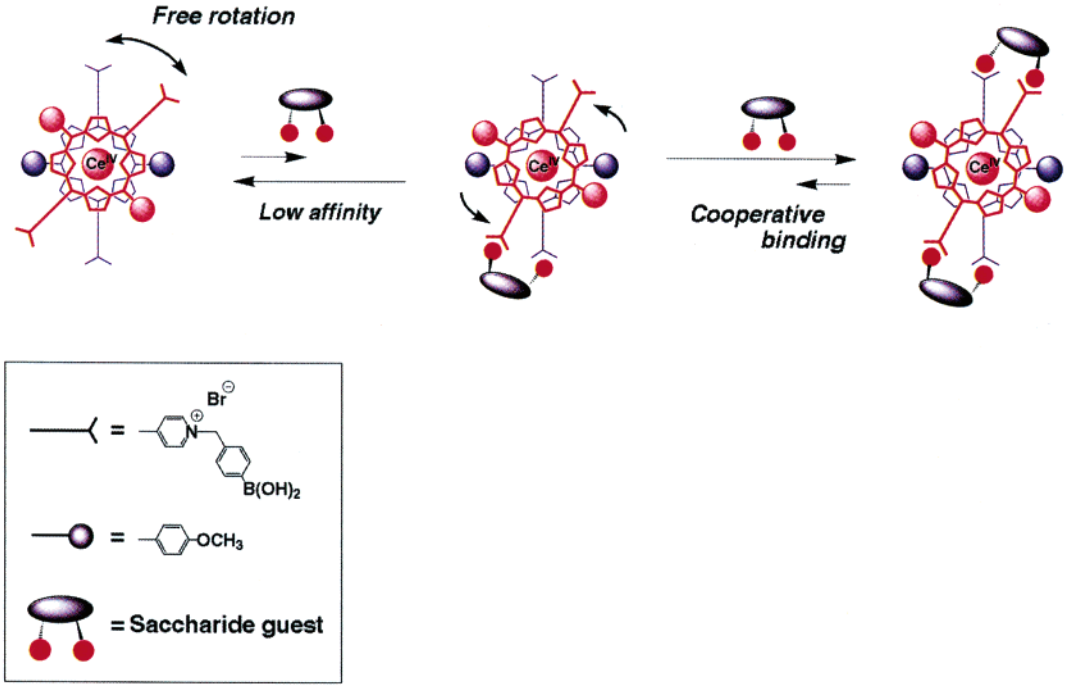

Figure 67. Cooperative saccharide binding via a rotational mechanism in a cerium(IV) bis(porphyrin) complex. Reprinted with permission from ref 705. Copyright 2001 American Chemical Society.

ments,[698−701] and alkali ion binding to lanthanum(III) double-decker molecules adorned with crown ether moieties.[702] By appending carboxylate groups onto cerium(IV) bis(porphyrinato) double deckers, positive homotropic allosteric binding of anions was also observed. Binding of the above analytes to the complex, in all cases, either hinders or immobilizes the porphyrin to rotation.

A lanthanum(III) triple-decker porphyrin complex (**175** and **176**) was also investigated by the Shinkai group (Figure 68).[703] The rates of rotation of the lanthanum triple deckers were much faster than

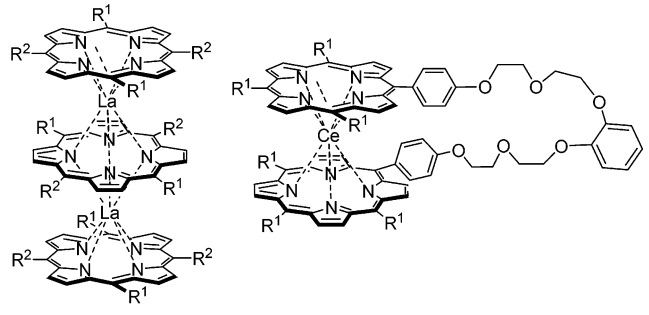

175 R^1 = H; R^2 = *p*-MePhenyl-
176 R^1 = H; R^2 = *p*-MeOPhenyl-

177

Figure 68. Triple-decker molecular rotor (**175**−**176**) and a molecular oscillator (**177**).

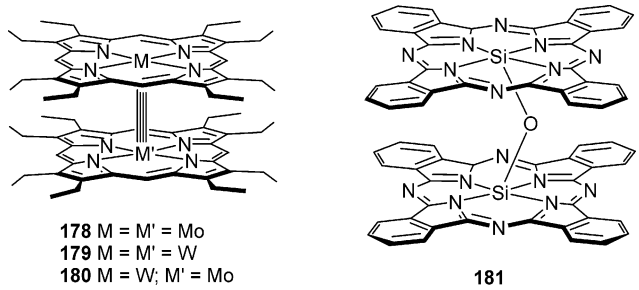

178 M = M' = Mo
179 M = M' = W
180 M = W; M' = Mo

181

Figure 69. Bis(porphyrin) sandwich complex (left) bound by metal−metal quadruple bonds and a phthalocyanine dimer (right) with a μ-oxo silicon linker.

those of the corresponding double deckers, which in turn were much faster than those in the cerium(IV) double deckers. The reason is presumably due to the increased ionic size of lanthanum(III) (118 pm) versus cerium(IV) (97 pm). The ability to change the size of the metal ion to achieve a change in the rotational barrier imparts a tunability in the molecular design of such systems for useful applications.

Aida and co-workers[704] also reported a molecular oscillator based on a cerium(IV) bis(tetraphenylporphyrinate) complex (**177**) wherein the two "decks" were tethered together by a crown ether chain (Figure 68). Since the complex could not rotate by 360°, it simply oscillated back and forth. The authors did not investigate metal ion binding to the crown ether, which may be useful to lock the dimer complex to a single orientation and could be useful for sensor applications by metal binding to the crown ether portion. Several reviews[705,706] have appeared recently on the concepts of allosteric interactions with an emphasis on bis(porphyrinato) complexes.

Porphyrin complexes such as those discussed in section 5.2, wherein the metal sits within the porphyrin ring and connecting the two metal centers via a linker to create a 2:2 porphyrin−metal structure also creates a carousel structure, are shown in Figure 69. Collman and co-workers[707−709] have pioneered the study of rotations in dimeric metal−porphyrin complexes which involve a formal metal−metal quadruple bond.[710,711] In their seminal paper,[707] they measured the barriers to rotation in three different binuclear molybdenum(II) porphyrins (**178**−**180**) using DNMR and found them to be identical within experimental error (~10 kcal mol^{-1}). This was consistent with the spectroscopic evidence of Trogler and Gray, who predicted a δ-bond energy of 10 kcal mol^{-1} for quadruply bonded metals. In the mono-*meso*-tolyloctaethylporphyrin dimers of molybdenum and tungsten, $[Mo(TOEP)]_2$ (**178**) and $[W(TOEP)]_2$ (**179**),[708,712] the Collman group found barriers ($\Delta G^{\ddagger}$) of 10.8 and 12.9 kcal mol^{-1}, respectively, using DNMR methods. This is interesting in light of the fact that all measurements show that the W−W quadruple bond is longer that the Mo−Mo quadruple bond. Another interesting feature is that both molecules prefer an eclipsed ground state with the porphyrin rings lying directly above and below each other, unlike the staggered state for the 2:1 complexes, as shown in Figure 64. In the mixed W−Mo system (TOEP)W−Mo(TOEP) (**180**),[709] the barrier to rotation ($\Delta G^{\ddagger}$) was 10.6 kcal mol^{-1}. Kim et al.[713] studied the rotation of dimeric tungsten−TPP complexes $[W(TPP)]_2$, which involves a formal rotation about a tungsten−tungsten quadruple bond, and found it to be ($\Delta G^{\ddagger}$) 11.3 kcal mol^{-1} by NMR line shape analysis. Previously, Yang et al.[714] had shown that the barrier to rotation ($\Delta G^{\ddagger}$) about a formal molybdenum−molybdenum quadruple bond in $[Mo(TPP)]_2$ was 6.3 kcal mol^{-1}.

Binstead, Reimers, and Hush[715] have investigated the rotation of phthalocyanine dimers and trimers bridged by μ-oxo-silicon linkers (e.g., **181**) by photoelectron spectroscopy.[716,717] They concluded that stacks of μ-oxo silicon phthalocyanines[718] can be simply derived from the dimers, and they believe that through-stack coupling could be tuned "by application of external geometric constraints". They believe nanotechnological applications, such as a ratchet-drive mechanism, could result.

5.4.5. Metal Atoms as "Ball Bearings"

Shionoya and co-workers[719−721] have developed a double-decker sandwich system that coordinates three silver ions between the decks of the carousel which act as ball bearings for rotation of the sandwich complex. Initially, they studied[719] the complexation of silver with two disk-shaped tridentate ligands bearing imidazole ligands and found a complex in which two disks bound three silver ions to form a sandwich complex and one with four disks held together by four silver ions in a tetrahedral fashion (Figure 70). Exploiting this discovery,[720] they increased the steric bulk of the disks with toluene groups and changed the silver binding moieties to thiazolyl and 2-pyridyl groups. The tolyl groups served to force the thiazolyl groups out of the plane of the central benzene ring for more efficient binding to silver. Complexation of three silver ions with two disks resulted in the quantitative conversion into a sandwich complex which had a distinct helicity (as evidenced by X-ray crystallography). To verify the helicity in solution, they used chiral counterions and observed the interconversion ($P \rightleftharpoons M$) by NMR. For the disk with 2-pyridyl groups, they found that the $P \rightleftharpoons M$ interconversion occurred above 328 K, and for the thiazolyl system, it is fast even at 303 K.

Shionoya and co-workers[721] extended these investigations in an attempt to observe driven motion using their ball bearing system. Using the more

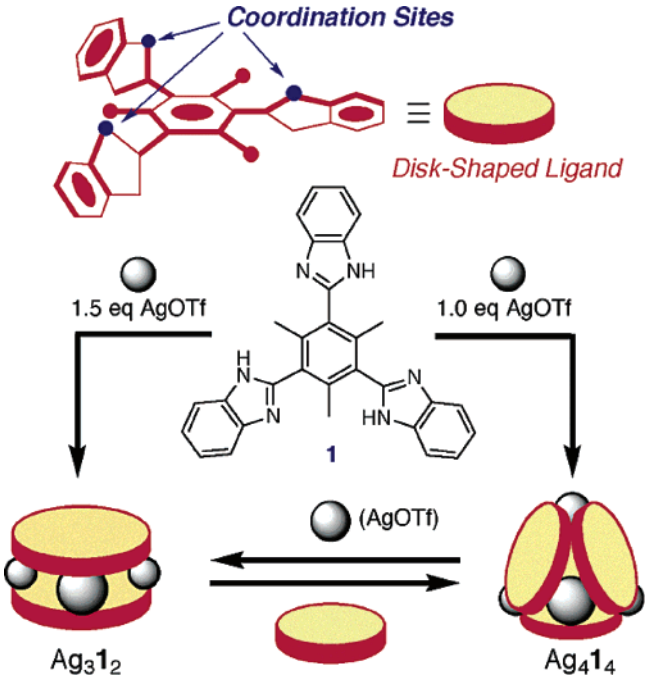

Figure 70. Complexation of disks into superstructures using silver ions. Reprinted with permission from ref 719. Copyright 2002 American Chemical Society.

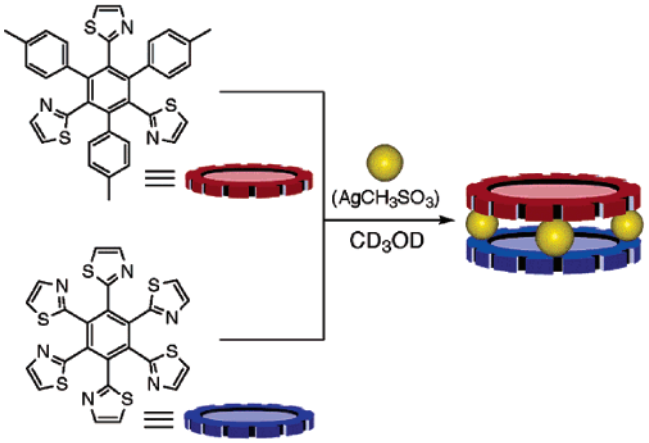

Figure 71. Molecular carousel formed by the quantitative self-assembly of two polythiazolylbenzene disks with three silver ions. Reprinted with permission from ref 721. Copyright 2004 American Chemical Society.

fluxional thiazolyl disk molecules, they synthesized a disk with six such units on a central benzene ring (Figure 71). Using this disk and the tris(thiazolyl) disk, they coordinated the two rings in a heterotopic fashion to three silver ions. From variable-temperature NMR, they found that ligand exchange between the nitrogens of the hexakis(thiazolyl) disk and the silver ions led to reversible rotation ($P \rightleftharpoons M$ interconversion). By line shape analysis, they found that the free energy for rotation ($\Delta G^{\ddagger}_{298}$) was ~14 kcal mol^{-1} ($\Delta H^{\ddagger} = \sim$12 kcal mol^{-1} and $\Delta S^{\ddagger} = \sim -$6.4 kcal mol^{-1}). They propose a transition state wherein the silver ions are coordinated to three thiazoyl nitrogens (Figure 72). The advantage of these systems is their quantitative assembly in solution and matching sixfold barriers to rotation. It remains to be seen how robust they are, but it appears to be an interesting system to study.

Shinkai and co-workers[145] discovered that binding silver ions to the concave π-clefts of cerium(IV) porphyrins (three Ag^+ ions per cerium double decker) actually increased the rate of rotation of the ensemble. When no silver ions were present, the rate of rotation was 200 s^{-1} ($\Delta G^{\ddagger}_{293} = 14.1$ kcal mol^{-1}), and when three silver ions were present, the rate increased slightly to 220 s^{-1} ($\Delta G^{\ddagger}_{233} = 11.0$ kcal mol^{-1}). They conclude that the silver ion binding induces a conformational change in the bis(porphyrin) system that removes interactions and makes rotation easier, such as decreasing the amount of π bonding and/or increasing the distance between the decks. In this way, the silver ions act as molecular "grease" to facilitate the rotation of the disks. This is similar to what was observed in the catenated porphyrin system discussed earlier, where adding a species that would seem to slow the rotation actually served to speed it up. While the silver ions might intuitively appear to be a steric nuisance to the rotation of the sandwich complex, they impart conformational changes that allow the disks to rotate with less hindrance. These results appear to defy logic when thinking about similar systems on the macroscopic scale, but at the molecular scale, interesting things happen that cannot be reconciled with such "macroscopic" thinking.

5.5. Rope-Skipping Rotors and Gyroscopes

A "rope-skipping" rotor (**182**) consists of a cyclic core to whose opposite ends are attached the two ends of a chain that can swing around the core (Figure 73). Taking the core as an immobile reference frame, this evokes images of children skipping rope in the street. These compounds have also been called paddlanes,[722] which intuitively brings about images of a paddle on a steam ship if one considers the chain to provide an immobile reference frame within which the cyclic system rotates. This dichotomy reminds us again of the ambiguities associated with the notions of a rotator and a stator in a molecular rotor. In an isolated molecule, both will move relative to an external frame, and the concepts are strictly applicable only for molecular rotors attached to a macroscopic body.

Some of the intramolecularly linked porphyrin systems discussed in section 5.2.3 fit this definition. Rope-skipping rotors also distantly resemble gyroscopes, in that if the rope were turning fast enough to create a "shield" around the interior, a rotator inside would be shielded like a gyroscope. More realistically, we use the term molecular gyroscope for molecular rotors similar to rope-skipping rotors but carrying more than one chain around the central core. Here, too, in an isolated molecule the core and the shield will both rotate, and it will not be easy to tell the stator apart from the rotator.

The parent compound for rope-skipping rotors is cyclophane. Figure 73 shows several examples of cyclophanes, such as [2.2]metacyclophane (**183**) and [3.3]paracyclophane (**184**), where the numbers in the brackets indicate the chain length of the tethers holding the two benzene rings. For compounds with only one aromatic group, the number in the bracket

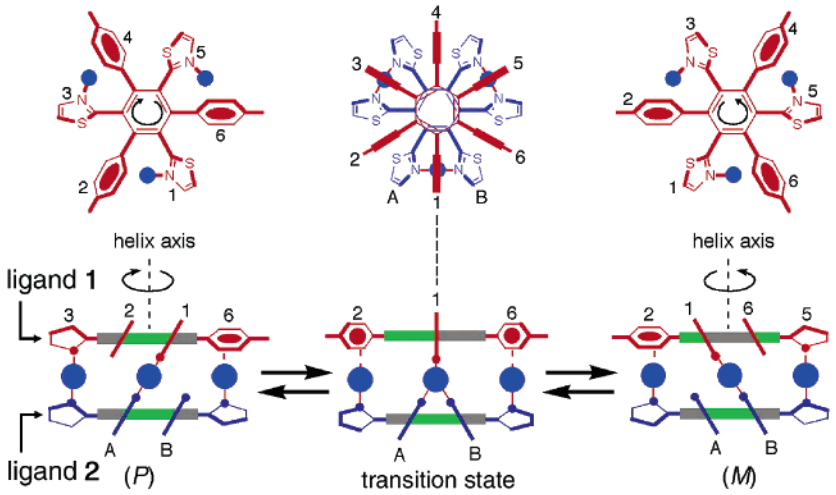

Figure 72. Cartoon representation of the P ⇌ M interconversion of the carousels investigated by Shionoya and co-workers. Reprinted with permission from ref 721. Copyright 2004 American Chemical Society.

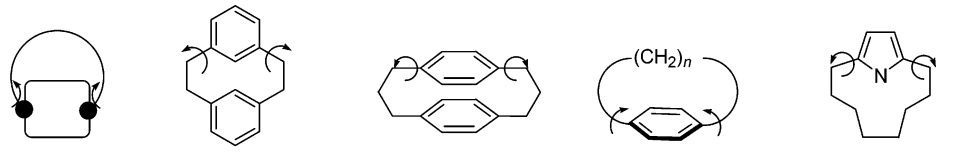

Figure 73. Rope-skipping rotors.

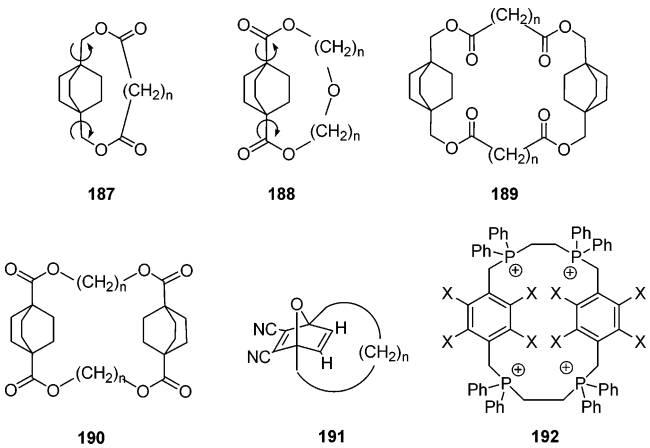

Figure 74. Some rope-skipping rotors and paddlanes.

indicates the chain length, as shown for [*n*]paracyclophane (**185**), and the number in parentheses indicates the substitution pattern, as shown for [8]-(2,5)pyrrolophane (**186**). Early work on rope-skipping and hindered rotation in cyclophanes has been covered elsewhere[165] and will not be reviewed here. Several monographs and reviews dedicated to cyclophanes, including their rotational dynamics, have been published.[723,724]

Molecular rope-skipping paddlanes were discovered by Ginsburg and collaborators[722] in 1973. Attempting to synthesize the singly linked [2.2.2]bicyclooctane, rope-skipping rotors **187** and **188**, they were only able to isolate the dimeric structures **189** and **190** (Figure 74). They reported "no extraordinary behavior of protons...in the room-temperature NMR" and performed no further analysis on the systems. Helder and Wynberg[725] did perform variable-temperature NMR measurements on rope-skipping rotor **191** (*n* = 8) and found temperature dependence presumably related to rotation. A unique paddlane structure was synthesized by Venkataramu et al.[726] (**192**), but they made no attempt to investigate the dynamics.

Vögtle and Mew[727] synthesized a rope-skipping rotor in which the central unit is a triptycene (Figure 75). Compound **194** (*n* = 8, 12) was synthesized by the pyrolysis of the disulfone **193** (*n* = 8, 12). NMR analysis showed that the triptycenes could not rotate inside the cavity of the chain for any length. Models indicated that the chain was wedged between two phenyl groups of the triptycene, which is borne out in the diastereotopicity of the phenyl protons (2:1 ratio, indicating that two phenyl groups are equivalent while the third is in a magnetically different environment). Dignan and Miller[728] found similar results for a triptycene-based cyclophane. Gakh et al.[729,730] synthesized an analogous triptycene with crown ether tethers [**195**; X = $O(CH_2CH_2O)_2$ or OCH_2-CH_2O]. NMR and crystal data showed the center of the crown ether chain to be in one of the cavities of the triptycene. Binding to Tl^+ distorted the structure of the chain. These authors have also investigated bis(triptycyl) paddle wheel systems (**196**),[730,731] which undergo fast rotation above 60 °C and for which the rotation is frozen below −40 °C.

A wholly different type of rope-skipping rotor, based on organometallic platinum complex **197** (*n* = 1, 5, 9,11) was recently described by Gladysz and collaborators (Figure 76).[732] Although the P−Pt−P axis can rotate, only the smaller chlorine atom is able to pass under the methylene chain, and therefore, the molecule can oscillate back and forth. At room temperature, the oscillation is fast for *n* = 5, 9, and

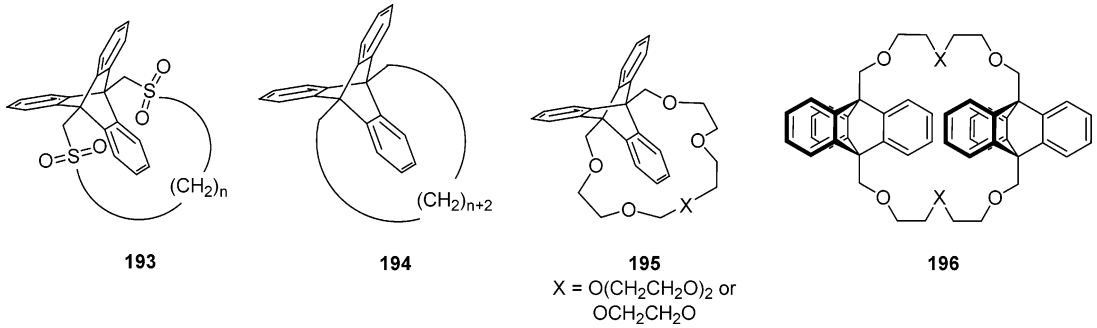

Figure 75. Triptycene-based rope-skipping rotors.

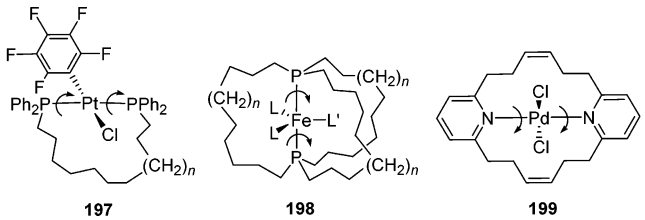

Figure 76. Organometallic rope-skipping rotors. Progenitors to molecular gyroscopes.

11 but slow for $n = 1$. The lower limit for the rotational barrier ($\Delta G^{\ddagger}$) for the smallest chain is 17.4 kcal mol^{-1}. For the second-shortest chain ($n = 5$), the upper limit to the activation process ($\Delta G^{\ddagger}$) was found to be 8.4 kcal mol^{-1}. Given that the shortest chain does not rotate fast up to 95 °C (no coalescence up to this temperature) and the second-shortest chain rotates too quickly even at −90 °C (no coalescence down to this temperature), the authors propose a 15-member macrocycle ($n = 3$) to measure the exact barrier of an oscillation within their experimental capabilities.

The Gladysz group has used the same synthetic strategy to synthesize molecular gyroscope structures (**198**; $n = 2, 4, 6$), in which the ligands on the pentacoordinate iron rotate within the cage formed by the methylene linkers, as shown in Figure 76.[733] From the parent (L = L′ = CO), they replaced one CO by an isoelectronic NO ligand and investigated the dynamics of the system with ^{13}C DNMR. They found the enthalpy of rotation ($\Delta H^{\ddagger}$) to be 9.5 kcal mol^{-1} for $n = 6$ by line shape analyses of the temperature-dependent spectrum. For $n = 4$, warming the solution led to line broadening, but the compound decomposed at higher temperatures. The two choices of shorter tethers each showed two sets of signals at room temperature, indicating that rotation is slow on the NMR time scale. The inclusion of a dipole moment in the molecule opens possibilities for driven motion in a rotating electric field (see section 3). The fact that the rotator is "protected" by the cage also leads to intriguing options for regular arrays of dipolar rotors capable of communicating through electrostatic interactions. The cage could be used to keep the dipoles separated, whether in a solid-state device or on a surface, and their mechanical interference small.

Previously, Ng and Lambert[734] synthesized a palladium complex employing similar chemistry to form a two-armed molecular gyroscope (**199**) in a surprising 80% yield. These compounds are analogous to the supramolecular inclusion compounds which will be discussed in the next section, with the advantage of having a covalent axle to hold the rotator in place.

Molecular turnstiles are closely related to paddlanes and are thus considered here in the rope-skipping section. The first rationally designed molecular turnstile was synthesized and studied by Moore and Bedard (Figure 77).[735] They attached a

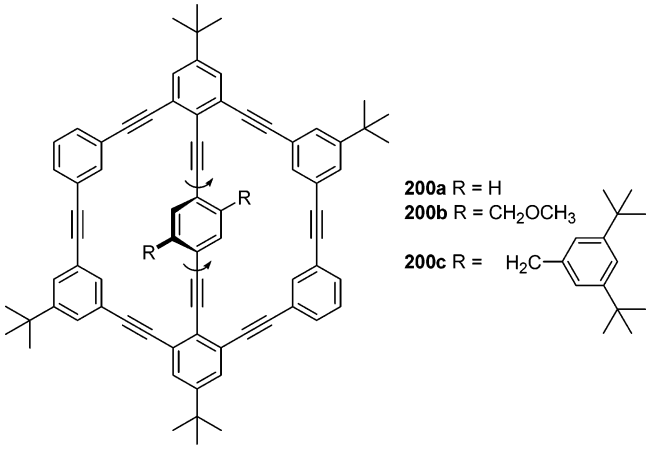

Figure 77. Molecular turnstile.

substituted *p*-diethynylbenzene group to the interior of a phenylethynyl macrocyclic framework and observed the rotation of the internal phenylene group as a function of its substituents (R = −H, −CH_2-OCH_3, −CH_2O-3,5-di-*tert*-butylphenyl). They studied the differentially substituted molecules using DNMR. Compound **200a** rotates too quickly to be studied by NMR methods. As discussed in section 5.3, the intrinsic barrier to rotation about triple bonds is very low, and in the absence of steric hindrance, the rotational barrier here is likely to be less than 1 kcal mol^{-1}, well below the limit for DNMR measurements. For **200b**, rotation is still very fast and the barrier to rotation ($\Delta G^{\ddagger}$) was estimated to be 13.4 kcal mol^{-1}, due to steric interactions between the methoxymethylene groups and the macrocyclic framework. Compound **200c** is sterically very bulky, and rotation was not observed. This compound is thus conformationally locked. The authors hoped to use these conformationally bistable molecules in new types of solids or liquid crystals in the hope that they would respond to external electric fields. To the best of our knowledge, however, these studies have not been carried out by these authors. However, they have been taken up by others[84,85] more recently on similar molecules

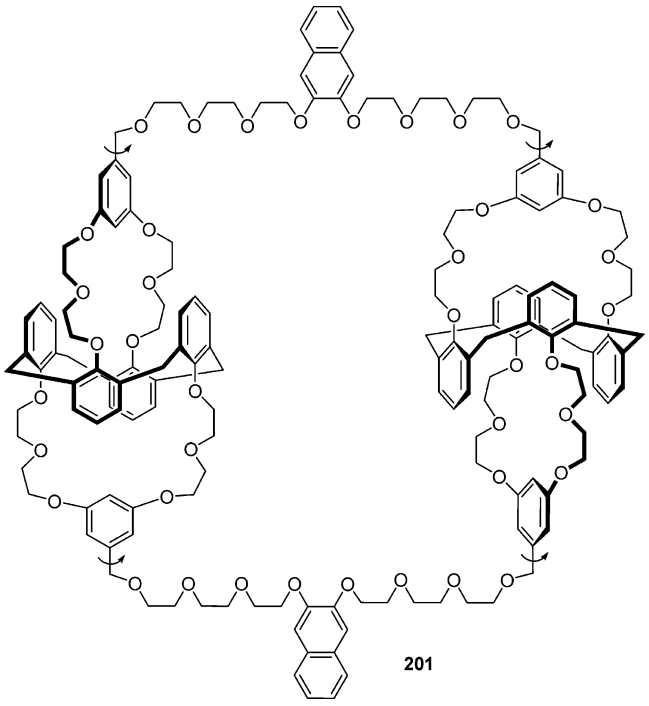

Figure 78. Molecular mill.

in solid-state studies (section 6.1). İpek and Varnali[736] used semiempirical calculations (PM3) to investigate Moore's turnstile (**200**) for R = H, F, Cl, CN, CH_3, OCH_3, and CH_2OCH_3. They found that H, F, and Cl do not interfere with spindle rotation, while CN, CH_3, OCH_3, and CH_2OCH_3 block the rotation of the inner substituted phenyl ring. They found significant distortions in the transition state as the inner phenyl group passes through the plane containing the macrocycle.

Another molecular turnstile (**201**), referred to as a "molecular mill", was designed and synthesized by the Vicens group,[737] using two calix[4]-bis-crown ethers as the rotational elements in a framework of a naphtho polyether diol (Figure 78). They performed molecular modeling studies on the system and found that the calix[4]arene moieties would be able to rotate independently of one another. However, they gave no experimental evidence to support the calculations.

5.6. Rotators in Inclusion (Supramolecular) Complexes

Supramolecular chemistry, or "chemistry beyond the molecule",[738] is chemistry that involves binding by interactions between molecules and not by covalent bonds, and it is considered one of the greater advances of the latter half of the last century, leading to Nobel Prizes in chemistry for Jean-Marie Lehn,[739] Donald Cram,[740] and Charles Pedersen.[741] "Conventional chemistry" deals with the construction of molecules from atoms, while supramolecular chemistry is based on the construction of larger ordered arrays from molecular building blocks. Traditional chemistry has a length scale of approximately 1−100 Å, while that of supramolecular chemistry is an order of magnitude higher, or ∼1−100 nm. Many reviews exist which discuss the principles of supramolecular science,[738−740,742−746] and a number of groups have been interested in molecular nanoscience derived from supramolecular chemistry.[738] Several groups have investigated rotational processes in inclusion complexes, which will be covered in this section. Much of the published work on the dynamic behavior of molecules in supramolecular complexes concerns the association and dissociation properties of such species, and we will not discuss these here. In some cases, we felt obliged to deviate from our stated criterion and to discuss examples involving whole-molecule rotations. We believe these instances represent structures which may ultimately lead to useful nanoscience applications or are important in the general understanding of rotational phenomena.

5.6.1. Rotation in Host–Guest Complexes

In general, electrostatic effects dominate the inclusion of guests into their hosts and steric effects dominate the rotation of the guests inside the framework of the supramolecular host. For example, using variable-temperature NMR techniques, Hilmersson and Rebek[747] found that benzene rotates rapidly inside a cylindrical cavitand while *p*-xylene tumbles slowly and toluene shows an intermediate rotational rate. Behr and Lehn[748] used ^2H and ^{13}C NMR relaxation experiments to investigate the rotations of alkyl groups on guest molecules in complexes of *p*-methylcinnamate, *m*-methylcinnamate, and *p-tert*-butylphenate in α-cyclodextrin (α-CD). Upon inclusion, the reorientation times increase by a factor of 4. For the cinnamates, the methyl groups showed hindered rotation, indicating that they were inside or in contact with the CD. In contrast, the *tert*-butyl group in the phenate is likely outside the cavity. They concluded that there is weak coupling between the host and the guest in these compounds, that is, very little change to both the host and guest upon complexation. Thus, their individual motions are weakly coupled in the complex.

Lehn and co-workers investigated ammonium cryptates (e.g., **202**, Figure 79) and initially[749] found

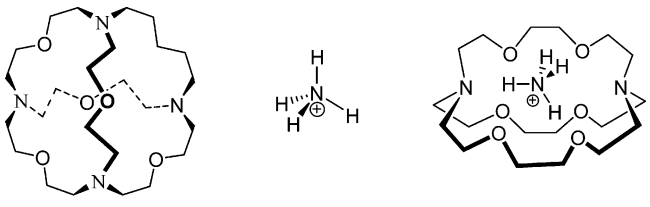

Figure 79. Ammonium cryptate molecules.

by ^2D NMR techniques that the ammonium ion does not rotate in the cavity of the cryptate. Semiempirical calculations on the complex gave a barrier (E_{calc}) of 23 kcal mol^{-1} for rotation of the ammonium ion about the C_3 axis of the cryptate. In another system (**203**),[750] they did find rotation of the included ammonium ion. The crystal structure showed that the ammonium ion is hydrogen-bonded in the cavity, and they studied the dynamics by NMR. At room temperature, the complex is fluxional, but below 228 K, motion is frozen and the methylene protons on the cryptate cage are also frozen. The free energy of activation for

the symmetrization process was found to be 10.5 ± 0.5 kcal mol^{-1}.[750] Interestingly, all the carbons of the cryptand have a similar correlation time (τ_c), which allowed the authors to conclude that it is an "isotropic rotor". The fast reorientation inside the cavity indicates that the ammonium ion is only weakly coupled to the host, and they labeled this complex an "anisodynamic supramolecule". Compound **202**, where the ammonium was tightly held by the host and did not rotate inside the cavity,[749,750] was labeled an "isodynamic supramolecule".

Many macrocyclic hosts in supramolecular inclusion complexes are not spherically symmetric. Many are oblong, having a long axis and two shorter axes. The supramolecular terminology is often analogous to that used for describing planetary regions. For example, the poles terminating the longitudinal axis are often referred to as the northern and southern hemispheres and those of the equatorial axis, the eastern and western hemispheres. Therefore, elliptically shaped guests can fit differentially into the host and, when asymmetric, can be probed by DNMR for rotation of the host in the guest. Figure 80 shows one

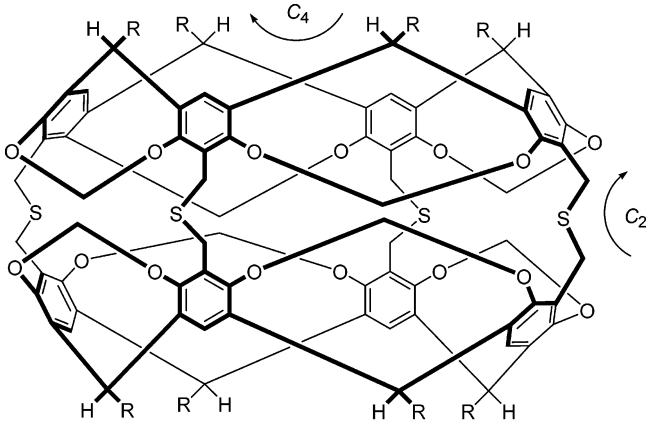

204

Figure 80. "Football-shaped" carceplex.

such host, a carceplex (**204**), synthesized by Cram and co-workers[751] in which the guests $CH_3OH\cdot HOCH_3$, $CH_3CN\cdot NCCH_3$, CH_3CN, CH_3CH_2OH, $(CH_3)_2NCHO$, $CH_3COCH_2CH_3$, and $CH_3CH_2COCH_2CH_3$ were included. The host is "shaped like a U.S. football, fattest at its equator and narrower at the poles".[751] Four C_2 axes of symmetry exist about the equatorial plane, and a C_4 axis exists along the longitudinal plane, in addition to five mirror planes. By probing the protons along the periphery of the host by NMR, rotations of the included guests could be monitored. In all cases, the long axis of the guest lined up with the long axis of the carcerand. For inclusion of $H\cdot CH_3COCH_2CH_3$, the authors found that rotation about the long axis was fast on the NMR time scale, while rotation about the short axis (which exchanges the ends of the guest) was slow and observable. For the symmetrical $H\cdot CH_3CH_2COCH_2CH_3$ molecule, only one type of signal is observed, as end-to-end exchange cannot be probed due to the symmetries of the host and the guest. For the smaller guests, $H\cdot CH_3CH_2OH$, $H\cdot(CH_3)_2NCHO$, $H\cdot CH_3OH\cdot HOCH_3$, and $H\cdot CH_3CN$, rotation about all axes was found to be fast on the NMR time scale.

A similar carceplex (**205**, Figure 81) was synthesized by Cram and co-workers and studied for rota-

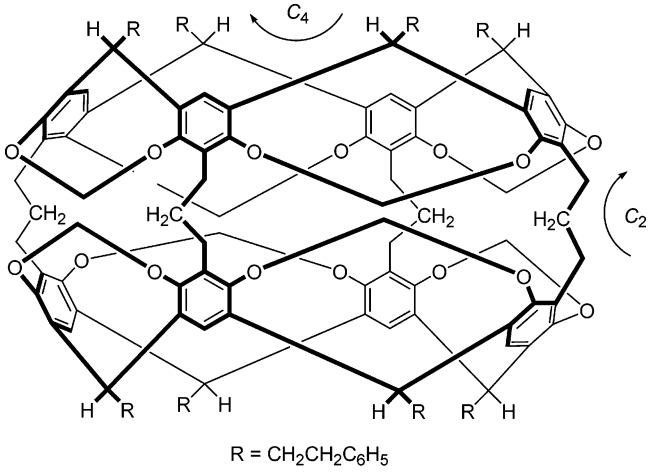

205

Figure 81. A carcerand.

tion of dimethyl sulfoxide (DMSO), *N*,*N*-dimethylformamide (DMF), and *N*,*N*-dimethylacetamide (DMAA) guests.[752,753] They found that the long axes of the guests were coincident with the long axis of the carcerand. A combination of ^{13}C and ^{1}H NMR showed that DMAA was only able to rotate about its long axis (up to 175 °C), while DMF could rotate about all its axes, even at very low temperatures (−37 °C). For DMSO, down to −2 °C, it could likewise rotate about all its axes, but below this temperature, it was restricted to rotation about its long axis. Interestingly, the authors also measured the bond rotation of the C−N amide bond of DMAA and DMF in the complex. For DMAA, the rotational barrier was ∼1 kcal mol^{-1} higher in the carceplex than that in the free amide, while, in DMF, the barrier was ∼2 kcal mol^{-1} *lower* inside the cage than in solvent. This implies that the inside of the host is a mixture of vacuum and guest and that solvent effects outside the cage are greater than the steric effects inside the cage.

Likewise, Cram and co-workers[754] investigated rotations of guests in carcerands of the type shown in Figure 82 (**206**; one enantiomer shown; the other enantiomer and the *meso* compound not shown). In

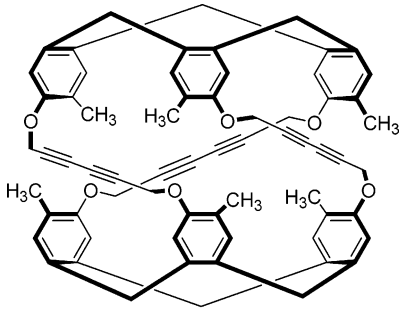

206

Figure 82. A carcerand.

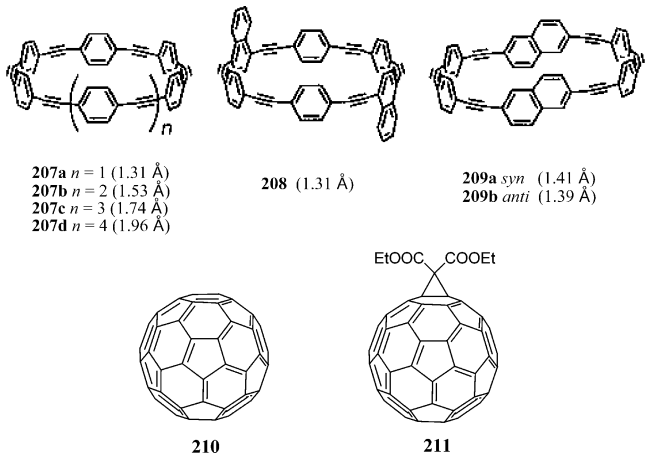

Figure 83. Nanobelts for fullerene cages. The inside diameters of the belts are shown in parentheses. The top figure was reprinted with permission from ref 764. Copyright 2003 Wiley-VCH.

looking at CPK models, they determined that chloroform "provides the largest common surface between host and guest without any rotational constraint of host vs. guest, unlike the model of [*tert*-butanol] whose OH fits better in the equatorial rather than in the polar caps of the host. Dichloromethane in models 'rattles' when shaken, and thus the cavity is a mixture of vacuum and guest." However, they did not probe the rotation experimentally. The above studies are important for understanding the rotations of molecules fully included into larger species and represent noncovalent analogues of the molecular gyroscopes discussed previously (where the rotator is fully protected by a cage). A likely next step toward nano-machinery would be to probe dipolar guests in solid-state structures of such supermolecules via an electric field. In section 6.3, we will touch on some examples of "solid-state inclusion complexes".

Bonechi et al.[755] found that acetonitrile (CH_3CN) behaves as a "free"[645] rotor in the cavity of a calixarene by ^{13}C NMR relaxation measurements and supported by molecular mechanics and dynamics. Calixarenes form cone-shaped structures and can include small organic guest molecules.[756−759] In this example, the acetonitrile group sits in the cavity of the calixarene with the cyano portion pointing toward the cone opening. Reorientational motion of the acetonitrile guest was 2 orders of magnitude faster than that of the calixarene host.

Kawase and co-workers have pioneered the study of fullerenes complexed into "nanobelts" made of aromatic units—cyclic *para*-phenyleneacetylenes (Figure 83).[760−762] These belts (**207**−**209**) were shown to complex small organic molecules[762] and fullerenes,[763,764] which showed interesting dynamic properties. A variable-temperature NMR analysis showed that C_{60} (**210**) rotates rapidly inside ring **207a**, even at −100 °C.[763] With the less symmetrical bis(ethoxycarbonyl)-methanofullerene (**211**), two singlets appeared for the aromatic protons at −100 °C, whereas they were a singlet at room temperature. This implies hindered rotation of the larger fullerene derivative in the ring. No crystal structure could be obtained from the C_{60} complex, most likely due to rotation of the cage in the macrocycle and hence disorder in the crystal. However, the substituted fullerene gave a crystal structure (**207a·211**) from toluene. The authors find that the ester groups "lean on the aromatic rings...and therefore the aromatic protons of [the nanoring] act like a gear wheel hindering easy rotation of the guest". The possibility of gearing in these molecules may present an interesting application for molecular devices. In the crystal structure, the ring adopts a bowl shape, because the fullerene is larger than the cavity of the ring, and a larger "belt" might fully include the spherical guest.

To remove the symmetry from the ring (and increase the likelihood of rotational isomers) as well as to increase the inside diameter, the authors synthesized two new ring structures with naphthalene units, either 1,4- or 2,6-substituted (**208** and **209**, respectively).[764] Figure 83 shows the interior diameter of the rings as calculated by the semiempirical AM1 method. The 1,4-substituted naphthalene derivative (**208**) has the same interior dimensions as **207a**, and the 2,6-substituted ring (**209**) has the same dimensions as a C_{70} molecule. For **207a**·C_{70}, the authors found two signals at −100 °C, indicating that the center of the fullerene is not aligned with the center of the macrocycle, and rotation is fast at this temperature. They proposed that it occurs about the long axis of the fullerene (C_{70} has lower symmetry than C_{60}). The new complexes, **208**·C_{60}, **208**·C_{70}, and **209**·C_{70} also showed fast rotation down to low temperatures.

5.6.2. Rotation in Self-Assembled Architectures

In this section we briefly discuss several examples of rotations in "self-assembled architectures", defined as compounds derived from individual molecules to create a supermolecule in solution and held together by noncovalent bonds. We note the similarities to crystal engineering (section 6) and to self-assembly of molecules on surfaces (section 7), but the molecules discussed here are not crystalline in that they do not form coordination networks derived from unit cells, nor is their assembly related to any surface phenomenon.

Whitesides and co-workers[765−769] have investigated supramolecular complexes made from hydrogen-bonded components. These "rosette"[770] structures self-assemble in solution and are composed of cyanuric acid derivatives (isocyanuric acids and barbituric acids) and of a synthesized molecular "hub". The hub is designed with the correct geometry and stereochemistry to self-assemble the cyanuric acids in solution, as shown in Figure 84.[771] The authors found coalescence of the signals in the NMR and proposed that it was caused either by a rotation of a cyanuric acid in the aggregate or by an association−dissociation mechanism, wherein one molecule formally dissociates, rotates by 180°, and returns to the complex (Figure 85). The barrier ($\Delta G^{\ddagger}$) was found to be between 13 and 15 kcal mol^{-1}, but the possible two isomerization pathways could not be distinguished. Use of optically active isocyanuric acid derivatives[768] led to formation of diastereomers, but

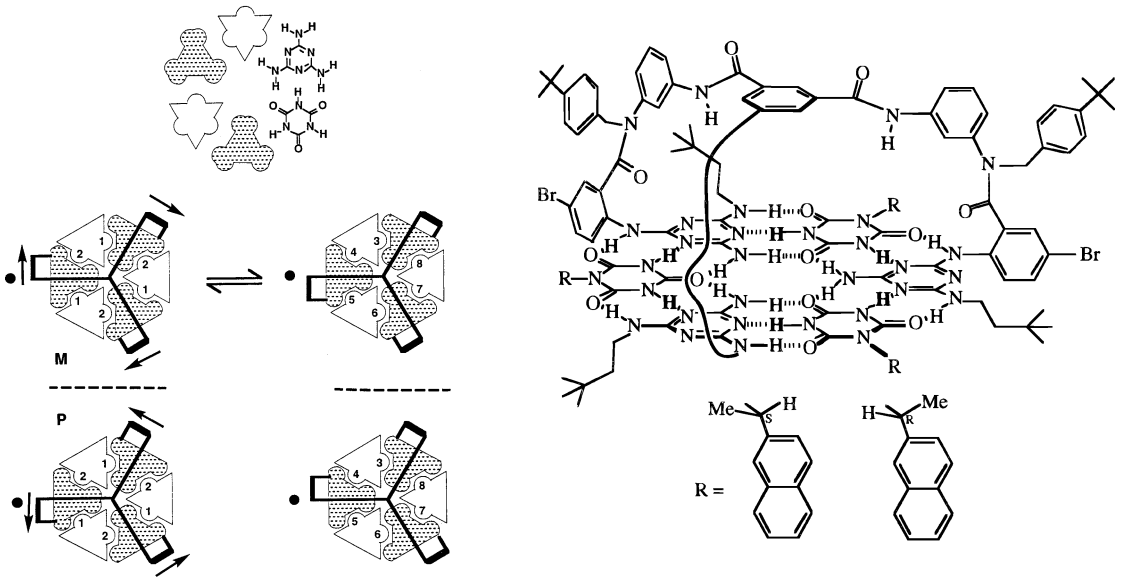

Figure 84. Self-assembled aggregates (as viewed from above) made from an isocyanuric acid component (open geometrical figure), melamine (shaded geometrical figure), and a three-armed "hub" molecule. The chiral complexes shown on the left have C_3 and C_1 symmetry, and the enantiomers are shown below the dashed line, which represents a mirror plane. Helical chirality is represented by the *M* and *P* as defined by the arrows. The C_3 and C_1 isomers can be conceptually interconverted by rotation of the spoke denoted with the dot. The numbers in the isocyanuric acid component are related to the number of imine protons observed, which are used for determination of the isomeric distribution. Reprinted with permission from ref 768. Copyright 1997 American Chemical Society.

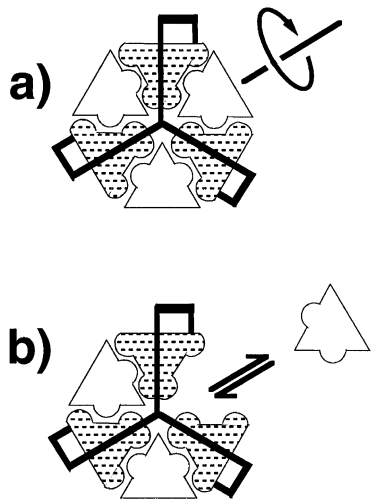

Figure 85. Two possible rotation mechanisms for Whitesides' self-assembled "hub" compounds: (a) intracomplex rotation and a (b) dissociation−rotation−association process. Reprinted with permission from ref 768. Copyright 1997 American Chemical Society.

this did not aid in the understanding of the process that leads to rotation of the cyanuric acid components. To the best of our knowledge, the mechanism has not yet been elucidated, and because this is not a clear example of intracomplex rotation, we will not discuss it further.

Reinhoudt and co-workers[772−776] have similarly investigated rotational phenomena in self-assembled molecular cage structures (Figure 86) composed of cyanuric and barbituric acid derivatives and in complexes with melamine and a calixarene (the hub). They began with calix[4]arene **212a** containing melamine substituents and self-assembled the structures in a variety of solvents with 2 equiv of the barbiturates (diethylbarbituric acid or DEB) or cyanurates (cyanuric acid or CYA) to give complexes containing three units of the calixarene and six units of the acids: (**212a**)$_3$(DEB)$_6$ and (**212a**)$_3$(CYA)$_6$. Complexation involved the cooperative interaction of 36 hydrogen bonds[149] in a manner similar to those described above for the Harvard group[777] and also investigated by Lehn and co-workers.[778] Using a enantiomerically pure calixarene, they found that the assembly process led to supramolecular chiral structures (with six stereogenic centers).[774,775] The complexes can form in three isomers as shown in Figure 87: D_3, C_{3h}, and C_s.

Dynamical processes were also found in these self-assembled structures when complexed with three molecules of alizarine (**213**).[776] A complex of (**212a**)$_3$(DEB)$_6$(**213**)$_3$ was crystallized and shown to have a threefold axis of rotation, with the alizarine hydroxyl groups pointing away from this axis (Figure 88).[776] Only one of the three possible isomers,[775] C_{3h}, is found in the crystal structure, whereas (**212a**)$_3$(DEB)$_6$ crystallizes with D_3 symmetry. Upon addition of alizarine to the (**212a**)$_3$(DEB)$_6$, the complex spontaneously rearranges to accommodate the guests. The final complex can be thought of as a supramolecular rotamer of the original. Using the fact that cyanurates form stronger hydrogen bonds to melamine,[779,780] the DEB molecules were then replaced by titration with butyl cyanurate to give (**212a**)$_3$(BuCYA)$_6$, which resulted in the release of the guest (Figure 89). The cyanurates have a different geometry than the barbiturates and are not able to accommodate the guest alizarine. The (**212a**)$_3$(BuCYA)$_6$ supramolecule is again of D_3 symmetry, and thus, the authors showed that the supermolecule can exist in two "rotameric" states. Although it can be converted from one to the other and back again, thereafter, no further change is possible. They have also observed the rotation of

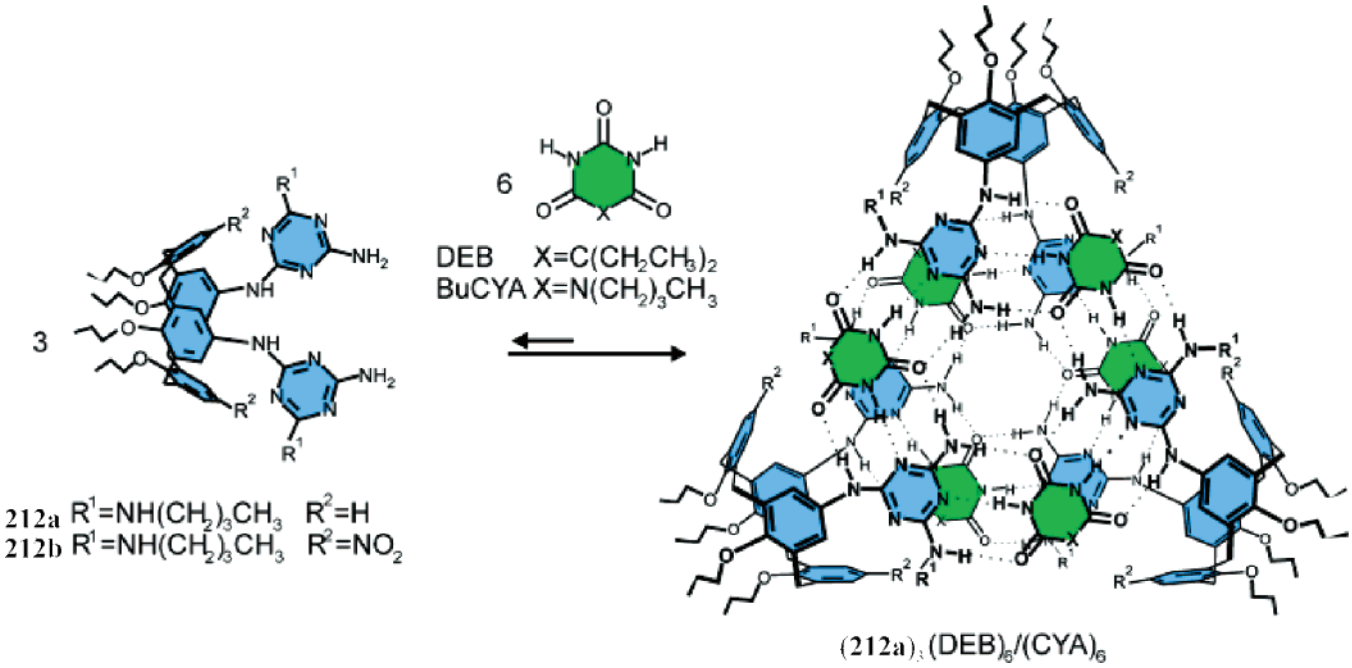

Figure 86. Rosette structure synthesized by Reinhoudt and co-workers. Reprinted with permission from ref 776. Copyright 2003 Wiley-VCH.

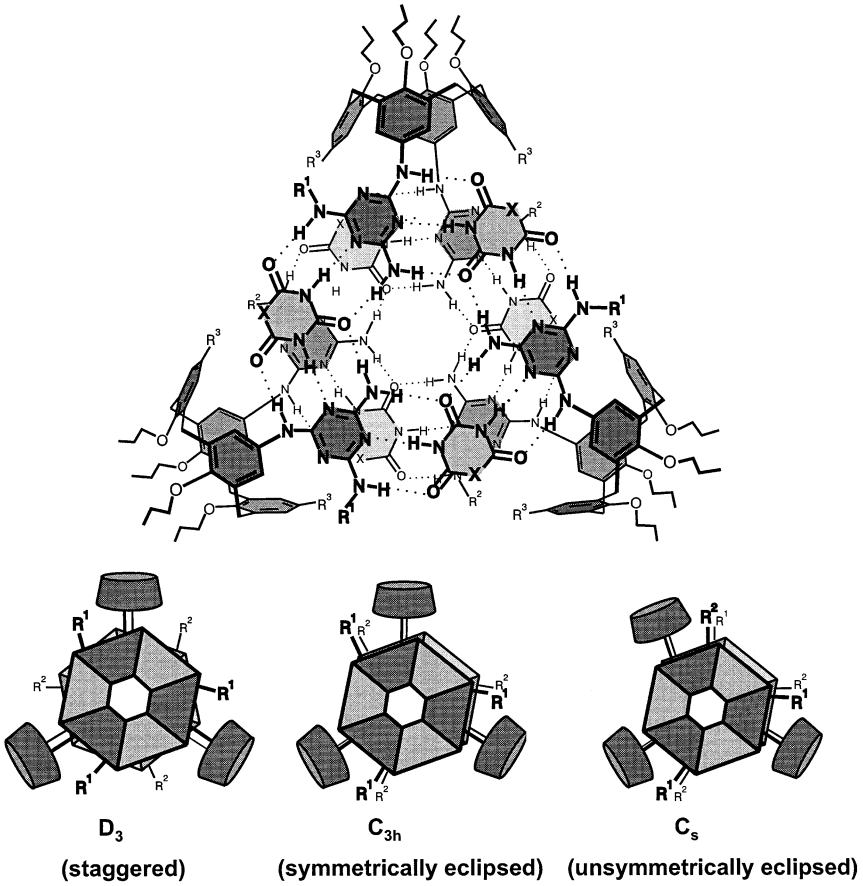

Figure 87. Three geometries for a hydrogen-bonded rosette structure. Reprinted with permission from ref 775. Copyright 2000 American Chemical Society.

inclusion complexes adsorbed to a surface using near-field scanning optical microscopy (NSOM).[781]

5.6.3. Rotations in Molecular "Onion" Complexes

Molecules within molecules are an interesting area of research,[782] and the potential for the inner molecule rotating inside the cavity formed by the outer molecule may be exploited to yield interesting properties. Several examples of such systems are the so-called fullerene "onion" compounds[783,784] and nanotube "peapod" complexes.[785−787] The potential for useful devices being achieved from this design is not

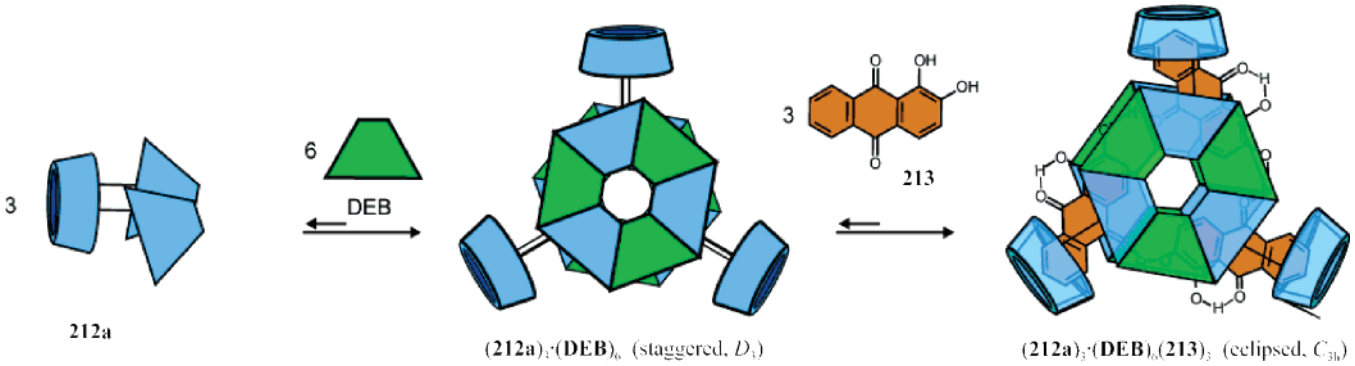

Figure 88. Self-assembled molecular rotor. Addition of alizarine (**213**) causes the structure to rotate from a staggered conformation to the eclipsed rotamer. Reprinted with permission from ref 776. Copyright 2003 Wiley-VCH.

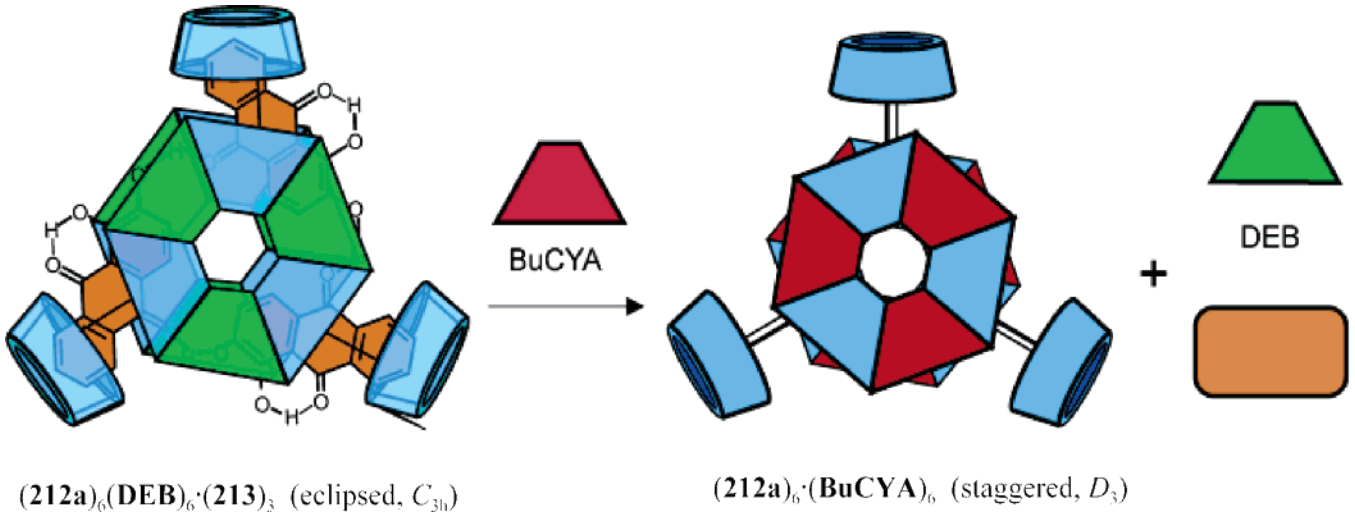

Figure 89. Conformational switching by a molecular rotor based on supramolecular chemistry. Addition of butyl cyanurate (BuCYA) causes replacement of the diethylbarbituric acid (DEB) units and expulsion of the alizarine molecule, causing the structure to rotate from an eclipsed to a staggered geometry. Reprinted with permission from ref 776. Copyright 2003 Wiley-VCH.

yet known. Here we discuss such molecules, including those in which a guest is encapsulated inside a host, which in turn is included inside a larger host.

An early example of such a system was discovered by Vögtle and Müller,[788] who crystallized γ-cyclodextrin with coronates and cryptates. These complexes were later shown by X-ray diffraction[789−791] to be comprised of an alkali metal bound inside the cryptand and surrounded by either one or two cyclodextrins. These types of molecules were called *cascade complexes*. To the best of our knowledge, rotational phenomena have not yet been observed in such structures.

Rebek and co-workers[792] have synthesized capsules inside capsules, reminiscent of Russian Matroshka dolls (Figure 90), which can be used to bind guests, and they observed rotational processes. Upon encapsulation of **215** into inclusion complex **214**, a simple pattern was observed in the NMR spectrum, implying fast, nondirectional rotation. However, when K^+-filled cryptate **216** was encapsulated into **214**, the NMR signals were split into two sets, which led the researchers to conclude that the desymmetrization was due to restricted guest rotation. They argued that both the cation and its thiocyanate (SCN^-) anion are encapsulated, with one ion occupying the upper half and the other the lower. The ions can switch

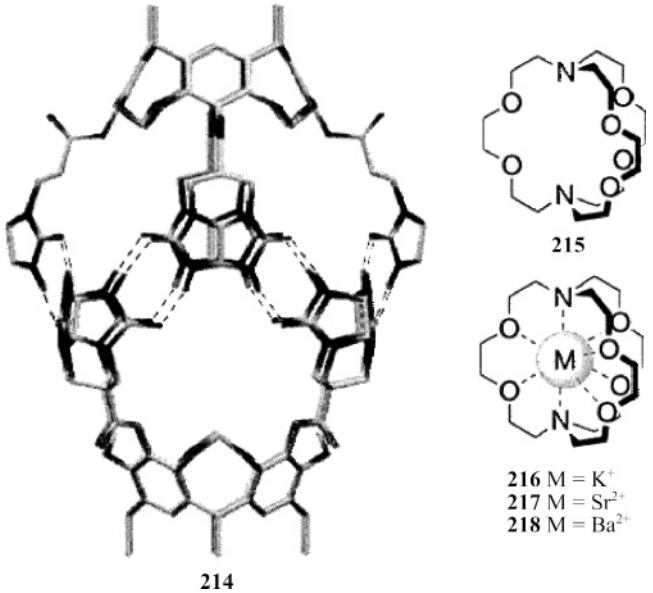

Figure 90. Inclusion complexes inside inclusion complexes—chemical Matroshka dolls. Reprinted with permission from ref 792. Copyright 1999 American Chemical Society.

positions, but this process is slow on the NMR time scale. This was supported by the ^{13}C NMR study of an isotopically labeled thiocyanate ($S^{13}CN^-$) and the

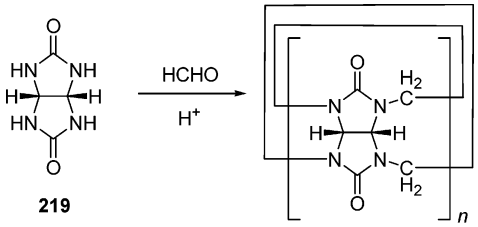

Figure 91. Synthesis of curcurbit[*n*]uril.

fact that a larger anionic salt of potassium did not form the inclusion complex.

A fascinating new area of research is centered around cucurbiturils.[87,88,793−795] Cucurbit[*n*]urils (**220**[*n*]) are synthesized from the glycouril (**219**) and formaldehyde under acidic conditions, where the *n* denotes the number of methyleneglycouril units in the cycle (Figure 91). They were first synthesized in 1905[796] but were not investigated further until the early 1980s, when Freeman, Mock, and Shih fully characterized the products of the reaction.[797] The six-membered macrocycle **220**[6] is the most commonly formed product. Like other macroscopic cylinders, cucurbiturils bind a variety of guests, including xenon,[798] water,[799] THF,[800−802] and pyridine,[803] among others. Larger cucurbiturils are known, and **220**[5] is the smallest formed under these reaction conditions.

Day and co-workers[804,805] synthesized a *gyroscane* consisting of a smaller cucurbit[5]uril (**220**[5]) inside a larger curcurbit[10]uril (**220**[10]) host (Figure 92), and they showed that the smaller **220**[5] rotates rapidly inside the host. The complex was crystallized from concentrated hydrochloric acid, and the crystal structure showed that the **220**[5] is directly in the middle of **220**[10] but that its axis is 64° inclined to that of the host. There is a chloride ion in the center of the guest and two water molecules (or hydronium ions) between the **220**[5] and **220**[10] cages. The authors only performed the variable-temperature NMR measurements down to 2 °C, and they did not see any splitting of the signals. This implies that the guest is rotating rapidly inside the host. Because the guest is inclined with respect to the host, they referred to this as "gyroscope-like motion", which leads to the dynamic averaging of the NMR signals for the host *and* the guest. For this to occur, the guest molecule **220**[5] must undergo both axial rotation and precession inside of the **220**[10] macrocycle.

Blanch and co-workers[806] investigated the use of *o*-carborane (**221**) as a template for the assembly of cucurbit[7]uril (Figure 93). *o*-Carborane is a nearly spherical (icosahedral) unit which is included in the spherical curcurbituril, and the authors viewed it as a model for a molecular bearing. Although the carborane can dissociate from the host (slowly at room temperature), the complexes are rather robust, surviving aqueous acids, ion exchange chromatography, and vacuum-drying at 80 °C. The NMR spectrum showed only a single resonance for the two carborane C−H units, indicating that the guest rotates rapidly inside the host. A low-temperature NMR analysis was precluded by insolubility.

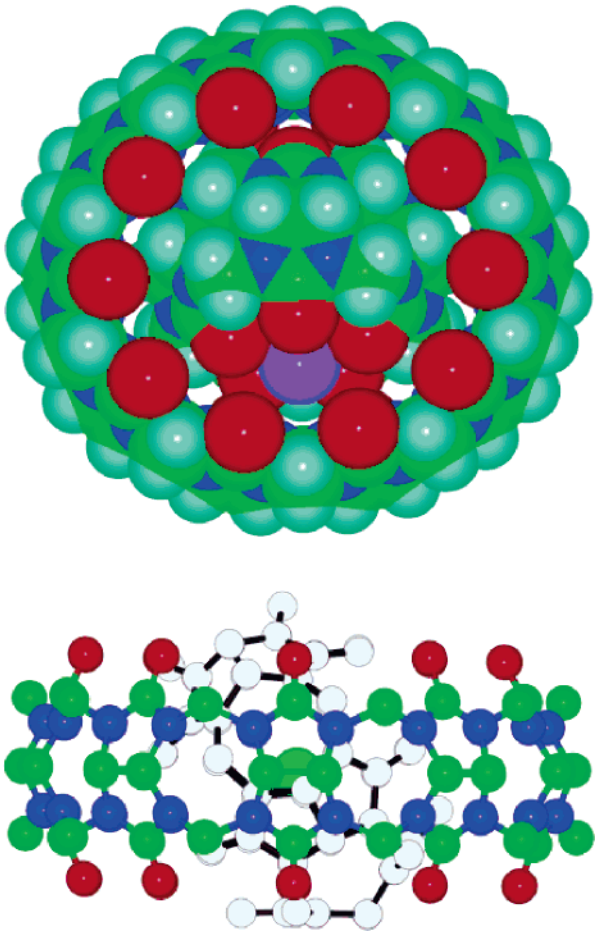

Figure 92. Molecular *gyroscane*: a curcurbit[5]uril (**220**[5]) encapsulated inside a curcurbit[10]uril (**220**[10]): (a, top) axial view (space-filling); (b, bottom) side elevation (ball-and-stick). Color code: C, green; N, blue; O, red; H, cyan; O (water), magenta. Reprinted with permission from ref 804. Copyright 2002 Wiley-VCH.

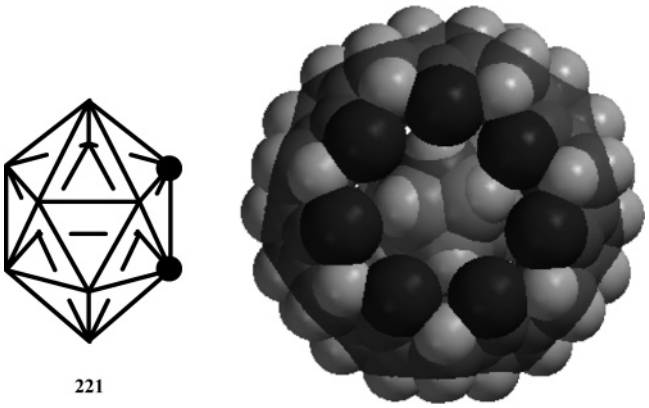

Figure 93. *o*-Carborane (**221**; ● = carbon, all other vertexes are boron) included in a curcurbit[7]uril (axial view). Reprinted with permission from ref 806. Copyright 2001 American Chemical Society.

5.7. Driven Unidirectional Molecular Rotors

A system capable of unidirectional motion is a precursor to a true molecular motor. To produce useful work, a molecular motor will require a supply of energy. Similarly, a unidirectional rotor also requires a supply of energy, even if it is not capable of producing useful work and thus is no motor according to our definition. Learning how to drive a

molecular rotor unidirectionally appears to be a useful and much simpler first step to learning how to drive it to do useful work.

A short review on unidirectional rotors has recently appeared,[807] and the authors preferred the term motor to describe these unidirectional systems. We, however, favor the view that useful work (e.g., pumping a liquid) must be produced by a system that is to earn the term molecular motor. So far, in our opinion no artificial system has achieved this goal, although some discussed in the following section come close and although the point could be argued depending on the definition of useful work. In the following section, we describe the first step—the synthetic design of molecules which undergo unidirectional rotation.

5.7.1. Light-Driven Unidirectional Molecular Rotors

Feringa and co-workers have pioneered the field of chirooptic molecular switches[144,808−810] and expanded on their findings to develop actively driven molecular rotors.[811,812] A number of groups have investigated photochemical cis/trans isomerization, ring closure, and charge-transfer processes[813] as potential means for bistable switches, where the read-out generally depends on the changes in the optical properties that accompany these conversions.[808,810] As early as 1956, Hirshberg[814,815] noted that the photochromism displayed by a spiropyran and its subsequent conversion to a merocyanine dye might be applicable as a molecular memory device. A recent survey of photochromism is available.[70]

The concept of using the information stored in different enantiomers (namely, their opposite responses to polarized light) is the basis for chirooptical switching, assuming the enantiomers can be switched readily and nondestructively. And, if the enantiomers can be read out at wavelengths different from those used to switch them, the read-out process could likewise be nondestructive. Many previous systems had failed due to fatigue, destructive read-out, and side reactions caused by photochemical processes.[808] Toward the goal of making bistable switches, Feringa and co-workers initially investigated sterically crowded systems based on helicenes (**222** and **223**) connected via double bonds, with the output being helical reversal between *P* and *M* forms (as shown in Figure 94).[816−819] The stability to racemization for many such molecules is quite high ($\Delta G^{\ddagger}$ ~25−30 kcal mol^{-1}), depending on the heteroatoms in the rings and groups on the periphery.[811] These initial discoveries led to the attempted synthesis of a molecular brake (Figure 95). The authors proposed that if a rotationally mobile group is on the lower ring system and the compound is photochemically switched, the rotation will be halted and hence the group acts a molecular brake.[820] However, *trans*-**224** actually had a higher barrier to rotation than *cis*-**224** by 0.7 kcal mol^{-1} due to the fact that the methyl groups on the rotator interacted more strongly with the allylic methylene groups in the trans form than with the naphthalene fragment in the cis form. The flexibility of the naphthalene unit allows it to move out of the way and let the rotor pass. Again, an intuitively well-designed system presents problems when shrunk to the molecular level.

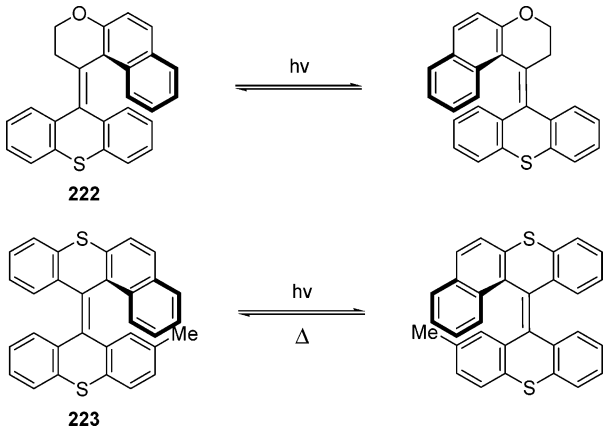

Figure 94. Helicity reversal by the isomerization of double bonds in sterically crowded systems.

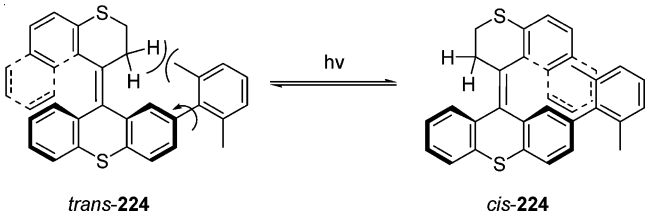

Figure 95. Attempted realization of a molecular brake in sterically crowded alkenes.

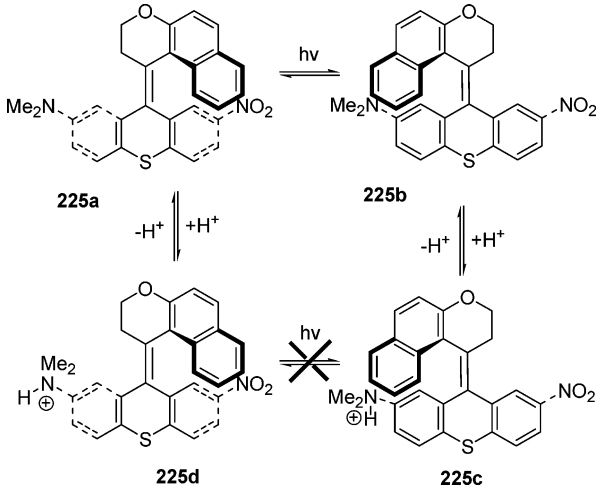

Figure 96. Four-stage molecular switch.

To design a molecular rotor that could perform a 360° turn, Feringa and co-workers synthesized a four-station molecular switch (Figure 96). This was accomplished by using a dimethylamino group (**225**) as a proton acceptor which acted as a brake to block the switching process.[821] State **225a** can be converted to **225b** by light-induced isomerization of the double bond. Protonation of the dimethylamino group effectively locks the molecule in the conformation shown in **225c**. Protonation of **225a** also leads to the trivial protonated form, **225d**. Interconversion of **225c** and **225d** could not be accomplished by irradiation, effectively showing the braking action of the protonated amine. Such a system shows promise for memory elements, but the use of acidic conditions in solution is not desirable.

To create a unidirectional molecular rotor, the Feringa group needed to include the components required for such a system: repetitive, unidirectional motion and a consumption of energy. Building on previous work on phenanthrylidenes in collaboration with the group of Harada[822−826] and using a similar strategy to that in the four-state switch, they developed a unidirectional molecular rotor (**226**).[122,827] The stations shown in Figure 97 can be populated indi-

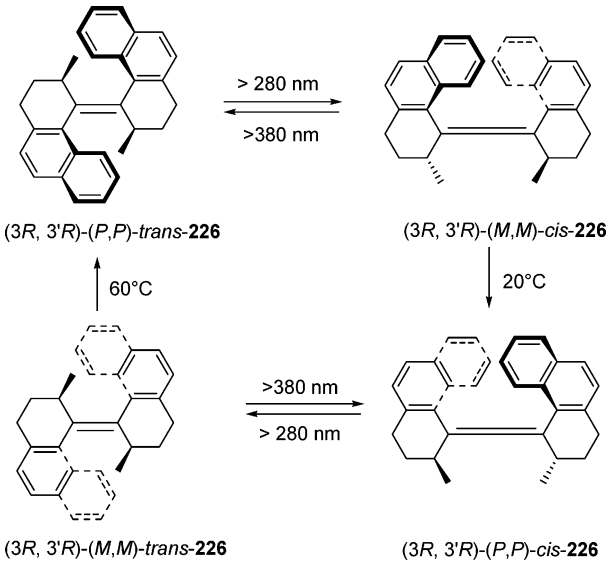

Figure 97. Unidirectional, light-driven molecular rotor.

vidually, or the entire system can be kept at >60 °C, and under irradiation, continuous 360° unidirectional motion was found. The interconversion of the isomers was followed by NMR and UV−vis spectroscopies and the directionality by CD spectroscopy. In this system, the light energy is required for the molecules to enter the sterically strained *M,M* configurations in an energetically uphill process, and the more stable *P,P* isomers are formed in thermal, energetically downhill processes. The input of light energy therefore allows unidirectionality without violating the second law of thermodynamics.

A second-generation unidirectional molecular rotor (**227**) was synthesized and studied by Feringa and co-workers (Figure 98).[828] In this system, they made a distinct upper and lower portion of the rotor molecule, indicating the possibility that the lower portion could be used to link the rotor to other molecules or to a surface. Again, four different stages were observed which could be interconverted and monitored by CD spectroscopy. In this case, unlike that of the first generation rotor, the unidirectional motion is dictated by a single stereocenter—the methyl group on the top fragment.

Feringa and co-workers[829,830] had previously studied the femtosecond spectroscopy of a number of related overcrowded alkenes (**228**) to determine the rates of photoisomerization, which were found to be quite fast (<300 ps). To determine the tunability of the second-generation system, they investigated the effects of changing the heteroatoms in the framework (Figure 99) as shown in Table 5. In looking at the thermally activated helix inversion from the less

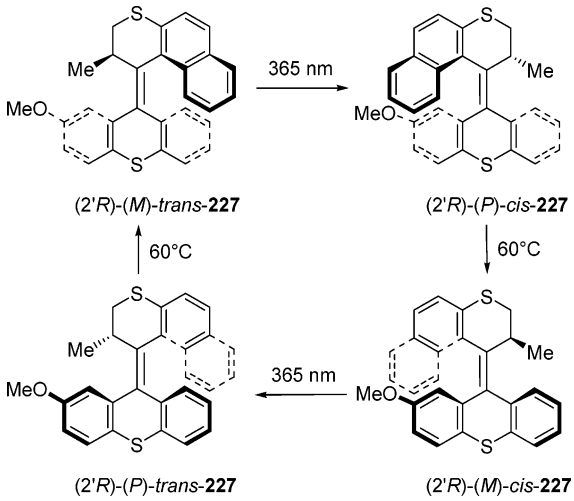

Figure 98. Second-generation light-driven molecular rotor.

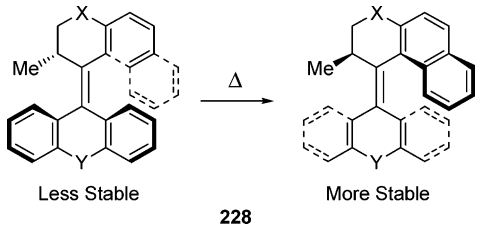

Figure 99. Light-induced isomerization in crowded alkenes.

Table 5. Characteristic Energies and Half-lives for the Thermally Activated Helix Inversion for the Molecule Shown in Figure 99[a]

compd **228**	$\Delta G^{\ddagger}$ (kcal mol^{-1})	$t_{1/2}$ at 25 °C
X = S, Y = S	25.3	215 h
X = S, Y = O	24.1	26.3 h
X = CH_2, Y = S	21.9	40 min

[a] Changing the heteroatoms (X and Y) in the framework changes the energies for thermal isomerization

stable *P* isomer to the more stable *M* isomer, they found that replacing a sulfur by an oxygen on the lower half lowered the barrier to rotation ($\Delta G^{\ddagger}$) by 1.2 kcal mol^{-1}. When the sulfur on the upper half of the molecule was replaced by a CH_2 group, the barrier ($\Delta G^{\ddagger}$) decreased by 3.4 kcal mol^{-1} and the half-life decreased from 215 h to 40 min.[812,831] Retardation of the motion was observed for other derivatives,[832] and a smaller version of the second-generation rotor was designed.[833] The ability to tailor the properties by changing the atoms in the framework leads to an important design principle. However, one of the drawbacks of light-induced molecular machinery is resiliency of the molecules under the duress of constant switching by a high energy source, especially when bonds are broken and formed (as a π bond is in the case of switchable alkenes). To the best of our knowledge, no tests have been performed as to the fidelity of these devices, that is, the number of switching cycles possible before photobleaching or another process leads to the degradation of the switches. Many alkenes are stable to such switching processes, but tests on the compounds described above have yet to be performed.

Feringa and co-workers have also investigated these unidirectional molecular rotors in liquid crystals,[834] showing that the motion of the rotor can lead to a change in the macroscopic material, manifested as a change in the color. They had observed a similar phenomenon with other chiral molecular switches in liquid crystals.[835] Recently, they have shown that the chirality of a liquid crystal phase can be reversed when a photochromic switch is incorporated into the individual molecules.[836] Others have proposed photochemically driven molecular rotors based on liquid crystal molecules.[837−840]

Zerbetto and co-workers have studied the effect of rotation in rotaxanes by external electric fields[841] as well as photochemical stimuli.[842] Stepwise circumrotation of a small ring about a larger ring containing individual stations using light, heat, and chemical stimuli in a catenated structure has been investigated by Leigh et al.[843] With one smaller ring within a larger one containing three stations, unidirectional rotation could not be achieved. However, in a significant accomplishment, when two smaller rings were catenated onto a larger four-stage ring (a [3]catenane), the smaller rings prevented rotation in the reverse direction and the overall movement was unidirectional. This important area of research has been reviewed recently,[807] and catenanes lie outside the scope of the present review as defined in the Introduction.

Fujimura and co-workers[844] performed a computational study of 2-chloro-5-methylcyclopenta-2,4-diene carbaldehyde (**229**; R = Cl) as an example of a chiral molecular rotor by quantum dynamics (Figure 100).

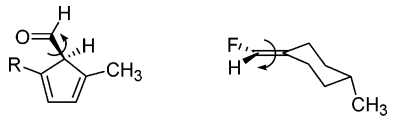

229 **230**

Figure 100. Molecules for the study of light-driven molecular rotation.

The simulations were done in a one-dimensional potential representing the internal rotation of the −CHO group against the cyclopentadiene system. This rotation has an asymmetric potential, and unidirectional rotation can occur when the −CHO dipole moment interacts with a linearly polarized electric field. The cyclopentadienyl part was assumed artificially fixed in space, and a 30 ps long linearly polarized laser pulse at 124 cm^{-1} (3.72 THz) with a maximum field strength of 3.4 GV/m was introduced in the calculation. At this field strength, the dipole−electric field interaction was comparable to the potential barrier, and unidirectional rotation was predicted.

Similar methods were applied to randomly oriented ensembles of the same molecule to study the influence of linearly and circularly polarized laser pulses.[120] In both cases, the ensemble average of the angular momentum reversed when the symmetry of the molecule was reversed. Whereas linearly polarized laser fields induced rotation in the molecular coordinate system, circularly polarized fields induced rotation in the laboratory fixed frame.

These results were obtained while energy dissipation, which is of critical importance, was ignored. It was included through a quantum master equation method.[119] In an intense laser field, unidirectional rotation was calculated to occur in the intuitive direction, while, at intensities below threshold, rotation in the other direction may occur.

Fujimura and co-workers showed the feasibility of pump−dump femtosecond laser pulses to initiate unidirectional rotation in **229** (R = H) by quantum dynamics simulations in a one-dimensional potential.[845] Whereas IR frequencies were studied so far, and the dynamics on the ground state was investigated, electronic excitations with UV−vis laser pulses were studied within a two-state model. If the minimum in the ground state does not correspond to a minimum in the excited state, a torque with the directionality defined by the chirality of the molecule acts upon vertical excitation from the ground-state minimum. If the wave packet is transferred back into the ground state by a time-correlated dump pulse before it arrives at the minimum in the excited state, the angular momentum accumulated in the excited state is preserved and rotational excitation results.

Electronic excitations combined with librational excitation by IR laser pulses are also suitable to induce molecular rotation. This was shown by Manz and colleagues using 1D quantum dynamics simulations for (4-methylcyclohexylidene)fluoromethane (**230**; Figure 100),[846] which exists as aR and aS enantiomers, which interconvert through a 180° rotation about the double bond. The molecule was initially assumed to be present entirely as the aR enantiomer. A linearly polarized IR laser pulse resonant with the librational mode was applied to induce rotational excitation in the ground state. A subsequent UV laser pulse was applied to elevate the rotational wave packet. Due to local asymmetry of the excited state in the region of the ground-state minimum, unidirectional rotation was induced. Once directional rotation stops, the direction of rotation cannot be predicted any more, because of the inversion symmetry of the rotational potential. Thus, the use of this particular design for nanotechnology seems limited, but the principle is very interesting.

This series of publications reports high level quantum dynamics calculations of molecular rotors, which do not invoke the approximations made in classical molecular dynamics. The computational demands do not allow the study of large systems. In fact, the studies were done on a one-dimensional potential, and energy dissipation effects cannot be estimated from this type of calculation.

5.7.2. Chemically Driven Rotors

Kelly and co-workers have investigated molecular brakes,[847,848] ratchets, and chemically driven unidirectional molecular rotors.[849−851] The molecular brake was based on a bipyridyl unit connected to a triptycene moiety, in which the triptycene could rotate readily in the system (Figure 101), similar to molecules we have discussed previously. When Hg^{2+} is added to the system, the bipyridyl unit is complexed and attains a planar conformation, similar to

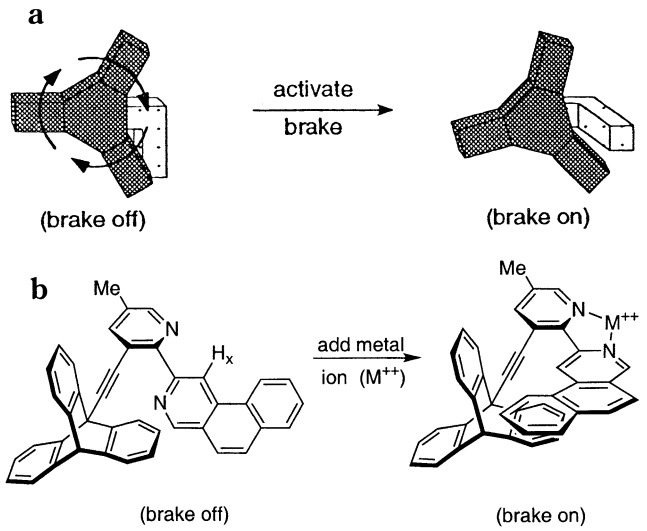

Figure 101. Molecular brake shown (a) schematically and (b) in its molecular form. Reprinted with permission from ref 849. Copyright 2001 American Chemical Society.

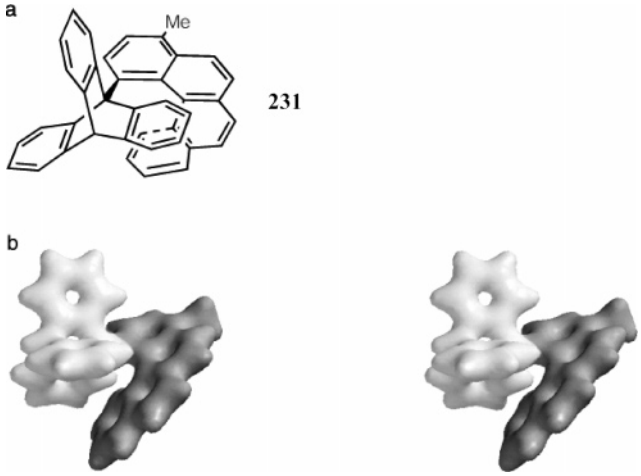

Figure 102. Attempted design of a unidirectional rotor (a) based on the helical twist of the benzophenanthrene unit, which imparts a chirality as shown in the space-filling models (b). Reprinted with permission from ref 856. Copyright 2000 American Chemical Society.

that observed in Rebek's bipyridyl system (section 5.1.4; Figure 16). In this configuration, the triptycene can no longer rotate. The rotational arrest can be observed by NMR, and thus, a braking action can be observed.

In 1963, Feyman laid out the framework for the design of a gas-driven molecular ratchet and pawl system which could be used to theoretically lift a flea.[852] In his discussion, he then proceeded to show how this cannot be true, based on the second law of thermodynamics. In the present article, we have seen in section 3 and repeatedly thereafter how macroscopic analogies are likely to break down as a system gets smaller, because Brownian motion (kT terms) begins to dominate. In section 5.7.1, we saw an example of a unidirectional motor by Feringa and co-workers. In this case, light energy had to be used as an input—unidirectional motion cannot be obtained without the input of energy, whether it be thermal, electrical, chemical, or another form.

Kelly and co-workers made and studied a system that showed that the second law survives, even if at first sight intuition might tell us otherwise.[853,854] Similar to the molecular brake, they designed a molecule composed of a triptycene connected to phenanthrene and benzophenanthrene (**231**) units (Figure 102). The phenanthrene and benzophenanthrene are helical and thus would appear to impart a differential preference for rotation in one direction. However, as Feynman explained, and transition-state theory also tells us, if the thermal bath provides enough energy for rotation, it provides enough energy for rotation in either sense, and bidirectional rotation is indeed what the group found by using a combination of coalescence and spin polarization-transfer NMR ($\Delta G^{\ddagger} \geq 25$ kcal mol^{-1}). Predictably, no preferred rotation in one direction was observed and the conclusion was that the second law is indeed valid.[855]

Kelly and co-workers then set out to produce a chemically driven molecular rotor (**232**),[140,856,857] using the high-energy phosgene molecule as an input, much like ATP is used to drive biochemical motors (Figure 103). The system is a derivative of their ratchet and pawl system, but it contains functional groups that reversibly react with the phosgene. As shown in Figure 103, addition of phosgene and triethylamine to **232** converts the aniline group in the triptycene unit to an isocyanate which can then, after rotation, react with a hydroxypropyl tether on the helicene to form a urethane linkage. However, the urethane is in an undesirable conformation and uses thermal energy from the bath to rotate (again in the same direction; the reverse direction is restricted by the now-formed urethane link) to a more stable conformation. Addition of water then cleaves the urethane to give a rotamer of the original starting atropisomer. Although this represents a simple system, it provides a proof that unidirectional motion can be obtained in molecular frames with the correct input of energy. Feringa (for light energy), Kelly (for chemical energy), and Leigh (for light and chemical energy) have now shown this. Another important feature of all three systems is the ability to harness the random fluctuations in the thermal bath, in properly designed systems, to still obtain unidirectional motion. These relatively simple, albeit important, examples were useful in proving these concepts, and they open the doors for further exploitation in these realms.

6. Rotors in Solids

In this section, we will cover molecular rotations within large structures including solids, liquid crystals, and related systems. As noted at the outset, we only deal with well characterized pure compounds and not with mixtures such as polymers. Even so, subjective decisions had to be made for inclusion of material into this subset of the review. For instance, we did not include numerous instances of rotation in crystals that were not a result of design but happened to be discovered. For instance, we do not discuss "bicycle pedal rotation" in crystals of *trans*-stilbenes[858−860] and *trans*-azobenzenes,[861,862] in which the double bond turns around the single bond that attaches it to the phenyl rings while the rings remain

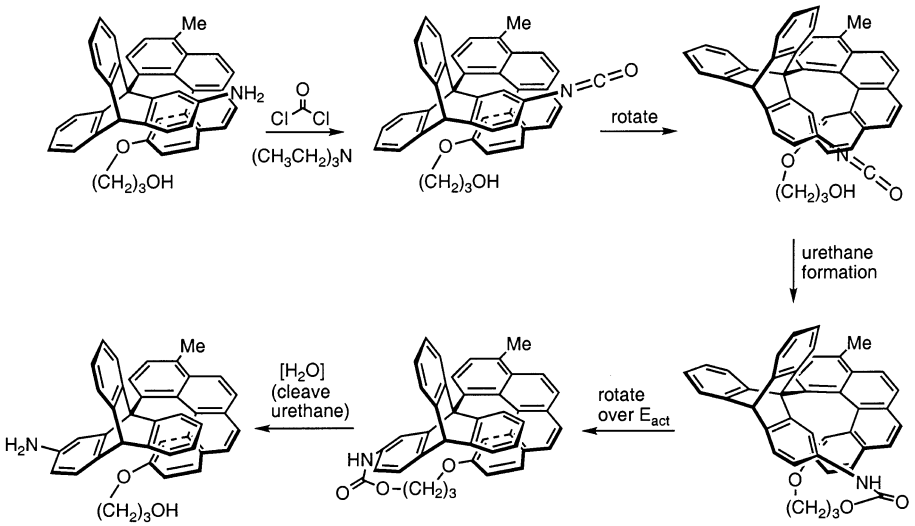

Figure 103. Chemically driven unidirectional molecular rotor. Reprinted with permission from ref 856. Copyright 2000 American Chemical Society.

stationary. As mentioned in the Introduction, we were particularly concerned with including structures that in our judgment may be ultimately useful in nanoscience applications. This makes molecules in solids and especially on surfaces considerably more relevant than molecules floating freely in solution, and we have accordingly discussed them in more detail.

However, in dealing with rotors in solids, we will only discuss a few topical areas which we believe fit the criterion of potential relevance to the building of molecular devices: in particular, the use of crystal design to incorporate rotational phenomena into solid structures. As stated earlier, we do not consider the rotations of whole molecules, even though the crystal environment could be considered to act as a stator with respect to such rotation. Therefore, we do not discuss the phenomenon of molecular rotation in the *plastically crystalline state*,[863] where orientational disorder is caused by the rotations of entire molecules in the crystal (plastic crystals),[864,865] or the rotational diffusion of molecules in zeolites[866] or other solids.[867] The dynamics of plastic crystals as well as other glassy solids, studied by NMR, has been reviewed recently by Böhmer et al.[173] Instead, we will concern ourselves here with the rotations of an individual part of a molecule (rotator) within the framework of a larger molecule (stator) which is itself in the framework of a solid, such as a crystal. We also look here at geared rotations in some solids, as this is related to our discussion in the solution-based rotors section (section 5), but again, we only consider cases in which the gearing involves a part of the molecule (rotator).

Crystal design is rapidly becoming one of the fastest growing fields in chemistry and physics today.[868−872] Whether for the design of porous solids, solid-state magnets, designer catalysts, or other crystal-related phenomena, much progress has been made recently. In a sense, crystal engineering is attempting to learn to design solid-state properties in the same fashion as chemists have been designing molecular properties. This is reminiscent of the supramolecular chemistry discussed in section 5.6. There, large structures were made by the noncovalent assembly of molecules. The principles are similar in crystal engineering, where forces typically much weaker than a chemical bond dictate the packing in a solid. With knowledge of the types of structures that lead to different crystal packing, molecules can be synthetically designed to give known superstructures with built-in substructures. A number of early researchers discovered that rotational processes can be observed in solids with a variety of techniques, but the phenomenon is not widely known among chemists, who frequently think of all crystals as being internally rigid, as most of them of course are. Recently, several groups have become interested in using crystal design to produce crystals containing tailored rotor molecules that have low rotational barriers and in harnessing such internal rotation to make designer solids that can be used for rotoelectronic applications. In this regard, the contributions of Garcia-Garibay's group, starting with their initial outline of their research program,[873] are particularly systematic and noteworthy and are discussed in detail in section 6.1. Their molecules contain a rotator mounted on an axle whose ends are shielded by bulky protecting groups intended to prevent neighbors from interfering with the motion of the rotator.

Many methods, including X-ray diffraction, neutron diffraction, inelastic neutron scattering (INS), quasi-elastic neutron scattering (QENS), dielectric spectroscopy, solid-state NMR experiments, and others, are available to the chemist and physicist interested in studying dynamic processes in solids, liquid crystals, and other macromolecular species. For the reasons cited in section 4.1 for solution-state NMR, including ease of use and availability of spectrometers, solid-state NMR has become one of the favorites in the understanding of solid-state structures. Between solid-state NMR and X-ray diffraction,[874,875] different, yet complementary, data can be obtained on molecular motions in solid-state samples.

The data obtained from crystal diffraction experiments give the mean position of the atoms and the probability density of their average displacement from the mean position, expressed in the familiar

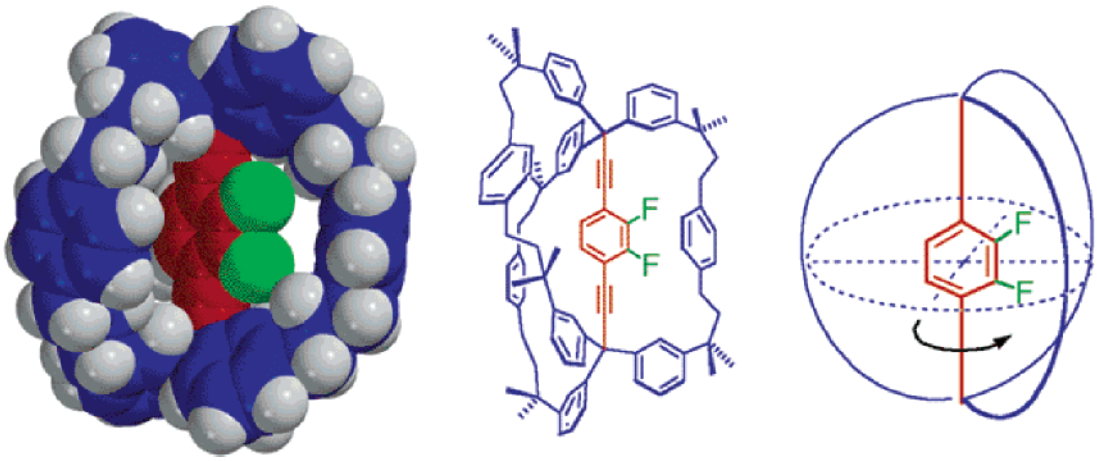

Figure 104. Proposed solid-state molecular gyroscope. The structure on the left is a space-filling model of that in the center, and the picture on the right schematically depicts the "gyroscope". Reprinted with permission from ref 85. Copyright 2002 American Chemical Society.

thermal or vibrational ellipsoids. The data can then be extrapolated, often with some assumptions, to give values of force constants and rotational barriers in crystals. From X-ray crystallography, information about the translational, vibrational, and rotational (librational) motions of a molecule or parts of a molecule can be obtained. In contrast, solid-state NMR experiments give information on the local structure of the molecule, which may or may not correlate with information about the extended structure.

In section 5.4.1, we discussed how solid-state relaxation measurements were used to determine the rotational barriers in ferrocene (**146**, M = Fe; Figure 57) and related compounds. Similarly, Maverick and Dunitz[876] were able to determine the rotational barriers for a series of crystalline metallocenes, for which diffraction data were available over a wide range of temperatures. Although the data agreed quite well, different space groups yielded different values, which indicates a further complication relative to solution studies. For ferrocene in a triclinic unit cell, they obtained a value of 1.8 kcal mol^{-1}, which agrees nicely with the data reported in section 5.4.1. Dunitz and co-workers have pointed out that the results agree well, even if the underlying assumptions are quite different.[872] Spectroscopy gives information about the rate (e.g., frequencies, relaxation times) versus temperature, assuming an Arrhenius type behavior, whereas the torsional amplitude method[872] (e.g., Dunitz and White[877]) uses classical Boltzmann averaging to estimate the rotational barrier height at a given temperature. In the words of Dunitz and co-workers,[872] "In a sense, one can say that spectroscopy sees the rate at which molecules cross the barrier, while diffraction sees the bottom of the potential well; we derive roughly the same barrier height as long as the potential is approximately sinusoidal." Thus, the two methods are complementary. Bernard and Wasylishen[878] have recently reviewed fluxional processes for some organometallic compounds, including metallocenes, in the solid state, and we will not discuss them further here.

6.1. Phenylene Group Rotations

Garcia-Garibay and co-workers have investigated designed crystals in which phenylene groups could rotate in the cavity created by the substituents on the phenylene rotator[84,85,873,879–881] and refer to the systems as "molecular gyroscopes". This is not the usage of the term that we have adopted presently (section 5.5). The structures discussed by these authors are closely related to the turnstiles of Moore and co-workers[735] discussed in section 5.5, but they are nonplanar. The goal of the Garcia-Garibay group is to design a molecule that encompasses a fully enclosed cavity containing a chemically bonded rotator (Figure 104). This would then be a true molecular analogue of a gyroscope. If the phenylene carried substituents that would make it dipolar, it could then be addressed by an external electric field. A recent publication from the laboratory of Gladysz describes a true molecular gyroscope, albeit with a nonpolar rotator, but the rotator is not of the phenylene type[733] and they did not study the dynamics in the solid state (see section 5.5).

In a preliminary study,[873] 1,4-bis(3,3,3-triphenylpropynyl)benzene (**233**), which has no dipole, was synthesized and crystallized from benzene, which was included in the crystal (Figure 105). From

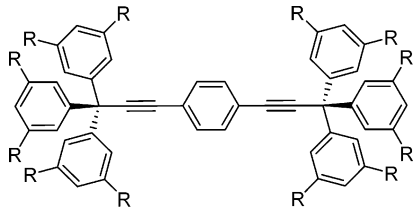

233 R = H
234 R = *t*-Bu

Figure 105. Molecular rotor designed with the intent of allowing the phenylene rotator to turn in a crystalline solid.

dynamic ^{13}C cross-polarization and magic-angle spinning (CPMAS) NMR, the authors found a splitting of 60 Hz at ~255 K, giving a time constant of rotation of 7.7 ms and a barrier ($\Delta G^{\ddagger}_{255}$) of 12.8 kcal mol^{-1}. From quadrupolar echo ^{2}H NMR line-shape analysis,

they found an upper limit for the rate of rotation of 10^4 s^{-1}, giving an activation barrier of 14.6 kcal mol^{-1} for the desolvated structure—only ~2 kcal mol^{-1} higher than that for the clathrate structure. Later,[880] the same group synthesized the dodecakis-*tert*-butyl analogue (**234**) to counteract intercalation and found that the twofold flip occurs at 100 MHz (10^8 s^{-1}) in the solid state at ambient temperature. This compound crystallized in a propeller conformation. They also made a deuterated phenylene analogue to investigate the ^2H NMR. Unfortunately, the rotation was faster than the upper limit of the experiment, 10^8 s^{-1} at 293 K, and at 193 K, the rotation was slower than the lower limit of the experiment, 10^3 s^{-1}. Spectra at intermediate temperatures could not be fitted to a single rate constant. This implies that loss of crystallinity gives amorphous solids, and even with the bulky groups, interdigitation in the crystal was still observed.

The Garcia-Garibay group[84] also reported the dynamics of 1,4-bis(3,3,3-triphenylpropynyl)benzene (**233**), which was crystallized from benzene. They found one molecule of the rotor with two benzene molecules included. Using ^{13}C CPMAS NMR, it was shown that the phenylene groups undergo rapid twofold flipping with a rate of 1.3×10^2 s^{-1} ($\tau = 77$ ms) at 18 °C ($\Delta G^{\ddagger}_{255} \sim 12.8$ kcal mol^{-1}). The included benzene molecules are also in a "state of rapid rotation". Since the benzenes are in a T-shape conformation, the authors considered the system to be possibly geared, even though the twofold rotation of the phenylene against the sixfold rotation of the benzenes would be inefficient. They found (by ^{13}C CPMAS NMR and quadrupolar echo ^2H NMR lineshape analysis between 200 and 330 K) that the twofold flipping occurs in the kilohertz regime while the sixfold flipping occurs above 100 MHz. They also studied solvent-free crystals grown from dichloromethane. They found rotation rates ranging from 1.5×10 s^{-1} at 297 K to 3.8×10^6 s^{-1} at 385 K and an activation barrier (E_a) of 14.6 kcal mol^{-1} for the solvent-free crystals. This is only ~2 kcal mol^{-1} higher than that for the clathrate crystals, so gearing in the clathrated structures is unlikely.

In an attempt to shield the rotator more, Garcia-Garibay and co-workers[85] also used triptycene end groups (Figure 106) to form the cavity and showed that various groups could be used as the rotator, such as anthracene, pyrene, and biphenyl. Again, none of these structures bear a dipole moment, and the authors explored the gas-phase rotational potentials, crystallization behavior, and thermal properties. All molecules rotated fast on the NMR time scale, which was supported by semiempirical AM1 calculations, which showed essentially frictionless rotation. From X-ray crystallography, the authors found that the close packing interactions that hinder the rotator rotation come from interdigitation, wherein triptycenes fill the void space between two triptycenes on an adjacent molecule in the crystal.

Again, they made the triptycene units bulkier by adding methyl groups to increase the free space in which the phenylene unit can rotate (Figure 106, R = *tert*-butyl).[881] The crystal structure indicates more

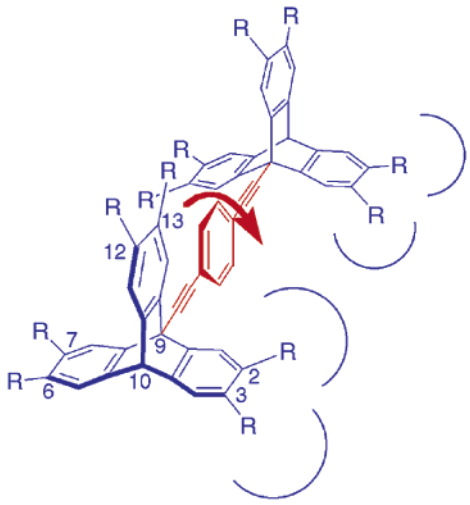

Figure 106. Example of a phenylene rotator with triptycyl blocking groups designed to allow the phenyl group to rotate in a crystal when the rotor crystallizes. R = H, *tert*-butyl, as discussed in the text. Reprinted with permission from ref 85. Copyright 2002 American Chemical Society.

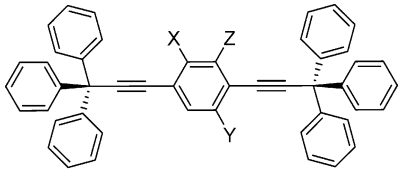

235 X = H; Y = F; Z = H
236 X = H; Y = CN; Z = H
237 X = H; Y = NO_2; Z = H
238 X = H; Y = NH_2; Z = H
239 X = NH_2; Y = H; Z = NH_2
240 X = H; Y = NH_2; Z = NO_2

Figure 107. Dipolar rotors for examination of rotation in the solid phase.

void space through which the rotator can turn, and from the atomic displacement parameters in the crystal data, they were able to estimate a rotational barrier of only 3.3 kcal mol^{-1} (at 100 K and assuming a twofold flipping model).

In their first examples of dipolar rotors (**235**−**240**), Garcia-Garibay and co-workers[879] synthesized a series of dipolar phenylenes on the trityl framework and determined the effects of crystallization on rotation (Figure 107). The dipoles ranged from 0.74 to 7.30, but the volumes only differed by ~5%, and some crystals showed positional disorder. They studied the molecules using ^{13}C CPMAS NMR. All signals were averaged at room temperature, and the overlapping peaks did not allow them to get quantitative data. The crystal disorder is by inversion, and therefore rotation cannot be the cause, but a 180° or 360° rotation could cause the disorder in some of the molecules.

Compound **235** was crystallized in both a desolvated and a clathrate form and characterized by Price, Garcia-Garibay, and co-workers as a crystalline dielectric.[141] Utilizing dielectric spectroscopy, ^2H NMR, and variable-temperature X-ray crystallography, the authors demonstrated a rapid thermal response of the molecular rotors to the applied electric field with a measured barrier to rotation of

~14 kcal mol^{-1} and found a twofold rotational potential with a well asymmetry of about 1.5 kcal mol^{-1}. The observed behavior of the rotors was relatively monodisperse with about two-thirds of the active rotors having indistinguishable barriers to rotation. The observed asymmetry was shown to result from steric interactions between the dipolar rotators and the nonrotating portions of neighboring molecules via the interdigitation mechanism discussed above. This steric effect dominated the dipolar rotor−rotor interactions, which are weak for the relatively small dipole of the singly fluorinated phenylene group.

6.2. Geared Rotations in Solids

Hexammine metal complexes $[M(NH_3)_6]X_2$ (where M is a metal, usually divalent, and X is a counteranion) have six ammonia groups ligated to the central metal in an octahedral fashion. Due to the steric bulk surrounding the metal, correlated rotations of the individual ammonia ligands can be visualized, and this phenomenon was found in a number of studies. Rotations in $[Ni(NH_3)_6]X_2$ crystals (X = Cl, Br, I) have been studied by EPR,[882−885] and observed line-width variations have been explained in terms of correlated rotations of the NH_3 groups.[886] Trapp and Shyr[887] proved this by looking at the EPR spectra of $[Ni(NH_3)_6]X_2$ in $[Zn(NH_3)_6]X_2$ and $[Cd(NH_3)_6]X_2$ hosts (where X = Cl, Br, I). Above the critical temperature (T_c), the complexes existed in a perfectly octahedral environment, and below the T_c, the motion is frozen. Stankowski et al.[888] have studied rotations in $[Ni(NH_3)_6](BF_4)_2$ and found a T_c approaching room temperature, which agrees with specific heat measurements.[889] Sczaniecki[890] found four angular minima and four angular maxima in an electrostatic calculation of a model compound comprised of six NH_3 groups as a function of the correlated rotation of all the protons. Even though such a correlated system might find use in a nanoscience application, these compounds suffer from low stability, even at room temperature.

Correlated rotations in crystals of [(alkoxycarbonyl)methyl]cobalttricarbonyltriphenylphosphine $[ROC(O)CH_2Co(CO)_3PPh_3]$[891−893] were studied computationally for $CH_3CH_2OC(O)CH_2Co(CO)_3PPh_3$.[894] The crystalline phases of these molecules contain enantiomeric pairs based on the chiral conformations of the triphenylphosphine ligand (helical chirality, *P*/*M*) and the ester fragment (*re*/*si*). Each enantiomer has one conformation of the ester group, interconversion is very fast, and the selectivity is high. Using semiempirical methods and molecular mechanics, the authors found[894] correlated rotation of the coaxial rotors and bevel gearlike rotation for the interconversion. Interestingly, they also predicted a coupled conrotation in this system, which provide the molecule with a path to stereochemical inversion. The ester group and the carbonyl groups on the cobalt are so tightly meshed that they must rotate in the same direction. The carbonyl groups then engage the PPh_3 groups, which rotate in a disrotatory fashion. The gearing here is inefficient because the three-toothed $Co(CO)_3$ gear is coupled to the two-toothed Ph groups on the phosphine and the ester fragment likewise behaves as a two-toothed gear. To invert the helicity, the PPh_3 group and the ester fragment must change conformations, and it was found that this stereochemical transmission of information from one end of the molecule to the other occurs readily, implying that communication through this geared system offers an interesting mechanism for "gear trains" discussed in section 5.1.5. Therefore, although the gearing is inefficient, it nonetheless works to some degree. The authors of this study dub the system a "clockwork analogue unimolecular machine" and suggest its use in molecular memory.

6.3. Solid-State Inclusion Complexes

In section 5.6, we discussed rotations in inclusion complexes that were prepared and measured in solution. Here, we discuss a related area of chemistry concerning inclusion compounds in the solid state, including the preparation of such compounds without solvent. Although diffusion through solids is generally much slower than diffusion through a solution, it nonetheless can be exploited for solvent-free synthesis,[895] which has important environmental and cost advantages.[896] Although these systems have gained interest recently, solid-state reactions have been known for over a century. Mixing quinone and hydroquinone to give quinhydrone was discovered by Ling and Baker in 1893.[897] The use of crystalline guests to control reaction outcomes in the solid state is also a growing field. Enantioselective reactions in a crystal can be compared to those in biological systems in that the solid holds the substrate in a required conformation to obtain an enantiopure product upon reaction, much like enzymes do in biological transformations. In many cases, the bound substrate is held in a certain conformation which yields an optically active product upon reaction. Here, we consider the case where the bound conformation is a rotamer.

Toda et al.[898] discovered that when mixing solid 1,1,6,6-tetraphenylhexa-2,4-diyne-1,6-diol (**241**) with 1 equiv of benzophenone, the same inclusion complex forms as when they are crystallized from solution and its formation could be monitored by IR spectroscopy (Figure 108). They have also shown that gaseous

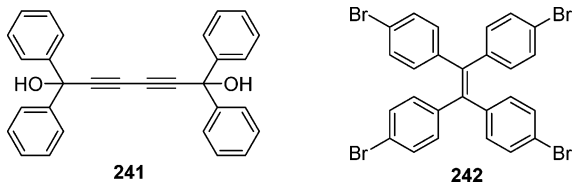

241 242

Figure 108. Host structures for solid-state inclusion compounds.

guests in achiral crystalline hosts show chiral switching of the host molecules.[899] Crystalline hosts and gaseous guests form inclusion complexes in which the guests can be removed by heating.[898] For chiral switching of a host molecule in the presence of an included guest, tetra(*p*-bromophenyl)ethene (**242**) has been shown to form a chiral state upon contact with THF, dioxane, benzene, *p*-xylene, and *β*-picoline

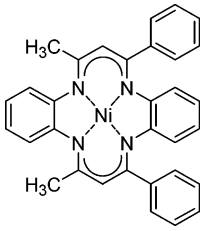

Figure 109. Tetraazaannulene nickel complex.

vapors.[900] The chirality results from the phenyl rings adopting a propeller structure (see section 5.1.5 and Figure 19), imparting a helicity on the host molecules. The mechanism that leads to the dynamical behavior of the molecules in the solid state is unknown. To probe this mechanism, Toda and coworkers[899] investigated the phenomenon in chiral derivatives of tartaric acid and binaphthyl. For the tartaric acid derivative, an inclusion complex was formed with acetone while the binaphthyl derivative formed a complex with DMF. Both compounds showed fast intramolecular rotation in the crystal to accommodate the guest molecules and resulted in the formation of chiral crystals.

Ward and co-workers[901] found that supramolecular host frameworks consisting of guanidinium (G) and 4,4′-biphenyldisulfonate (BPDS) ions, with included aryl guests, [$(G)_2$(BPDS)(guest)], formed geared systems wherein the BPDS moieties relay guest orientations from one pore to the next. The information transfer occurs by rotation of the S−C_{Ar} bond or conformational twisting of the biphenyl C_{Ar}−C_{Ar} bond.

Ripmeester, Ratcliffe, and co-workers have studied the dynamics of guests in clathrate hydrates (hosts made of water)[902−907] and have reviewed the fluxionality of guest molecules in solid-state inclusion complexes with cyclodextrins and other clathrate structures.[904] Guest dynamics in clathrate hydrates have been studied since the 1960s, mostly with dielectric spectroscopy.[908] Recent advances in NMR spectroscopy have allowed for further study of these inclusion complexes.[909,910]

Soldatov et al.[911] investigated C_{60} molecules included into crystals of the tetrazaannulene nickel(II) complex shown in Figure 109. Macrocyclic dibenzotetraazaannulenate metal complexes had previously been shown to form inclusion complexes with fullerenes and other species in the solid state as well as in solution.[912−917] In the crystal state, the concave surfaces of the tetraazaannulene form a cavity which can incorporate the C_{60} molecule. By investigating the solid with ^{13}C CPMAS NMR, the authors[911] found rapid pseudoisotropic rotation of the C_{60} molecule in the cavities. At −100 °C, the fullerene is disordered over two orientations, related by a 30° rotation about the sixfold axis of C_{60}. A related discussion of rotational processes in solid C_{60} can be found in section 6.5.2.

A number of groups have turned the tables and looked at molecules included *inside* open-cage fullerenes.[918−921] Levitt and colleagues[922] investigated molecular hydrogen trapped inside such a cage, as shown in Figure 110, by solid-state ^{1}H MAS NMR spectroscopy. They observed a small anisotropy

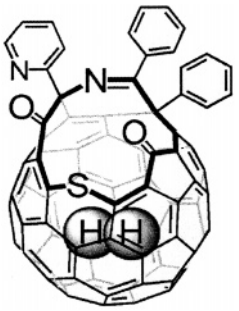

Figure 110. Molecular hydrogen included in an open-cage fullerene. Reprinted with permission from ref 922. Copyright 2004 American Chemical Society.

(∼2.3%) of the H_2 rotation in the cage and estimated the correlation time for H_2 rotation to be 2.3 ps at 295 K and 15.3 ps at 119 K (with a linear dependence between these two values). Computationally, Cross[923] investigated the hydrogen molecule completely enclosed in a C_{60} molecule at the Hartree−Fock level. In this study, it was found that H_2 was free to rotate and translate within the cage, with the bonds of rings of the cage causing a small torque on the included molecule. As in the experimental work above,[922] a very small anisotropy of the hydrogen rotation was also found in the calculated structure.

6.4. Rotations in Other Macromolecular Species

Vorderwisch et al.[924] have studied the influence of guest molecules on the rotations of NH_3 groups in Hofmann clathrates via inelastic neutron scattering (INS). Hofmann clathrates are molecules of the type $M(NH_3)_2M'(CN)_4 \cdot mG$ (abbreviated M−M′−G) where M and M′ are metals, G are guest molecules, and m is the number of guest molecules G per unit host.[925] The clathrates form stacked sheets containing the metals M and M′ and the cyano groups, which usually form a collinear arrangement with the two metals (M−CN−M′). Two NH_3 groups are bound to M and protrude from both sides of the sheets, with the guest molecules trapped between the sheet and the NH_3 groups. When G is a nonpolar guest (benzene or biphenyl), nearly uniaxial rotation of the NH_3 groups was observed, but when G was a polar guest (water, aniline, phenol, dioxane), dipolar interactions between the guest and the NH_3 groups led to hindered rotations. In INS, this is evidenced by the presence of tunneling lines in the spectra, instead of transitions between rotational wells. The first example of INS on Ni−Ni−C_6D_6 was by Wegener et al.,[926] who found uniaxial quantum rotation of the NH_3 groups at 1.8 K. Kearly et al.[927] examined the effects of changing the central metal ion in M−Ni−C_6D_6 clathrates (M = Cu, Fe, Mn, Ni, Zn) and found only small changes in the rotational energy measured by INS.

Würger[157] has developed an analytical method for explaining the temperature dependence on the line width in the EPR spectra of Hofmann clathrates. In this formulation, based on rotor−rotor coupling, the widths are dependent on the rotor level occupation and the three-proton spin degeneracies in the initial and final states and provides a good fit to the experimental spectra. Rogalsky et al.[89] have similarly

investigated the neutron scattering line widths from a theoretical standpoint. In a joint theoretical and experimental investigation, they investigated Ni−Ni−(biphenyl)$_2$ via INS and developed a theoretical model for calculating the INS line widths at finite temperatures using a stochastic perturbation potential analogous to the classical Langevin equation (see section 3). The behavior for the studied molecule is deemed classical for the coupling of the phonons to the rotor, with a $g = g_{\rho\rightarrow\sigma}\sqrt{T}$ temperature dependence. The finding that the system displays a classical relationship is surprising given the quantum nature of the rotor transitions discovered previously. The authors state that a better understanding of the coupling strength will be required to validate this conclusion.

Enders and Mintz[928] have investigated the rotations in dimyristoylphosphatidylcholine bilayers using dielectric spectroscopy as a function of temperature in the frequency range from 4 to 12 GHz. They find a steplike dielectric response as a function of temperature at the chain melting phase transition and conclude that it is due to a phase transition of the acyl chains. At low temperatures, the chains are all-trans. As the temperature is raised, rigidity is lost and the chains begin rotating between different gauche conformations. The gauche conformation has a small dipole moment (<0.1 D), which allows observation of the transition via dielectric spectroscopy. The amplitude of the observed dielectric signal is interpreted as due to gearlike cooperative rotational motions of chains within large chain clusters.

Asthaler et al.[929] investigated the dynamics of octamethylethynylferrocene (OMFA) with quasielastic nuclear forward scattering (QNFS) from 61 to 257 K at photon energy 14.413 keV along with variable energy X-ray powder diffraction. Previous studies[930−933] have shown that this molecule displays a sharp decrease of the Lamb−Mössbauer factor at 248 K, well below its melting point (436 K). Herber and coworkers[930,931] have suggested librational coupling of the molecule to the rotations of the cyclopentadienyl rings. Using the QNFS technique with synchrotron radiation, the authors found that the rotation of the OMFA molecules above 246 K "occurs on a timescale faster than the nuclear lifetime of ^{57}Fe, i.e. their libration or rotation frequency is well above 7×10^6 Hz".

6.5. Carbon Nanotubes and Fullerenes

6.5.1. Carbon Nanotube Gears

Since their discovery, carbon nanotubes inspired thoughts about their use in rotational nanodevices. They are classified as single-wall carbon nanotubes (SWNTs) or multiwall carbon nanotubes (MWNTs). SWNTs consist of finite sheets of graphite, folded in one direction to build a cylinder; MWNTs are built when two or more SWNTs of different size are inserted inside each other.

Two SWNTs with *o*-phenylene substituents on their outer side were studied computationally in a molecular gear arrangement.[934] Both nanotubes were restricted to be parallel and close enough to make the substituents on both tubes geared. Constant angular velocity was added to the atoms at the end of one nanotube, and the transfer of rotational energy from one tube to the other was studied by constant energy molecular dynamics simulations. At temperatures below 1000 K, the gear functioned at a frequency of 5 THz. Above these temperatures, angular momentum transfer was impaired by substituent slippage. At higher frequencies, centrifugal effects stabilized the substituents, and slippage did not occur below 2000 K.

The response of such a molecular gear to a linearly polarized laser field was also computed.[935] Artificial charges were placed on atoms at the end of one nanotube. Laser frequencies between 100 and 140 GHz were used, and the electric field strength was 6.14×10^7 V/m. After an initial period of ~50 ps, both the charged as well as the uncharged nanotubes were predicted to exhibit steady unidirectional rotation. While a single dipolar nanotube changed its directionality several times within 500 ps, the presence of the second, nonpolar nanotube stabilized the unidirectional rotation in the gear arrangement.

In multiwall carbon nanotubes (MWNTs), two or more SWNTs of different diameter are mechanically interlocked with a common principal axis. MWNTs are comparably rigid, and their relative rotational coordinate is unambiguously defined. Because of symmetry considerations (see section 3), the rotational potential is expected to be low. For low temperatures, it was argued that classical MD is not adequate for the simulations of nanotubes, because they pool energy in low energy vibrational modes.[936] Semiclassical rigid body mechanics methods were then applied to demonstrate that MWNT bearings behave in a superrotatory (in analogy to superfluidic) fashion under certain conditions at low temperatures.

MWNTs were studied using a simple model potential without atomistic resolution, with neglect of rotational barriers.[937] A MWNT with an dipolar inner tube was studied under application of a linearly polarized laser field by molecular dynamics,[938] with an intensity between 0.249 GW/cm^2 and 6.24 TW/cm^2. Rotation was observed upon the application of the laser field, but a beat pattern between rotation and pendulum-like motion was also observed. The beats grew with increasing intensity of the laser field. The induction of rotational motion was more successful when a second laser field was applied with the same polarization, but at the frequency of a higher harmonic. Chiral MWNTs with asymmetric rotational potentials were also proposed to act as Brownian motors driven by temperature modulations.[939]

The potentials between different pairs of finite length nanotubes were studied in two dimensions (the relative translation along the principal axis x, and the relative rotational angle α), using a pairwise 6−12 Lennard-Jones potential.[940] Different types of potentials were found: (i) isolated minima with high energy barriers in both directions, (ii) minima connected by low barriers along α, (iii) minima connected by low barriers along x, (iv) minima connected by low

barriers along a linear combination of x and α, and (v) isolated maxima.

In case iv, a net translation is obtained following the minimum energy path for rotation. Applications as nanodrills and electromechanic nanodevices were discussed for this type of MWNT.[941,942] Rotation and translation are correlated if the magnitude of the externally applied forces is small compared to the energy barriers which separate the individual helical minima. The operational mode was classified to be accelerated if the applied external force exceeds kT, in which case stochastic fluctuations are insignificant. For kT larger than the applied force, a Fokker−Plank mode was defined, where the applied force merely adds a drift to dominating thermal fluctuations. This classification is similar to a scheme used by Michl and co-workers,[92,91] but it does not consider frequency-dependent friction.

The use of carbon nanotubes in computational studies of molecular rotors is attractive but carries some ambivalence. Their near perfect cylindrical shape grants them some very promising properties. However, some of the computational studies seem a little detached from the current state of art in experimental capabilities. For example, there are no general methods to substitute nanotubes in defined positions. Furthermore, their incorporation into supermolecular designs has not been addressed and poses a big challenge, although it was already achieved on a larger scale.[943] Future progress in this field, which is still in its early childhood, will be anticipated with excitement.

6.5.2. Fullerene Clusters

The rotational dynamics of C_{60} molecules in condensed phases have been probed by NMR,[944,945] QENS,[946] and INS,[947] each of which indicates fast rotation of the individual units. The phase transition between unhindered rotation and a situation in which C_{60} reorients by jumps to symmetry-equivalent orientations is thought to occur at ~250 K,[948−951] with the former occurring above this temperature. The crystal structure changes from a simple cubic (sc) structure at low temperature to a face-centered cubic (fcc) structure above the transition temperature.[948] Johnson and co-workers[949] used solid-state NMR (T_1 relaxation) to study the two phases as a function of the molecular reorientation time, τ. The high-temperature phase, called the rotator phase, has an activation energy (E_a) of 1.4 kcal mol^{-1}, while the low-temperature phase, the ratchet phase, has an activation energy (E_a) of 4.2 kcal mol^{-1}. This behavior is similar to that found in solid adamantane.[952,953]

Deleuze and Zerbetto[954] have used unimolecular reaction rate theory and molecular mechanics simulations to determine the temperature-dependent rate constants for the spinning of buckminsterfullerene clusters [$(C_{60})_n$; $n = 3-13$]. Previously, the nearly spherical C_{60} molecules were found to rotate ("spin") in the solid state at 10^9 s^{-1} at 233 K and immeasurably slowly at 123 K.[955] A value of 1.8×10^{10} s^{-1} was reported at 283 K.[949] Deleuze and Zerbetto[954] found rates which seem to converge toward those measured in the solid phase as the cluster size increases. The largest rate constants were obtained in the smallest clusters, and the barriers increase as more C_{60} molecules are added, approaching a "magic" number of 13 (full encapsulation of the central C_{60}), with a barrier (E_{calc}) of 2 kcal mol^{-1}. The room-temperature rate constants fall in the nanosecond regime (E_a between 0.2 and 2.0 kcal mol^{-1}), which can be extrapolated to twelve cages surrounding one C_{60} (full coverage) of 2.2−3.0 kcal mol^{-1}. A number of other groups have used theory to study solid-state rotations in C_{60}.[956−959]

The rotation of C_{60} crystals is controllable by external magnetic fields. Above the transition temperature, Lebedev and co-workers[947] found the rotations of the fullerenes to decrease when the magnetic field increased. Such a system could have potential uses in magnetic storage devices. C_{60} clusters have also been shown to act as *molecular bearings* when placed between two graphite sheets.[960]

7. Rotors on Surfaces

Along with rotors in solids, surface-mounted rotors appear to have the best potential in nanoscience, and we cover them in considerable detail. This is made easier by the relative paucity of published results.

Rotors attached to macroscopic surfaces always rotate relative to the macroscopic object that they are attached to. The orientation of the surface is known although not always in atomistic detail, the rotational motion of the rotator takes place in a space fixed frame, and there is no doubt which part of the molecule is the rotator and which, if any, the stator. Some of the techniques that are very important in studies of rotors in solution and the solid phase, such as NMR, cannot be used, and additional experimental methods become applicable, such as scanning miscroscopy. To further delimit the scope of our review, we recall the size of molecular rotors and more or less arbitrarily rule that objects such as rotational actuators based on multiwalled carbon nanotubes[961,962] are not molecular.

Similarly as molecular rotors inside solids, those on surfaces can occur naturally and have been studied for some time. However, they, too, can be designed, synthesized, and tailored for rotoelectronic applications. Indeed, the development of artificial surface-mounted rotors characterized by one or two mounts carrying a relatively rigid axle with a covalently attached rotator has been the emphasis of the Boulder group of chemists and physicists whose work is described in section 7.2.

7.1. Physisorbed Rotors

Although this review does not generally deal with the rotation of a whole molecule, we need to discuss it at least briefly when it comes to certain molecules on a surface, but we make no claim of comprehensive coverage of the rotation of simple molecules physisorbed on surfaces. These have been studied by a variety of techniques. While their applicability for nanomachinery is limited, they represent the simplest structure that can act as an R-type rotor or rotational switch. Rotation of H_2 adsorbed to Cu(510)

was studied by electron energy loss spectroscopy (EELS).[963,964] Scanning tunneling microscopy (STM) and atomic force miscroscopy (AFM) methods were also used in the study of simple physisorbed molecules. A STM tip can be used to apply torque on individual molecules at low coverage, where the molecules do not interact with each other, and the rotational potential reflects the surface symmetry. This was first observed by Mo in a study of antimony dimers on Si(001)[965] and was later interpreted by means of resonant inelastic electron tunneling.[966] At room temperature, the STM tip was used to push individual Sb_2 molecules from one rotational minimum into the next one. The minimum orientations were found to be 90° apart, consistent with the 001 symmetry of the surface. The energy barrier was estimated to be approximately 2.3 kcal mol^{-1} (0.1 eV).

Molecular oxygen was studied on a Pt(111) surface.[967] The adsorbed oxygen molecules appeared pear-shaped in the STM image, centered on hollow sites of the fcc lattice. To induce rotation, the STM tip was placed over the brighter of the two oxygen atoms, and the voltage was increased until a drop in the tunneling current was observed. A rescan of the area showed that the molecule had undergone a 120° rotation, consistent with the 111 symmetry of the surface. The energy barrier to rotation was found to be in a range from 3.5 to 4.0 kcal mol^{-1}. The same method was used to study acetylene on Cu(001),[968] Cu(100),[969] and Pd(111).[970]

Veerman et al.[781] studied dendritic molecules physisorbed on glass by near-field scanning optical microscopy (NSOM). The molecules have an architecture based on palladium coordination chemistry and a single rhodamine B chromophore. A solution of the molecules was spin coated on glass to yield a sample with several tens of molecules per square micrometer. The polarization of absorption and emission was monitored during NSOM scans. Observing the same molecule over a period of time, it was found that there is rotational motion of the fluorescent cores on a time scale of milliseconds to seconds.

Rotational switching of copper tetra-3,5-di-*tert*-butylphenylporphyrin (**243**; Figure 111) was studied

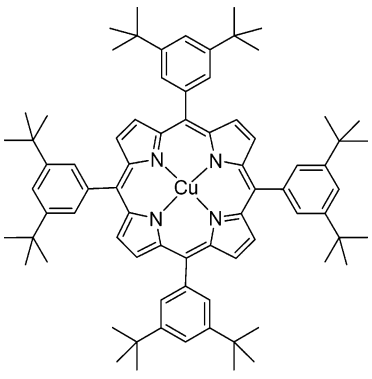

243

Figure 111. Copper tetra-3,5-di-*tert*-butylphenylporphyrin (**243**) can act as rotational switch when adsorbed on a Cu surface.

by AFM/STM methods on Cu(100)[971,972] and Cu(211).[973] Compound **243** is a disk-shaped molecule with four rotatable di-*tert*-butylphenyl legs, similar to the molecules we discussed in section 5.2. It is an altitudinal RS rotor, where the central porphyrin system is the stator. Each leg is a rotator and can adopt two orientations, one roughly parallel with the central disk and the other one roughly perpendicular. The orientation of one leg was controlled using an AFM tip under ultrahigh vacuum (UHV) conditions at room temperature. During this process, the force versus tip sample distance was derived. In this curve, one peak was assigned to the ~90° rotation of the leg. By integration of this peak, the work required to switch the leg was calculated to be 6.76 kcal mol^{-1}. The rotation of one of the legs was utilized to implement a single-molecule switch. When all four legs are in plane with the disk, the electronic coupling of the porphyrin's π-systems to the surface is stronger than that in a state where one leg is rotated, and the porphyrin−surface distance is thus increased. Thus, the STM junction resistance was switched from 670 MΩ to 2.1 GΩ. This established a single-molecule electric ON/OFF switch. It was discussed in the context of power consumption and heat dissipation within electronic devices. The very low switching energy of the rotational switch is promising to reduce the heat removal requirements, but many other problem have to be solved before such switches could find application in electronics. Compound **243** also behaved as an azimuthal rotational switch, where the rotator was switched by an AFM tip between two stable states. Measurements done on the rotor in either state did not rely on free or quasi-free rotation, and dynamical rotational motion was not the subject of interest.

Thermal switching of a surface-adsorbed molecule between an unhindered and a rotationally hindered state was observed by STM imaging.[75,974] The molecule studied was hexa-*tert*-butyldecacyclene (HB-DC) (Figure 112), an approximately disk-shaped molecule, adsorbed on a Cu(100) surface. There are no chemical bonds to the surface, and the rotational potential is dictated by the intermolecular interactions with the surface and with neighboring adsorbed molecules.

In densely packed monolayers, the rotation of individual HB-DC molecules was suppressed. At a coverage far below a monolayer, individual molecules could not be observed by STM, because of the high surface mobility. At a coverage just below the monolayer, the authors studied molecules adsorbed next to a defect of the 2D lattice. These molecules can occupy two distinct states. In one state, they build a perfect lattice with four of their five neighbors (the fifth one is not placed on a lattice point due to the defect). In the other state, the molecule is displaced to the next minimum of the metal surface toward the defect. By STM it was observed that molecules occupying the first state do not rotate (Figure 113A, C), while the molecules in the second state showed azimuthal rotation (Figure 113B, D). It was concluded that the interactions between the adsorbed molecules suppress the rotation. Molecular mechanics calculations of a model system support these observation. For the first state, a rotational barrier

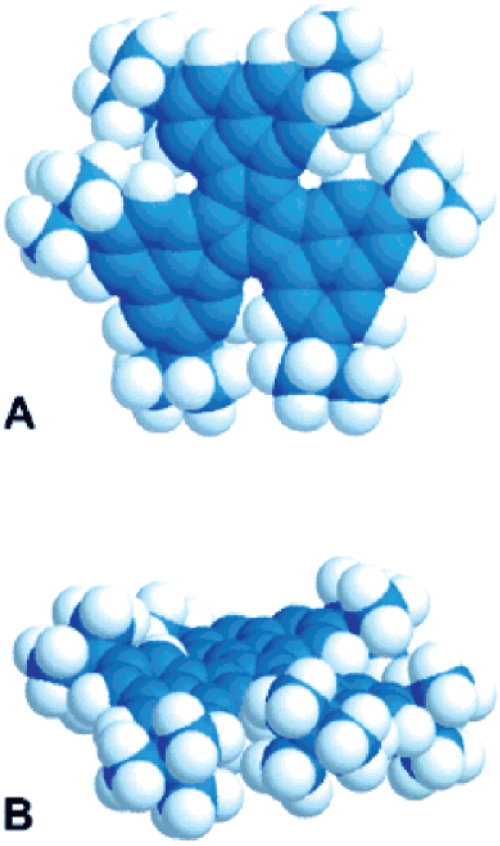

Figure 112. Space-filling model of hexa-*tert*-butyl decacyclene (HB-DC) from the top (A) and side (B). Reprinted with permission from *Science* (http://www.aaas.org), ref 974. Copyright 1998 AAAS.

of 27.9 kcal mol^{-1} was found, and for the second one, a barrier of only 6.9 kcal mol^{-1} was found. A barrier of 10.0 kcal mol^{-1} was obtained for sliding along the surface from one state to the other, and this agrees with the observation of infrequent thermal transitions between the two states.

Hersam and co-workers studied planar, square-shaped copper phthalocyanine (CuPc) on a H-passivated Si(100) surface by STM under ultrahigh vacuum.[975] Individual dangling bonds were created by feedback controlled lithography,[976] which provided templates for rapid absorption of the molecules from the gas phase. Two attachment types with different characteristics were identified. In the first one, CuPc appeared square-shaped in the STM image. The size of 16 Å × 16 Å matched the expected size of the molecule. In the second one, a circular image with a diameter of 35 Å was observed in the STM. The authors concluded that one of the *o*-phenylene rings was attached to a Si dangling bond and the CuPc was able to rotate around this attachment. Thus, the diameter of the feature in the STM was doubled in size compared to the one of the first molecule. When copper atoms of CuPc were complexed by NH_3 prior to absorption, the rotational attachment type predominated.

Collective rotation of chiral molecular rotors was observed by Tabe and Yokohama,[977] who studied Langmuir monolayers of OPOB on glycerol (Figure 114). It builds a liquid crystal monolayer with a coherent tilt angle constrained to ~20° and a domain size of ~1 mm. The intensity observed in reflected

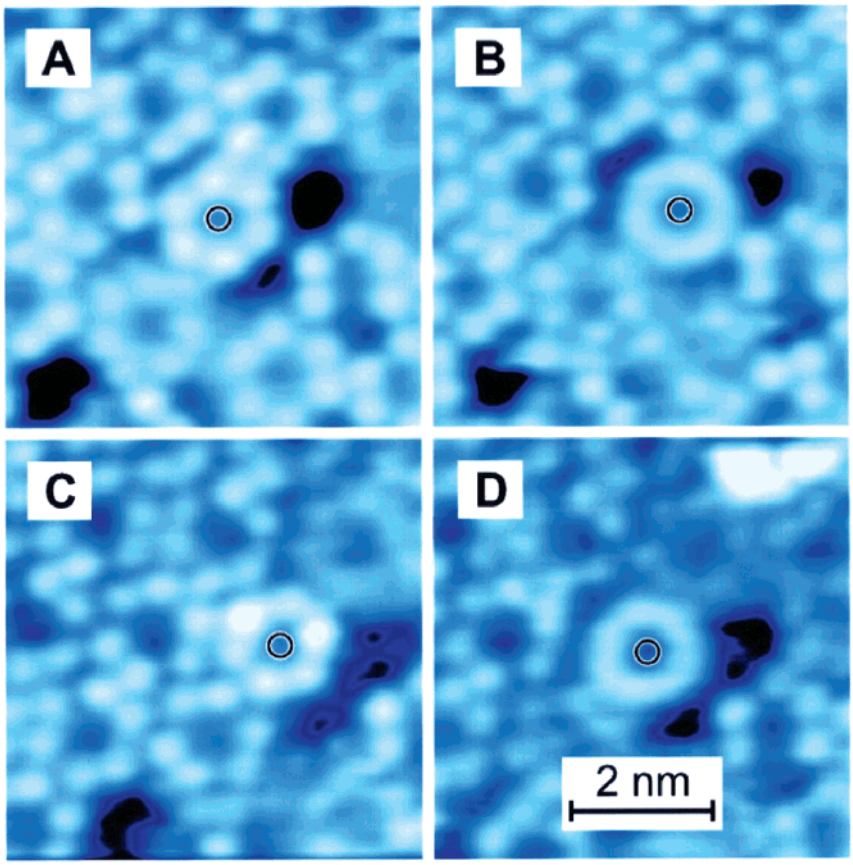

Figure 113. HB-DC on Cu(100) in rotating (B, D) and frozen (A, B) states. Reprinted with permission from *Science* (http://www.aaas.org), ref 974. Copyright 1998 AAAS.

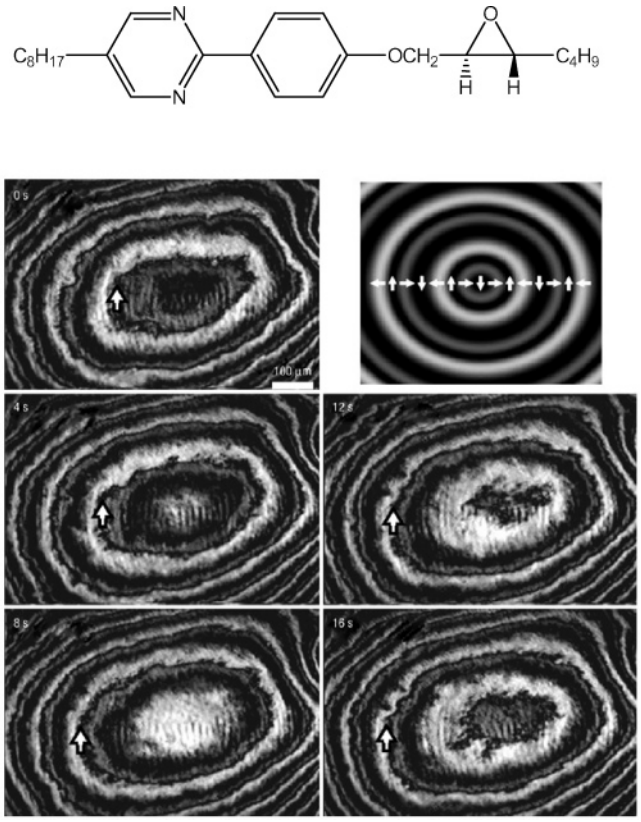

Figure 114. Structure of (*R*)-OPOB and its rotation in a monolayer on glycerol, as seen by polarizing microscopy. Reprinted with permission from ref 977. Copyright 2004 Nature Publishing Group.

light polarizing microscopy correlates with the azimuthal precession angle of the molecular axes within the monolayer. After monolayer formation, concentric rings developed within the monolayer, where the molecules in each ring were oriented in the same direction. The rings differed from their neighbors through the polarization direction. On a time scale of seconds, collective rotation was observed as the polarization direction of the rings changed (Figure 114). For the *R* enantiomer the precession occurred clockwise, and for the *S* enantiomer it occurred counterclockwise. The experiment was repeated with 14 chiral and 9 achiral liquid crystal compounds. All chiral monolayers showed similar rotation; the achiral ones did not. The rotation was studied as a function of air humidity and the water content of the glycerol phase. The frequency of rotation depended linearly on the difference in vapor pressure between the gas and liquid phases. Thus, it was determined that the driving force of the rotation is transfer of water through the monolayer. It was estimated that the average torque per molecule is on the order of $10^{-11}kT$ to $10^{-10}kT$. This emphasizes that this approach to rotation cannot be observed for single molecules, where random thermal motion is dominant, but becomes detectable in the study of two-dimensional arrays.

Molecular mechanics MM3 calculations were performed for benzylic amide [2]catenane **244** and the corresponding thiophenyl catenane **245** (Figure 115) on a graphite surface[978] by methods described previously.[843,979] A finite two-layer model of graphite was

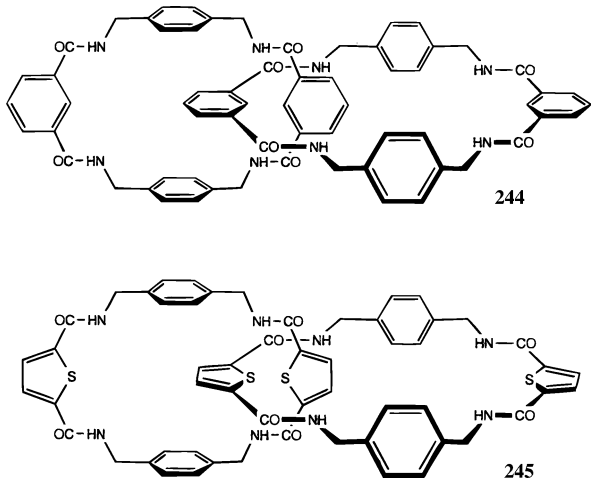

Figure 115. Benzylic amide [2]catenane (**244**) and thiophenylic amide [2]catenane (**245**). Reprinted with permission from ref 978. Copyright 2000 American Chemical Society.

used, and a large number of catenane conformations was created by applying rigid rotations to both rings. After optimization of the structure on top of the graphite surface, two types of physisorbed structures were identified for each catenane. In one, both rings lie flat on the surface, whereas, in the other one, one ring lies flat and the other one is perpendicular to the surface. In the former, circumrotation cannot be easily achieved, and in the latter, partial circumrotation rates are comparable to rates in solution (due to the complexity of the system, full circumrotation was not studied). The azimuthal rotation of the whole catenane on the surface was calculated to have a barrier in the range from 1 to 8 kcal mol^{-1}.

7.2. Chemisorbed Rotors

It is our belief that rotors firmly attached to a surface are the best choice for molecular devices and that much of the solution work can be viewed as preparatory. So far, only relatively few attempts have been made to attach artificial rotors chemically to a surface, to characterize their orientation, and then to study their rotational behavior.

Hydroxyl groups on silica surfaces are very simple, naturally occurring examples of chemisorbed surface-mounted rotors. Ryason and Russel[980] determined their rotational barriers from the temperature dependence of the half width of their IR absorption bands, and they found values of ~0.9 kcal mol^{-1}.

The distribution of energy barriers of azimuthal chloromethyl rotors, $(-O)_3Si-CH_2Cl$, and dichloromethyl rotors, $(-O)_3Si-CHCl_2$, embedded in a monolayer of $(-O)_3Si-Me$ groups on fused silica was determined by dielectric relaxation and compared with molecular modeling results.[981] The samples were made by vapor deposition of methyltrichlorosilane/chloromethyltrichlorosilane mixtures onto fused silica substrates patterned with interdigitated gold electrodes with gaps of 10 μm. The surfaces were characterized by Auger spectroscopy to determine the chloromethyl/methyl ratio, and the thickness of the monolayer was determined to be 3−5 Å by ellipsometry. The capacitance and the dissipation factor were

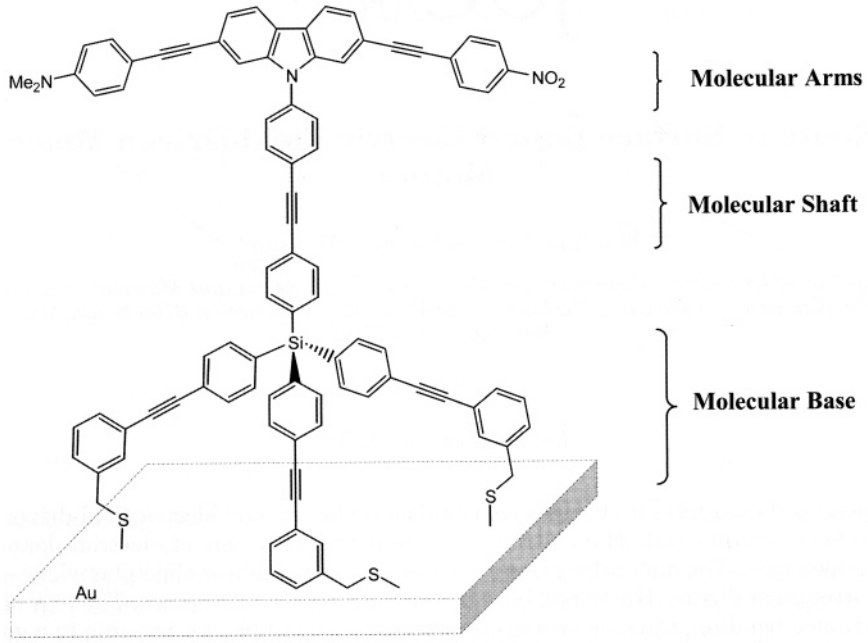

Figure 116. Structure of an azimuthal rotor designed to attach to gold surfaces as shown. Reprinted with permission from ref 983. Copyright 2003 American Chemical Society.

measured at 1 and 10 kHz in a temperature range from 4 to 300 K for samples containing dipolar rotors, for a sample made with pure methyltrichlorosilane, and for a sample of bare fused silica. At lower temperatures, there are peaks that appear in the chloromethyl samples exclusively. In the temperature range studied, dipole relaxation occurs predominantly through thermally activated hopping. Therefore, rotational barriers can be deduced from eq 33 (section 3.2.3.2). The barriers were widely distributed, with 75% of the signal observed between 1.5 and 3.0 kcal mol^{-1}, and the wide distribution was attributed to the proximity of the amorphous silica surface. The barriers were compared to molecular modeling results, where a chloromethyl rotor was attached at nine different sites to a 5.5×5.5 nm^2 model of a fused silica surface. The attachment was modeled by replacing three surface hydroxyl groups by one rotor, and torsional potentials for the rotation of the chloromethyl group were calculated by the universal force field (UFF)[982] method. The torsional barriers of a chloromethyl rotor attached to a crystalline quartz (100) surface were also calculated. Comparing both barrier distributions to the dielectric data, it was concluded that the fused silica samples have a rather disordered surface.

Thus, the challenge is to design rotors which provide narrow barrier distributions, which is essential for any use in nanotechnology, even if they are attached to amorphous surfaces. RS rotors, where the first-order environment of a rotator is part of the molecule, and thus clearly defined, are a promising approach toward narrower barrier distributions. This type of rotor has been synthesized, for example, by Jian and Tour (Figure 116).[983] It is designed to be attached to a gold surface, but no measurements have been reported to date.

Another approach to rotors with homogeneous barriers is to incorporate only a spacer such as a $-C\equiv C-$ group into the axle. The rotating dipole is then elevated higher above the surface, where the main cause of inhomogeneities, nonbonding surface−rotor interactions, are weaker. An example is the $(-O)_3Si-C\equiv C-CH_2Cl$ rotor discussed below.

Vacek and Michl[123] used molecular dynamics with the UFF potential to investigate the response of grid-mounted, chiral, propeller-shaped azimuthal molecular rotors to a flow of a supersonic rare gas beam directed parallel to the rotor axle. The rotor structures were based on a octahedral Re complex in which the Re atom carries three bidentate ligands (Figure 117). It is attached to the two oxygens of a 3-cyanobicyclo[1.1.1]pent-1-ylmalonic dialdehyde, whose nitrile group provides a link to the carrier grid. Its other two chirally disposed ligands are derivatives of *o*-phenanthroline and represent the two blades of the rotor. On the outside edge, one phenanthroline carries a BF_2^- group and the other a NMe_2^+ group, forming a strongly dipolar zwitterionic structure. The size of these blades was considered minimal in view of the requirement that they not be hidden by the carrier grid from the applied stream of gas, and a larger set of blades was also examined. Attachment to the carrier grid, composed of nine dirhodium tetracarboxylate connectors linked into nine squares with twelve [2]staffanedicarboxylates, is provided by the nitrile substituent on the malonic dialdehyde ligand. This is located axially on one of the Rh atoms in the central connector.

Helium, neon, argon, and xenon were used to drive the rotor, and the density and velocity of the gas beam were varied. In all simulations, the density of the gas was relatively high for the sake of computational efficiency. It was observed that the excitation of rotational motion through momentum transfer from the gas atoms competes with the induction of pendulum-like motion, where the axle of the rotor is bent. This effect became more pronounced for the

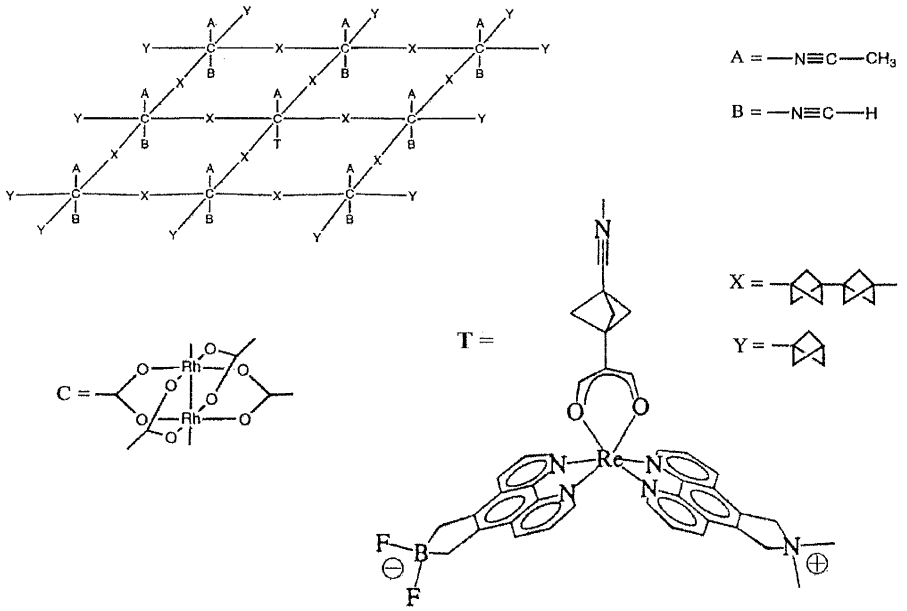

Figure 117. Structure of a rhenium complex used for a molecular dynamics simulation of a molecular rotor. Reproduced with permission from ref 123. Copyright 1997 The Royal Society of Chemistry.

heavier gases. For argon and xenon, continuous rotation was never obtained. If induction of rotational motion was successful, the rotor assumed a steady state with approximately constant angular velocity, after an initial period of hesitation. Rotational frequencies of up to 37 GHz for the bigger rotor and 21 GHz for the smaller rotor were observed. The efficiency of energy transfer from the gas into rotational motion was judged by the average rotational period, the average angular momentum, and the temperature equivalent (T_{eq}) of the rotational motion. The best induction of rotation was found for a high-density beam of light rare gas atoms with a high velocity at low temperatures. The performance was also judged by the ratio of the average energy stored in the steady-state rotational motion of the rotator and the loss of translational energy of the gas stream, integrated over the time it took to reach steady-state rotation. The temperature equivalent T_{eq} of the kinetic energy stored in the induced rotation mode in the steady state was more than 2000 K, high above the room temperature of the rest of the system.

The smaller of the rotors (Figure 117) was also studied by molecular dynamics when driven by a rotating electric field of frequency in a range between 3.2 and 400 GHz and field strengths between 10 and 700 MV/m.[91] The dipole moment of the rotor, ~42 D, is perpendicular to the axle of rotation, and the rotational barrier is negligible. In most simulations there was no significant heating of the grid polymer or the rotator. However, the temperature equivalent of the rotational mode was significantly higher when rotational motion was successfully induced, reflecting the mechanical nature of this mode. A phase diagram for the rotor response was derived from the simulations. Five regimes of rotor motion were characterized by the value of the average lag: synchronous, asynchronous, and three random regimes of motion. These regimes are discussed in section 3.2.1.

Below ~40 GHz, the average lag per turn a was frequency independent. The breakoff field E_{bo}, below which the rotor fails to respond to the rotating field, was approximately equal to kT/μ and the critical field E_c, above which the rotor becomes synchronous, 2.3 kT/μ. At these frequencies, the driving field needs to overcome opposition from random thermal motion (section 3.2.1). At frequencies above 40 GHz, friction was identified as the dominant opponent of the driving force. At these frequncies, E_{bo} and E_c increased linearly in the log−log phase diagram, and the slope suggested that the friction constant of the system is a linear function of the frequency ν ($\nu = \omega/2\pi$).

A "tilted washboard" model for the response of the rotor was developed, and it allowed a definition of a phenomenological friction constant η and its evaluation from a fit to the values of $a(E,\nu)$ obtained from the molecular dynamics runs, as discussed in section 3.2.1.2. The fitting of a at frequencies above 40 GHz yielded $\eta/\nu = 1.14$ eVps/THz. Below 20 GHz, such fitting of η is not possible, since the rotor behavior is dictated by thermal fluctuations.

A further development of the phenomenological model was reported by Horinek and Michl[92] in a molecular modeling study of chloropropynyl rotors, $(-O)_3Si-C\equiv C-CH_2Cl$, on fused silica.[984] The rotor was attached to a model fused silica surface, which contained ~3500 atoms. Two types of surface attachment were studied: In surface 1, the rotors were attached by replacing surface hydroxyl groups. For surface 2, a full methylsilyl monolayer was constructed on the surface, and the rotor was incorporated into the monolayer at different places. The rotational potentials of both rotor ensembles were calculated with the UFF potential. The barriers of rotation ranged from 0.65 to 3.1 kcal mol^{-1}. While generally lower than the barriers of the shorter $(-O)_3Si-CH_2Cl$ rotors, these barriers were much higher than that of the rotors shown in Figure 117.[981]

The barriers on the rotors on surface 2 were somewhat higher than those for the rotors on surface 1. The barrier distribution was still rather broad. The shape of the rotational potential was related to the polar angle of the rotor axle. Rotors that were nearly perpendicular to the surface had a potential with one minimum and one maximum, dictated by the van der Waals attraction of the chlorine substituent to the surface. Rotors that were more tilted toward the surface had potentials with two or three minima and maxima, since now the methylene hydrogens interacted with the surface as well, and their barriers were higher.

One of the rotors, which had a barrier of 0.75 kcal/mol, was studied by molecular dynamics. It was shown that these dipolar rotors act as energy absorbing antennas when they are exposed to rotating electric field in the GHz range: a system with a dipolar rotor absorbed 10 times more energy than a system with a nonpolar propynyl rotor. When the torsional barriers were artificially suppressed and a rotating electric field was applied, the rotors showed synchronous response. Fourier transform of the angle versus time curves showed two distinct peaks, one at the frequency of the applied electric field and a second one at a frequency that scales as $\sqrt{E}$, which was assigned to librational motion in the electric field potential $\mu E \cos \omega t$ (see section 3.2.1.1). When a rotating electric field potential was applied with the barriers switched on, Fourier transform of the angle versus time curves generally showed a broad frequency response. Phase diagrams of rotational motion were obtained at several temperatures. These diagrams show in which ranges of electric field frequency and amplitude the rotor responds by synchronous rotation (see section 3.2.1). Rather different behavior was found for driving frequencies above and below 500 Ghz. Below this frequency, friction effects are small relative to thermal energy and cogging effects of the intrinsic potential. The driving force has to overcome the random thermal motion term kT or the intrinsic barrier W, whichever of the two is larger (this depends on temperature), before the rotor turns synchronously, and neither one depends on field frequency, such that the average lag a is independent of the driving frequency ν. This result is very similar to the one observed[91] in work with the smaller of the rotors of Figure 117. The friction effects again grow with increasing driving frequency, and above 500 GHz, they become the major opponent of the driving force. A frequency-dependent phenomenological friction constant was derived using the tilted work board model (section 3.2.1.2). Between 500 and 1000 GHz, a linear relation $\eta/(\nu - 0.5) = 0.26$ eV ps/THz was obtained. Because of the non-negligible rotational barrier height, the phenomenological model had to be elaborated considerably.

Triptycene-based rotors (Figure 118) were studied on Si(100)-2 × 1 with the semiempirical AM1 method.[985] A flat silicon cluster served as the model system of the surface. Two methods of binding of the triptycene to the silicon were studied: binding through an oxygen atom, −O−, and binding through a carboxy group, $-CO_2-$. The remaining dangling bonds on the Si cluster were saturated by hydrogen atoms. The rotational potential was calculated for both modes of attachment. The attachment through $-CO_2-$ yielded a rotational barrier of 1.4 kcal mol^{-1}, and the attachment through −O−, a barrier of 3.7 kcal mol^{-1}. The lower barrier of the carboxy attachment is a result of the increased flexibility. This barrier increases to approximately 20 kcal mol^{-1} when a C_{60} fullerene is attached next to the triptycene on the surface, acting as a brake (Figure 118). In a molecular gear arrangement, where two triptycenes are mounted on the surface 7.68 D apart, the authors studied whether the rotation of one triptycene drives the rotation of the neighboring one. The barrier for slippage was estimated to be on the order of 9 kcal mol^{-1}, high enough to allow angular momentum transfer between neighboring triptycenes but too low for synchronous transfer. The issue of how rotation is to be initially induced in a surface mounted triptycene was not addressed.

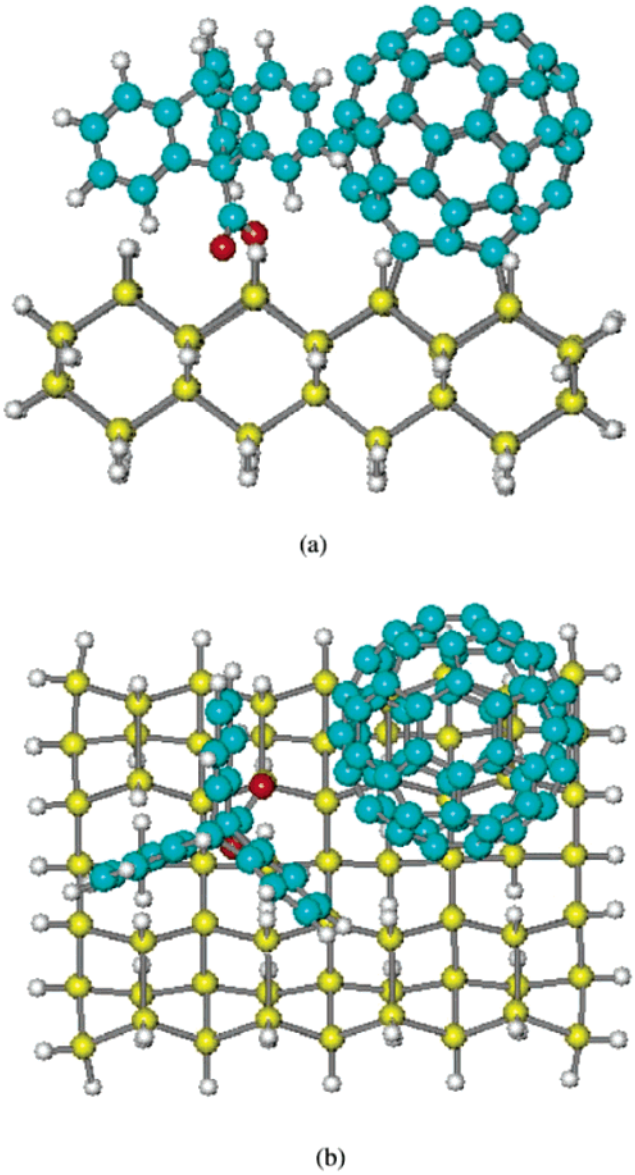

Figure 118. Structure of a triptycene-based rotor in the vicinity of C_{60} on Si(100). Reprinted with permission from ref 985. Copyright 2003 IOP Publishing Limited.

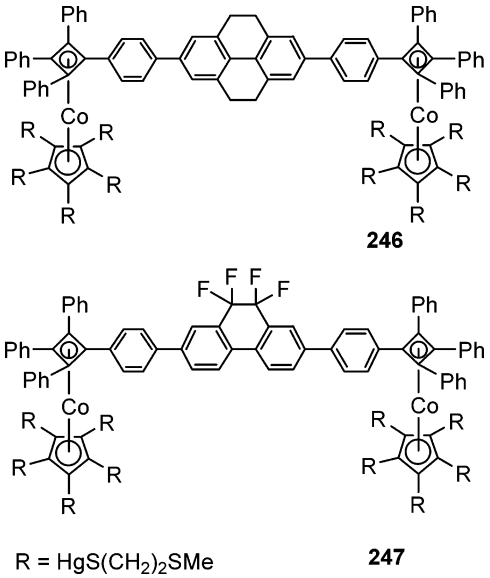

Figure 119. A nonpolar (**246**) and a dipolar (**247**) altitudinal rotor.

A surface-mounted nonpolar altitudinal rotor **246** and its dipolar analogue **247** have been synthesized in the laboratory of Michl (Figure 119).[114] In solution, the rotational barriers were too low to be measured by NMR (~3 kcal mol^{-1} calculated). Both rotors were adsorbed on the (111) surface of gold at monolayer and submonolayer coverages (Figure 120), and the process was monitored by ellipsometry, a quartz microbalance, and X-ray photoelectron spectroscopy (XPS). Even through some of the sulfur atoms were oxidized within days when exposed to air as judged by XPS, the rotors were immobilized over hours in STM images. After further studies, it was concluded that the mercury atoms contribute significantly to the binding,[986] explaining why the rotor still attaches after the sulfur atoms are oxidized. The surface area per molecule was determined by STM to be about 2−3 × 4−5 nm^2. This compares well to the value of 9 nm^2 calculated for the expected conformation with all 10 sulfur-containing chains spread over the surface. It also compares well with the footprint size of 8.5 nm^2 obtained from a compression isotherm on a Hg/CH_3CN interface in an electrochemical Langmuir trough. The average orientation of the rotator was determined by grazing incidence IR spectroscopy. To find out whether the rotators in these surface-mounted rotors are actually capable of turning, an STM tip was placed above the surface, and the local work function was measured by barrier height imaging (BHI).[987] About two-thirds of the dipolar rotors and none of the nonpolar rotors showed different work functions depending on the direction of the STM electric field, appearing as bright spots in BHI (Figure 120). The difference in work function was interpreted as due to the reorientation of the dipolar rotor in the direction of the electric field imposed by the STM tip. Repeated scans of the same surface area revealed that the same molecule can switch back and forth between bright and dark states (blink).

The dynamical response of the surface mounted rotor was studied by molecular modeling using the UFF potential including image charges inside the gold substrate. Electronic friction within the metal was handled by Langevin dynamics. All three pairs of enantiomers which originate from the helical P/M symmetry of both tetraarylcyclobutadienes and the rotator in **247** were studied. Two conformations of the tentacles which attach the rotor to the surface

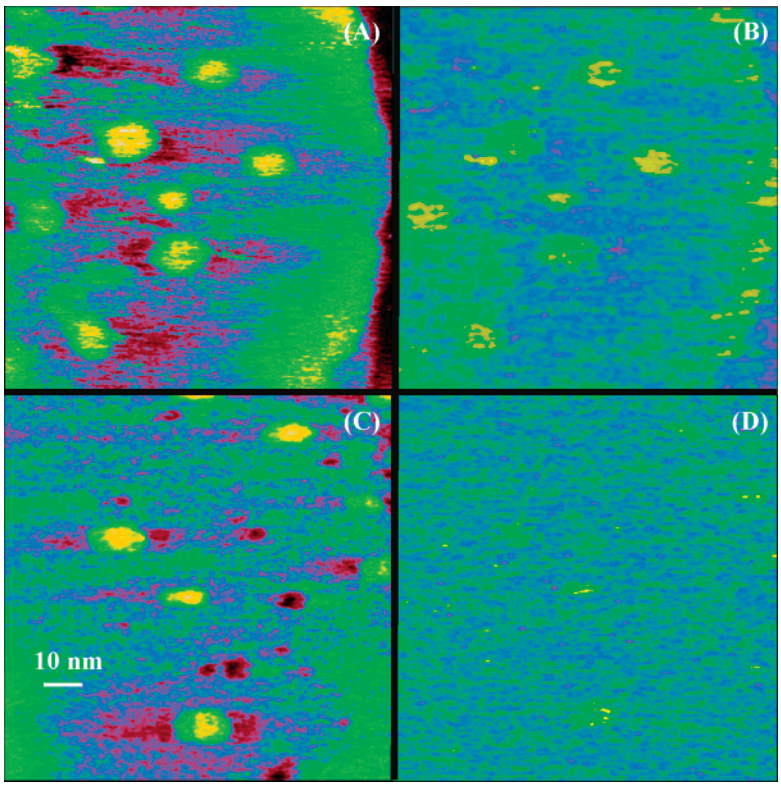

Figure 120. Images of altitudinal rotors on Au (111): (A) STM, **246**; (B) BHI, **246**; (C) STM, **247**; (D) BHI, **247**. Reprinted with permission from ref 114. Copyright 2004 American Chemical Society.

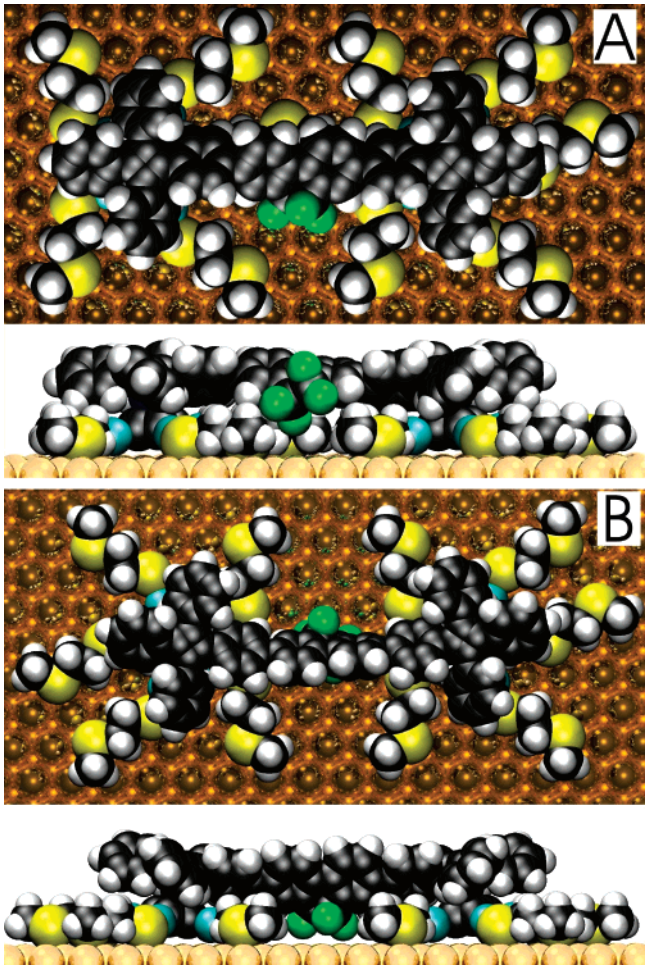

Figure 121. Eclipsed (A) and staggered (B) conformations of the one diastereomer of **247** on Au(111). Reprinted with permission from ref 114. Copyright 2004 American Chemical Society.

which represent structures with maximal (A) and minimal (B) rotator−tentacle interaction were examined (Figure 121). In conformation B the realignment of the rotator through a typical electric field imposed by a STM tip is energetically possible for all pairs of enantiomers; in conformation A, it is not and the rotator is blocked. Assuming some small mobility of the tentacles on the surface, it was concluded that the blinking is caused by changes of tentacle conformation.

Molecular dynamics simulations of the gold mounted rotor at low temperature showed that two of the conformers respond to alternating electric fields with unidirectional rotation, while the third one does not. The symmetry of the calculated rotational potentials was used to explain this observation. The computer simulations predicted subharmonic resonances (section 3.2.1.3) in the unidirectional response of the rotor. At room temperature, the rotor's proclivity toward unidirectional rotation is expected to be overshadowed by the random interconversion between the stereoisomers, which requires the average directionality to be zero. It is however fairly clear how to amend the rotor design to provide steady unidirectionality in the driven rotation.

One approach toward molecular electronics[988,989] is the attachment of conducting molecules to a gold surface through thiol groups ("molecular alligator clips"). Molecular rotors bridging a gap between two gold surfaces could act as molecular rectifiers if their conductivity depends on the angle of rotation, either through changes in the electronic structure or through connection or separation of two conducting elements of the molecule. A computational study of 9-hydro-10-carboxamide-acridine-2,7-dithiol (**248**, Figure 122)

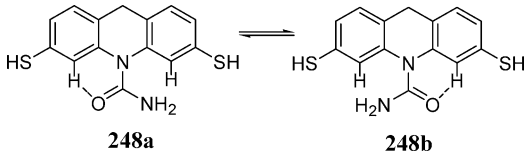

Figure 122. 9-Hydro-10-carboxamide-acridine-2,7-dithiol, a switchable dipolar molecule for the theoretical study of electrical conductance in applied electric field.

has been reported.[990] The dipolar carboxamide has two favored orientations at angles of ~30° and ~150°. With a strong electric field along the gap, the dipole can be oriented. Calculations based on transport Green functions predicted that, upon application of small potentials, electrical conductance through the molecule will be higher in the case where the dipole points in the direction of the current.

Troisi and Ratner studied the two rotors shown in Figures 123 and 124 theoretically as examples of

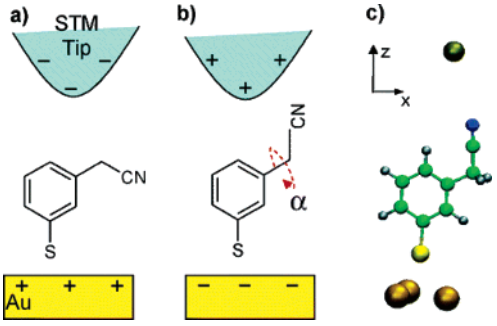

Figure 123. Schematic of a contact-modulated CMR, with two conformations shown (a, b). Part c shows the atoms included in the conductance calculations. Reprinted with permission from ref 143. Copyright 2004 American Chemical Society.

"conformational molecular rectifiers" (CMR).[143] Both molecules attach to gold surfaces through their thiol groups. They have a dipolar rotating part whose orientation can be controlled by a strong electric field when placed in a tunneling junction. The *I/V* curves of both molecules were calculated by a Green's function approach. In both cases, they show significant rectification, where the latter molecule seems to be the most promising, albeit synthetically most demanding.

7.3. Wheels on Surfaces

Wheels, one of the most revolutionizing inventions in history, are characterized by rolling motion on surfaces. This is a special combination of altitudinal rotation and translation along the surface. Similar to the macroscopic world, where wheels replace sliding high friction motion by smooth rolling, mo-

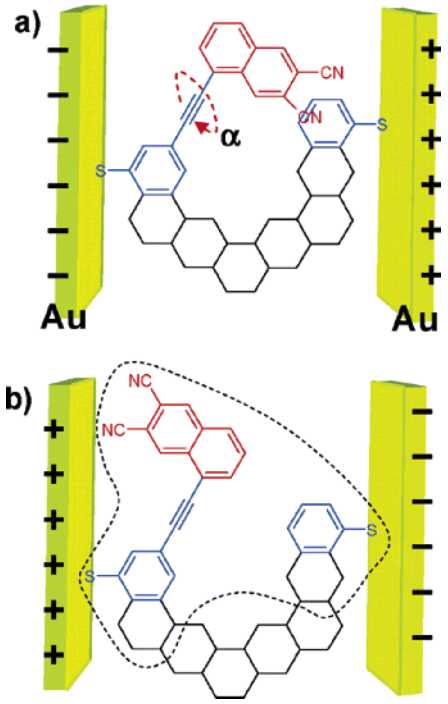

Figure 124. Conformational molecular rectifiers based on rotational motion. Reprinted with permission from ref 143. Copyright 2004 American Chemical Society.

lecular wheels were studied under the aspect of low friction surface mobility.

The tribological effects of a layer of fullerene acting as ball bearings intercalated between two layers of graphite were studied experimentally, and ultralubricant behavior was found.[991] Kang and Hwang reported a molecular dynamics study of C_{60} and $K@C_{60}$ as molecular ball bearings and found $K@C_{60}$ to be the better lubricant due to its higher bulk modulus.[992]

Molecular versions of rolling wheels were designed[993,994] in theoretical studies by attaching fluxional molecules to a surface with a high density of dangling bonds. Cyclopentadienyl was studied[993] on the (111) surface of Si and Ge by DFT calculations (B3LYP, 3-21G, and 6-31G** basis sets) of small model systems for a full surface. The transition barriers were calculated for bond fluctuations which result in a net translation of the cyclopentadienyl on the surface. The predicted corresponding rates at room temperature are in the range from $\sim 10^4$ to ~ 1 Hz.

Hypostrophene rolling on Al(100) through degenerate Cope rearrangements (Figure 125) was studied by quantum chemical calculations (HF and B3LYP) with a 3-21G basis for Al atoms and 6-31G** otherwise.[994] The barrier found was 16.9 kcal mol^{-1} for a rolling motion, whereas for a sliding motion on the surface the barrier was approximately five times higher.

The advantage of molecular wheels is that they stick to the surface better than physisorbed molecules, which have an equal or better mobility on the surface. The large scale comparison, where wheels increase the efficiency of sliding motion, does not hold.

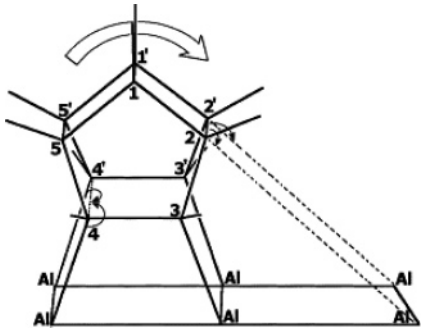

Figure 125. Rolling mechanism for hypostrophene on Al-(100). Reprinted with permission from: Das, B.; Sebastian, K. L. Adsorbed hypostrophene: can it roll on a surface by rearrangement of bonds? *Chem. Phys. Lett.* **2000**, *330*, 433–439. Copyright 2000 Elsevier.

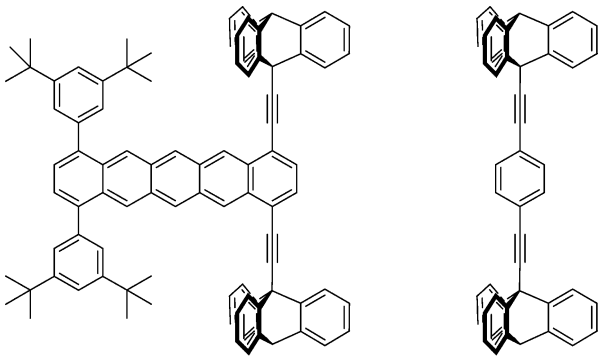

249 **250**

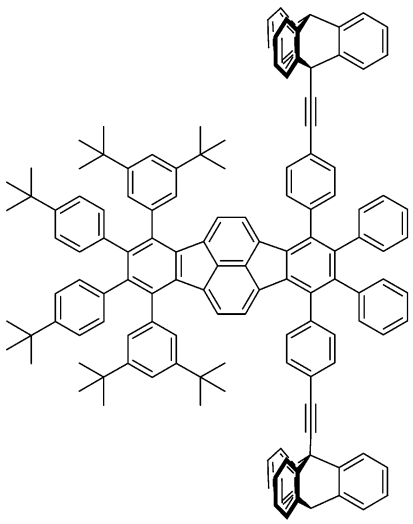

251

Figure 126. Some molecular barrows.

Another route toward molecular rolling was pursued by the design of molecular barrows. The molecular barrow **249** shown in Figure 126 contains "handles" on one side which can be pushed by an STM tip. On the other side, two triptycene "wheels" are attached through ethynyl spacers. Theoretically, it was shown that the tunneling current between the tip placed above the central board of the barrow and the surface should change as a function of wheel rotation. The simpler molecule **250** was synthesized, and two bright lobes corresponding to the two wheels were observed by STM on Cu(100) at 12 K.[995]

However, there was no evidence that the wheels roll, and molecular mechanics calculations indicated that the central polycence is not stiff enough to transmit the pressure applied by the tip. Furthermore, there is only little resistance to sliding motion on the Cu(100) surface without rotation of the wheels. To overcome the first problem, the more rigid molecular barrow **251** was designed and synthesized,[996] but no STM studies have been reported at this time.

Here, the classical comparison to large scale wheels is more appropriate. The idea of the barrow's wheels compares to the wheels mentioned earlier as macroscopic wheels compare to logs used in ancient Egypt to haul bricks. Nevertheless, their advantage over sliding motion needs to be demonstrated. As mentioned by the authors, molecular machines can only endure UHV conditions for an extended time if they are connected by chemical bonds. The barrows attach to surfaces through van der Waals forces and are therefore prone to surface desorption. In our opinion, physisorbed molecular rotors are not likely to find much application.

Chemisorbed rotors are attached to a surface by one or more chemical bonds. Their stronger attachment energies make them less vulnerable to destruction by surface desorption than physisorbed rotors, which are only loosely attached to their substrate. On the other hand, the bonding to the surface restricts their motion and may give rise to higher rotational barriers. It was found so far that surface inhomogeneities significantly broaden the energy barrier distribution. For most applications in nanomachinery, low barriers and narrow energy distributions would be ideal. RS rotors are more complicated structures and require a more sophisticated synthesis, but their rotational potential can be controlled to a higher degree.

8. Conclusions and Outlook

We have attempted to provide a comprehensive overview of the current state of artificial molecular rotors. The breadth of the subject is fascinating. It ranges from preparative chemistry to theoretical physics, and rapid progress is occurring on all fronts.[997] It also ranges from fundamental to application-oriented studies. We expect a gradual shift of emphasis from studies of rotor molecules floating freely in solution to systems in which they are mounted on surfaces or inside solids. Some of the current challenges are a demonstration of coherent motion in regular arrays of dipolar rotors, demonstration of advanced methods for driving unidirectional rotation, realization of structures that minimize rotational energy dissipation by friction, and demonstration of fluid flow−rotor interactions, initially with flow-driven rotors and ultimately perhaps with rotor-driven flow.

Actual molecular machinery still remains a distant goal. Near-term applications are more likely to come in electronics, optoelectronics, and possibly nanofluidics. For instance, it does not take much imagination to envisage a delay line in which a pulse of rotational excitation propagates through a ferroelectric array of dipolar rotors at a speed much slower than the speed of sound in solids, permitting a miniaturization of this important constituent of analogue electronics. The dielectric response of dipolar rotors is inherently nonlinear, and this suggests their possible use in varactors (variable capacitors) and elsewhere. Modulation of optical signals at microwave or THz frequencies is another attractive possibility.

Achieving nanoscience goals using molecular rotors will take a collaborative effort among chemists, physicists, engineers, biochemists, and others. Amalgamating these disciplines is quite difficult, but knowledge of each is key to understanding the intricacies of this new field. The first truly functional device will most likely come out of such a collaboration.

9. References

(1) Arnold, B. R.; Balaji, V.; Downing, J. W.; Radziszewski, J. G.; Fisher, J. J.; Michl, J. *J. Am. Chem. Soc.* **1991**, *113*, 2910.
(2) *Merriam Webster's Collegiate Dictionary*, 10th ed.; Simon & Schuster, Inc.: New York, 1993.
(3) Itoh, H.; Takahashi, A.; Adachi, K.; Noji, H.; Yasuda, R.; Yoshida, M.; Kinosita, K., Jr. *Nature* **2004**, *427*, 465 and references therein.
(4) Aksimentiev, A.; Balabin, I. A.; Fillingame, R. H.; Schulten, K. *Biophys. J.* **2004**, *86*, 1332 and references therein.
(5) Boyer, P. D. *Nature* **1999**, *402*, 247.
(6) Boyer, P. D. *Angew. Chem., Int. Ed.* **1998**, *37*, 2296.
(7) Walker, J. E. *Angew. Chem., Int. Ed.* **1998**, *37*, 2308.
(8) Kinosita, K., Jr.; Yasuda, R.; Noji, H.; Ishiwata, S.; Yoshida, M. *Cell* **1988**, *93*, 21.
(9) *Molecular Motors*; Schliwa, M., Ed.; Wiley-VCH: Weinheim, 2003.
(10) Schliwa, M.; Woelke, G. *Nature* **2003**, *422*, 759.
(11) Vale, R. D.; Milligan, R. A. *Science* **2000**, *288*, 88.
(12) Schatzki, T. F. *J. Polym. Sci.* **1962**, *67*, 496.
(13) Boyer, R. F. *Rubber Chem. Technol*. **1963**, *34*, 1303.
(14) Schatzki, T. F. *J. Polym. Sci., Part C* **1966**, *14*, 139.
(15) Boyer, R. F. *Macromolecules* **1973**, *6*, 288.
(16) Boyd, R. H.; Breitling, S. M. *Macromolecules* **1974**, *7*, 855.
(17) Gurler, M. T.; Crabb, C. C.; Dahlin, D. M.; Kovac, J. *Macromolecules* **1983**, *16*, 398.
(18) David, L.; Girard, C.; Dolmazon, R.; Albrand, M.; Etienne, S. *Macromolecules* **1996**, *29*, 8343 and references therein.
(19) Moro, G. J. *J. Phys. Chem.* **1996**, *100*, 16419 and references therein.
(20) Wolgemuth, C. W.; Powers, T. R.; Goldstein, R. E. *Phys. Rev. Lett.* **2000**, *84*, 1623 and references therein.
(21) Hugel, T.; Holland, N. B.; Cattani, A.; Moroder, L.; Seitz, M.; Gaub, H. E. *Science* **2002**, *296*, 1103 and references therein.
(22) Holland, N. B.; Hugel, T.; Neuert, G.; Cattani-Scholz, A.; Renner, C.; Oesterhelt, D.; Moroder, L.; Seitz, M.; Gaub, H. E. *Macromolecules* **2003**, *36*, 2015 and references therein.
(23) *The American Heritage Dictionary of the English Language*, 4th ed.; 2000.
(24) Schill, G. *Catenanes, Rotaxanes, and Knots*; Academic Press: New York, 1971.
(25) *Molecular Catenanes, Rotaxanes and Knots*; Sauvage, J.-P., Dietrich-Buchecker, C., Eds.; Wiley-VCH: Weinheim, 1999.
(26) Balzani, V.; Venturi, M.; Credi, A. *Molecular Devices and Machines*; Wiley-VCH: Weinheim, 2003.
(27) Amabilino, D. B.; Stoddart, J. F. *Chem. Rev.* **1995**, *95*, 2725.
(28) Fyfe, M. C. T.; Stoddart, J. F. *Acc. Chem. Res.* **1997**, *30*, 393.
(29) Balzani, V.; Gómez-López, M.; Stoddart, J. F. *Acc. Chem. Res.* **1998**, *31*, 405.
(30) Raymo, F. M.; Stoddart, J. F. *Chem. Rev.* **1999**, *99*, 1643.
(31) Balzani, V.; Credi, A.; Raymo, F.; Stoddart, J. F. *Angew. Chem., Int. Ed.* **2000**, *39*, 3348.
(32) Pease, A. R.; Stoddart, J. F. *Struct. Bonding* **2001**, *99*, 189.
(33) Pease, A. R.; Jeppesen, J. O.; Stoddart, J. F.; Luo, Y.; Collier, C. P.; Heath, J. R. *Acc. Chem. Res.* **2001**, *34*, 433.
(34) Tseng, H.-R.; Stoddart, J. F. In *Modern Arene Chemistry*; Astruc, D., Ed.; Wiley-VCH: Weinheim, 2002; pp 574−599.
(35) Liu, J.; Gómez-Kaifer, M.; Kaifer, A. E. *Struct. Bonding* **2001**, *99*, 142.
(36) Ballardini, R.; Balzani, V.; Credi, A.; Gandolfi, M. T.; Venturi, M. *Acc. Chem. Res.* **2001**, *34*, 445.
(37) Chambron, J. C.; Dietrich-Buchecker, C.; Sauvage, J.-P. In *Comprehensive Supramolecular Chemistry*; Atwood, J. L., Lehn,

J.-M., Davies, J. E. D., MacNicol, D. D., Vögtle, F., Eds.; Elsevier: Amsterdam, 1996; Volume 9, p 43.
(38) Dietrich-Buchecker, C. O.; Sauvage, J.-P. *Chem. Rev.* **1987**, *87*, 795.
(39) Sauvage, J.-P. *Acc. Chem. Res.* **1990**, *23*, 319.
(40) Chambron, J.-C.; Dietrich-Buchecker, C. O.; Sauvage, J.-P. *Top. Curr. Chem.* **1993**, *165*, 131.
(41) Chambron, J.-C.; Dietrich-Buchecker, C. O.; Heitz, V.; Nierengarten, J.-F.; Sauvage, J.-P.; Pascard, C.; Guilhem, J. *Pure Appl. Chem.* **1995**, *67*, 233.
(42) Sauvage, J.-P. *Acc. Chem. Res.* **1998**, *31*, 611.
(43) Collin, J.-P.; Dietrich-Buchecker, C.; Gaviña, P.; Jimenez-Molero, M. C.; Sauvage, J.-P. *Acc. Chem. Res.* **2001**, *34*, 477.
(44) Raehm, L.; Sauvage, J.-P. *Struct. Bonding* **2001**, *99*, 55.
(45) Collin, J.-P.; Kern, J.-M.; Raehm, L.; Sauvage, J.-P. In *Molecular Switches*; Feringa, B. L., Ed.; Wiley-VCH: Weinheim, 2001; pp 249−280.
(46) Hunter, C. A. *Chem. Soc. Rev.* **1994**, 101.
(47) Vögtle, F.; Dünnwald, T.; Schmidt, T. *Acc. Chem. Res.* **1996**, *29*, 451.
(48) Vögtle, F.; Jäger, R.; Händel, M.; Ottens-Hildebrandt, S. *Pure Appl. Chem.* **1996**, *68*, 225.
(49) Jäger, R.; Vögtle, F. *Angew. Chem., Int. Ed. Engl.* **1997**, *36*, 931.
(50) Schalley, C. A.; Beizai, K.; Vögtle, F. *Acc. Chem. Res.* **2001**, *34*, 465 and references therein.
(51) Armspach, D.; Ashton, P. R.; Ballardini, R.; Balzani, V.; Godi, A.; Moore, C. P.; Prodi, L.; Spencer, N.; Stoddart, J. F.; Tolley, M. S.; Wear, T. J.; Williams, D. J. *Chem.—Eur. J.* **1995**, *1*, 33.
(52) Harada, A. *Acc. Chem. Res.* **2001**, *34*, 456.
(53) Lee, J. W.; Kim, K. *Top. Curr. Chem.* **2003**, *228*, 111.
(54) Shipway, A. N.; Katz, E.; Willner, I. *Struct. Bonding* **2001**, *99*, 237.
(55) Benniston, A. C. *Chem. Soc. Rev.* **1996**, 427.
(56) Breault, G. A.; Hunter, C. A.; Mayers, P. C. *Tetrahedron* **1999**, *55*, 5265.
(57) Raymo, F. M.; Stoddart, J. F. In *Templated Organic Synthesis*; Diederich, F., Stang, P. J., Eds.; Wiley-VCH: Weinheim, 2000; pp 75−104.
(58) Raymo, F. M.; Stoddart, J. F. In *Molecular Switches*; Feringa, B. L., Ed.; Wiley-VCH: Weinheim, 2001; pp 219−248.
(59) Haidekker, M. A.; Brady, T.; Wen, K.; Okada, C.; Stevens, H. Y.; Snell, J. M.; Frangos, J. A.; Theodorakis, E. A. *Biorg. Med. Chem.* **2002**, *10*, 3627.
(60) Viriot, M. L.; Carre, M. C.; Geoffroy-Chapotot, C.; Brembilla, A.; Muller, S.; Stoltz, J.-F. *Clin. Hemorheol. Microcirc.* **1998**, *19*, 151.
(61) Iio, T.; Takahashi, S.; Sawada, S. *J. Biochem.* **1993**, *113*, 196.
(62) Haidekker, M. A.; Brady, T. P.; Chalian, S. H.; Akers, W.; Lichlyter, D. *Bioorg. Chem.* **2004**, *32*, 274−289 and references therein.
(63) Loutfy, R. O. *Macromolecules* **1983**, *16*, 678 and references therein.
(64) Loutfy, R. O.; Arnold, B. A. *J. Phys. Chem.* **1982**, *86*, 4205 and references therein.
(65) Grabowski, Z. R.; Rotkiewicz, K.; Rettig, W. *Chem. Rev.* **2003**, *103*, 3899.
(66) Saltiel, J.; Sun, Y. P. In *Photochromism, Molecules and Systems in Studies in Organic Chemistry 40*; Dürr, H., Bouas Laurent, H., Eds.; Elsevier: Amsterdam, 1990; Chapter 3.
(67) Ross, D. L.; Blanc, J. In *Photochromism in Techniques of Chemistry*; Brown, G. H., Ed.; Wiley-Interscience: New York, 1971; Volume 3, Chapter 5.
(68) Birge, R. R. *Biochim. Biophys. Acta* **1990**, *1016*, 293.
(69) Hartley, G. S. *Nature* **1937**, *140*, 281.
(70) See special issue on Photochromism: *Chem. Rev.* **2000**, *100*, 1683−1890.
(71) Holmes, R. R. *Acc. Chem. Res.* **1979**, *12*, 257.
(72) Montgomery, C. D. *Phosphorous, Sulfur Silicon Relat. Elem.* **1993**, *84*, 23.
(73) Mann, B. E. In *Comprehensive Organometallic Chemistry*; Wilkinson, G., Stone, F. G. A., Abel, E. W., Eds.; Pergamon: Oxford, 1982; Vol. 2, pp 89−179.
(74) Montgomery, C. D. *J. Chem. Educ.* **2001**, *78*, 844 and references therein.
(75) Joachim, J.; Gimzewski, J. K. *Struct. Bonding* **2001**, *99*, 1.
(76) Reif, F. *Fundamentals of Statistical and Thermal Physics*; McGraw-Hill: New York, 1965; p 370.
(77) Purcell, E. M. *Am. J. Phys.* **1977**, *45*, 3.
(78) Astumian, R. D.; Hanggi, P. *Phys. Today* **2002**, *55*, 33.
(79) Coffey, W. T.; Kalmykov, Y. P.; Titov, S. V. *Phys. Rev. E* **2002**, *65*, 032102.
(80) Coffey, W. T.; Kalmykov, Y. P.; Titov, S. V. *Phys. Rev. E* **2003**, *67*, 0621115.
(81) de Jonge, J. J.; Ratner, M. A.; de Leeuw, S. W.; Simonis, R. O. *J. Phys. Chem. B* **2004**, *108*, 2666.
(82) de Leeuw, S. W.; Solvaeson, D.; Ratner, M. A.; Michl, J. *J. Phys. Chem. B* **1998**, *102*, 3876.
(83) Sim, E.; Ratner, M. A.; de Leeuw, S. W. *J. Phys. Chem. B* **1999**, *103*, 8663.
(84) Dominguez, Z.; Dang, H.; Strouse, M. J.; Garcia-Garibay, M. A. *J. Am. Chem. Soc.* **2002**, *124*, 7719.
(85) Godinez, C. E.; Zepeda, G.; Garcia-Garibay, M. A. *J. Am. Chem. Soc.* **2002**, *124*, 4701.
(86) Karczmarke, J.; Wright, J.; Corkum, P.; Ivanov, M. *Phys. Rev. Lett.* **1999**, *82*, 3420.
(87) Lee, J. W.; Samal, S.; Selvapalam, N.; Kim, H.-J.; Kim, K. *Acc. Chem. Res.* **2003**, *36*, 621.
(88) Kim, K. *Chem. Soc. Rev.* **2002**, *31*, 96.
(89) Rogalsky, O.; Voderwisch, P.; Hüller, A.; Hautecler, S. *J. Chem. Phys.* **2002**, *116*, 1063.
(90) Reif, F. *Fundamentals of Statistical and Thermal Physics*; McGraw-Hill: New York, 1965; p 563.
(91) Vacek, J.; Michl, J. *Proc. Natl. Acad. Sci.* **2001**, *98*, 5481.
(92) Horinek, D.; Michl, J. *J. Am. Chem. Soc.* **2003**, *125*, 11900.
(93) Debye, P. *Polar Molecules*; Chemical Catalog Company: New York, 1929; p 85.
(94) Landau, L. D.; Lifshitz, E. M. *Fluid Mechanics*; Pergamon Press: Oxford, 1959.
(95) Williams, A. M.; Jiang, Y.; Ben-Amotz, D. *Chem. Phys.* **1994**, *180*, 119.
(96) Horng, M.-L.; Gardecki, J. A.; Maroncelli, M. *J. Phys. Chem. A* **1997**, *101*, 1030.
(97) Halle, B.; Davidovic, M. *Proc. Natl. Acad. Sci. U.S.A.* **2003**, *100*, 12135.
(98) Kubo, R. *Rep. Prog. Phys. Part 1* **1966**, *29*, 255.
(99) The specific fluctuation dissipation theorem for rotational Brownian motion is found in: Zwanzig, R. *Nonequilibrium Statistical Mechanics*; Oxford: Oxford, 2001; p 13.
(100) Callen, H. B.; Welton, T. A. *Phys. Rev.* **1951**, *83*, 34.
(101) Callen, H. B.; Greene, R. F. *Phys. Rev.* **1952**, *86*, 702.
(102) The discussion follows: (a) Zwanzig, R. *Nonequilibrium Statistical Mechanics*; Oxford: Oxford, 2001; p 3. and (b) Reif, F. *Fundamentals of Statistical and Thermal Physics*; McGraw-Hill: New York, 1965; p 567.
(103) See, for instance: Reif, F. *Fundamentals of Statistical and Thermal Physics*; McGraw-Hill: New York, 1965; p 249.
(104) Zwanzig, R. *Nonequilibrium Statistical Mechanics*; Oxford University Press: Oxford, 2001; p 5.
(105) Allen, H. C.; Cross, P. C. *Molecular Vib-Rotors; The Theory and Interpretation of High-Resolution Infra-Red Spectra*; Wiley: New York, 1963; p 77.
(106) For a discussion of torsional entropy as a function of bond type, see: Mammen, M.; Shakhnovich, E. I.; Whitesides, G. M. *J. Org. Chem.* **1998**, *63*, 3168.
(107) Saebø, S.; Almlöf, J.; Boggs, J. E.; Stark, J. G. *THEOCHEM* **1989**, *200*, 361.
(108) Sipachev, V. A.; Khaikin, L. S.; Grikina, O. E.; Nikitin, V. S.; Trætteberg, M. *J. Mol. Struct.* **2000**, *523*, 1.
(109) Jackson, J. D. *Classical Electrodynamics*; Wiley: New York, 1962; p 143.
(110) For a discussion of dipole−dipole interactions in a quantum rotor system, see: Shima, H.; Nakayama, T. *Phys. Rev. B* **2004**, *69*, 035202.
(111) For a recent review, see: Hochli, U. T.; Knorr, K.; Loidl, A. *Adv. Phys.* **2002**, *51*, 589.
(112) Special issue on Ratchets and Brownian Motors: Basics, Experiments, and Applications: *Appl. Phys. A* **2003**, *75*, 167.
(113) Reimann, P. *Phys. Rep.* **2002**, *361*, 57.
(114) Zheng, X.; Mulcahy, M.-E.; Horinek, D.; Galeotti, F.; Magnera, T. F.; Michl, J. *J. Am. Chem. Soc.* **2004**, *126*, 4540.
(115) Horinek, D.; Michl, J. Unpublished results.
(116) Baranova, N. B.; Zel'dovich, B. Y. *Chem. Phys. Lett.* **1978**, *57*, 435.
(117) Mischel, M.; Voss, A.; Pohl, H. A. *J. Biol. Phys.* **1982**, *10*, 223.
(118) Villeneuv, D. M.; Aseyev, S. A.; Dietrich, P.; Spanner, M.; Ivanov, M. Y.; Corkum, P. B. *Phys. Rev. Lett.* **2000**, *85*, 542.
(119) Hoki, K.; Yamaki, M.; Koseki, S.; Fujimura, Y. *J. Chem. Phys.* **2003**, *119*, 12393.
(120) Hoki, K.; Yamaki, M.; Koseki, S.; Fujimura, Y. *J. Chem. Phys.* **2003**, *118*, 497.
(121) Fujimura, Y.; Gonzalez, L.; Kroner, D.; Manz, J.; Mehdaoui, I.; Schmidt, B. *Chem. Phys. Lett.* **2004**, *386*, 248.
(122) Koumura, N.; Zijlstra, R. W. J.; van Delden, R. A.; Harada, N.; Feringa, B. L. *Nature* **1999**, *401*, 152.
(123) Vacek, J.; Michl, J. *New J. Chem.* **1997**, *21*, 1259.
(124) The exception is thermal ratchets discussed in section 3.2.3.3.
(125) Reif, F. *Fundamentals of Statistical and Thermal Physics*; McGraw-Hill: New York, 1965; p 566.
(126) Landauer, R.; Swanson, J. A. *Phys. Rev.* **1961**, *121*, 1668.
(127) Kramers, H. A. *Physica* **1940**, *7*, 284.
(128) Kramers found that, for a potential barrier with a smooth maximum, the attempt frequency was well approximated by the librational frequency for any viscosity. However, he also discusses a wide variety of situations where this approximation may need to be altered.
(129) This result can be obtained from eq 20.
(130) McCrum, N. G.; Read, B. E.; Williams, G. *Anelastic and Dielectric Effects in Polymeric Solids*; Dover: New York, 1967; p 12.

(131) McCrum, N. G.; Read, B. E.; Williams, G. *Anelastic and Dielectric Effects in Polymeric Solids*; Dover: New York, 1967; p 16.
(132) Daniel, V. V. *Dielectric Relaxation*; Academic: London, 1967; p 24.
(133) In practice, the values of s in this case can be significant compared to kT (a few kcal mol^{-1}) and this effect can be observed in the relaxation rate as shown in eq 36.
(134) Daniel, V. V. *Dielectric Relaxation*; Academic: London, 1967; p 23.
(135) Jackson, J. D. *Classical Electrodynamics*; Wiley: New York, 1962; p 144.
(136) The numerator of this equation can be interpreted as the sum of the rates, by all possible paths, into well i. For instance, for $i = 1$, the numerator is $\Gamma_{21}\Gamma_{31} + \Gamma_{32}\Gamma_{21} + \Gamma_{23}\Gamma_{31}$. The denominator then is the compilation of such sums for all wells.
(137) Effects from the modification of the barrier energy due to the applied field are required to cancel in most situations. In equilibrium, the populations in each well will be consistent with Boltzmann statistics, which depend on the relative well energies only. This is reflected by the consistency of eqs 44 and 45, which utilize the Boltzmann factor, with the master equation approach derived from rates of hopping into and out of the wells.
(138) Jackson J. D. *Classical Electrodynamics*; Wiley: New York, 1962; p 157.
(139) See, for instance, refs 112 and 113.
(140) Kelly, T. R.; De Silva, H.; Silva, R. A. *Nature* **1999**, *401*, 150.
(141) Horansky, R. D.; Clarke, L. I.; Price, J. C.; Khuong, T.-A. V.; Jarowski, P. D.; Garcia-Garibay, M. A. Submitted for publication.
(142) Rozenbaum, V. M. *Phys. Rev. B* **1996**, *53*, 6240.
(143) Troisi, A.; Ratner, M. A. *Nano Lett.* **2004**, *4*, 591.
(144) Feringa, B. L.; van Delden, R. A.; ter Wiel, M. K. J. In *Molecular Switches*; Feringa, B. L., Ed.; Wiley-VCH: Weinheim, 2001; pp 123−163.
(145) Ikeda, M.; Takeuchi, M.; Shinkai, S.; Tani, F.; Naruta, Y.; Sakamoto, S.; Yamaguchi, K. *Chem.—Eur. J.* **2002**, *8*, 5542.
(146) See, for instance, refs 148, 391, and 417.
(147) Rozenbaum, V. M.; Ogenko, V. M.; Chuiko, A. A. *Sov. Phys. Usp.* **1991**, *34*, 883.
(148) Iwamura, H.; Mislow, K. *Acc. Chem. Res.* **1988**, *21*, 175.
(149) Lindner, A. B.; Grynszpan, F.; Biali, *J. Org. Chem.* **1993**, *58*, 6662.
(150) Coluccini, C.; Grilli, S.; Lunazzi, L.; Mazzanti, A. *J. Org. Chem.* **2003**, *68*, 7266.
(151) For an ordered system with a significant torsional barrier, the net orientation, which depends on the relative energy of the wells in the torsional potential, could be influenced by electrostatic interactions. The dynamics of such a system would still be dominated by thermally activated hopping, and the rotor would fall into the hindered rotor section under our classification.
(152) Rozenbaum, V. M.; Ogenko, V. M. *Sov. Phys. Solid State* **1984**, *26*, 877.
(153) Belobrov, P. I.; Gekht, R. S.; Ignatchenko, V. A. *Sov. Phys. JETP* **1983**, *57*, 636.
(154) Brankov, J. G.; Danchev, D. M. *Physica A* **1987**, *144*, 128.
(155) Rozenbaum, V. M. *Sov. Phys. JETP* **1991**, *72*, 1028.
(156) Rozenbaum, V. M. *Phys. Rev. B* **1995**, *51*, 1290.
(157) Würger, A. *Phys. Rev. Lett.* **2002**, *88*, 063002.
(158) Bates, A. R.; Stevens, K. W. H. *J. Phys. C* **1969**, *2*, 1573.
(159) Binsch, G. *Top. Stereochem.* **1968**, *3*, 97.
(160) Kessler, H. *Angew. Chem., Int. Ed. Engl.* **1970**, *9*, 219.
(161) *Dynamic Nuclear Magnetic Resonance Spectroscopy*; Jackman, L. M., Cotton, F. A., Eds.; Academic Press: New York, 1975.
(162) Kaplan, J. I.; Fraenkel, G. *NMR of Chemically Exchanging Systems*; Academic Press: New York, 1980.
(163) Lambert, J. B.; Nienhuis, R. J.; Keepers, J. W. *Angew. Chem., Int. Ed. Engl.* **1981**, *20*, 487.
(164) Sandström, J. *Dynamic NMR Spectroscopy*; Academic Press: New York, 1982.
(165) Ōki, M. *Applications of Dynamic NMR Spectroscopy to Organic Molecules*; Methods in Stereochemical Analysis Volume 4; VCH: Weinheim, 1985.
(166) Ōki, M. *The Chemistry of Rotational Isomers*; Springer-Verlag: Berlin, 1993.
(167) Pons, M.; Millet, O. *Prog. Nucl. Magn. Reson. Spectrosc.* **2001**, *38*, 267.
(168) Ernst, R. R.; Bodenhausen, G.; Wokaun, A. *Principles of Nuclear Magnetic Resonance in One and Two Dimensions*; Oxford Science Publications: Oxford, 1990.
(169) Perrin, C. L.; Dwyer, T. *Chem. Rev.* **1990**, *90*, 935.
(170) Neuhaus, D.; Williamson, M. P. *The Nuclear Overhauser Effect in Structural and Conformational Analysis*; VCH: New York, 1989.
(171) Spiess, H. W. *Colloid Polym. Sci.* **1983**, *261*, 193.
(172) Spiess, H. W. *Adv. Polym. Sci.* **1985**, *66*, 23.
(173) Böhmer, R.; Diezemann, G.; Hinze, G.; Rössler, E. *Prog. Nucl. Magn. Reson. Spectrosc.* **2001**, *39*, 191.
(174) Gordy, W.; Smith, W. V.; Trambarulo, R. F. *Microwave Spectroscopy*; Wiley: New York, 1953.
(175) Strandberg, M. W. P. *Microwave Spectroscopy*; Wiley: New York, 1954.
(176) Townes, C. H.; Schawlow, A. L. *Microwave Spectroscopy*; McGraw-Hill: New York, 1955.
(177) Bryce, D. L.; Wasylishen, R. E. *Acc. Chem. Res.* **2003**, *36*, 327.
(178) Smith, A. L. *Applied Infrared Spectroscopy: Fundamentals, Techniques, and Analytical Problem-Solving*; Wiley: New York, 1979.
(179) Griffiths, P. R.; de Haseth, J. A. *Fourier Transform Infrared Spectroscopy*; Wiley: New York, 1986.
(180) Günzler, H.; Gremlich, H.-U. (trans. Blümich, M.-J.) *IR Spectroscopy: An Introduction*; Wiley: VCH: 2002.
(181) *Fourier Transform Raman Spectrosopy*; Chase, D. B., Rabolt, J. F., Eds.; Academic Press: San Diego, CA, 1994.
(182) Ferraro, J. R.; Nakamoto, K.; Brown, C. W. *Introductory Raman Spectroscopy*, 2nd ed.; Academic Press: Boston, MA, 2003.
(183) *Infrared and Raman Spectroscopy: Methods and Applications*; Schrader, B., Ed.; Wiley-VCH: Weinheim, 1995.
(184) Suëtaka, W.; Yates, J. T. *Surface Infrared and Raman Spectroscopy: Methods and Applications*; Plenum Press: New York, 1995.
(185) *Circular Dichroism: Principles and Applications*, 2nd ed.; Berova, N., Nakanishi, K., Woody, R. W., Eds.; Wiley-VCH: New York, 2000.
(186) Lightner, D. A.; Gurst, J. E. *Organic Conformational Analysis and Stereochemistry from Circular Dichroism Spectroscopy*; Wiley-VCH: New York, 2000.
(187) An overview of dielectric spectroscopy can be found in: (a) Daniel, V. V. *Dielectric Relaxation*; Academic: London, 1967. or (b) McCrum, N. G.; Read, B. E.; Williams, G. *Anelastic and Dielectric Effects in Polymeric Solids*; Dover: New York, 1967.
(188) See ref 141 or 981.
(189) McCrum, N. G.; Read, B. E.; Williams, G. *Anelastic and Dielectric Effects in Polymeric Solids*; Dover: New York, 1967; p 4.
(190) Frenkel, D., Smit, B., Eds. *Understanding Molecular Simulations*; Academic Press: San Diego, CA, 2002.
(191) Tuzun, R. E.; Noid, D. W.; Sumpter, B. G. *Nanotechnology* **1995**, *6*, 64.
(192) Christie, G. H.; Kenner, J. *J. Chem. Soc.* **1922**, *121*, 614.
(193) Adams, R.; Yuan, H. C. *Chem. Rev.* **1933**, *12*, 261.
(194) Eliel, E. L.; Wilen, S. H.; Doyle, M. P. *Basic Organic Stereochemistry*; Wiley: New York, 2001; Chapter 13.
(195) Eliel, E. L.; Wilen, S. H.; Mander, L. N. *Stereochemistry of Organic Compounds*; Wiley: New York, 1994; Chapter 14.
(196) Ōki, M. *Top. Stereochem.* **1983**, *14*, 1.
(197) Berg, U.; Liljefors, T.; Roussel, C.; Sandström, J. *Acc. Chem. Res.* **1985**, *18*, 80.
(198) Berg, U.; Sandström, J. *Adv. Phys. Org. Chem.* **1989**, *25*, 1.
(199) Mislow, K.; Gust, D.; Finocchiaro, P.; Boettcher, R. J. *Fortschr. Chem. Forsch.* **1974**, *47*, 1.
(200) Mislow, K. *Acc. Chem. Res.* **1976**, *9*, 26 and references therein.
(201) Mislow, K. *Chemtracts: Org. Chem.* **1989**, *2*, 151.
(202) Hrovat, D. A.; Borden, W. T.; Eaton, P. E.; Kahr, B. *J. Am. Chem. Soc.* **2001**, *123*, 1289.
(203) Oberg, E.; Jones, F. D.; Horton, H. L.; Ryffell, H. H. *Machinery's Handbook: A Reference Book for the Mechanical Engineer, Designer, Manufacturing Engineer, Draftsman, Toolmaker, and Machinist*, 26th ed.; Industrial Press: New York, 2000.
(204) Ng, J. M. K.; Fuerstman, M. J.; Grzybowski, B. A.; Stone, H. A.; Whitesides, G. M. *J. Am. Chem. Soc.* **2003**, *125*, 7948 and references therein.
(205) Bell and Robinson. *J. Chem. Soc.* **1927**, 2234.
(206) Kuhn and Albrecht. *Annalen* **1927**, *455*, 272.
(207) Kuhn and Albrecht. *Annalen* **1927**, *458*, 221.
(208) Yuan, H. C.; Adams, R. *J. Am. Chem. Soc.* **1932**, *54*, 4434.
(209) Mills, W. H.; Elliott, K. A. C. *J. Chem. Soc.* **1928**, 1291.
(210) Mills, W. H.; Breckenridge, J. G. *J. Chem. Soc.* **1932**, 2209.
(211) Mills, W. H.; Kelham, R. M. *J. Chem. Soc.* **1937**, 274.
(212) Adams, R.; Dankert, L. J. *J. Am. Chem. Soc.* **1940**, *62*, 2191.
(213) Adams, R.; Dunbar, J. E. *J. Am. Chem. Soc.* **1958**, *80*, 3649.
(214) Mills, W. H.; Dazeley, G. H. *J. Chem. Soc.* **1939**, 460.
(215) Adams, R.; Miller, M. W. *J. Am. Chem. Soc.* **1940**, *62*, 53.
(216) Adams, R.; Anderson, A. W.; Miller, M. W. *J. Am. Chem. Soc.* **1941**, *63*, 1589.
(217) Wittig, G.; Oppermann, A.; Faber, K. *J. Prakt. Chem.* **1941**, *158*, 61.
(218) Adams, R.; Mecorney, J. W. *J. Am. Chem. Soc.* **1945**, *67*, 798.
(219) Kuhn, R. In *Stereochemie*; Freudenberg, H., Ed.; Franz Deutike: Leipzig-Wien, 1933; pp 803−824.
(220) Lewis, G. N.; Magel, T. T.; Lipkin, D. *J. Am. Chem. Soc.* **1942**, *64*, 1774.
(221) Newman, M. S.; Deno, N. C. *J. Am. Chem. Soc.* **1951**, *73*, 3644.
(222) Deno, N. C.; Jaruzelski, J. J.; Schriesheim, A. *J. Org. Chem.* **1953**, *18*, 155.
(223) Colter, A. K.; Schuster, I. I.; Kurland, R. J. *J. Am. Chem. Soc.* **1965**, *87*, 2278.
(224) Kurland, R. J.; Schuster, I. I.; Colter, A. K. *J. Am. Chem. Soc.* **1965**, *87*, 2279.

(225) Schuster, I. I.; Colter, A. K.; Kurland, R. J. *J. Am. Chem. Soc.* **1968**, *90*, 4679.
(226) Sundaralingam, M.; Jensen, L. H. *J. Am. Chem. Soc.* **1966**, *88*, 198.
(227) Akkerman, O. S. *Recl. Trav. Chim. Pays-Bas* **1967**, *86*, 755.
(228) Kwart, H.; Alekman, S. *J. Am. Chem. Soc.* **1968**, *90*, 4482.
(229) van der Linde, R.; Dornseiffen, J. W.; Veenland, J. U.; de Boer, Th. J. *Tetrahedron Lett.* **1968**, 525.
(230) Adams, R.; Campbell, J. *J. Am. Chem. Soc.* **1950**, *72*, 153.
(231) Breslow, R.; Kaplan, L.; LaFollette, D. *J. Am. Chem. Soc.* **1968**, *90*, 4056.
(232) Rakshys, J. W.; McKinley, S. V.; Freedman, H. H. *J. Am. Chem. Soc.* **1970**, *92*, 3518.
(233) Rakshys, J. W.; McKinley, S. V.; Freedman, H. H. *J. Am. Chem. Soc.* **1971**, *93*, 6522.
(234) Kessler, H.; Rieker, A.; Rundel, W. *Chem. Commun*. **1968**, 475.
(235) Bergman, J. J.; Chandler, W. D. *Can. J. Chem.* **1972**, *50*, 353.
(236) Kessler, H.; Rieker, A.; Rundel, W. *Chem. Commun*. **1968**, 475.
(237) Nelander, B.; Sunner, S. *J. Am. Chem. Soc.* **1972**, *94*, 3576.
(238) Lauer, D.; Staab, H. A. *Chem. Ber.* **1969**, *102*, 1631.
(239) Sabacky, M. J.; Johnson, S. M.; Martin, J. C.; Paul, I. C. *J. Am. Chem. Soc.* **1969**, *91*, 7542.
(240) Riecker, A.; Kessler, H. *Tetrahedron Lett.* **1969**, 1227.
(241) Akkerman, O. S.; Coops, J. *Recl. Trav. Chim. Pays-Bas* **1970**, *89*, 673.
(242) Brydes, S.; Harrington, L. E.; McGlinchey, M. J. *Coord. Chem. Rev.* **2002**, *233*−*234*, 75.
(243) Thematic issue on Atropisomerism: *Tetrahedron* **2004**, *60*, 4325−4558.
(244) Kemp, J. D.; Pitzer, K. S. *J. Chem. Phys.* **1936**, *4*, 749.
(245) Kemp, J. D.; Pitzer, K. S. *J. Am. Chem. Soc.* **1937**, *59*, 276.
(246) Kohlrausch, K. W. *Z. Phys. Chem.* **1932**, *18B*, 61.
(247) Mizushima, S. *Structure of Molecules and Internal Rotation*; Academic Press: New York, 1954.
(248) Mizushima, S.; Morino, Y.; Higashi, K. *Sci. Pap. Inst. Phys. Res.* **1934**, *25*, 159.
(249) It is interesting to note that the origin of the rotational barrier in ethane is still being debated. For two opposing viewpoints, see: (a) Bickelhaupt, F. M.; Baerends, E. J. *Angew. Chem., Int. Ed.* **2003**, *42*, 4183. and (b) Weinhold, F. *Angew. Chem., Int. Ed.* **2003**, *42*, 4188.
(250) Gutowsky, H. S.; Holm, C. H. *J. Chem. Phys.* **1956**, *25*, 1228.
(251) Gutowsky, H. S. In *Dynamic Nuclear Resonance Spectroscopy*; Jackman, L. M., Cotton, F. A., Eds.; Academic Press: New York, 1975; pp 1−21.
(252) Uncuta, C.; Păun, I.; Deleanu, C.; Plăveti, M.; Balaban, A. T.; Roussel, C. *New J. Chem.* **1997**, *21*, 1055.
(253) Newman, M. S.; LeBlanc, J. R.; Karnes, H. A.; Axelrod, G. *J. Am. Chem. Soc.* **1964**, *86*, 868.
(254) Arnett, E. M.; Bollinger, J. M. *J. Am. Chem. Soc.* **1964**, *86*, 4729.
(255) Dix, D. T.; Fraenkel, G.; Karnes, H. A.; Newman, M. S. *Tetrahedron Lett.* **1966**, 517.
(256) Mannschreck, A.; Ernst, L. *Chem. Ber.* **1971**, *104*, 228.
(257) Nilsson, B.; Martinson, P.; Olsson, K.; Carter, R. E. *J. Am. Chem. Soc.* **1973**, *95*, 5615.
(258) Nilsson, B.; Martinson, P.; Olsson, K.; Carter, R. E. *J. Am. Chem. Soc.* **1974**, *96*, 3190.
(259) Dahlberg, E.; Nilsson, B.; Olsson, K.; Martinson, P. *Acta Chem. Scand., Ser. B* **1975**, *29*, 300.
(260) Carter, R. E.; Nilsson, B.; Olsson, K. *J. Am. Chem. Soc.* **1975**, *97*, 6155.
(261) Olah, G. A.; Comisarow, M. B.; Namanworth, E.; Ramsey, B. *J. Am. Chem. Soc.* **1967**, *89*, 5259.
(262) Sandel, V. R.; McKinley, S. V.; Freedman, H. H. *J. Am. Chem. Soc.* **1968**, *90*, 495.
(263) Brownstein, S.; Worsfold, D. J. *Can. J. Chem.* **1972**, *50*, 1246.
(264) Fraenkel, G.; Russell, J. G.; Chen, Y.-H. *J. Am. Chem. Soc.* **1973**, *95*, 3208.
(265) Cupas, C. A.; Bollinger, J. M.; Haslanger, M. *J. Am. Chem. Soc.* **1968**, *90*, 5502.
(266) Mannschreck, A.; Ernst, L. *Chem. Ber.* **1971**, *104*, 228.
(267) Peeling, J.; Rowbotham, J. B.; Ernst, L.; Schaefer, T. *Can. J. Chem.* **1974**, *52*, 2414.
(268) Peeling, J.; Ernst, L.; Schaefer, T. *Can. J. Chem.* **1974**, *52*, 849.
(269) Mannschreck, A.; Muensch, H. *Tetrahedron Lett.* **1968**, 3227.
(270) Nelander, B.; Sunner, S. *J. Am. Chem. Soc.* **1972**, *94*, 3576.
(271) Newsereff, G. P.; Sternhell, S. *Tetrahedron Lett.* **1967**, 2539.
(272) Janzen, E. G.; Gerlock, J. L. *J. Am. Chem. Soc.* **1967**, *89*, 4902.
(273) Hounshell, W. D.; Iroff, L. D.; Iverson, D. J.; Wroczynski, R. J.; Mislow, K. *Isr. J. Chem.* **1980**, *20*, 65.
(274) Förster, H.; Vögtle, F. *Angew. Chem., Int. Ed. Engl.* **1977**, *16*, 429.
(275) Hopff, H. *Chimia* **1964**, *18*, 140.
(276) Hopff, H.; Gati, A. *Helv. Chim. Acta* **1965**, *48*, 140.
(277) Siegel, J.; Gutiérrez, A.; Schweiser, W. B.; Ermer, O.; Mislow, K. *J. Am. Chem. Soc.* **1986**, *108*, 1569.
(278) Mislow, K. *Chimia* **1986**, *40*, 395.
(279) Siegel, J.; Gutiérrez, A.; Schweiser, W. B.; Ermer, O.; Mislow, K. *J. Am. Chem. Soc.* **1986**, *108*, 1569.
(280) Schuster, I. I.; Weissensteiner, W.; Mislow, K. *J. Am. Chem. Soc.* **1986**, *108*, 6661.
(281) Weissensteiner, W.; Schuster, I. I.; Blount, J. F.; Mislow, K. *J. Am. Chem. Soc.* **1986**, *108*, 6664.
(282) Singh, M. D.; Siegel, J.; Biali, S. E.; Mislow, K. *J. Am. Chem. Soc.* **1987**, *109*, 3397.
(283) Biali, S. E.; Mislow, K. *J. Org. Chem.* **1988**, *53*, 1318.
(284) Chance, J. M.; Kahr, B.; Buda, A. B.; Toscano, J. P.; Mislow, K. *J. Org. Chem.* **1988**, *53*, 3226.
(285) Iverson, D. J.; Hunter, G.; Blount, J. F.; Damewood, J. R., Jr.; Mislow, K. *J. Am. Chem. Soc.* **1981**, *103*, 6073.
(286) Hunter, G.; Weakley, T. J. R.; Weissensteiner, W. *J. Chem. Soc., Perkin Trans. 2* **1987**, 1633.
(287) Marsau, P. *Acta Crystallogr.* **1965**, *18*, 851.
(288) Hunter, G.; Iverson, D. J.; Mislow, K.; Blount, J. F. *J. Am. Chem. Soc.* **1980**, *102*, 5942.
(289) McGlinchey, M. J. *Can. J. Chem.* **2001**, *79*, 1295 and references therein.
(290) McGlinchey, M. J. *Adv. Organomet. Chem.* **1992**, *34*, 285.
(291) Downton, P. A.; Mailvaganam, B.; Frampton, C. S.; Sayer, B. G.; McGlinchey, M. J. *J. Am. Chem. Soc.* **1990**, *112*, 27.
(292) Mailvaganam, B.; Frampton, C. S.; Sayer, B. G.; Top, S.; McGlinchey, M. J. *J. Am. Chem. Soc.* **1991**, *113*, 1177.
(293) Kilway, K. V.; Siegel, J. S. *J. Am. Chem. Soc.* **1991**, *113*, 2332.
(294) Kilway, K. V.; Siegel, J. S. *J. Am. Chem. Soc.* **1992**, *114*, 255.
(295) Li, L.; Decken, A.; Sayer, B. G.; McGlinchey, M. J.; Brégaint, P.; Thépot, J.-Y.; Toupet, L.; Hamon, J.-R.; Lapinte, C. *Organometallics* **1994**, *13*, 682.
(296) Mailvaganam, B.; Sayer, B. G.; McGlinchey, M. J. *J. Organomet. Chem.* **1990**, *395*, 117.
(297) Zuaretz, N.; Golan, O.; Biali, S. E. *J. Org. Chem.* **1991**, *56*, 2444.
(298) Marks, V.; Nahmany, M.; Gottlieb, H. E.; Biali, S. E. *J. Org. Chem.* **2002**, *67*, 7898.
(299) Simaan, S.; Siegel, J. S.; Biali, S. E. *J. Org. Chem.* **2003**, *68*, 3699.
(300) Metzger, J. V.; Chanon, M. C.; Roussel, C. M. *Rev. Heteroatom Chem.* **1997**, *16*, 1.
(301) Bianchini, R.; Chiappe, C.; Lenoir, D.; Meyer, B. *Gazz. Chim. Ital.* **1995**, *125*, 453.
(302) Columbus, I.; Biali, S. E. *J. Org. Chem.* **1994**, *59*, 3402.
(303) Columbus, I.; Biali, S. E. *J. Org. Chem.* **1993**, *58*, 7029.
(304) Bock, H.; Nagel, N. *Z. Naturforsch.* **1998**, *53b*, 792.
(305) Bock, H.; Nagel, N. *Z. Naturforsch.* **1998**, *53b*, 805.
(306) Hopf, H.; Mlynek, C.; Klein, D.; Traetteberg, M.; Bakken, P. *Eur. J. Org. Chem.* **2001**, 1385.
(307) Anderson, J. E.; de Meijere, A.; Kozhushkov, S. I.; Lunazzi, L.; Mazzanti, A. *J. Org. Chem.* **2003**, *68*, 8494.
(308) Kiefl, C. *Eur. J. Org. Chem.* **2000**, 3279.
(309) Wimmer, R.; Müller, N. *J. Magn. Reson.* **1997**, *129*, 1.
(310) Hopf, H.; Hänel, R.; Trætteberg, M.; Bakken, P. *Eur. J. Org. Chem.* **1998**, *467*, 7.
(311) Laerdahl, J. K.; Fægri, K.; Rømming, C.; Swang, O.; Midtgård, T.; Schöffel, K. *J. Mol. Struct.* **1998**, *445*, 89.
(312) Neumann, M. A.; Plazanet, M.; Johnson, M. R.; Trommsdorff, H. P. *J. Chem. Phys.* **2004**, *120*, 885 and references therein.
(313) Pophristic, V.; Goodman, L. *J. Phys. Chem. A* **2003**, *107*, 3538.
(314) Sutherland, I. O.; Ramsay, M. V. J. *Tetrahedron* **1965**, *21*, 3401.
(315) Rebek, J., Jr.; Trend, J. E. *J. Am. Chem. Soc.* **1978**, *100*, 4315.
(316) Rebek, J., Jr.; Trend, J. E.; Wattley, R. V.; Chakravorti, S. *J. Am. Chem. Soc.* **1979**, *101*, 4333.
(317) Rebek, J., Jr.; Costello, T.; Wattley, R. V. *Tetrahedron Lett.* **1980**, *21*, 2379.
(318) Rebek, J., Jr.; Wattley, R. V. *J. Heterocycl. Chem.* **1980**, *17*, 749.
(319) Bott, G.; Field, L. D.; Sternhell, S. *J. Am. Chem. Soc.* **1980**, *102*, 5618.
(320) Finocchiaro, P. *Gazz. Chim. Ital.* **1975**, *105*, 149.
(321) Meurer, K. P.; Vögtle, F. *Top. Curr. Chem.* **1985**, *127*, 1.
(322) Rappoport, Z.; Biali, S. E. *Acc. Chem. Res.* **1997**, *30*, 307.
(323) Allen, M.; Moir, R. Y. *Can. J. Chem.* **1959**, *37*, 1799.
(324) Montaudo, G.; Finocchiaro, P.; Trivellone, E.; Bottino, F.; Maravigna, P. *Tetrahedron* **1971**, *27*, 2125.
(325) Fuji, K.; Oka, T.; Kawabata, T.; Kinoshita, T. *Tetrahedron Lett.* **1998**, *39*, 1373.
(326) Casarini, D.; Grilli, S.; Lunazzi, L.; Mazzanti, A. *J. Org. Chem.* **2001**, *66*, 2757.
(327) Grilli, S.; Lunazzi, L.; Mazzanti, A. *J. Org. Chem.* **2001**, *66*, 5853.
(328) Casarini, D.; Lunazzi, L.; Verbeek, R. *Tetrahedron* **1996**, *52*, 2471.
(329) Grilli, S.; Lunazzi, L.; Mazzanti, A.; Casarini, D.; Fermoni, C. *J. Org. Chem.* **2001**, *66*, 488.
(330) Grilli, S.; Lunazzi, L.; Mazzanti, A.; Mazzanti, A. *J. Org. Chem.* **2001**, *66*, 748.
(331) Gust, D.; Mislow, K. *J. Am. Chem. Soc.* **1973**, *95*, 1535.
(332) Gust, D.; Mislow, K. *J. Am. Chem. Soc.* **1973**, *95*, 7019.
(333) Gust, D.; Mislow, K. *J. Am. Chem. Soc.* **1973**, *95*, 7029.
(334) Montaudo, G.; Caccamese, S.; Finocchiaro, P.; Bottino, F. *Tetrahedron Lett.* **1970**, 887.
(335) Montaudo, G.; Caccamese, S.; Finocchiaro, P. *J. Am. Chem. Soc.* **1971**, *93*, 4202.

(336) Montaudo, G.; Finocchiaro, P.; Caccamese, S.; Bottino, F. *J. Am. Chem. Soc.* **1971**, *93*, 4208.
(337) Montaudo, G.; Finocchiaro, P.; Maravigna, P. *J. Am. Chem. Soc.* **1971**, *93*, 4214.
(338) Weissensteiner, W.; Scharf, J.; Schlögl, K. *J. Org. Chem.* **1987**, *52*, 1210.
(339) Weissensteiner, W. *Monatsh. Chem.* **1992**, *123*, 1135.
(340) Strekowski, L.; Lee, H.; Lin, S.-Y.; Czarny, A.; Van Derveer, D. *J. Org. Chem.* **2000**, *65*, 7703.
(341) Finocchiaro, P.; Gust, D.; Mislow, K. *J. Am. Chem. Soc.* **1974**, *96*, 2165.
(342) Finocchiaro, P.; Gust, D.; Mislow, K. *J. Am. Chem. Soc.* **1974**, *96*, 2176.
(343) Finocchiaro, P.; Gust, D.; Mislow, K. *J. Am. Chem. Soc.* **1974**, *96*, 3198.
(344) Finocchiaro, P.; Gust, D.; Mislow, K. *J. Am. Chem. Soc.* **1974**, *96*, 3205.
(345) Lockhart, J. C.; McDonnell, M. B.; Clegg, W.; Hill, M. N. S. *J. Chem. Soc., Perkin Trans. 2* **1987**, 639.
(346) Foces-Foces, C.; Cano, F. H.; Martínez-Ripoll, M.; Faure, R.; Roussel, C.; Claramunt, R. M.; López, C.; Sanz, D.; Elguero, J. *Tetrahedron: Asymmetry* **1990**, *1*, 65.
(347) Ito, S.; Morita, N.; Asao, T. *Tetrahedron Lett.* **1992**, *33*, 6669.
(348) Hellwinkel, D.; Melan, M.; Egan, W.; Degel, C. R. *Chem. Ber.* **1975**, *108*, 2219.
(349) Glaser, R.; Blount, J. F.; Mislow, K. *J. Am. Chem. Soc.* **1980**, *102*, 2777.
(350) Wille, E. E.; Stephenson, D. S.; Capriel, P.; Binsch, G. *J. Am. Chem. Soc.* **1982**, *104*, 405.
(351) Howell, J. A. S.; Palin, M. G.; Yates, P. C.; McArdle, P.; Cunningham, D.; Goldschmidt, Z.; Gottlieb, H. E.; Herzoni-Langerman, D. *J. Chem. Soc., Perkin Trans. 1* **1992**, 1769.
(352) Howell, J. A. S.; Fey, N.; Lovatt, J. D.; Yates, P. C.; McArdle, P.; Cunningham, D.; Sadeh, E.; Gottlieb, H. E.; Goldschmidt, Z.; Hursthoude, M. B.; Light, M. E. *J. Chem. Soc., Dalton Trans.* **1999**, 3015.
(353) Schlögl, K.; Weissensteiner, W.; Widhalm, M. *J. Org. Chem.* **1982**, *47*, 5025.
(354) Willem, R.; Pepermans, H.; Hallenga, K.; Gielen, M.; Dams, R.; Geise, H. J. *J. Org. Chem.* **1983**, *48*, 1890.
(355) Bonini, B. F.; Grossi, L.; Lunazzi, L.; Macciantelli, D. *J. Org. Chem.* **1986**, *51*, 517.
(356) Rappoport, Z.; Biali, S. E. *Acc. Chem. Res.* **1988**, *21*, 422 and references therein.
(357) Rappoport, Z.; Biali, S. E. *Acc. Chem. Res.* **1997**, *30*, 307 and references therein.
(358) Schmittel, M.; Keller, M.; Burghart, A.; Rappoport, Z.; Langels, A. *J. Chem. Soc., Perkin Trans. 2* **1998**, 869.
(359) Gur, E.; Kaftory, M.; Biali, S. E.; Rappoport, Z. *J. Org. Chem.* **1999**, *64*, 8144.
(360) Willem, R.; Pepermans, H.; Hoogzand, C.; Hallenga, K.; Gielen, M. *J. Am. Chem. Soc.* **1981**, *103*, 2297.
(361) Willem, R.; Jans, A.; Hoogzand, C.; Gielen, M.; Van Binst, G.; Pepermans, H. *J. Am. Chem. Soc.* **1985**, *107*, 28.
(362) Brydges, S.; McGlinchey, M. J. *J. Org. Chem.* **2002**, *67*, 7688.
(363) Gust, D. *J. Am. Chem. Soc.* **1977**, *99*, 6980.
(364) Gust, D.; Patton, A. *J. Am. Chem. Soc.* **1978**, *100*, 8175.
(365) Patton, A.; Dirks, J. W.; Gust, D. *J. Org. Chem.* **1979**, *44*, 4749.
(366) Pepermans, H.; Willem, R.; Gielen, M.; Hoogzand, C. *J. Org. Chem.* **1986**, *51*, 301.
(367) Grilli, S.; Lunazzi, L.; Mazzanti, A.; Pinamonti, M. *J. Org. Chem.* **2002**, *67*, 5733.
(368) Kawada, Y.; Iwamura, H. *Tetrahedron Lett.* **1981**, *22*, 1533.
(369) Furuta, T.; Tanaka, K.; Tsubaki, K.; Fuji, K. *Tetrahedron* **2004**, *60*, 4431.
(370) Haywood-Farmer, J.; Battiste, M. A. *Chem. Ind.* **1971**, 1232.
(371) Bart, J. C. J. *Acta Crystallogr., B* **1968**, *24*, 1277.
(372) Almenningen, A.; Bastiansen, O.; Skancke, P. N. *Acta Chem. Scand.* **1958**, *12*, 1215.
(373) Pepermans, H.; Gielen, M.; Hoogzand, C.; Willem, R. *Bull. Soc. Chim. Belg.* **1983**, *92*, 65.
(374) Mailvaganam, B.; McCarry, B. E.; Sayer, B. G.; Perrier, R. E.; Faggiani, R.; McGlinchey, M. J. *J. Organomet. Chem.* **1987**, *335*, 213.
(375) Mailvaganam, B.; Sayer, B. G.; McGlinchey, M. J. *J. Organomet. Chem.* **1990**, *395*, 177.
(376) Gupta, H. K.; Brydges, S.; McGlinchey, M. J. *Organometallics* **1999**, *18*, 115.
(377) Harrington, L. E.; Britten, J. F.; McGlinchey, M. J. *Can. J. Chem.* **2003**, *81*, 1180.
(378) Harrington, L. E.; Britten, J. F.; Hughes, D. W.; Bain, A. D.; Thépot, J.-Y.; McGlinchey, M. J. *J. Organomet. Chem.* **2002**, *656*, 243.
(379) Knop, O.; Rankin, K.; Cameron, T. S.; Boyd, R. J. *Can. J. Chem.* **2002**, *80*, 1351 and reference therein.
(380) Ōki has reviewed much of his work in this area in refs 165, 166, and 196.
(381) Yamamoto, G.; Ōki, M. *J. Org. Chem.* **1983**, *48*, 1233.
(382) Yamamoto, G. *Pure Appl. Chem.* **1990**, *62*, 569.
(383) Nemoto, T.; Ohashi, Y.; Yamamoto, G. *Acta Crystallogr.* **1996**, *C52*, 716.
(384) Nachbar, R. B.; Hounshell, W. D.; Naman, V. A.; Wennerström, O.; Guenzi, A.; Mislow, K. *J. Org. Chem.* **1983**, *48*, 1227.
(385) Yamamoto, G.; Ōki, M. *Bull. Chem. Soc. Jpn.* **1986**, *59*, 3597.
(386) Yamamoto, G. *Bull. Chem. Soc. Jpn.* **1989**, *62*, 4058.
(387) Houndshell, W. D.; Johnson, C. A.; Guenzi, A.; Cozzi, F.; Mislow, K. *Proc. Natl. Acad. Sci. U.S.A.* **1980**, *77*, 6961.
(388) Cozzi, F.; Guenzi, A.; Johnson, C. A.; Mislow, K. *J. Am. Chem. Soc.* **1981**, *103*, 957.
(389) Kawada, Y.; Iwamura, H. *J. Am. Chem. Soc.* **1981**, *103*, 958.
(390) Kawada, Y.; Iwamura, H. *Tetrahedron Lett.* **1981**, *22*, 1533.
(391) Kawada, Y.; Iwamura, H. *J. Am. Chem. Soc.* **1983**, *105*, 5498.
(392) Chance, J. M.; Geiger, J. H.; Mislow, K. *J. Am. Chem. Soc.* **1989**, *111*, 2326.
(393) Chance, J. M.; Geiger, J. H.; Okamoto, Y.; Aburatani, R.; Mislow, K. *J. Am. Chem. Soc.* **1990**, *112*, 3540.
(394) Yamamoto, G.; Kaneko, M.; Ohkuma, M.; Minoura, M. *Chem. Lett.* **2003**, *32*, 964.
(395) Shvo, Y.; Taylor, E. C.; Mislow, K.; Raban, M. *J. Am. Chem. Soc.* **1967**, *89*, 4910.
(396) Siddall, T. H.; Garner, R. H. *Can. J. Chem.* **1966**, *44*, 2387.
(397) Stewart, W. H.; Siddall, T. H. *Chem. Rev.* **1970**, *70*, 517.
(398) Mannschreck, A. *Tetrahedron Lett.* **1965**, 1341.
(399) Staab, H. A.; Lauer, D. *Tetrahedron Lett.* **1966**, 4593.
(400) Ackerman, J. H.; Laidlaw, G. M.; Snyder, G. A. *Tetrahedron Lett.* **1969**, 3879.
(401) Ackerman, J. H.; Laidlaw, G. M. *Tetrahedron Lett.* **1969**, 4487.
(402) Cuyegkeng, M. A.; Mannschreck, A. *Chem. Ber.* **1987**, *120*, 803.
(403) Azumaya, I.; Yamaguchi, K.; Okamoto, I.; Kagechika, H.; Shudo, K. *J. Am. Chem. Soc.* **1995**, *117*, 9083.
(404) Ahmed, A.; Bragg, R. A.; Clayden, J.; Lai, L. W.; McCarthy, C.; Pink, J. H.; Westlund, N.; Yasin, S. A. *Tetrahedron* **1998**, *54*, 13277.
(405) Clayden, J.; McCarthy, C.; Helliwell, M. *Chem. Commun.* **1999**, 2059.
(406) Bowles, P.; Clayden, J.; Tomkinson, M. *Tetrahedron Lett.* **1995**, *36*, 9219.
(407) Bowles, P.; Clayden, J.; Helliwell, M.; McCarthy, C.; Tomkinson, M.; Westlund, N. *J. Chem. Soc., Perkin Trans. 1* **1997**, 2607.
(408) Clayden, J. *Angew. Chem., Int. Ed. Engl.* **1997**, *36*, 949.
(409) Clayden, J. *Synlett* **1998**, 810.
(410) Clayden, J. *Angew. Chem., Int. Ed. Engl.* **1997**, *36*, 949.
(411) Clayden, J.; Lai, L. W.; Helliwell, M. *Tetrahedron: Asymmetry* **2001**, *12*, 695.
(412) Bowles, P.; Clayden, J.; Helliwell, M.; McCarthy, C.; Tomkinson, M.; Westlund, N. *J. Chem. Soc., Perkin Trans. 1* **1997**, 2607.
(413) Clayden, J.; Pink, J. H.; Yasin, S. A. *Tetrahedron Lett.* **1998**, *39*, 105.
(414) Clayden, J.; Westlund, N.; Wilson, F. X. *Tetrahedron Lett.* **1999**, *40*, 3331.
(415) Clayden, J.; Lai, L. W. *Angew. Chem., Int. Ed.* **1999**, *38*, 2556.
(416) Clayden, J.; Lai, L. W. *Tetrahedron Lett.* **2001**, *42*, 3163.
(417) Clayden, J.; Pink, J. H. *Angew. Chem., Int. Ed.* **1998**, *37*, 1937.
(418) Bragg, R. A.; Clayden, J. *Org. Lett.* **2000**, *2*, 3351.
(419) Johnston, E. R.; Fortt, R.; Barborak, J. C. *Magn. Reson. Chem.* **2000**, *38*, 932.
(420) Bragg, R. A.; Clayden, J.; Morris, G. A.; Pink, J. H. *Chem. Eur. J.* **2002**, *8*, 1279.
(421) Hellwinkel, D.; Lindner, W.; Wilfinger, H. J. *Chem. Ber.* **1974**, *107*, 3989.
(422) Trahanovsky, W. S.; Kowalski, D. J.; Avery, M. J. *J. Am. Chem. Soc.* **1974**, *96*, 1502.
(423) Aylett, B. J.; Taghipour, M. T. *J. Organomet. Chem.* **1983**, *249*, 55.
(424) Harrington, L. E.; Cahill, L. S.; McGlinchey, M. J. *Organometallics* **2004**, *23*, 2884.
(425) Gearing in organometallic metal complexes of phenyl rings was previously discussed in sections 5.1.5 and 5.1.6.
(426) Kimura, T.; Sakurai, T.; Shima, M.; Mukaida, M.; Nomura, T. *Inorg. Chim. Acta* **1983**, *69*, 135.
(427) Howell, J. A. S.; Palin, M. G.; Tirvengadum, M.-C.; Cunningham, D.; McArdle, P.; Goldschmidt, Z.; Gottlieb, H. E. *J. Organomet. Chem.* **1991**, *413*, 269.
(428) Braga, D.; Grepiani, F.; Johnson, B. F. G.; Lewis, J.; Mortinelli, M. *J. Chem. Soc., Dalton Trans.* **1990**, 1847.
(429) Deeming, A. J.; Forth, C. S.; Hogarth, G.; Markham, D.; Prince, J. O.; Steed, J. W. *Chem. Commun.* **2002**, 2230.
(430) Hounshell, W. D.; Iroff, L. D.; Wrocztnski, R. J.; Mislow, K. *J. Am. Chem. Soc.* **1978**, *100*, 5212.
(431) Bock, H.; Meuret, J.; Ruppert, K. *J. Organomet. Chem.* **1993**, *462*, 31.
(432) Frey, J.; Schottland, E.; Rappoport, Z.; Bravo-Zhivotovskii, D.; Nakash, M.; Botoshansky, M.; Kaftory, M.; Apeloig, Y. *J. Chem. Soc., Perkin Trans. 2* **1994**, 2555.
(433) Haquette, P.; Dagorne, S.; Welter, R.; Jaouen, G. *J. Organomet. Chem.* **2003**, *682*, 240.
(434) *The Porphyrin Handbook*; Kadish, K. M., Smith, K. M., Guilard, R., Eds.; Academic Press: New York, 2000; Vols. 1−10.

(435) Volumes 11−20 were published in 2003 and dealt with biological and medical aspects of porphyrins as well as many aspects of phthalocyanine chemistry: *The Porphyrin Handbook*; Kadish, K. M., Smith, K. M., Guilard, R., Eds.; Academic Press: New York, 2003; Vols. 11−20.
(436) Wasielewski, M. R. *Chem. Rev.* **1992**, *92*, 435.
(437) Lukas, A. S.; Wasielewski, M. R. In *Molecular Switches*; Wiley-VCH: Weinheim, 2001; pp 1−35.
(438) Harriman, A.; Sauvage, J.-P. *Chem. Soc. Rev.* **1996**, *25*, 41.
(439) Hayashi, T.; Ogoshi, H. *Chem. Soc. Rev.* **1997**, *26*, 355.
(440) Medforth, C. J.; Haddad, R. E.; Muzzi, C. M.; Dooley, N. R.; Jaquinod, L.; Shyr, D. C.; Nurco, D. J.; Olmstead, M. M.; Smith, K. M.; Ma, J.-G.; Shelnutt, J. A. *Inorg. Chem.* **2003**, *42*, 2227 and references therein.
(441) Medforth, C. J. In *The Porphyrin Handbook*; Kadish, K. M., Smith, K. M., Guilard, E., Eds; Academic Press: New York, 2000; Vol. 5; pp 3−74.
(442) Scheer, H.; Katz, J. J. In *Porphyrins and Metalloporphyrins*; Smith, K. M., Ed.; Elsevier: Amsterdam, 1975; p 399.
(443) Janson, T.; Katz, J. J. In *The Porphyrins*; Dolphin, D., Ed.; Academic Press: New York, 1979; Vol. IV, Chapter 1.
(444) Gottwald, L. K.; Ullman, E. F. *Tetrahedron Lett.* **1969**, *36*, 3071.
(445) Fleischer, E. B. *Acc. Chem. Res.* **1970**, *3*, 105.
(446) Walker, F. A.; Avery, G. L. *Tetrahedron Lett.* **1971**, *52*, 4949.
(447) Eaton, S. S.; Eaton, G. R.; Holm, R. H. *J. Organomet. Chem.* **1972**, *39*, 179.
(448) Bonnet, J. J.; Eaton, S. S.; Holm, R. H.; Ibers, J. A. *J. Am. Chem. Soc.* **1973**, *95*, 2141.
(449) Eaton, S. S.; Eaton, G. R. *Chem. Commun*. **1974**, 576.
(450) Eaton, S. S.; Eaton, G. R. *J. Am. Chem. Soc.* **1975**, *97*, 3660.
(451) Eaton, S. S.; Eaton, G. R. *J. Am. Chem. Soc.* **1977**, *99*, 6594.
(452) Eaton, S. S.; Fishwild, D. M.; Eaton, G. R. *Inorg. Chem.* **1978**, *17*, 1542.
(453) Dirks, J. W.; Underwood, G.; Matheson, J. C.; Gust, D. *J. Org. Chem.* **1979**, *44*, 2551.
(454) Hatano, K.; Anzai, K.; Kubo, T.; Tamai, S. *Bull. Chem. Soc. Jpn.* **1981**, *54*, 3518.
(455) Vicente, A. G. H.; Nurco, D. J.; Shetty, S. J.; Medforth, C. J.; Smith, K. M. *Chem. Commun.* **2001**, 483.
(456) Young, R.; Chang, C. K. *J. Am. Chem. Soc.* **1985**, *107*, 898.
(457) Collman, J. P. *Acc. Chem. Res.* **1977**, *10*, 265 and references therein.
(458) Collman, J. P.; Decréau, R. A.; Zhang, C. *J. Org. Chem.* **2004**, *69*, 3546.
(459) Mansuy, M.; Battione, P.; Renaud, J.-P.; Guerin, P. *Chem. Commun.* **1985**, 155.
(460) Boitrel, B.; Lecas, A.; Renko, Z.; Rose, E. *Chem. Commun*. **1985**, 1820.
(461) Groves, J. T.; Myers, R. S. *J. Am. Chem. Soc.* **1983**, *105*, 5791.
(462) Walker, F. A.; Buehler, J.; West, J. T.; Hinds, J. L. *J. Am. Chem. Soc.* **1983**, *105*, 6923.
(463) Hatano, K.; Anzai, K.; Nishino, A.; Fujii, K. *Bull. Chem. Soc. Jpn.* **1985**, *58*, 3653.
(464) Zimmer, B.; Bulach, V.; Drexler, C.; Erhardt, S.; Hosseini, M. W.; De Cian, A. *New. J. Chem.* **2002**, *26*, 43.
(465) Le Moigne, C.; Picaud, T.; Boussac, A.; Loock, B.; Momenteau, M.; Debois, A. *Inorg. Chem.* **2003**, *42*, 6081.
(466) Collman, J. P.; Brauman, J. I.; Collins, T. J.; Iverson, B.; Sessler, J. L. *J. Am. Chem. Soc.* **1981**, *103*, 2450.
(467) Collman, J. P.; Brauman, J. I.; Collins, T. J.; Iverson, B. L.; Lang, G.; Pettman, R. B.; Sessler, J. L.; Walters, M. A. *J. Am. Chem. Soc.* **1983**, *105*, 3038.
(468) Freitag, R. A.; Mercer-Smith, J. A.; Whitten, D. G. *J. Am. Chem. Soc.* **1981**, *103*, 1226.
(469) Freitag, R. A.; Whitten, D. G. *J. Phys. Chem.* **1983**, *87*, 3918.
(470) Knyukshto, V.; Zenkevich, E.; Sagun, E.; Shulga, A.; Bachilo, S. *Chem. Phys. Lett.* **1998**, *297*, 97.
(471) Fujimoto, T.; Umekawa, H.; Nishino, N. *Chem. Lett.* **1992**, 37.
(472) Crossley, M. J.; Field, L. D.; Forster, A. J.; Harding, M. M.; Sternhall, S. *J. Am. Chem. Soc.* **1987**, *109*, 341.
(473) The barrier in the fluoro analogue was measured via ^{19}F NMR, while the others were measured by HPLC determination of the concentration after equilibration at high temperature.
(474) Bourgeois, J.-P.; Diederich, F.; Echegoyen, L.; Nierengarten, J.-F. *Helv. Chim. Acta* **1998**, *81*, 1835.
(475) Armaroli, N.; Marconi, G.; Echegoyen, L.; Bourgeois, J.-P.; Diederich, F. *Chem.—Eur. J.* **2000**, *6*, 1629.
(476) Bonifazi, D.; Diederich, F. *Chem. Commun.* **2002**, 2178.
(477) Bonifazi, D.; Scholl, M.; Song, F.; Echegoyen, L.; Accorsi, G.; Armaroli, N.; Diederich, F. *Angew. Chem., Int. Ed.* **2003**, *42*, 4966.
(478) Diederich, F.; Kessinger, R. In *Templated Organic Synthesis*; Diederich, F., Stang, P. J., Eds.; Wiley-VCH: Weinheim, 2000; pp 189−218.
(479) Nierengarten, J.-F.; Oswald, L.; Nicoud, J.-F. *Chem. Commun.* **1998**, 1545.
(480) Okuno, Y.; Kamikado, T.; Yokoyama, S.; Mashiko, S. *J. THEOCHEM* **2002**, *594*, 55.
(481) Avilov, I. V.; Zen'kevich, É. I.; Sagun, E. I.; Shul'ga, A. M.; Filatov, I. V. *Opt. Spectrosc.* **2003**, *95*, 696.
(482) Shachter, A. M.; Fleisher, E. B.; Haltiwanger, R. C. *Chem. Commun.* **1988**, 960.
(483) Fleisher, E. B.; Shachter, A. M. *Inorg. Chem.* **1991**, *30*, 3763.
(484) Drain, C. M.; Lehn, J.-M. *Chem. Commun.* **1994**, 2313.
(485) Kimura, A.; Funatsu, K.; Imamura, T.; Kido, H.; Sasaki, Y. *Chem. Lett.* **1995**, 207.
(486) Alessio, E.; Macchi, M.; Heath, S.; Marzilli, L. G. *Chem. Commun.* **1996**, 1411.
(487) Kimura, A.; Funatsu, K.; Imamura, T.; Kido, H.; Sasaki, Y. *Chem. Lett.* **1995**, 207.
(488) Kariya, N.; Imamura, T.; Sasaki, Y. *Inorg. Chem.* **1997**, *36*, 833.
(489) Funatsu, K.; Kimura, A.; Imamura, T.; Ichimura, A.; Sasaki, Y. *Inorg. Chem.* **1997**, *36*, 1625.
(490) Kariya, N.; Imamura, T.; Sasaki, Y. *Inorg. Chem.* **1998**, *37*, 1658.
(491) Funatsu, K.; Imamura, T.; Ichimura, A.; Sasaki, Y. *Inorg. Chem.* **1998**, *37*, 1798.
(492) Alessio, E.; Geremia, S.; Mestroni, S.; Iengo, E.; Srnova, I.; Slouf, M. *Inorg. Chem.* **1999**, *38*, 869.
(493) Alessio, E.; Geremia, S.; Mestroni, S.; Srvona, I.; Slouf, M.; Gianferrara, T.; Prodi, A. *Inorg. Chem.* **1999**, *38*, 2527.
(494) Kaufmann, T.; Shamsai, B.; Ju, R. S.; Bau, R.; Miskelly, G. M. *Inorg. Chem.* **1995**, *34*, 5073.
(495) Mak, C. C.; Bampos, N.; Sanders, J. K. M. *Chem. Commun.* **1999**, 1085.
(496) Anderson, H. L.; Hunter, C. A.; Sanders, J. K. M. *Chem. Commun.* **1989**, 226.
(497) Hwang, I.-W.; Cho, H. S.; Jeong, D. H.; Kim, D.; Tsuda, A.; Nakamura, T.; Osuka, A. *J. Phys. Chem. B* **2003**, *107*, 9977.
(498) Darling, C. L.; Goh, P. K. Y.; Bampos, N.; Feeder, N.; Montalti, M.; Prodi, L.; Johnson, B. F. G.; Sanders, J. K. M. *Chem. Commun.* **1998**, 2031.
(499) Imamura, T.; Fukushima, K. *Coord. Chem. Rev.* **2000**, *198*, 133.
(500) Wojaczyński, J.; Latos-Grażyński, L. *Coord. Chem. Rev.* **2000**, *204*, 113.
(501) Choi, M.-S.; Yamazaki, T.; Yamazaki, I.; Aida, T. *Angew. Chem., Int. Ed.* **2004**, *43*, 150.
(502) Gust, D.; Moore, T. A. *Top. Curr. Chem.* **1991**, *159*, 103.
(503) Holten, D.; Bocian, D. F.; Lindsey, J. S. *Acc. Chem. Res.* **2002**, *35*, 57 and references therein.
(504) Thamyongkit, P.; Speckbacher, M.; Diers, J. R.; Kee, H. L.; Kirmaier, C.; Holten, D.; Bocian, D. F.; Lindsey, J. S. *J. Org. Chem.* **2004**, *69*, 3700.
(505) Prathapan, S.; Johnson, T. E.; Lindsey, J. S. *J. Am. Chem. Soc.* **1993**, *115*, 7519.
(506) Wagner, R. W.; Lindsey, J. S. *J. Am. Chem. Soc.* **1994**, *116*, 9759.
(507) Seth, J.; Palaniappan, V.; Wagner, R. W.; Johnson, T. E.; Lindsey, J. S.; Bocian, D. F. *J. Am. Chem. Soc.* **1996**, *118*, 11194.
(508) Strachen, J.-P.; Gentemann, S.; Seth, J.; Kalsbeck, W. A.; Lindsey, J. S.; Holten, D.; Bocian, D. F. *Inorg. Chem.* **1998**, *37*, 1191.
(509) Bothner-By, A. A.; Dadok, J.; Johnson, T. E.; Lindsey, J. S. *J. Phys. Chem.* **1996**, *100*, 17551.
(510) Wagner, R. W.; Seth, J.; Yang, S. I.; Kim, D.; Bocian, D.; Holten, D.; Lindsey, J. S. *J. Org. Chem.* **1998**, *63*, 5042.
(511) Li, J.; Ambroise, A.; Yang, S. I.; Diers, J. R.; Seth, J.; Wack, C. R.; Bocian, D. F.; Holten, D.; Lindsey, J. S. *J. Am. Chem. Soc.* **1999**, *121*, 8927.
(512) Sazanovich, I. V.; Kirmaier, C.; Hindin, E.; Yu, L.; Bocian, D. F.; Lindsey, J. S.; Holten, D. *J. Am. Chem. Soc.* **2004**, *126*, 2664.
(513) Yu, L.; Muthukumaran, K.; Sazanovich, I. V.; Kirmaier, C.; Hindin, E.; Diers, J. R.; Boyle, P. D.; Bocian, D. F.; Holten, D.; Lindsey, J. S. *Inorg. Chem.* **2003**, *42*, 6629.
(514) Kilså, K.; Kajanus, J.; Mårtensson, J.; Albinsson, B. *J. Phys. Chem. B* **1999**, *103*, 7329.
(515) Andréasson, J.; Zetterqvist, H.; Kajunus, J.; Mårtensson, J.; Albinsson, B. *J. Phys. Chem. A* **2000**, *104*, 9307.
(516) Andréasson, J.; Kajunus, J.; Mårtensson, J.; Albinsson, B. *J. Am. Chem. Soc.* **2000**, *122*, 9844.
(517) Kilså, K.; Kajanus, J.; Macpherson, A. N.; Mårtensson, J.; Albinsson, B. *J. Am. Chem. Soc.* **2001**, *123*, 3069.
(518) Kilså, K.; Kajunas, J.; Larsson, S.; Macpherson, A. N.; Mårtensson, J.; Albinsson, B. *Chem.—Eur. J.* **2001**, *7*, 2122.
(519) Kyrychenko, A.; Albinsson, B. *Chem. Phys. Lett.* **2002**, *366*, 291.
(520) Kyrychenko, A.; Andréasson, J.; Mårtensson, J.; Albinsson, B. *J. Phys. Chem. B* **2002**, *106*, 12613.
(521) Andréasson, J.; Kodis, G.; Ljungdahl, T.; Moore, A. L.; Moore, T. A.; Gust, D.; Mårtensson, J.; Albinsson, B. *J. Phys. Chem. A* **2003**, *107*, 8825.
(522) Pettersson, K.; Kilså, K.; Mårtensson, J.; Albinsson, B. *J. Am. Chem. Soc.* **2004**, *126*, 6710.
(523) Okuno, Y.; Mashiko, S. *Thin Solid Films* **2003**, *438−439*, 215.
(524) Nakano, A.; Osuka, A.; Yamazaki, I.; Yamazaki, T.; Nishimura, Y. *Angew. Chem., Int. Ed.* **1998**, *37*, 3023.
(525) Nakano, A.; Yamazaki, T.; Nishimura, Y.; Yamakazi, I.; Osuka, A. *Chem.—Eur. J.* **2000**, *6*, 3254.

(526) Nakano, A.; Osuka, A.; Yamazaki, T.; Nishimura, Y.; Akimoto, S.; Yamazaki, I.; Akira, I.; Murakami, M.; Miyasaka, H. *Chem.—Eur. J.* **2001**, *7*, 3134.
(527) Aratani, N.; Osuka, A.; Kim, Y. H.; Jeong, D. H.; Kim, D. *Angew. Chem., Int. Ed.* **2000**, *39*, 1458.
(528) Osuka, A.; Shimidzu, H. *Angew. Chem., Int. Ed. Engl.* **1997**, *36*, 135.
(529) See: Lindsey, J. S. In *The Porphyrin Handbook*; Kadish, K. M., Smith, K. M., Guilard, R., Eds.; Academic Press: New York, 2000; Vol. 1, pp 45−118.
(530) Peng, X.; Aratani, N.; Takagi, A.; Matsumoto, T.; Kawai, T.; Hwang, I.-W.; Ahn, T. K.; Kim, D.; Osuka, A. *J. Am. Chem. Soc.* **2004**, *126*, 4468.
(531) Sessler, J. L.; Johnson, M. R.; Lin, T.-Y.; Creager, S. E. *J. Am. Chem. Soc.* **1988**, *110*, 3659.
(532) Nagata, T.; Osuka, A.; Maruyama, K. *J. Am. Chem. Soc.* **1990**, *112*, 3054.
(533) Osuka, A.; Nakajima, S.; Nagata, T.; Maruyama, K.; Toriumi, K. *Angew. Chem., Int. Ed. Engl.* **1991**, *30*, 582.
(534) Sessler, J. L.; Capuano, V. L.; Harriman, A. *J. Am. Chem. Soc.* **1993**, *115*, 4618.
(535) Helms, A.; Heiler, D.; McLendon, G. *J. Am. Chem. Soc.* **1991**, *113*, 4325.
(536) Osuka, A.; Nakajima, S.; Nagata, T.; Muruyama, K.; Toriumi, K. *Angew. Chem., Int. Ed. Engl.* **1991**, *30*, 582.
(537) Helms, A.; Heiler, D.; McLendon, G. *J. Am. Chem. Soc.* **1991**, *113*, 4325.
(538) Arnold, D. P.; Mahendran, M.; Johnson, A. W. *J. Chem. Soc., Perkin Trans. 1* **1978**, 366.
(539) Arnold, D. P.; Nitschinsk, L. J. *Tetrahedron* **1992**, *48*, 8781.
(540) Arnold, D. P.; Heath, G. A. *J. Am. Chem. Soc.* **1993**, *115*, 12197.
(541) Anderson, H. L. *Inorg. Chem.* **1994**, *33*, 972.
(542) Lin, V. S.-Y.; Therien, M. J. *Chem.—Eur. J.* **1995**, *1*, 645.
(543) Piet, J. J.; Warman, J. M.; Anderson, H. L. *Chem. Phys. Lett.* **1997**, *266*, 70.
(544) Anderson, H. L. *Chem. Commun.* **1999**, 2323.
(545) Piet, J. J.; Taylor, P. N.; Anderson, H. L.; Osuka, A.; Warman, J. M. *J. Am. Chem. Soc.* **2000**, *122*, 1749.
(546) Piet, J. J.; Taylor, P. N.; Wegewijs, P. N.; Anderson, H. L.; Osuka, A.; Warman, J. M. *J. Phys. Chem. B* **2001**, *105*, 97.
(547) Ogawa, K.; Ohashi, A.; Kobuke, Y.; Kamada, K.; Ohta, K. *J. Am. Chem. Soc.* **2003**, *125*, 13356.
(548) Lin, V. S.-Y.; DiMagno, S. G.; Therien, M. J. *Science* **1994**, *264*, 1105.
(549) Lin, V. S.-Y.; Therien, M. J. *Chem.—Eur. J.* **1995**, *1*, 645.
(550) Susumo, K.; Therien, M. J. *J. Am. Chem. Soc.* **2002**, *124*, 4298.
(551) See, for example: Stomphorst, R. G.; Koehorst, R. B. M.; van der Zwan, G.; Benthem, B.; Schaafsma, T. J. *J. Porphyrins Phthalocyanines* **1999**, *3*, 346.
(552) Burrell, A. K.; Officer, D. L.; Reid, D. C.; Scott, S. M.; Gordon, K. C. *J. Porphyrins Phthalocyanines* **2000**, *4*, 627.
(553) Helms, A.; Heiler, D.; McLendon, G. *J. Am. Chem. Soc.* **1991**, *113*, 4325.
(554) Hsiao, J.-S.; Krueger, B. P.; Wagner, R. W.; Johson, T. E.; Delaney, J. K.; Mauzerall, D. C.; Fleming, G. R.; Lindsey, J. S.; Bocian, D. F.; Donohoe, R. J. *J. Am. Chem. Soc.* **1996**, *118*, 11181.
(555) Klose, T.; Peters, M. *Chem. Commun.* **1976**, 881.
(556) Dieckmann, H.; Chang, C. K.; Traylor, T. G. *J. Am. Chem. Soc.* **1971**, *93*, 4068.
(557) Almog, J.; Baldwin, J. E.; Huff, J. *J. Am. Chem. Soc.* **1975**, *97*, 227.
(558) Almog, J.; Baldwin, J. E.; Dyer, R. L.; Peters, M. K. *J. Am. Chem. Soc.* **1975**, *97*, 226.
(559) Almog, J.; Baldwin, J. E.; Crossley, M. J.; Debernardis, J. F.; Dyer, R. L.; Huff, J. R.; Peters, M. K. *Tetrahedron* **1981**, *37*, 3589.
(560) Momenteau, M.; Loock, B.; Mispelter, J.; Bisagni, E. *New J. Chem.* **1979**, *3*, 77.
(561) Chang, C. K. *J. Am. Chem. Soc.* **1977**, *99*, 2819.
(562) Collman, J. P.; Braumann, J. I.; Fitzgerald, J. P.; Hampton, P. D.; Naruta, Y.; Sparapany, J. W.; Ibers, J. A. *J. Am. Chem. Soc.* **1988**, *110*, 3477.
(563) Naruta, Y.; Tani, F.; Muruyama, K. *Chem. Lett.* **1989**, 1269.
(564) Boitrel, B.; Lecas, A.; Renko, Z.; Rose, E. *Chem. Commun.* **1985**, 1820.
(565) Almog, J.; Baldwin, J. E.; Huff, J. *J. Am. Chem. Soc.* **1975**, *97*, 227.
(566) Ogoshi, H.; Sugimoto, H.; Yoshida, Z. *Tetrahedron Lett.* **1976**, 4477.
(567) Ogoshi, H.; Sugimoto, H.; Yoshida, Z. *Tetrahedron Lett.* **1976**, 4481.
(568) Battersby, A. R.; Buckley, D. G.; Hartley, S. G.; Turnbull, M. D. *Chem. Commun.* **1976**, 879.
(569) Baldwin, J. E.; Chang, C. K. *J. Am. Chem. Soc.* **1977**, *99*, 2819.
(570) Ward, B.; Wang, C.-B.; Chang, C. K. *J. Am. Chem. Soc.* **1981**, *103*, 5236.
(571) Leighton, P.; Sanders, J. K. M. *Chem. Commun.* **1984**, 854.
(572) Leighton, P.; Sanders, J. K. M. *Chem. Commun.* **1984**, 856.
(573) Hamilton, A. D.; Rubin, H.-D.; Bocarsly, A. B. *J. Am. Chem. Soc.* **1984**, *106*, 7255.
(574) Leighton, P.; Sanders, J. K. M. *Chem. Commun.* **1985**, 24.
(575) Abraham, R. J.; Leighton, P.; Sanders, J. K. M. *J. Am. Chem. Soc.* **1985**, *107*, 3472.
(576) Hamilton, A.; Lehn, J.-M.; Sessler, J. L. *J. Am. Chem. Soc.* **1986**, *108*, 5158.
(577) Leighton, P.; Sanders, J. K. M. *J. Chem. Soc., Perkin Trans. 1* **1987**, 2385.
(578) Lisicki, M. A.; Mishra, P. K.; Bothner-By, A. A.; Lindsey, J. S. *J. Phys. Chem.* **1988**, *92*, 3400.
(579) Blaskó, A.; Garcia, B.; Bruice, T. C. *J. Org. Chem.* **1993**, *58*, 5738.
(580) Traylor, T. G. *Acc. Chem. Res.* **1981**, *14*, 102.
(581) Ganesh, K. N.; Sanders, J. K. M. *Chem. Commun.* **1980**, 1129.
(582) Ganesh, K. N.; Sanders, J. K. M.; Waterton, J. C. *J. Chem. Soc., Perkin Trans. 1* **1982**, 1617.
(583) Krieger, C.; Dernbach, M.; Voit, G.; Carell, T.; Staab, H. A. *Chem. Ber.* **1993**, *126*, 811.
(584) Staab, H. A.; Voit, G.; Weiser, J.; Futscher, M. *Chem. Ber.* **1992**, *125*, 2303.
(585) Staab, H. A.; Weiser, J.; Futscher, M.; Voit, G.; Rueckemann, A.; Christine, A. *Chem. Ber.* **1992**, *125*, 2285.
(586) Staab, H. A.; Weiser, J.; Baumann, E. *Chem. Ber.* **1992**, *125*, 2275.
(587) Krieger, C.; Weiser, J.; Staab, H. A. *Tetrahedron Lett.* **1985**, *26*, 6055.
(588) Wieser, J.; Staab, H. A. *Angew. Chem., Int. Ed. Engl.* **1984**, *23*, 623.
(589) Heitele, H.; Pöllinger, F.; Kremer, K.; Michel-Beyerle, M. E.; Futscher, M.; Voit, G.; Weiser, J.; Staab, H. A. *Chem. Phys. Lett.* **1992**, *188*, 270.
(590) Pöllinger, F.; Heitele, H.; Michel-Beyerle, M. E.; Anders, C.; Futscher, M.; Staab, H. A. *Chem. Phys. Lett.* **1992**, *198*, 645.
(591) Wagner, R. W.; Johnson, T. E.; Lindsey, J. S. *Tetrahedron* **1997**, *53*, 6755.
(592) Gunter, M. J.; Johnston, M. R. *Chem. Commun.* **1992**, 1163.
(593) Gunter, M. J.; Hockless, D. C. R.; Johnston, M. R.; Skelton, B. W.; White, A. H. *J. Am. Chem. Soc.* **1994**, *116*, 4810.
(594) Gunter, M. J.; Johnston, M. R. *Chem. Commun.* **1994**, 829.
(595) Anelli, P. L.; Ashton, P. R.; Ballardini, R.; Balzani, V.; Delgado, M.; Gandolfi, M. T.; Goodnow, T. T.; Kaifer, A. E.; Philp, D.; Pietraszkiewicz, M.; Prodi, L.; Reddington, M. V.; Slawin, N.; Spencer, N.; Stoddart, J. F.; Vicent, C.; Williams, D. J. *J. Am. Chem. Soc.* **1992**, *114*, 193.
(596) Collman, J. P.; Elliot, C. M.; Halbert, T. R.; Tovrog, B. S. *Proc. Natl. Acad. Sci. U.S.A.* **1977**, *74*, 18.
(597) Collman, J. P.; Marrocco, M.; Denisovich, P.; Koval, C.; Anson, F. C. *J. Electroanal. Chem. Interfacial Electrochem.* **1979**, *101*, 117.
(598) Collman, J. P.; Denisovich, P.; Konai, Y.; Marrocco, M.; Koval, C.; Anson, F. C. *J. Am. Chem. Soc.* **1980**, *102*, 6027.
(599) Collman, J. P.; Chong, A. O.; Jameson, G. B.; Oakley, R. T.; Rose, E.; Schmittou, E. R.; Ibers, J. A. *J. Am. Chem. Soc.* **1981**, *103*, 516.
(600) Collman, J. P.; Anson, F. C.; Barnes, C. E.; Bencosme, S.; Geiger, T.; Evitt, E. R.; Kreh, R. P.; Meier, K.; Pettman, R. B. *J. Am. Chem. Soc.* **1983**, *105*, 2694.
(601) Collman, J. P.; Bencosme, S.; Durand, R. R., Jr.; Kreh, R. P.; Anson, F. C. *J. Am. Chem. Soc.* **1983**, *105*, 2699.
(602) Collman, J. P.; Bencosme, S.; Barnes, C. E.; Miller, B. D. *J. Am. Chem. Soc.* **1983**, *105*, 2704.
(603) Durand, R. R., Jr.; Bencosme, C. S.; Collman, J. P.; Anson, F. C. *J. Am. Chem. Soc.* **1983**, *105*, 2710.
(604) Baldwin, J. E.; Perlmutter, P. *Top. Curr. Chem.* **1984**, *121*, 181.
(605) Dolphin, D.; Hiom, J.; Paine, J. B. *Heterocycles* **1981**, *16*, 417.
(606) Wasielewski, W. R.; Niemczyk, M. P.; Svec, W. A. *Tetrahedron Lett.* **1982**, *23*, 3215.
(607) Abdalmuhdi, I.; Chang, C. K. *J. Org. Chem.* **1985**, *50*, 411.
(608) Dubowchik, G. M.; Hamilton, A. D. *Chem. Commun.* **1985**, 90.
(609) Dubowchik, G. M.; Hamilton, A. D. *Chem. Commun.* **1986**, 665.
(610) Cowan, J. A.; Sanders, J. K. M.; Beddard, G. S.; Harrison, R. J. *Chem. Commun.* **1987**, 55.
(611) Tran-Thi, T. H.; Lipskier, J. F.; Maillard, P.; Momenteau, M.; Lopez-Castillo, J.-M.; Jay-Gerin, J.-P. *J. Phys. Chem.* **1992**, *96*, 1073.
(612) Zhang, H.-Y.; Yu, J.-Q.; Bruice, T. C. *Tetrahedron* **1994**, *50*, 11339.
(613) Leighton, P.; Cowan, J. A.; Abraham, R. J.; Sanders, J. K. M. *J. Org. Chem.* **1988**, *53*, 733.
(614) Hunter, C. A.; Sanders, J. K. M. *J. Am. Chem. Soc.* **1990**, *112*, 5525.
(615) Anderson, H. L.; Hunter, C. A.; Meah, M. N.; Sanders, J. K. M. *J. Am. Chem. Soc.* **1990**, *112*, 5780.
(616) Hunter, C. A.; Meah, M. N.; Sanders, J. K. M. *J. Am. Chem. Soc.* **1990**, *112*, 5773.
(617) Tashiro, K.; Aida, T.; Zheng, J.-Y.; Kinbara, K.; Saigo, K.; Sakamoto, S.; Yamaguchi, K. *J. Am. Chem. Soc.* **1999**, *121*, 9477.

(618) Nishioka, T.; Tashiro, K.; Aida, T.; Zheng, J.-Y.; Kinbara, K.; Saigo, K.; Sakamoto, S.; Yamaguchi, K. *Macromolecules* **2000**, *33*, 9182.
(619) Zheng, J.-Y.; Tashiro, K.; Hirabayashi, Y.; Kinbara, K.; Saigo, K.; Aida, T.; Sakamoto, S.; Yamaguchi, K. *Angew. Chem., Int. Ed.* **2001**, *40*, 1858.
(620) Yashiro, K.; Hirabayashi, Y.; Aida, T.; Saigo, K.; Fujiwara, K.; Komatsu, K.; Sakamoto, S.; Yamaguchi, K. *J. Am. Chem. Soc.* **2002**, *124*, 12086.
(621) Yamaguchi, T.; Ishii, N.; Tashiro, K.; Aida, T. *J. Am. Chem. Soc.* **2003**, *125*, 13934.
(622) Sun, D.; Tham, F. S.; Reed, C. A.; Chaker, L.; Burgess, M.; Boyd, P. D. W. *J. Am. Chem. Soc.* **2000**, *122*, 10704.
(623) Kubo, Y.; Sugasaki, A.; Ikeda, M.; Sugiyasu, K.; Sonoda, K.; Ikeda, A.; Takeuchi, M.; Shinkai, S. *Org. Lett.* **2002**, *4*, 925.
(624) Kubo, Y.; Ikeda, M.; Sugasaki, A.; Takeuchi, M.; Shinkai, S. *Tetrahedron Lett.* **2001**, *42*, 7435.
(625) Shoji, Y.; Tasjiro, K.; Aida, T. *J. Am. Chem. Soc.* **2004**, *126*, 6570.
(626) Liberles, A.; Matlosz, B. *J. Org. Chem.* **1971**, *36*, 2710.
(627) Stølevik, R.; Bakken, P. *J. Mol. Struct.* **1990**, *239*, 205.
(628) Okuyama, K.; Hasegawa, T.; Ito, M.; Mikami, N. *J. Phys. Chem.* **1984**, *88*, 1711.
(629) Young, J. K.; Moore, J. S. In *Modern Acetylene Chemistry*; Stang, P. J.. Diederich, F., Eds.; VCH: Weinheim, 1995; Chapter 12.
(630) Toyota, S.; Yamamori, T.; Asakura, M.; Ōki, M. *Bull. Chem. Soc. Jpn.* **2000**, *73*, 205.
(631) Toyota, S.; Yamamori, T.; Makino, T.; Ōki, M. *Bull. Chem. Soc. Jpn.* **2000**, *73*, 2591.
(632) Toyota, S.; Yamamori, T.; Makino, T. *Tetrahedron* **2001**, *57*, 3521.
(633) The first hindered bis(9-triptycyl)ethyne derivatives were prepared by Mew and Vögtle: Mew, P. K. T.; Vögtle, F. *Angew. Chem., Int. Ed. Engl.* **1979**, *18*, 159. The rotational barrier ($\Delta G^{\ddagger}$) for compound **VVVa4** was found to be 15.6 kcal mol^{-1}.
(634) Toyota, S.; Iida, T.; Kunizane, C.; Tanifuji, N.; Yoshida, Y. *Org. Biomol. Chem.* **2003**, *1*, 2298.
(635) Toyota, S.; Makino, T. *Tetrahedron Lett.* **2003**, *44*, 7775.
(636) Glass, T. E. *J. Am. Chem. Soc.* **2000**, *122*, 4522.
(637) Raker, J.; Glass, T. E. *J. Org. Chem.* **2001**, *66*, 6505.
(638) Raker, J.; Glass, T. E. *Tetrahedron* **2001**, *57*, 10233.
(639) Kealy, T. J.; Pauson, P. L. *Nature* **1951**, *168*, 1039.
(640) Wilkinson, G.; Rosenblum, M.; Whiting, M. C.; Woodward, R. B. *J. Am. Chem. Soc.* **1952**, *74*, 2125.
(641) Woodward, R. B.; Rosenblum, M.; Whiting, M. C. *J. Am. Chem. Soc.* **1952**, *74*, 3458.
(642) Jaffé, H. H. *J. Chem. Phys.* **1953**, *21*, 156.
(643) Moffitt, W. *J. Am. Chem. Soc.* **1954**, *76*, 3386.
(644) Richmond, H. H.; Freiser, H. *J. Am. Chem. Soc.* **1955**, *77*, 2022.
(645) This is the term used in these publications and one that we have attempted to avoid in this review. Every rotor molecule will have some intrinsic barrier to rotation *W*, and the term is generally used in the literature to describe rotation which could not be observed with the particular method being used to probe a rotation. Although one could argue for its usage in such a relative way, we avoid it for clarity purposes.
(646) Holm, C. H.; Ibers. J. A. *J. Chem. Phys.* **1959**, *30*, 885.
(647) Mulay, L. N.; Attalla, A. *J. Am. Chem. Soc.* **1963**, *85*, 702.
(648) Makova, M.; Karimov, Y. S.; Kochetkova, N. S.; Leonova, E. V. *Teor. Eksp. Khim.* **1972**, *8*, 259.
(649) Makova, M. K.; Leonova, E. V.; Karimov, Y. S.; Kochetkova, N. S. *J. Organomet. Chem*. **1973**, *55*, 185.
(650) Luke, W. D.; Streitweiser, A. *J. Am. Chem. Soc.* **1981**, *103*, 3241.
(651) *Ferrocenes*; Togni, A., Hayashi, T., Eds.; VCH: Weinheim, 1995. *Metallocenes*; Togni, A., Halterman, R. L., Eds.; Wiley-VCH: Weinheim, 1998; Vols. 1−2.
(652) Castellani, M. P.; Wright, J. M.; Geib, S. J.; Rheingold, A. L.; Trogler, W. C. *Organometallics* **1986**, *5*, 1116.
(653) Thornberry, M. P.; Slebodnick, C.; Deck, P. A. *Organometallics* **2000**, *19*, 5352.
(654) Okuda, J.; Herdweck, E. *Chem. Ber.* **1988**, *121*, 1899.
(655) Abel, E. W.; Long, N. J.; Orrell, K. G.; Osborne, A. G.; Šik, V. *J. Organomet. Chem.* **1991**, *403*, 195.
(656) Okuda, J. *Top. Curr. Chem.* **1991**, *160*, 97.
(657) Carella, A.; Jaud, J.; Rapenne, G.; Launay, J.-P. *Chem. Commun.* **2003**, 2434.
(658) Trofimenko, S. *Scorpionates: The Coordination Chemistry of Polypyrazolylborate Ligands*; Imperial College Press: London, 1999.
(659) Long, N. *Metallocenes: An Introduction to Sandwich Complexes*; Blackwell Science: Oxford, 1998.
(660) *Ferrocenes*; Togni, A., Hayashi, T., Eds.; VCH: Weinheim, 1995. *Metallocenes*; Togni, A., Halterman, R. L., Eds.; Wiley-VCH: Weinheim, 1998; Vols. 1−2.
(661) Albright, T. A. *Acc. Chem. Res.* **1982**, *15*, 149.
(662) McGlinchey, M. J. *Adv. Organomet. Chem.* **1992**, *34*, 285.
(663) Rausch, M. D.; Westover, G. F.; Mintz, E.; Reisner, G. M.; Bernal, I.; Clearfield, A.; Troup, J. M. *Inorg. Chem.* **1979**, *18*, 2605.
(664) Uno, M.; Shirai, K.; Ando, K.; Komatsuzaki, N.; Tanaka, T.; Sawada, M.; Takahashi, S. *Chem. Lett.* **1995**, 7.
(665) Stevens, A. M.; Richards, C. J. *Tetrahedron Lett.* **1997**, *38*, 7805.
(666) Hawthorne, M. F.; Zink, J. I.; Skelton, J. M.; Bayer, M. J.; Liu, C.; Livshits, E.; Baer, R.; Neuhauser, D. *Science* **2004**, *303*, 1849.
(667) Warren, L. F., Jr.; Hawthorne, M. F. *J. Am. Chem. Soc.* **1970**, *92*, 1157.
(668) Hansen, F. V.; Hazell, R. G.; Hyatt, C.; Stucky, G. D. *Acta Chem. Scand. A* **1973**, *27*, 1210.
(669) Hawthorne, M. F.; Dunks, G. B. *Science* **1972**, *178*, 462.
(670) Hawthorne, M. F.; et al. *J. Am. Chem. Soc.* **1968**, *90*, 879.
(671) Lucazeau, G.; Chhor, K.; Sourisseau, C.; Dianoux, A. *Chem. Phys.* **1983**, *76*, 307.
(672) Gilson. D. F. R.; Gomez, G.; Butler, I. S.; Fitzpatrick, P. J. *Can. J. Chem.* **1983**, *61*, 737.
(673) Eisenberg, A.; Shaver, A.; Tsutsui, T. *J. Am. Chem. Soc.* **1980**, *102*, 1416.
(674) For an introduction to mechanical spectroscopy, see: Eisenberg, A.; Eu, B. C. *Annu. Rev. Mater. Sci.* **1976**, *6*, 335.
(675) Gilson, D. F. R.; Gomez, G. *J. Organomet. Chem.* **1982**, *240*, 41.
(676) Adams, H.; Bailey, N. A.; Mann, B. E.; Taylor, B. F.; White, C.; Yavari, P. *J. Chem. Soc., Dalton Trans.* **1987**, 1947.
(677) Mynott, R.; Lehmkuhl, H.; Kreuzer, E.-M.; Joussen, E. *Angew. Chem., Int. Ed. Engl.* **1990**, *29*, 289.
(678) Du Plooy, K. E.; Marais, C. F.; Carlton, L.; Hunter, R.; Boeyens, J. C. A. *Inorg. Chem.* **1989**, *28*, 3855.
(679) Okuda, J. *J. Organomet. Chem.* **1989**, *375*, C13.
(680) Albright, T. A. *J. Organomet. Chem.* **1991**, *403*, 145.
(681) Coville, N. J.; du Plooy, K. E.; Pickl, W. *Coord. Chem. Rev.* **1992**, *116*, 1.
(682) Okuda, J. *J. Organomet. Chem.* **1988**, *356*, C43.
(683) Winter, C. H.; Dobbs, D. A.; Zhou, X.-X. *J. Organomet. Chem.* **1991**, *403*, 145.
(684) Castellani, M. P.; Geib, S. J.; Rheingold, A. L.; Trogler, W. C. *Organometallics* **1987**, *6*, 2524.
(685) Wadepohl, H. In *Unusual Structures and Physical Properties in Organometallic Chemistry*; Gielen, M., Willem, R., Wrackmeyer, B., Eds.; Wiley: New York, 2002; Chapter 7.
(686) Girolami, G. S.; Gorlin, P. A.; Suslick, K. S. *Inorg. Chem.* **1994**, *33*, 626.
(687) Buchler, J. W.; Eiermann, V.; Hanssum, H.; Heinz, G.; Rüterjans, H.; Schwarzkopf, M. *Chem. Ber.* **1994**, *127*, 589.
(688) Buchler, J. W.; Heinz, G. *Chem. Ber.* **1996**, *129*, 201.
(689) Buchler, J. W.; Heinz, G. *Chem. Ber.* **1996**, *129*, 1073.
(690) Tashiro, K.; Konishi, K.; Aida, T. *Angew. Chem., Int. Ed. Engl.* **1997**, *36*, 856.
(691) Takeuchi, M.; Imada, T.; Ikeda, M.; Shinkai, S. *Tetrahedron Lett.* **1998**, *39*, 7897.
(692) Tashiro, K.; Konishi, K.; Aida, T. *J. Am. Chem. Soc.* **2000**, *122*, 7921.
(693) Takeuchi, M.; Imada, T.; Shinkai, S. *Angew. Chem., Int. Ed.* **1998**, *37*, 2096.
(694) Takeuchi, M.; Imada, T.; Shinkai, S. *J. Am. Chem. Soc.* **1996**, *118*, 10658.
(695) Takeuchi, M.; Imada, T.; Shinkai, S. *Bull. Chem. Soc. Jpn.* **1998**, *71*, 1117.
(696) Sugasaki, A.; Ikeda, M.; Takeuchi, M.; Robertson, A.; Shinkai, S. *J. Chem. Soc., Perkin Trans. 1* **1999**, 3259.
(697) Shinkai, S. In *Molecular Switches*; Feringa, B. L., Ed.; Wiley-VCH: Weinheim, 2001; pp 281−307.
(698) Sugasaki, A.; Sugiyasu, K.; Ikeda, M.; Takeuchi, M.; Shinkai, S. *J. Am. Chem. Soc.* **2001**, *123*, 10239.
(699) Ikeda, M.; Tanida, T.; Takeuchi, M.; Shinkai, S. *Org. Lett.* **2000**, *2*, 1803.
(700) Sugasaki, A.; Ikeda, M.; Takeuchi, M.; Koumoto, K.; Shinkai, S. *Tetrahedron* **2000**, *56*, 4717.
(701) Sugasaki, A.; Ikeda, M.; Takeuchi, M.; Shinkai, S. *Angew. Chem., Int. Ed.* **2000**, *39*, 3839.
(702) Robertson, A.; Ikeda, M.; Takeuchi, M.; Shinkai, S. *Bull. Chem. Soc. Jpn.* **2001**, *74*, 883.
(703) Ikeda, M.; Takeuchi, M.; Shinkai, S.; Tani, F.; Naruta, Y. *Bull. Chem. Soc. Jpn.* **2001**, *74*, 739.
(704) Tashiro, K.; Fujiwara, T.; Konishi, K.; Aida, T. *Chem. Commun.* **1998**, 1121.
(705) Shinkai, S.; Ikeda, M.; Sugasaki, A.; Takeuchi, M. *Acc. Chem. Res.* **2001**, *34*, 494.
(706) Takeuchi, M.; Ikeda, M.; Sugasaki, A.; Shinkai, S. *Acc. Chem. Res.* **2001**, *34*, 865.
(707) Collman, J. P.; Woo, L. *Proc. Natl. Acad. Sci. U.S.A.* **1984**, *81*, 2592.
(708) Collman, J. P.; Garner, J. M.; Hembre, R. T.; Ha, Y. *J. Am. Chem. Soc.* **1992**, *114*, 1292.
(709) Collman, J. P.; Harford, S. T.; Franzen, S.; Eberspacher, T. A.; Shoemaker, R. K.; Woodruff, W. H. *J. Am. Chem. Soc.* **1998**, *120*, 1456.
(710) Cotton, F. A. *Acc. Chem. Res.* **1978**, *11*, 225.
(711) Trogler, W. C.; Gray, H. B. *Acc. Chem. Res.* **1978**, *11*, 232.
(712) See also: Collman, J. P.; Garner, J. M.; Woo, L. K. *J. Am. Chem. Soc.* **1989**, *111*, 8141.
(713) Kim, J. C.; Goeden, V. L.; Lee, B. M. *Polyhedron* **1996**, *15*, 57.

(714) Yang, C. H.; Dzugan, S. J.; Goedken, V. L. *Chem. Commun.* **1986**, 1313.
(715) Binstead, R. A.; Reimers, J. R.; Hush, N. S. *Chem. Phys. Lett.* **2003**, *378*, 654.
(716) Hush, N. S.; Cheung, A. S. *Chem. Phys. Lett.* **1977**, *47*, 1.
(717) Hush, N. S.; Woolsey, I. S. *Mol. Phys.* **1971**, *21*, 465.
(718) Esposito, J. N.; Lloyd, J. E.; Kenney, M. E. *Inorg. Chem.* **1966**, *5*, 1979.
(719) Hiraoka, S.; Yi, T.; Shiro, M.; Shionoya, M. *J. Am. Chem. Soc.* **2002**, *124*, 14510.
(720) Hiraoka, S.; Harano, K.; Tanaka, T.; Shiro, M.; Shionoya, M. *Angew. Chem., Int. Ed.* **2003**, *42*, 5182.
(721) Hiraoka, S.; Shiro, M.; Shionoya, M. *J. Am. Chem. Soc.* **2004**, *126*, 1214.
(722) Hahn, E. H.; Bohm, H.; Ginsburg, D. *Tetrahedron Lett.* **1973**, 507.
(723) *Cyclophanes*; Keehn, P. M., Rosenfeld, S. M., Eds.; Academic Press: New York, 1983; Vols. 1 and 2.
(724) Vögtle, F. *Cyclophane Chemistry*; Wiley and Sons: Chichester, U.K., 1993.
(725) Helder, R.; Wynberg, H. *Tetrahedron Lett.* **1973**, 4321.
(726) Venkataramu, S. D.; El-Deek, M.; Berlin, K. D. *Tetrahedron Lett.* **1976**, 3365.
(727) Vögtle, F.; Mew, P. K. T. *Angew. Chem., Int. Ed. Engl.* **1978**, *17*, 60.
(728) Dignan, J. C.; Miller, J. B. *J. Org. Chem.* **1967**, *32*, 490.
(729) Gakh, A. A.; Sachleben, R. A.; Bryan, J. C.; Moyer, B. A. *Tetrahedron Lett.* **1995**, *36*, 8163.
(730) Gakh, A. A.; Sachleben, R. A.; Bryan, J. C. *Chemtech* **1997**, 26.
(731) Bryan, J. C.; Sachleben, R. A.; Gakh, A. A.; Bunick, G. J. *J. Chem. Crystallogr.* **1999**, *29*, 513.
(732) Bauer, E. B.; Hampel, F.; Gladysz, J. A. *Organometallics* **2003**, *22*, 5567.
(733) Shima, T.; Hampel, F.; Gladysz, J. A. *Angew. Chem., Int. Ed.* **2004**, *43*, 5537.
(734) Ng, P. L.; Lambert, J. N. *Synlett* **1999**, 1749.
(735) Bedard, T. C.; Moore, J. S. *J. Am. Chem. Soc.* **1995**, *117*, 10662.
(736) İpek, S. G.; Varnali, T. *THEOCHEM* **1999**, *468*, 201.
(737) Asfari, Z.; Naumann, C.; Kaufmann, G.; Vicens, J. *Tetrahedron Lett.* **1998**, *39*, 9007.
(738) Lehn, J.-M. *Angew. Chem., Int. Ed. Engl.* **1990**, *29*, 1304.
(739) Lehn, J.-M. *Angew. Chem., Int. Ed. Engl.* **1988**, *27*, 89.
(740) Cram, D. J. *Angew. Chem., Int. Ed. Engl.* **1988**, *27*, 1009.
(741) Pedersen, C. J. *Chem. Scr.* **1988**, *28*, 229.
(742) Lehn, J.-M. *Science* **1985**, *227*, 849.
(743) Cram, D. J. *Nature* **1993**, *356*, 29.
(744) Cram, D. J.; Cram, J. M. In *Container Molecules and Their Guests*; Stoddart, J. F., Ed.; Monographs in Supramolecular Chemistry; Royal Society of Chemistry: Cambridge, U.K., 1994.
(745) Hof, F.; Craig, S. L.; Nuckolls, C.; Rebek, J., Jr. *Angew. Chem., Int. Ed.* **2002**, *41*, 1488.
(746) Special Issue on Supramolecular Chemistry and Self-Assembly: *Science* **2002**, *295*, 2400.
(747) Hilmersson, G.; Rebek, J., Jr. *Magn. Reson. Chem.* **1998**, *36*, 663.
(748) Behr, J.-P.; Lehn, J.-M. *J. Am. Chem. Soc.* **1976**, *98*, 1743.
(749) Graf, E.; Kintzinger, J.-P.; Lehn, J.-M.; LeMoigne, J. *J. Am. Chem. Soc.* **1982**, *104*, 1672.
(750) Dietrich, B.; Kintzinger, J.-P.; Lehn, J.-M.; Metz, B.; Zahidi, A. *J. Phys. Chem.* **1987**, *91*, 6600.
(751) Bryant, J. A.; Blanda, M. T.; Vincenti, M.; Cram, D. J. *J. Am. Chem. Soc.* **1991**, *113*, 2167.
(752) Bryant, J. A.; Blanda, M. T.; Vincenti, M.; Cram, D. J. *Chem. Commun.* **1990**, 1403.
(753) Sherman, J. C.; Knobler, C. B.; Cram, D. J. *J. Am. Chem. Soc.* **1991**, *113*, 2194.
(754) Cram, D. J.; Tanner, M. E.; Kiepert, S. J.; Knobler, C. B. *J. Am. Chem. Soc.* **1991**, *113*, 8909.
(755) Bonechi, C.; Donati, A.; Martini, S.; Rossi, C.; Arduini, A.; Pochini, A.; Lonetti, B.; Baglioni, P. *J. Phys. Chem. B* **2004**, *108*, 7603.
(756) Yamada, A.; Murase, T.; Kikukawa, K.; Arimura, T.; Shinkai, S. *J. Chem. Soc., Perkin Trans.* **1991**, 793.
(757) Shimizu, K. D.; Rebek, J., Jr. *Proc. Natl. Acad. Sci. U.S.A.* **1995**, *92*, 12403.
(758) Antony, J. H.; Dolle, A.; Fliege, T.; Geiger, A. *J. Phys. Chem. A* **1997**, *101*, 4517.
(759) Meier, U. C.; Detellier, C. *J. Phys. Chem. A* **1999**, *103*, 9204.
(760) Kawase, T.; Darabi, H. R.; Oda, M. *Angew. Chem., Int. Ed. Engl.* **1996**, *35*, 2664.
(761) Kawase, T.; Ueda, N.; Yanaka, K.; Seirai, Y.; Oda, M. *Tetrahedron Lett.* **2001**, *42*, 5509.
(762) Kawase, K.; Seirai, Y.; Darabi, H. R.; Oda, M.; Sarakai, Y.; Tashiro, K. *Angew. Chem., Int. Ed.* **2003**, *42*, 1621.
(763) Kawase, T.; Tanaka, K.; Fujiwara, N.; Darabi, H. R.; Oda, M. *Angew. Chem., Int. Ed.* **2003**, *42*, 1624.
(764) Kawase, T.; Tanaka, K.; Seirai, Y.; Shiono, N.; Oda, M. *Angew. Chem. Int. Ed.* **2003**, *42*, 5597.
(765) Whitesides, G. M.; Simanek, E. E.; Mathias, J. P.; Seto, C. T.; Chin, D. N.; Mammen, M.; Gordon, D. M. *Acc. Chem. Res.* **1995**, *28*, 37 and references therein.
(766) Li, X.; Chin, D. N.; Whitesides, G. M. *J. Org. Chem.* **1996**, *61*, 1779.
(767) Chin, D. N.; Simanek, E. E.; Li, X.; Wazeer, M. I. M.; Whitesides, G. M. *J. Org. Chem.* **1997**, *62*, 1891.
(768) Simanek, E. E.; Qiao, S.; Choi, I. S.; Whitesides, G. M. *J. Org. Chem.* **1997**, *62*, 2619.
(769) Simanek, E. E.; Isaacs, L.; Li, X.; Wand, C. C. C.; Whitesides, G. M. *J. Org. Chem.* **1997**, *62*, 8994.
(770) Mathias, J. P.; Simanek, E. E.; Zerkowski, J. A.; Seto, C. T.; Whitesides, G. M. *J. Am. Chem. Soc.* **1994**, *116*, 4316.
(771) Simanek, E. E.; Wazeer, M. I. M.; Mathias, J. P.; Whitesides, G. M. *J. Org. Chem.* **1994**, *59*, 4904.
(772) Vreekamp, R. H.; Hubert, M.; van Duynhoven, J. P. M.; Verboom, W.; Reinhoudt, D. N. *Angew. Chem., Int. Ed. Engl.* **1996**, *35*, 1215.
(773) Timmerman, P.; Vreekamp, R. H.; Hulst, R.; Verboom, W.; Reinhoudt, D. N.; Rissanen, K.; Udachin, K. A.; Ripmeester, J. *Chem.—Eur. J.* **1997**, *3*, 1823.
(774) Prins, L. J.; Huskens, J.; de Jong, F.; Timmerman, P.; Reinhoudt, D. N. *Nature* **1999**, *398*, 498.
(775) Prins, L. J.; Jolliffe, K. A.; Hulst, R.; Timmerman, P.; Reinhoudt, D. N. *J. Am. Chem. Soc.* **2000**, *122*, 3617.
(776) Kerckhoffs, J. M. C. A.; van Leeuwen, F. W. B.; Spek, A. L.; Kooijman, H.; Crego-Calama, M.; Reinhoudt, D. N. *Angew. Chem., Int. Ed.* **2003**, *42*, 5717.
(777) See refs 765−769.
(778) Marsh, A.; Silvestri, M.; Lehn, J.-M. *Chem. Commun.* **1996**, 1527 and references therein.
(779) Prins, L. J.; De Jong, F.; Timmerman, P.; Reinhoudt, D. N. *Nature* **2000**, *408*, 181.
(780) Bielejewska, A. G.; Marjo, C. E.; Prins, L. J.; Timmerman, P.; De Jong, F.; Reinhoudt, D. N. *J. Am. Chem. Soc.* **2001**, *123*, 7518.
(781) Veerman, J. A.; Levi, S. A.; van Veggel, F. C. J. M.; Reinhoudt, D. N.; van Hulst, N. F. *J. Phys. Chem. A* **1999**, *103*, 11264.
(782) Highlight: Schalley, C. A. *Angew. Chem., Int. Ed.* **2002**, *41*, 1513.
(783) Kroto, H. W. *Nature* **1992**, *359*, 670.
(784) Cumings, J.; Zettl, A. *Science* **2000**, *289*, 602.
(785) Smith, B. W.; Monthioux, M.; Luzzi, D. E. *Nature* **1998**, *396*, 323.
(786) Sloan, J.; Kirkland, A. I.; Hutchison, J. L.; Green, M. L. H. *Chem. Commun.* **2002**, 1319.
(787) Chen, J.; Dong, J. *J. Phys: Condensed Matter* **2004**, *16*, 1401.
(788) Vögtle, F.; Müller, W. M. *Angew. Chem., Int. Ed. Engl.* **1979**, *18*, 623.
(789) Kamitori, S.; Hirotsu, K.; Higuchi, T. *Chem. Commun.* **1986**, 690.
(790) Kamitori, S.; Hirotsu, T.; Higuchi, T. *J. Am. Chem. Soc.* **1987**, *109*, 2409.
(791) Kamitori, S.; Hirotsu, K.; Higuchi, T. *Bull. Chem. Soc. Jpn.* **1988**, *61*, 3825.
(792) Lützen, A.; Renslo, A. R.; Schalley, C. A.; O'Leary, B. M.; Rebek, J., Jr. *J. Am. Chem. Soc.* **1999**, *121*, 7455.
(793) Mock, W. L. *Top. Curr. Chem.* **1995**, *175*, 1.
(794) Mock, W. L. In *Comprehensive Supramolecular Chemistry*; Vögtle, F., Ed.; Pergamon: Oxford, U.K., 1996; Vol. 2, p 477.
(795) Gerasko, O. A.; Samsonnenko, D. G.; Fedin, V. P. *Russ. Chem. Rev.* **2002**, *71*, 741.
(796) Behrend, R.; Meyer, E.; Rusche, F. *Justus Liebigs Ann. Chem.* **1905**, *339*, 1.
(797) Freeman, W. A.; Mock, W. L.; Shih, N. Y. *J. Am. Chem. Soc.* **1981**, *103*, 7367.
(798) El Haouaj, M.; Luhmer, M.; Ko, Y. H.; Kim, K.; Bartik, K. *J. Chem. Soc., Perkin Trans. 2* **2001**, 804.
(799) Freeman, W. A. *Acta Crystallogr., B* **1984**, *40*, 382.
(800) Jeon, Y.-M.; Kim, J.; Whang, D.; Kim, K. *J. Am. Chem. Soc.* **1996**, *118*, 9790.
(801) Whang, D.; Heo, J.; Park, J. H.; Kim, K. *Angew. Chem., Int. Ed.* **1998**, *37*, 78.
(802) Heo, J.; Kim, S.-Y.; Whang, D.; Kim, K. *Angew. Chem., Int. Ed.* **1999**, *38*, 641.
(803) Fedin, V. P.; Virovets, A. V.; Sokolov, M. N.; Dybtsev, D. N.; Gerasko, O. A.; Clegg, W. *Inorg. Chem.* **2000**, *39*, 2227.
(804) Day, A. I.; Blanch, R. J.; Arnold, A. P.; Lorenzo, S.; Lewis, G. R.; Dance, I. *Angew. Chem., Int. Ed.* **2002**, *41*, 275.
(805) Day, A.; Arnold, A. P.; Blanch, R. J.; Snushall, B. *J. Org. Chem.* **2001**, *66*, 8094.
(806) Blanch, R. J.; Sleeman, A. J.; White, T. J.; Arnold, A. P.; Day, A. I. *Nano Lett.* **2002**, *2*, 147.
(807) Mandl, C. P.; König, B. *Angew. Chem., Int. Ed.* **2004**, *43*, 1622.
(808) Feringa, B. L.; Jager, W. F.; de Lange, B. *Tetrahedron* **1993**, *49*, 8267.
(809) Feringa, B. L.; Huck, N. P. M.; Schoevaars, A. M. *Adv. Mater.* **1996**, *8*, 681.
(810) Feringa, B. L.; van Delden, R. A.; Koumura, N.; Geertsema, E. M. *Chem. Rev.* **2000** *100*, 1789.
(811) Feringa, B. L. *Acc. Chem. Res.* **2001**, *34*, 504.

(812) Feringa, B. L.; Koumura, N.; van Delden, R. A.; ter Wiel, M. K. J. *Appl. Phys. A* **2002**, *75*, 301.
(813) Jörgensen, M.; Lerstrup, K.; Frederiksen, P.; Bjørnholm, T.; Sommer-Larsen, P.; Schaumburg, K.; Brunfeldt, K.; Bechgaard, K. *J. Org. Chem.* **1993**, *58*, 2785 and references therein.
(814) Hirshberg, Y. *J. Am. Chem. Soc.* **1956**, *78*, 2304.
(815) Hirshberg, Y. *New Sci.* **1960**, *7*, 1243.
(816) Wynberg, H.; Feringa, B. L. *J. Am. Chem. Soc.* **1977**, *99*, 692.
(817) de Lange, B.; Feringa, B. L.; Jager, W. F. *Mol. Cryst. Liq. Cryst.* **1992**, *217*, 129.
(818) Jager, W. F.; Feringa, B. L.; de Lange, B. *Mol. Cryst. Liq. Cryst.* **1992**, *217*, 133.
(819) Huck, N. P. M.; Jager, W. F.; de Lange, B.; Feringa, B. L. *Science* **1996**, *273*, 1686.
(820) Schoevaars, A. M.; Kruizinga, W.; Zijlstra, R. W. J.; Veldman, N.; Spek, A. L.; Feringa, B. L. *J. Org. Chem.* **1997**, *62*, 4943.
(821) Huck, N. P. M.; Feringa, B. L. *Chem. Commun.* **1995**, 1686.
(822) Harada, N.; Saito, A.; Koumura, N.; Uda, H.; de Lange, B.; Jager, W. F.; Wynberg, H.; Feringa, B. L. *J. Am. Chem. Soc.* **1997**, *119*, 7241.
(823) Harada, N.; Saito, A.; Koumura, N.; Roe, D. C.; Jager, W. F.; Zijlstra, R. W. J.; de Lange, B.; Feringa, B. L. *J. Am. Chem. Soc.* **1997**, *119*, 7249.
(824) Harada, N.; Koumura, N.; Feringa, B. L. *J. Am. Chem. Soc.* **1997**, *119*, 7256.
(825) Koumura, N.; Harada, N. *Chem. Lett.* **1998**, 1151.
(826) Zijlstra, R. W. J.; Jager, W. F.; de Lange, B.; van Duijnen, P. Th.; Feringa, B. L.; Goto, H.; Saito, A.; Koumura, N.; Harada, N. *J. Org. Chem.* **1999**, *64*, 1667.
(827) Feringa, B. L. *Nature* **2000**, *408*, 151.
(828) Koumura, N.; Geertsema, E. M.; Meetsma, A.; Feringa, B. L. *J. Am. Chem. Soc.* **2000**, *122*, 12006.
(829) Zijlstra, R. W. J.; van Duijnen, P. Th.; Feringa, B. L.; Steffen, K.; Duppen, K.; Wiersma, D. A. *J. Phys. Chem. A* **1997**, *101*, 9828.
(830) Schuddeboom, W.; Jonker, S. A.; Warman, J. M.; de Haas, M. P.; Vermeulen, M. J. W.; Jager, W. F.; de Lange, B.; Feringa, B. L.; Fesseden, R. W. *J. Am. Chem. Soc.* **1993**, *115*, 3286.
(831) Koumura, N.; Geertsema, E. M.; van Gelder, M. B.; Meetsma, A.; Feringa, B. L. *J. Am. Chem. Soc.* **2002**, *124*, 5037.
(832) Geertsema, E. M.; Koumura, N.; ter Wiel, M. K. J.; Meetsma, A.; Feringa, B. L. *Chem. Commun.* **2002**, 2962.
(833) ter Wiel, M. K. J.; van Delden, R. A.; Meetsma, A.; Feringa, B. L. *J. Am. Chem. Soc.* **2003**, *125*, 15076.
(834) van Delden, R. A.; Koumura, N.; Harada, N.; Feringa, B. L. *Proc. Natl. Acad. Sci. U.S.A.* **2002**, *99*, 4945.
(835) van Delden, R. A.; van Gelder, M. B.; Huck, N. P. M.; Feringa, B. L. *Adv. Funct. Mater.* **2003**, *13*, 319.
(836) van Delden, R. A.; Mecca, T.; Rosini, C.; Feringa, B. L. *Chem.—Eur. J.* **2004**, *10*, 61.
(837) Galstyan, T. V.; Drnoyan, V. *Phys. Rev. Lett.* **1997**, *78*, 2760.
(838) Palffy-Muhoray, P.; Kosa, T.; Weinan, E. *Braz. J. Phys.* **2002**, *32*, 552.
(839) Palffy-Muhoray, P.; Kosa, T.; Weinan, E. *Appl. Phys. A* **2002**, *75*, 293.
(840) Palffy-Muhoray, P.; Kosa, T.; Weinan, E. *Mol. Cryst. Liq. Cryst.* **2002**, *375*, 577.
(841) Bermudez, V.; Capron, N.; Gase, T.; Gatti, F. G.; Kajzar, F.; Leigh, D. A.; Zerbetto, F.; Zhang, S. *Nature* **2000**, *406*, 608.
(842) Gatti, F. G.; Leon, S.; Wong, J. K. Y.; Bottari, G.; Altieri, A.; Morales, M. A. F.; Teat, S. J.; Frochot, C.; Leigh, D. A.; Brouwer, A. M.; Zerbetto, F. *Proc. Natl. Acad. Sci.* **2003**, *100*, 10.
(843) Leigh, D. A.; Wong, J. K. Y.; Dehez, F.; Zerbetto, F. *Nature* **2003**, *424*, 174.
(844) Hoki, K.; Yamaki, M.; Fujimura, Y. *Angew. Chem., Int. Ed.* **2003**, *42*, 2976.
(845) Hoki, K.; Sato, M.; Yamaki, M.; Sahnoun, R.; González, L.; Koseki, S.; Fujimura, Y. *J. Phys. Chem. B* **2004**, *108*, 4916.
(846) Fujimura, Y.; González, L.; Kröner, D.; Manz, J.; Mehdaoui, I.; Schmidt, B. *Chem. Phys. Lett.* **2004**, *386*, 248.
(847) Kelly, T. R.; Bowyer, M. C.; Bhaskar, K. V.; Bebbington, D.; Garcia, A.; Lang, F.; Kim, M. H.; Jette, M. P. *J. Am. Chem. Soc.* **1994**, *116*, 3657.
(848) A simpler, and less effective, brake has been investigated by Bates and co-workers: Jog, P. V.; Brown, R. E.; Bates, D. K. *J. Org. Chem.* **2003**, *68*, 8240.
(849) Kelly, T. R. *Acc. Chem. Res.* **2001**, *34,* 514.
(850) Destelo, J. P.; Kelly, T. R. *Appl. Phys. A.: Mater. Sci. Proc.* **2002**, *75*, 337.
(851) Kelly, T. R.; Sestelo, J. P. *Struct. Bonding* **2001**, *99*, 19.
(852) Feynman, R.; Leighton, R. B.; Sands, M. *The Feynman Lectures on Physics*; Addison-Wesley: Reading, MA, 1963; p 46-1.
(853) Kelly, T. R.; Tellitu, I.; Sestelo, J. P. *Angew. Chem., Int. Ed. Engl.* **1997**, *36*, 1866.
(854) Kelly, T. R.; Sestelo, J. P.; Tellitu, I. *J. Org. Chem.* **1998**, *63*, 3655.
(855) Davis, A. P. *Angew. Chem., Int. Ed.* **1998**, *37*, 909.
(856) Kelly, T. R.; Silva, R. A.; De Silva, H.; Jasmin, S.; Zhao, Y. *J. Am. Chem. Soc.* **2000**, *122*, 6935.
(857) Destelo, J. P.; Kelly, T. R. *Appl. Phys. A* **2002**, *75*, 337.
(858) Galli, S.; Mercandelli, P.; Sironi, A. *J. Am. Chem. Soc.* **1999**, *121*, 3767.
(859) Harada, J.; Ogawa, K.; Tomoda, S. *Acta Crystallogr.* **1997**, *B53*, 662.
(860) Ogawa, K.; Sano, T.; Yoshimura, S.; Takeuchi, Y.; Toriumi, K. *J. Am. Chem. Soc.* **1992**, *114*, 1041.
(861) Saito, K.; Okada, M.; Akutsu, H.; Sorai, M. *Chem. Phys. Lett.* **2000**, *318*, 75.
(862) McGeorge, G.; Harris, R. K.; Batsanov, A. S.; Churakov, A. V.; Chippendale, A. M.; Bullock, J. F.; Gans, Z. *J. Phys. Chem. A* **1998**, *102*, 3505.
(863) *The Plastically Crystalline State*; Sherwood, J. N., Ed.; Wiley: Chicester, U.K., 1979.
(864) Gavezzotti, A. *Mol. Cryst. Liq. Cryst.* **1988**, *156*, 25.
(865) Gavezzotti, A. *New J. Chem.* **1982**, *6*, 443.
(866) Ghorai, P. Kr.; Yashonath, S. *J. Chem. Phys.* **2004**, *120*, 5315 and references therein.
(867) Kärger, J.; Ruthven, D. M. *Diffusion in Zeolites and Other Microporous Solids*; North: New York, 1985.
(868) Desiraju, G. R. *Crystal Design: Structure and Function*; Perspectives in Supramolecular Chemistry Volume 7; Wiley: Chichester, U.K., 2003.
(869) Stupp, S. I.; LeBonheur, V.; Walker, K.; Li, L. S.; Huggins, K. E.; Keser, M.; Amstutz, A. *Science* **1997**, *276*, 384.
(870) Russell, V. A.; Evans, C. C.; Li, W.; Ward, M. D. *Science* **1997**, *276*, 575.
(871) Desiraju, G. R. *Angew. Chem., Int. Ed. Engl.* **1995**, *34*, 2311.
(872) Dunitz, J. D.; Maverick, E. F.; Trueblood, K. N. *Angew. Chem., Int. Ed. Engl.* **1988**, *27*, 880.
(873) Dominguez, Z.; Strouse, H.; Garcia-Garibay, M. A. *J. Am. Chem. Soc.* **2002**, *124*, 2398.
(874) Warren, B. E. *X-ray Diffraction*; Addison-Wesley Publishing Company: Reading, MA, 1969.
(875) Suryanarayana, C.; Norton, M. G. *X-ray Diffraction: A Practical Approach*; Plenum Press: New York, 1998.
(876) Maverick, E. F.; Dunitz, J. D. *Mol. Phys.* **1987**, *62*, 451.
(877) Dunitz, J. D.; White, D. N. J. *Acta Crystallogr., A* **1973**, *29*, 93.
(878) Bernard, G. M.; Wasylishen, R. E. In *Unusual Structures and Physical Properties in Organometallic Chemistry*; Gielen, M., Willem, R., Wrackmeyer, B., Eds.; Wiley: New York, 2002; Chapter 4.
(879) Dominguez, Z.; Khuong, T.-A. V.; Dang, H.; Sanrame, C. N.; Nuñez, J. E.; Garcia-Garibay, M. A. *J. Am. Chem. Soc.* **2003**, *125*, 8827.
(880) Khuong, T.-A. V.; Zepeda, G.; Ruiz, R.; Khan, S. I.; Garcia-Garibay, M. A. *Cryst. Growth Des.* **2004**, *4*, 15.
(881) Godinez, C. E.; Zepeda, G.; Mortko, C. J.; Dang, H.; Garcia-Garibay, M. A. *J. Org. Chem.* **2004**, *69*, 1652.
(882) Palma-Vittorelli, M. B.; Palma, M. U.; Drewes, G. W. J.; Koerts, C. *Physica* **1960**, *26*, 922.
(883) Garofano, T.; Palma-Vittorelli, M. B.; Palma, M. U.; Persico, F. In *Proceedings of the International Conference on Paramagnetic Resonance*; Low, W., Ed.; 1962; Vol. 2, p 582.
(884) Palma-Vittorelli, M. B.; Palma, M. U.; Persico, F. *J. Phys. Soc. Jpn.* **1962**, *17*, 475.
(885) Aiello, G.; Palma, M. U.; Persico, F. *Phys. Lett. (Netherlands)* **1964**, *11*, 117.
(886) Bates, A. R.; Stevens, K. W. H. *J. Phys. C: Solid State Phys.* **1969**, *2*, 1573.
(887) Trapp, C.; Shyr, C.-I. *J. Chem. Phys.* **1971**, *54*, 196.
(888) Stankowski, J.; Janik, J. M.; Dezor, A.; Sczaniecki, B. *Phys. Status Solidi A* **1973**, *16*, K167.
(889) Grzybek, T.; Janik, J. M.; Mayer, J.; Pytasz, G.; Rachwalska, M. *Phys. Status Solidi A* **1973**, *16*, K165.
(890) Sczaniecki, P. B. *Acta Phys. Polonica A* **1994**, *86*, 1021.
(891) Galmab, V.; Pályi, G. *Coord. Chem. Rev.* **1984**, *59*, 203.
(892) Pályi, G.; Alberts, K.; Bartik, T.; Boese, R.; Fráter, G.; Herbrich, T.; Herfurth, A.; Kriebel, C.; Sorkau, A.; Tschoerner, C. M.; Zucchi, C. *Organometallics* **1996**, *15*, 3253.
(893) Kovács, I.; Ungváry, F. *Coord. Chem. Rev.* **1997**, *161*, 1.
(894) Bencze, L.; Pályi, G.; Kurdi, R. In *Metal Ligand Interactions*; Russo, N., Salahub, D. R.; Witko, M., Eds.; NATO Science Series II: Mathematics, Physics and Chemistry, Volume 116; Kluwer: Dordrecht, 2003; pp 343−354.
(895) Gavezzotti, A.; Simonetta, M. *Chem. Rev.* **1982**, *82*, 1.
(896) Tanaka, K.; Toda, F. *Chem. Rev.* **2000**, *100*, 1025.
(897) Ling, A. R.; Baker, J. L. *J. Chem. Soc.* **1893**, *63*, 1314.
(898) Toda, F.; Tanaka, K.; Sekikawa, A. *Chem. Commun.* **1987**, 279.
(899) Hirano, S.; Yoshizawa, K.; Toyota, S.; Toda, F.; Urbanczyk-Lipkowska, Z. *Mendeleev Commun.* **2003**, 141.
(900) Toda, F. *Enantiomer* **2002**, *7*, 59.
(901) Swift, J. A.; Reynolds, A. M.; Ward, M. D. *Chem. Mater.* **1998**, *10*, 4159.
(902) Ratcliffe, C. I.; Ripmeester, J. A. *J. Phys. Chem.* **1986**, *90*, 1259.
(903) Collins, M.; Ratcliffe, C. I.; Ripmeester, J. A. *J. Phys. Chem.* **1990**, *94*, 157.

(904) Ripmeester, J. A.; Ratcliffe, C. I. In *Inclusion Compounds, Volume 5: Inorganic and Physical Aspects of Inclusion*; Oxford University Press: Oxford, U.K., 1991; pp 37−85.
(905) Udachin, K. A.; Enright, G. D.; Ratcliffe, C. I.; Ripmeester, J. A. *J. Am. Chem. Soc.* **1997**, *119*, 11481.
(906) Udachin, K. A.; Ratcliffe, C. I.; Ripmeester, J. A. *J. Phys. Chem. B* **2001**, *105*, 4200.
(907) Ripmeester, J. A.; Ratcliffe, C. I.; Cameron, I. G. *J. Phys. Chem. B* **2004**, *108*, 929 and references therein.
(908) Davidson, D. W. In *Water, A Comprehensive Treatise*; Franks, F., Ed.; Pergamon Press: New York, 1972; Vol. 2.
(909) Davidson, D. W.; Ripmeester, J. A. In *Inclusion Compounds*; Atwood, J. L., Davies, J. E. D., MacNicol, D. D., Eds.; Academic Press: London, 1984; Vol. 3.
(910) Ripmeester, J. A.; Ratcliffe, C. I. In *Inclusion Compounds*; Atwood, J. L., Davies, J. E. D., MacNicol, D. D., Eds.; Oxford University Press: Oxford, U.K., 1991; Vol. 5.
(911) Soldatov, D. V.; Diamente, P. R.; Ratcliffe, C. I.; Ripmeester, J. A. *Inorg. Chem.* **2001**, *40*, 5660.
(912) Williams, R. M.; Zwier, J. M.; Verhoeven, J. W. *J. Am. Chem. Soc.* **1994**, *116*, 6965.
(913) Andrews, P. C.; Atwood, J. L.; Barbour, L. J.; Nichols, P. J.; Raston, C. L. *Chem.—Eur. J.* **1998**, *4*, 1384.
(914) Croucher, P. D.; Nichols, P. J.; Raston, C. L. *J. Chem. Soc., Dalton Trans.* **1999**, 279.
(915) Andrews, P. C.; Atwood, J. L.; Barbour, L. J.; Croucher, P. D.; Nichols, P. J.; Smith, N. O.; Skelton, B. W.; White, A. H.; Raston, C. L. *J. Chem. Soc., Dalton Trans.* **1999**, 2927.
(916) Croucher, P. D.; Marshall, J. M. E.; Nichols, P. J.; Raston, C. L. *Chem. Commun.* **1999**, 193.
(917) Hardie, M. J.; Raston, C. L. *Chem. Commun.* **1999**, 1153 and references therein.
(918) Saunders, M.; Cross, R. J.; Jiménez-Vásquez, H. A.; Shimshi, R.; Khong, A. *Science* **1996**, *271*, 1693.
(919) Murphy, T. A.; Pawlic, T.; Weidinger, A.; Höhne, M.; Alcala, R.; Spaeth, J.-M. *Phys. Rev. Lett.* **1996**, *77*, 1075.
(920) Rubin, Y.; Jarrosson, T.; Wang, G.-W.; Bartberger, M. D.; Houk, K. N.; Schick, G.; Saunders, M.; Cross, R. J. *Angew. Chem., Int. Ed.* **2001**, *40*, 1543.
(921) Murata, Y.; Murata, M.; Komatsu, K. *J. Am. Chem. Soc.* **2003**, *125*, 7152.
(922) Carravetta, M.; Murata, Y.; Murata, M.; Heinmaa, I.; Stern, R.; Tontcheva, A.; Samoson, A.; Rubin, Y.; Komatsu, K.; Levitt, M. H. *J. Am. Chem. Soc.* **2004**, *126*, 4092.
(923) Cross, R. J. *J. Phys. Chem. A* **2001**, *105*, 6943.
(924) Vorderwisch, P.; Hautecler, S.; Kearley, G. J.; Kubanek, F. *Chem. Phys.* **2000**, *261*, 157.
(925) Iwamoto, T. In *Inclusion Compounds; Volume 5: Inorganic and Physical Aspects of Inclusion*; Atwood, J. L., Davies, J. E. D., MacNicol, D. D., Eds.; Oxford University Press: Oxford, U.K., 1991; pp 177−212.
(926) Wegener, W.; Bostoen, C.; Coddens, G. *J. Phys.: Condens. Matter* **1990**, *2*, 3177.
(927) Kearly, G.; Büttner, H.; Fillaux, F.; Lautiè, M. *Phisica B* **1997**, *226*, 199.
(928) Enders, A.; Mintz, G. *Phys. Rev. A* **1985**, *32*, 2521.
(929) Asthalter, T.; Franz, H.; van Bürck, U.; Messel, K.; Screier, E.; Dinnebier, R. *J. Phys. Chem. Solids* **2003**, *64*, 677.
(930) Nowik, I.; Herber, R. H. *Inorg. Chim. Acta* **2000**, *310*, 191.
(931) Herber, R. H.; Nowik, I. *Hyperfine Interact.* **2000**, *126*, 127.
(932) Herber, R. H. *Inorg. Chim. Acta* **1999**, *291*, 74.
(933) Schottenberger, H.; Wurst, K.; Herber, R. H. *J. Organomet. Chem.* **2001**, *625*, 200.
(934) Han, J.; Globus, A.; Jaffe, R.; Deardorff, G. *Nanotechnology* **1997**, *8*, 95.
(935) Srivastava, D. *Nanotechnology* **1997**, *8*, 186.
(936) Tuzun, R. E.; Noid, D. W.; Sumpter, B. G. *Nanotechnology* **1995**, *6*, 64.
(937) Sohlberg, K.; Tuzun, R. E.; Sumpter, B. G.; Noid, D. W. *Nanotechnology* **1997**, *8*, 103.
(938) Tuzun, R. E.; Noid, D. W.; Sumpter, B. G. *Nanotechnology* **1995**, *6*, 52.
(939) Tu, Z. C.; Ou-Yang, Z. C. *J. Phys.: Condens. Matter* **2004**, *16*, 1287.
(940) Saito, R.; Matsuo, R.; Kimura, T.; Dresselhaus, G.; Dresselhaus, M. S. *Chem. Phys. Lett.* **2001**, *348*, 187.
(941) Lozovik, Y. E.; Minogin, A. V.; Popov, A. M. *JETP Lett.* **2003**, *77*, 759.
(942) Lozovik, Y. E.; Minogin, A. V.; Popov, A. M. *Phys. Lett. A* **2003**, *313*, 112.
(943) Fennimore, A. M.; Yuzvinsky, T. D.; Han, W.-Q.; Fuhrer, M. S.; Cumings, J.; Zettl, A. *Nature* **2003**, *424*, 408.
(944) Yannoni, C. S.; Johnson, R. D.; Meijer, G.; Bethune, D. S.; Salem, J. R. *J. Phys. Chem.* **1991**, *95*, 9.
(945) Tycko, R.; Dabbagh, R. C.; Fleming, R. M.; Haddon, R. C.; Makhija, A. V.; Zahurak, S. M. *Phys. Rev. Lett.* **1991**, *67*, 1886.
(946) Neumann, D. A.; Copley, J. R. D.; Cappelletti, R. L.; Kamitakahara, W. A.; Lindstrom, R. M.; Creegan, K. M.; Cox, D. M.; Romanow, W. J.; Coustel, N.; McCauley, J. P., Jr.; Maliszewskyj, N. C.; Fischer, J. E.; Smith, A. B., III. *Phys. Rev. Lett.* **1991**, *67*, 3808.
(947) Lebedev, V. T.; Török, Gy.; Cser, L.; Budtov, V. P.; Sibilev, A. I. *Phys. Solid State* **2002**, *44*, 641.
(948) Heiny, P. A.; Fischer, J. E.; McGhie, A. R.; Romanow, W. J.; Denenstein, A. M.; McCauley, J. P., Jr.; Smith, A. B., III; Cox, D. E. *Phys. Rev. Lett.* **1991**, *66*, 2911.
(949) Johnson, R. D.; Yannoni, C. S.; Dorn, H. C.; Salem, J. R.; Bethune, D. S. *Science* **1992**, *255*, 1235.
(950) Cheng, A.; Klein, M. L. *Phys. Rev. B* **1992**, *45*, 1889.
(951) Kiefl, R. F.; Schneider, J. W.; MacFarlane, A.; Chow, K.; Duty, T. L.; Estle, T. L.; Hitti, B.; Lichti, R. L.; Ansaldo, E. J.; Schwab, C.; Percival, P. W.; Wei, G.; Wlodek, S.; Kojima, K.; Romanow, W. J.; McCauley, J. P., Jr.; Coustel, N.; Fischer, J. E.; Smith, A. B., III. *Phys. Rev. Lett.* **1992**, *68*, 1347.
(952) Reiley, H. A. *Mol. Cryst. Liq. Cryst.* **1969**, *101*, 9.
(953) Nordmann, C. E.; Schmitkons, D. L. *Acta Crystallogr.* **1965**, *18*, 764.
(954) Deleuze, M. S.; Zerbetto, F. *J. Am. Chem. Soc.* **1999**, *121*, 5281.
(955) Tycko, R.; Haddon, R. C.; Dabbagh, G.; Glarum, S. H.; Douglass, D. C.; Mujsce, A. M. *J. Phys. Chem.* **1991**, *95*, 518.
(956) Girifalco, L. A. *J. Phys. Chem.* **1992**, *96*, 858.
(957) Zubov, V. I.; Tretiakov, N. P.; Sanchez, J. F.; Caparica, A. A. *Phys. Rev. B* **1996**, *53*, 12080.
(958) Zubov, V. I.; Sanchez-Ortiz, J. F.; Teixeira Rabelo, J. N.; Zubov, I. V. *Phys. Rev. B* **1997**, *55*, 6747.
(959) Shen, J.-Q.; He, S.-L. *Phys. Rev. B* **2003**, *68*, 195421.
(960) Miura, K.; Kamiya, S.; Sasaki, N. *Phys. Rev. Lett.* **2003**, *90*, 055509.
(961) Fennimore, A. M.; Yuzvinsky, T. D.; Han, W.-Q.; Fuhrer, M. S.; Cumings, J.; Zettl, A. *Nature* **2003**, *424*, 408.
(962) Bourlon, B.; Glattli, D. C.; Miko, C.; Forró, L.; Bachtold, A. *Nano Lett.* **2004**, *4*, 709.
(963) Svensson, K.; Bengtson, L.; Bellman, J.; Hassel, M.; Person, M.; Anderson, S. *Phys. Rev. Lett.* **1999**, *83*, 124.
(964) Teillet-Billy, D.; Gauyacq, J. P. *Surf. Sci.* **2002**, *502−503*, 358.
(965) Mo, Y. W. *Science* **1993**, *261*, 886.
(966) Teillet-Billet, D.; Gauyacq, J. P.; Persson, M. *Phys. Rev. B* **2000**, *62*, R13306.
(967) Stipe, B. C.; Rezaei, M. A.; Ho, W. *Science* **1998**, *279*, 1907.
(968) Lauhon, L. J.; Ho, W. *J. Chem. Phys.* **1999**, *111*, 5633.
(969) Stipe, B. C.; Rezaei, M. A.; Ho, W. *Phys. Rev. Lett.* **1998**, *81*, 1263.
(970) Dunphy, J. C.; Rose, M.; Behler, S.; Ogletree, D. F.; Salmeron, M.; Sautet, P. *Phys. Rev. B* **1998**, *57*, R12705.
(971) Gimzewski, J. K.; Joachim, C. *Science* **1999**, *283*, 1683.
(972) Loppacher, Ch.; Guggisberg, M.; Pfeiffer, O.; Meyer, E.; Bammerlin, M.; Lüthi, R.; Schlittler, R.; Gimzewski, J. K.; Tang, H.; Joachim, C. *Phys. Rev. Lett.* **2003**, *90*, 066107.
(973) Moresco, F.; Meyer, G.; Rieder, K.-H.; Tang, H.; Gourdon, A.; Joachim, C. *Phys. Rev. Lett.* **2001**, *86*, 672.
(974) Gimzewski, J. K.; Joachim, C.; Schlittler, R. R.; Langlais, V.; Tang, H.; Johannsen, I. *Science* **1998**, *281*, 531.
(975) Hersam, M. C.; Guisinger, N. P.; Lyding, J. W. *Nanotechnology* **2000**, *11*, 70.
(976) Lyding, J. W.; Shen, T.-C.; Hubacek, J. S.; Tucker, J. R.; Abeln, G. C. *Appl. Phys. Lett.* **1994**, *64*, 2010.
(977) Tabe, Y.; Yokohame, H. *Nat. Mater.* **2004**, *2*, 806.
(978) Deleuze, M. *J. Am. Chem. Soc.* **2000**, *122*, 1130.
(979) Leigh, D. A.; Murphy, A.; Smart, J. P.; Deleuze, M. S.; Zerbetto, F. *J. Am. Chem. Soc.* **1998**, *120*, 6458.
(980) Ryason, P. R.; Russell, B. G. *J. Phys. Chem.* **1975**, *79*, 1276.
(981) Clarke, L. I.; Horinek, D.; Kottas, G. S.; Varaksa, N.; Magnera, T. F.; Hinderer, T. P.; Horansky, R. D.; Michl, J.; Price, J. C. *Nanotechnology* **2002**, *13*, 533.
(982) Rappe, A. K.; Casewit, C. J.; Colwell, K. S.; Goddard, W. A., III; Skiff, W. M. *J. Am. Chem. Soc.* **1992**, *114*, 10024.
(983) Jian, H.; Tour, J. M. *J. Org. Chem.* **2003**, *68*, 5091.
(984) These rotors were examined previously by dielectric spectroscopy, but their torsional barriers proved to be too low to be observable in the accessible temperature range: Clarke, L. I.; Price, J. C. Unpublished results.
(985) Hou, S.; Sagara, T.; Xu, D.; Kelly, T. R.; Ganz, E. *Nanotechnology* **2003**, *14*, 566.
(986) Mulcahy, M.-E.; Magnera, T. F.; Michl, J. Unpublished results.
(987) Sakai, A. In *Advances in Materials Research: Advances in Scanning Probe Microscopy*; Sakurai, T., Watanabe, Y., Eds.; Springer-Verlag: New York, 2000; p 143.
(988) *Molecular Electronics: Science and Technology*; Aviram, A., Ratner, M. A., Eds.; New York Academy of Sciences: New York, 1998.
(989) *Molecular Electronics II*; Aviram, A., Ratner, M. A., Mujica, V., Eds.; New York Academy of Sciences: New York, 2002.
(990) Kornilovitch, P. E.; Bratkovsky, A. M.; Williams, R. S. *Phys. Rev. B* **2002**, *66*, 245413.
(991) Miura, K.; Kamiya, S.; Sasaki, N. *Phys. Rev. Lett.* **2003**, *90*, 055509.
(992) Kang, J. W.; Hwang, H. J. *Nanotechnology* **2004**, *15*, 614.

(993) Das, B.; Sebastian, K. L. *Chem. Phys. Lett.* **2002**, *357*, 25.
(994) Das, B.; Sebastian, K. L. *Chem. Phys. Lett.* **2000**, *330*, 433.
(995) Joachim, C.; Tang, H.; Moresco, F.; Rapenne, G.; Meyer, G. *Nanotechnology* **2002**, *13*, 330.
(996) Jiminez-Bueno, G.; Rappene, G. *Tetrahedron Lett.* **2003**, *44*, 6261.
(997) Since the submission of this manuscript, a number of papers have been published in this field: Dahl, B. J.; Branchaud, B. P. *Tetrahedron Lett.* **2004**, *45*, 9599. Griessl, S. J. H.; Lackinger, M.; Jamitzky, F.; Markert, T.; Hietschold, M.; Heckl, W. M. *Langmuir* **2004**, *20*, 9403. Krause, M.; Hulman, M.; Kuzmany, H.; Dubay, O.; Kresse, G.; Vietze, K.; Seifert, G.; Wang, C.; Shinohara, H. *Phys. Rev. Lett.* **2004**, *93*, 137403. Hernández, J. V.; Kay, E. R.; Leigh, D. A. *Science* **2004**, *306*, 1532. Scarso, A.; Onagi, H.; Rebek, J., Jr. *J. Am. Chem. Soc.* **2004**, *126*, 12728. Hiraoka, S.; Hirata, K.; Shionoya, M. *Angew. Chem., Int. Ed.* **2004**, *43*, 3814. Khuong, T.-A. V.; Zepeda, G.; Sanrame, C. N.; Dang, H.; Bartberger, M. D.; Houk, K. N.; Garcia-Garibay, M. A. *J. Am. Chem. Soc.* **2004**, *126*, 14778. Carella, A.; Rapenne, G.; Launay, J.-P. *New J. Chem.* **2005**, *29*, 288. Astumian, R. D. *Proc. Natl. Acad. Sci.* **2005**, *102*, 1843. Philip, I.; Kaifer, A. E. *J. Org. Chem.* **2005**, *70*, 1558. Ercolani, G. *Org. Lett.* **2005**, *7*, 803. Akutagawa, T.; Shitagami, K.; Nishihara, S.; Takeda, S.; Hasegawa, T.; Nakamura, T.; Hosokoshi, Y.; Inoue, K.; Ikeuchi, S.; Miyazaki, Y.; Saito, K. *J. Am. Chem. Soc.* **2005**, *127*, 4397. Takamizawa, S.; Nakata, E.; Saito, T.; Akatsuka, T. *Inorg. Chem.* **2005**, *44*, 1362.

CR0300993